

Detection of bacterial contaminations in platelet concentrates using Raman spectroscopy and flow cytometry

Dissertation

zur

Erlangung des Doktorgrades (Dr. rer. nat.)

der

Mathematisch-Naturwissenschaftlichen Fakultät

der

Rheinischen Friedrich-Wilhelms-Universität Bonn

vorgelegt von

Manuel Schreiner

aus

Momberg

Bonn, März 2023

Angefertigt mit Genehmigung der Mathematisch-Naturwissenschaftlichen Fakultät der Rheinischen Friedrich-Wilhelms-Universität Bonn

1. Gutachter: Prof. Dr. Isabelle Bekeredjian-Ding

2. Gutachter: Prof Dr. Tanja Schneider

Tag der Promotion: 01.08.2023

Erscheinungsjahr: 2023

Table of contents

| | |
|---|-------------|
| TABLE OF CONTENTS | I |
| TABLES | VI |
| FIGURES | VIII |
| ABBREVIATIONS | XI |
| ZUSAMMENFASSUNG | XV |
| SUMMARY | XVII |
| 1 INTRODUCTION | 1 |
| 1.1 Bacterial contamination in platelet concentrates | 1 |
| 1.1.1 Current microbiological quality testing of blood products | 2 |
| 1.1.2 Transfusion-relevant bacteria reference strains | 6 |
| 1.1.3 Selection of representative reference strains for the detection of bacteria in PC | 10 |
| 1.1.3.1 <i>S. aureus</i> | 10 |
| 1.1.3.2 <i>K. pneumoniae</i> | 11 |
| 1.1.3.3 <i>S. epidermidis</i> | 12 |
| 1.1.3.4 <i>B. cereus</i> | 12 |
| 1.2 Flow cytometry | 14 |
| 1.2.1 Basics of flow cytometry | 14 |
| 1.2.2 The flow cytometry based BactiFlow® system | 16 |
| 1.2.3 Application of flow cytometry for the detection of bacteria in PC- status quo | 17 |
| 1.3 The Raman effect | 18 |
| 1.3.1 Raman spectroscopy of biological samples | 20 |
| 1.3.2 Raman microspectroscopy | 21 |
| 1.3.3 Design of a Raman experiment | 22 |
| 1.4 Raman data analysis | 22 |

| | | |
|----------|---|-----------|
| 1.4.1 | Raman spectra pre-processing..... | 23 |
| 1.4.2 | Multivariate data analysis for classification..... | 24 |
| 1.5 | Aim of the thesis | 25 |
| 2 | MATERIAL..... | 26 |
| 2.1 | Bacterial strains..... | 26 |
| 2.2 | Culture media and stock solutions..... | 26 |
| 2.3 | Consumables and devices | 30 |
| 3 | METHODS..... | 34 |
| 3.1 | Procurement and handling of PC | 34 |
| 3.1.1 | PC transfusion bags..... | 34 |
| 3.1.2 | Storage of PC..... | 34 |
| 3.1.3 | Welding of Luer-connection with sterile bag joint for PC sample collection..... | 34 |
| 3.1.4 | Base sterility test of PC using the BacT/ALERT® 3D automated culturing method | 34 |
| 3.2 | Sample preparations for PC spiked with bacterial strains | 35 |
| 3.2.1 | Bacterial reference strains for PC spiking | 35 |
| 3.2.2 | Preparation of cryopreserved bacterial strains | 35 |
| 3.2.3 | Cultivation of bacteria for PC spiking..... | 35 |
| 3.2.4 | Spiking of PC with defined contamination levels of bacteria..... | 36 |
| 3.2.5 | Enumeration of bacteria | 37 |
| 3.3 | Sample preparation for bacterial growth assays in PC | 37 |
| 3.3.1 | Transfer and splitting of PC into storage bags | 37 |
| 3.3.2 | Preparation of the spiking solution for bacterial growth assays in PC | 37 |
| 3.3.3 | Spiking of PC bags for bacterial growth assays | 38 |
| 3.3.4 | Sample collection of bacterial growth assays in PC..... | 38 |
| 3.3.5 | Evaluation of growth of <i>K. pneumoniae</i> in PC for Raman microspectroscopy measurements ... | 38 |
| 3.4 | Detection of bacteria in PC using Raman microspectroscopy | 39 |
| 3.4.1 | Preparation of Calcium fluoride (CaF ₂) microscopy slides | 39 |
| 3.4.2 | Raman measurements using the BioRam® Raman microspectroscope | 39 |

| | | |
|----------|--|-----------|
| 3.4.3 | Calibration measurements for Raman spectra | 40 |
| 3.4.4 | Raman measurements of PC samples | 40 |
| 3.5 | Analysis of Raman spectra | 41 |
| 3.5.1 | Structuring Raman data for reading into the software..... | 41 |
| 3.5.2 | Pre-processing of raw spectra with the Raman Analyst Software..... | 42 |
| 3.5.3 | Model cross-validation..... | 48 |
| 3.6 | Detection of bacteria in PC using flow cytometry | 50 |
| 3.6.1 | New flow cytometry method: Staining protocol for the detection of bacteria in PC..... | 50 |
| 3.6.2 | Validation of the LOD of flow cytometry for detection of bacteria in PC..... | 52 |
| 3.6.3 | Gating strategy for detection of bacteria in PC using the Kaluza flow cytometry analysis software version 2.1.1 | 52 |
| 3.6.4 | Analysis of flow cytometry data | 52 |
| 3.7 | Detection of bacteria in PC using the BactiFlow® system..... | 53 |
| 3.7.1 | Preparation of the BactiFlow® device before measurements | 53 |
| 3.7.2 | Preparation of working solutions for BactiFlow® Analysis..... | 53 |
| 3.7.3 | Sample processing for BactiFlow® analysis..... | 54 |
| 3.7.4 | Performing BactiFlow® Analysis..... | 54 |
| 3.7.5 | Comparison of BactiFlow® measurements with flow cytometric measurements..... | 55 |
| 4 | RESULTS..... | 56 |
| 4.1 | Detection of bacterial contaminations in PC using Raman microspectroscopy | 56 |
| 4.1.1 | Evaluation of the Raman data sets and confusion table results..... | 56 |
| 4.2 | Detection of bacterial contaminations in PC using flow cytometry | 58 |
| 4.2.1 | Definition of a universal gating strategy for the detection of bacteria in PC by flow cytometry | 58 |
| 4.2.2 | Comparison of flow cytometric bacteria detection in PC before and after the use of the platelet aggregation inhibitor Tirofiban during sample preparation..... | 62 |
| 4.2.3 | Detection of <i>S. aureus</i> in PC using an adjusted method protocol and detection gate | 66 |
| 4.2.4 | Calculation of the analytical accuracy of the flow cytometry method using area under the receiver operating characteristic curves | 68 |
| 4.2.5 | Screening for bacterial contaminations spiked in PC samples using the flow cytometry method under standardized conditions..... | 71 |

| | | |
|----------|--|------------|
| 4.2.5.1 | Bacterial detection in PC samples by the flow cytometry method is decreased by omitting the Tirofiban incubation step..... | 71 |
| 4.2.5.2 | Introduction of a Tirofiban incubation step leads to improved results in bacterial screening of PC by flow cytometry..... | 75 |
| 4.3 | Detection of bacterial contaminations in PC samples using the BactiFlow® system..... | 78 |
| 4.4 | Bacterial screening of bacteria grown in PC bags..... | 80 |
| 4.4.1 | Bacterial growth detection of transfusion-relevant bacteria in PC bags by the new flow cytometry method in comparison to BactiFlow®..... | 81 |
| 5 | DISCUSSION..... | 84 |
| 5.1 | Raman microspectroscopy..... | 84 |
| 5.1.1 | Challenges of bacterial contaminant detection in PC using Raman microspectroscopy..... | 84 |
| 5.1.2 | Improvement of bacterial detection in PC by Raman spectroscopy..... | 86 |
| 5.2 | Flow Cytometry..... | 90 |
| 5.2.1 | Development of the new flow cytometry method for the detection of bacteria in PC..... | 90 |
| 5.2.2 | Adaptation of the new flow cytometry protocol for the detection of <i>S. aureus</i> in PC..... | 93 |
| 5.2.3 | Comparison of BactiFlow® and the new flow cytometric detection method..... | 96 |
| 5.3 | Conclusions and Perspectives..... | 99 |
| 6 | LITERATURE..... | 102 |
| 7 | APPENDIX..... | 122 |
| 7.1 | Recipes of stock solutions and media..... | 122 |
| 7.2 | Result graphs flow cytometry method (WHO bacteria panel)..... | 124 |
| 7.3 | Detection of bacteria in PC without Tirofiban incubation step..... | 128 |
| 7.4 | Result graphs for the discrimination threshold of bacterial contaminations in PC..... | 130 |
| 7.5 | Mean number (CFU/ml) of bacteria spiked into PC and result graphs of the new flow cytometry method without Tirofiban..... | 132 |

| | | |
|-----|---|------------|
| 7.6 | Mean number (CFU/ml) of bacteria spiked into PC and result graphs of the new flow cytometry method with Tirofiban | 140 |
| 7.7 | Result graphs of BactiFlow® system | 145 |
| 7.8 | Raman parameter folder for the Raman Analyst Software | 149 |
| 7.9 | Titration of the optimal Triton X-100 concentration for the lysis of platelets | 150 |
| | ACKNOWLEDGEMENT | 151 |

Tables

| | |
|--|----|
| Table 1: Overview of commercially available PI systems..... | 5 |
| Table 2: Platelet Transfusion-Relevant Bacteria Reference Strains | 9 |
| Table 3: PEI PTRBR strains..... | 26 |
| Table 4: Culture medium | 27 |
| Table 5: General Solutions | 27 |
| Table 6: BactiFlow® Solutions and reagents | 28 |
| Table 7: general reagents and chemicals..... | 29 |
| Table 8: General consumables and blood products | 30 |
| Table 9: Devices | 31 |
| Table 10: Software | 33 |
| Table 11: Layout for BactiFlow® and Flow cytometry analysis experiments..... | 37 |
| Table 12: Overview of the recorded Raman spectra summarized in data sets | 48 |
| Table 13: Fluorescence dye for flow cytometry..... | 52 |
| Table 14: Enzymatic lysis solution for BactiFlow® | 53 |
| Table 15: Staining solution for BactiFlow® | 54 |
| Table 16: PC contaminated with $2.10-7.42 \times 10^5$ CFU/ml <i>K. pneumoniae</i> | 56 |
| Table 17: PC contaminated with $0.84-1.74 \times 10^6$ CFU/ml <i>K. pneumoniae</i> | 56 |
| Table 18: PC contaminated with $1.00-8.10 \times 10^7$ CFU/ml <i>K. pneumoniae</i> | 57 |
| Table 19: PC contaminated with $1.56-7.29 \times 10^8$ CFU/ml <i>K. pneumoniae</i> | 57 |
| Table 20: PC contaminated with $1.16-1.78 \times 10^9$ CFU/ml <i>K. pneumoniae</i> | 57 |
| Table 21: Overall detection of contaminated PC samples using the new flow cytometry method (without Tirofiban)..... | 73 |
| Table 22: Strain specific detection of contaminated PC samples using the new flow cytometry method (without Tirofiban) | 74 |
| Table 23: Overall detection of contaminated PC samples using the new flow cytometry method (with Tirofiban) | 76 |
| Table 24: Strain specific detection of contaminated PC samples using the new flow cytometry method (with Tirofiban) | 77 |
| Table 25: Overall detection of contaminated PC samples using the BactiFlow® system | 79 |
| Table 26: Detection of indicated bacterial strains spiked in PC samples using the BactiFlow® system | 80 |

| | |
|---|-----|
| Table 27: Recipe of NaCl 0.85 % (1 l) | 122 |
| Table 28: Recipe of PBS without Ca and Mg pH 7.1 (1 l) | 122 |
| Table 29: Recipe of PBS without Ca and Mg pH 7.1 + 1 mM EDTA (1l)..... | 123 |
| Table 30: Recipe of Standard-I-Agar (1 l) | 123 |
| Table 31: Mean number (CFU/ml) of bacteria spiked into PC samples (without Tirofiban) | 132 |
| Table 32: Mean number (CFU/ml) of bacteria spiked into PC samples (+ Tirofiban) | 140 |

Figures

| | |
|--|----|
| Figure 1: Bacterial species involved in transfusion-transmitted blood and blood product infections [42] (modified)..... | 8 |
| Figure 2: Scheme of the analysis point of a flow cytometer [176]..... | 16 |
| Figure 3: Jablonski diagram of Quantum Energy Transitions for Rayleigh and Raman Scattering [184], modified | 19 |
| Figure 4: Dependence of the intensity in spontaneous Raman Scattering [187]..... | 19 |
| Figure 5: Raman spectrum of a human platelet; important biological peaks and regions: | 21 |
| Figure 6: Growth curve of <i>K. pneumoniae</i> in PC at 20 °C (log ₁₀) | 39 |
| Figure 7: Data structure of Raman measurements | 42 |
| Figure 8: Mean plot of all sample spectra of the data set..... | 43 |
| Figure 9: Mean plot of each defined class..... | 43 |
| Figure 10: Data Pre-processing: Despiking | 44 |
| Figure 11: Data Pre-processing: Wavenumber axis calibration | 45 |
| Figure 12: Data-Pre-processing: Background correction | 46 |
| Figure 13: Data Pre-processing: Normalization | 47 |
| Figure 14: Data Pre-processing: Processed classes of data | 47 |
| Figure 15: k-fold cross validation | 49 |
| Figure 16: Representative illustration of k-fold cross validated test data sets (..... | 50 |
| Figure 17: Flow cytometric detection gate for <i>K. pneumoniae</i> in PC samples | 59 |
| Figure 18: Flow cytometric detection gate for <i>B. cereus</i> in PC samples..... | 59 |
| Figure 19: Flow cytometric detection gate for <i>S. epidermidis</i> in PC samples..... | 60 |
| Figure 20: Flow cytometric detection gate for <i>S. aureus</i> in PC samples..... | 60 |
| Figure 21: Gating strategy for bacterial detection in contaminated PC | 61 |
| Figure 22: Effects of Tirofiban on the flow cytometric detection of <i>K. pneumoniae</i> in PC. | 63 |
| Figure 23: Effects of Tirofiban on the flow cytometric detection of <i>B. cereus</i> in PC..... | 64 |
| Figure 24: Effects of Tirofiban on the flow cytometric detection of <i>S. epidermidis</i> in PC..... | 65 |
| Figure 25: Effects of Tirofiban on the flow cytometric detection of <i>S. aureus</i> in PC..... | 66 |
| Figure 26: Generation of an <i>S. aureus</i> - specific population gate | 67 |
| Figure 27: Effect of Tirofiban on <i>S. aureus</i> detection in PC without centrifugation prior to platelet lysis and DRAQ5™ staining..... | 67 |

| | |
|--|-----|
| Figure 28: Analysis of the classification performance of the flow cytometric method for contaminated and non-contaminated PC without the platelet aggregation inhibitor Tirofiban | 69 |
| Figure 29: Analysis of the classification performance of the flow cytometric method for contaminated and non-contaminated PC using the platelet aggregation inhibitor Tirofiban | 70 |
| Figure 30: AUROC analysis of <i>S. aureus</i> contaminated PC and non-contaminated PC | 71 |
| Figure 31: Flow cytometric detection of bacterial events of WHO Repository (PTRBR) strains spiked in PC samples at different concentrations without using Tirofiban | 72 |
| Figure 32: Flow cytometric detection of bacterial events of WHO Repository (PTRBR) strains spiked in PC samples at different concentrations with Tirofiban | 75 |
| Figure 33: Detected bacterial events of WHO Repository (PTRBR) strains spiked in PC samples at different contamination levels analysed with the BactiFlow® system | 78 |
| Figure 34: Growth of <i>K. pneumoniae</i> spiked in PC bags | 81 |
| Figure 35: Growth of <i>B. cereus</i> spiked in PC bags | 82 |
| Figure 36: Growth of <i>S. epidermidis</i> spiked in PC with 2-5 CFU/bag | 83 |
| Figure 37: Flow cytometric detection gate for <i>E. coli</i> in PC samples | 124 |
| Figure 38: Flow cytometric detection gate for <i>E. cloacae</i> in PC samples | 124 |
| Figure 39: Flow cytometric detection gate for <i>P. fluorescens</i> in PC samples | 125 |
| Figure 40: Flow cytometric detection gate for <i>P. mirabilis</i> in PC samples | 125 |
| Figure 41: Flow cytometric detection gate for <i>S. marcescens</i> in PC samples | 126 |
| Figure 42: Flow cytometric detection gate for <i>M. morgani</i> in PC samples | 126 |
| Figure 43: Flow cytometric detection gate for <i>S. pyogenes</i> in PC samples | 127 |
| Figure 44: Flow cytometric detection gate for <i>B. thuringiensis</i> in PC samples | 127 |
| Figure 45: Detection of 10 ⁵ CFU/ml <i>E. coli</i> in PC without Tirofiban incubation step | 128 |
| Figure 46: Detection of 10 ⁵ CFU/ml <i>E. cloacae</i> in PC without Tirofiban incubation step | 128 |
| Figure 47: Detection of 10 ⁵ CFU/ml <i>B. thuringiensis</i> in PC without Tirofiban incubation step | 129 |
| Figure 48: Comparison of detected events of contaminated and non-contaminated PC without Tirofiban | 130 |
| Figure 49: Comparison of detected events of contaminated and non-contaminated PC incubated with Tirofiban | 131 |
| Figure 50: PC spiked with <i>S. aureus</i> analysed with the new flow cytometry method without Tirofiban | 133 |
| Figure 51: PC spiked with <i>K. pneumoniae</i> analysed with the new flow cytometry method without Tirofiban | 134 |

| | |
|--|-----|
| Figure 52: PC spiked with <i>B. cereus</i> analysed with the new flow cytometry method without Tirofiban..... | 135 |
| Figure 53: PC spiked with <i>S. epidermidis</i> analysed with the new flow cytometry method without Tirofiban..... | 136 |
| Figure 54: PC spiked with <i>E. coli</i> analysed with the new flow cytometry method without Tirofiban | 137 |
| Figure 55: PC spiked with <i>E. cloacae</i> analysed with the new flow cytometry method without Tirofiban..... | 138 |
| Figure 56: PC spiked with <i>B. thuringiensis</i> analysed with the new flow cytometry method without Tirofiban..... | 139 |
| Figure 57: PC spiked with <i>K. pneumoniae</i> analysed with the new flow cytometry method with Tirofiban..... | 141 |
| Figure 58: PC spiked with <i>B. cereus</i> analysed with the new flow cytometry method with Tirofiban | 142 |
| Figure 59: PC spiked with <i>S. epidermidis</i> analysed with the new flow cytometry method with Tirofiban..... | 143 |
| Figure 60: PC spiked with <i>S. aureus</i> analysed with the new flow cytometry method with Tirofiban | 144 |
| Figure 61: PC spiked with <i>S. aureus</i> analysed with the BactiFlow® system..... | 145 |
| Figure 62: PC spiked with <i>K. pneumoniae</i> analysed with the BactiFlow® system | 146 |
| Figure 63: PC spiked with <i>B. cereus</i> analysed with the BactiFlow® system | 147 |
| Figure 64: PC spiked with <i>S. epidermidis</i> analysed with the BactiFlow® system..... | 148 |
| Figure 65: Parameters for pre-processing of Raman spectra using the Raman Analyst Software version 0.2.0.0 (Leibniz-IPHT; Jena, Germany) | 149 |
| Figure 66: Influence of lysis on bacteria and platelets by different concentrations of Triton X-100 | 150 |

Abbreviations

| | |
|-------------------------|--|
| (CA-)MRSA | (Community-acquired) methicillin-resistant <i>Staphylococcus aureus</i> |
| DNA | Deoxyribonucleic acid |
| AUROC | Area under the receiver operating characteristic curves |
| arb. u. | arbitrary units |
| <i>B. cereus</i> | <i>Bacillus cereus</i> |
| <i>B. thuringiensis</i> | <i>Bacillus thuringiensis</i> |
| BE | Blood establishments |
| CCD | Charge-coupled device |
| CD61 | Integrin beta-3 |
| CDP-plasma | Citrate-Phosphate-Dextrose-plasma |
| CE | Conformité européenne |
| CFU | Colony forming units |
| CI | Confidence interval |
| ClfA/B | Clumping factor A/B |
| CMV | Cytomegalovirus |
| Coa | Coagulase |
| DCCR | Drop coating deposition Raman |
| Dest. | Distilled |
| DRAQ5™ | Deep red-fluorescing bisalkylaminoanthraquinone number five |
| DRK | Deutsches Rotes Kreuz (German Red Cross) |
| <i>E. cloacae</i> | <i>Enterobacter cloacae</i> |
| <i>E. coli</i> | <i>Escherichia coli</i> |
| e. g. | Example given |
| ECDC | European centre for disease prevention and control |
| EDTA | Ethylenediaminetetraacetic acid |
| EMA | Ethidium monoazide |

| | |
|-----------------------|--|
| <i>et al.</i> | And others |
| EtOH | Ethanol |
| EU | European Union |
| Fig. | Figure |
| FSC | Forward scatter |
| GP | Glycoprotein |
| HBV | Hepatitis b virus |
| HCV | Hepatitis c virus |
| HIV | Human immunodeficiency virus |
| <i>K. pneumoniae</i> | <i>Klebsiella pneumoniae</i> |
| KBE | Kolonie Bildende Einheit (colony forming unit) |
| LDA | Linear discriminant analysis |
| LOD | Limit of detection |
| LP | Longpass filter |
| LPS | Lipopolysaccharide |
| LTA | Lipoteichoic acid |
| <i>M. morganii</i> | <i>Morganella morganii</i> |
| MSCRAMM | Microbial surface components recognizing adhesive matrix molecules |
| n | Number of experiments |
| NA | Numerical aperture |
| NAT | Nucleic acid test |
| NIR | Near infrared region |
| nm | Nano meter |
| OD | Optical density |
| <i>P. fluorescens</i> | <i>Pseudomonas fluorescens</i> |
| <i>P. mirabilis</i> | <i>Proteus mirabilis</i> |
| PAS | Platelet additive solution |
| PBS | Phosphate buffered saline |

| | |
|------------------------|-----------------------------------|
| PC | Platelet concentrate |
| PCA | Principal component analysis |
| PCR | Polymerase chain reaction |
| PEI | Paul-Ehrlich-Institute |
| pFA | Paraformaldehyde |
| PGN | Peptidoglycan |
| Ph. Eur. | European Pharmacopoeia |
| PI | Pathogen inactivation |
| PRT | Pathogen reduction technology |
| RGD | Arginylglycylaspartic acid |
| RMM | Rapid microbiological method |
| RNA | Ribonucleic acid |
| rpm | Rounds per minute |
| RRE | Resonance Raman effect |
| RRS | Resonance Raman spectroscopy |
| <i>S. aureus</i> | <i>Staphylococcus aureus</i> |
| <i>S. dysgalactiae</i> | <i>Streptococcus dysgalactiae</i> |
| <i>S. epidermidis</i> | <i>Staphylococcus epidermidis</i> |
| <i>S. gallolyticus</i> | <i>Streptococcus gallolyticus</i> |
| <i>S. marcescens</i> | <i>Serratia marcescens</i> |
| <i>S. pyogenes</i> | <i>Streptococcus pyogenes</i> |
| SD | Standard deviation |
| SERS | Surface-enhanced Raman scattering |
| SNR | Signal to noise ratio |
| SoHo | Substances of human origin |
| Sp. | Species |
| SSC | Side scatter |
| Ssp. | Species pluralis |
| STD | Standard |

| | |
|----------|--|
| Tab. | Table |
| PTRBR | Platelet transfusion-relevant bacteria reference strains |
| TTBI | Transfusion transmitted bacterial infection |
| TTID | Transfusion transmitted infectious diseases |
| UV (A/C) | Ultraviolet light (A/C) |
| VWbp | Von Willebrand factor binding protein |
| WHO | World Health Organisation |

Zusammenfassung

Die Transfusion von kontaminierten Thrombozyten-Konzentraten (TK) birgt aufgrund der idealen Wachstumsbedingungen für Bakterien während ihrer Lagerung das Risiko von systemischen Infektionen, welche zu einer tödlichen Sepsis führen können. Trotzdem wird die mikrobiologische Untersuchung von TK in Deutschland nur als stichprobenartige Qualitätskontrolle und zur Verlängerung der Haltbarkeit durchgeführt.

Der derzeitige Goldstandard der mikrobiologischen Qualitätsprüfung von Blutprodukten sind kulturbasierte Methoden. Hierbei werden bakterielle Kontaminationen auf der Grundlage morphologischer und metabolischer Merkmale identifiziert. Obwohl diese Methoden gut etabliert und zuverlässig sind, weisen sie spezifische Nachteile auf. Kulturbasierte Testmethoden haben, in Abhängigkeit von der Bakterienlast, bei ausreichend großen Probenvolumina eine hohe Nachweissensitivität. Diese Nachweismethode ist jedoch sehr zeitaufwändig und weist aufgrund der bevorzugten "negative-to-date" Produktfreigabe von TK deutliche Sicherheitsmängel auf. Um die Grenzen der etablierten Techniken in der Pathogendiagnostik von Blutprodukten zu überwinden, ist die Einführung von minimal-invasiven, schnellen und zuverlässigen Testmethoden entscheidend.

Im Rahmen dieser Arbeit wurde das Potenzial einer Kombination aus Raman-Spektroskopie und konfokaler Mikroskopie als kulturunabhängige, minimal-invasive Nachweismethode für bakterielle Kontaminationen in TK untersucht. Dazu wurden Raman-Spektren von TK analysiert, die mit Thrombozyten transfusionsrelevanten Bakterien Referenzstämmen (PTRBRs) kontaminiert wurden, sowie von nicht kontaminierten TK.

Es wurde eine Präprozessierung der Raman-Spektraldaten und eine multivariate Datenanalyse durchgeführt. Eine Klassifikation der Spektren in Bezug auf bakterielle Kontamination erfolgte auf Basis einer Hauptkomponentenanalyse (PCA) in Kombination mit einer linearen Diskriminanzanalyse (LDA) von Spektraldaten-Bibliotheken. Die Modelle wurden außerdem einer k-fachen Kreuzvalidierung unterzogen. Die Analysen wurden mit der Raman Analyst Software 0.2.0.0 (Leibniz-IPHT, Jena, Deutschland) durchgeführt und die Ergebnisse wurden in Konfusionstabellen zusammengefasst. Die Bestimmung der Nachweisgrenze von bakteriellen Verunreinigungen durch Raman Mikrospektroskopie zeigte, dass die Detektion in TK nur bei hoher Bakterien-Last ($>10^8$ KBE/ml) möglich war.

Die Durchflusszytometrie ermöglicht den raschen Nachweis von Mikroben, unabhängig von ihrer Kultivierbarkeit. Zusätzlich kann hierbei die quantitative Analyse der bakteriellen Belastung (Gesamtkeimzahl) erfolgen. Im Rahmen dieser Arbeit wurde ein neues Färbeprotokoll für Bakterien in TK unter Verwendung des DNA-interkalierenden Fluoreszenzfarbstoffs DRAQ5™ entwickelt. Durch eine

selektive Lyse mit Triton X-100 konnte der Großteil aller Thrombozyten in den Proben lysiert werden, um mögliche bakterielle Kontaminanten anzufärben. Vor diesem Lyseschritt wurde die Aktivierung und Aggregation der Thrombozyten mit dem Glykoprotein (GP) IIb/IIIa-Rezeptorblocker Tirofiban gehemmt, um die Effizienz der Lyse zu optimieren und ein Verklumpen der Probe im Verlauf der Probenbehandlung zu unterbinden. Zur Evaluation der Nachweisgrenze wurden die TK-Proben nach Zugabe definierter PTRBR Konzentrationen analysiert. Mittels Durchflusszytometrie war es möglich, bakterielle Kontaminationen von circa 10^3 - 10^5 KBE/ml in TK in weniger als 2 Stunden sicher nachzuweisen. Für *S. aureus* Kontaminationen in TK wurde eine speziell angepasste Nachweisstrategie entwickelt, wodurch es möglich war, Kontaminationen von 10^2 KBE/ml in weniger als 2 Stunden nachzuweisen.

In dieser Arbeit wurde eine neue Methodik für den durchflusszytometrischen Nachweis von transfusionsrelevanten Bakterien in TK entwickelt und mit dem validierten BactiFlow®-System verglichen. Die neue Anwendung bietet eine kostengünstige und herstellerunabhängige Alternative zu den derzeit genutzten durchflusszytometrischen mikrobiologischen Schnellmethoden.

Summary

Transfusion of contaminated platelet concentrates (PC) implicates the risk of systemic infections leading to fatal sepsis, due to ideal growth conditions for bacteria during storage. Despite that, microbiological testing of PC in Germany is only performed as a random quality control and for shelf-life extension.

The current gold standard of microbiological quality testing of blood products are culture-based methods. Here, bacterial contaminations are identified on the basis of morphological and metabolic characteristics. Although these methods are well established and reliable, they have specific drawbacks. Culture-based test methods have high detection sensitivity, depending on the bacterial load, when sample volumes are sufficiently large. However, this detection method is very time consuming and has significant safety deficiencies due to the preferred "negative-to-date" product release of PC. To overcome the limitations of established techniques in pathogen diagnostics of blood products, the introduction of minimally invasive, rapid and reliable testing methods is crucial.

In this thesis, the potential of a combination of Raman spectroscopy and confocal microscopy as a culture-independent, minimal-invasive detection method for bacterial contamination in PC was investigated. For this purpose, Raman spectra of PC contaminated with platelet transfusion-relevant bacteria reference strains (PTRBRs) and non-contaminated PC were analysed.

Preprocessing of Raman spectral data and multivariate data analysis were performed. Classification of spectra with respect to bacterial contamination was based on principal component analysis (PCA) combined with linear discriminant analysis (LDA) of spectral data libraries. Models were also subjected to k-fold cross-validation. Analyses were performed using Raman Analyst software 0.2.0.0 (Leibniz-IPHT, Jena, Germany) and results were summarized in confusion tables. Determination of the detection limit of bacterial contaminants by Raman microspectroscopy showed that detection in TPC was only possible at high bacterial loads ($>10^8$ CFU/ml).

Flow cytometry enables the rapid detection of microbes, regardless of their cultivability. In addition, quantitative analysis of the bacterial load (bioburden) can be performed. In this work, a new staining protocol for bacteria in PC was developed using the DNA-intercalating fluorescent dye DRAQ5™. Selective lysis with Triton X-100 allowed the majority of all platelets in the samples to be lysed to stain for possible bacterial contaminants. Prior to this lysis step, platelet activation and aggregation were inhibited with the glycoprotein (GP) IIb/IIIa receptor blocker Tirofiban to optimize lysis efficiency and prevent sample clumping during sample treatment. To evaluate the detection limit, the PC samples were analysed after addition of defined PTRBR concentrations. Using flow cytometry, it was possible to reliably detect bacterial contamination of approximately 10^3 - 10^5 CFU/ml in PC in less than 2 hours. For

S. aureus contaminations in PC, a specially adapted detection strategy was developed, making it possible to detect contamination levels of 10^2 CFU/ml in less than 2 hours.

In this thesis, a new methodology for flow cytometric detection of transfusion-relevant bacteria in PC was developed and compared with the validated BactiFlow® system. The new application offers a cost-effective and vendor-independent alternative to the currently used rapid flow cytometric microbiological methods.

1 Introduction

1.1 Bacterial contamination in platelet concentrates

Bacterial infection originating from transfusion of platelet concentrates (PC) represents one of the most important and persistent risks of transfusion in high income countries [1–4]. Reports of fatal transfusion reactions involving bacterial contaminated PC remain to be reported [5–8].

Since the introduction of nucleic acid testing (NAT), the risk of transfusion transmitted viral infections decreased below 1:1,000,000 cases [9–11], while the risk of transfusion transmitted bacterial infections (TTBI) is at least 100 times higher [12]. In particular, bacterial contaminations of PC are considered the most frequent infectious risk by transfusion and the contamination rate is estimated at approximately 100-2,000 cases per million PC [13–18]. At present, The risk of receiving a PC contaminated with bacteria is therefore considerably higher, than the risk of blood-borne viral infections post-transfusion, such as HIV, HCV and HBV [19–21].

The risk of a serious TTBI with development of a potentially fatal sepsis was evaluated by German hemovigilance data, reporting a frequency of TTBI of 1 in 94,000 PC, leading to fatal sepsis in 1 of 570,000 transfused PC between the years of 1997-2010 [22]. Similar findings were published by the American Red Cross, reporting a frequency of TTBI between 1:40,000 and 1:193,000 after PC transfusion, depending on the collecting procedure and a fatality rate of 1 in 500,000 transfused

Reasons for this are, among other factors, the specific storage conditions of PC. PC are stored shaking under constant oxygen supply providing ideal conditions for bacterial growth at 22 ± 2 °C [23] in nutrient-rich medium [24–26]. PC contain, depending on the preparation process, donor plasma and a platelet additive solution (PAS) [27,28]. Plasma is required for PASs, likely due to the glucose content, needed by platelets to maintain viability during storage [29]. Such additives in the storage solution of PC might serve as an additional energy source for some microorganisms, resulting in an enhanced growth behavior in PC [30]. The typical number of contaminating bacteria is initially very small, corresponding to 0.03-0.3 colony-forming units per ml (CFU/ml) [31], but storage conditions and composition of the storage media of PC can promote rapid growth of even very small numbers of bacteria to clinically relevant contamination levels [32]. Even a single viable bacterium can grow up to concentrations of 10^6 - 10^{10} CFU/ml within the shelf life of a PC and can cause a life-threatening bacteremia [33,34].

Preventive measures to reduce the risk of bacterial contamination of PC have been prescribed by the European Parliament and the Council in their general guidelines for the quality and safety of blood and blood components in the Directives 2002/98/EC and 2004/33/EC [35,36]. Furthermore, the “Guide to the Preparation, Use and Quality Assurance of Blood Components” issued by the European Directorate for the Quality of Medicines & HealthCare (EDQM) provides good handling practises for all blood products [37]. Notably, not all proposed measures are consistently implemented at blood establishments (BE) on a European or global level.

In Germany donor acceptance and exclusion criteria (Directive 2004/33/EC), skin disinfection procedures, aseptic blood collection and blood processing by utilization of sterile equipment, as well as leukocyte depletion (since 2000) and pre-donation sampling (since 2003) are implemented measures aimed to reduce serious adverse transfusion reactions [38].

The major source of bacterial contamination is derived from contact with the donor’s arm [39,40]. Therefore, most bacterial contamination of PC is due to contamination during blood collection by inadequate disinfection and incomplete removal of the skin core [41,42], as skin fragments with vital microbiota can enter the collection bag when a needle is inserted through the skin [43]. Multiple studies have evaluated skin disinfection in the context of blood donation and best practice donor arm disinfection techniques have led to a substantial reduction of viable bacteria on the upper layers of the skin [44]. However, sterile venipuncture cannot be guaranteed, due to inaccessibility of organisms present in the lower layers of the skin [45,46].

Another approach to reduce the risk of bacterial contamination of blood components is the disposal of the first part of the collected blood in the process of blood donation. This can prevent the contamination of blood components, caused by the introduction of skin bacteria at the time of venipuncture [47,48]. The implementation of a pre-donation sampling strategy reduced the contamination rate of PC from 0.17 % to 0.05 % with a reduction rate of 71 % at the Japanese Red Cross [49]. Ultimately, a residual risk cannot be completely ruled out [13,14,50]. Therefore, the requirements for microbiological diagnostic test sensitivity are particularly relevant and must allow a reliable estimation of the risks of microbiological contaminations in PC.

1.1.1 Current microbiological quality testing of blood products

The German Blood Working Party reduced the shelf-life of PC from 5 to 4 days in 2008 (4x 24 h, calculated from midnight on the day of collection) due to a disproportionate number of 5-day-old PC causing severe transfusion reactions [51]. To, among other things avoid supply shortages of PC, the German regulatory authority (Paul-Ehrlich-Institute, PEI) accepts the extension of PC shelf life

to 5 days after a validated, microbiological screening method was performed or a pathogen inactivation (PI) procedure was implemented [51–54].

The current gold standard of microbiological quality testing of blood products consists of culture-based screening methods and identifies bacterial contaminations by morphological and metabolic characteristics. In Europe, semi-automated blood culture systems, such as the BacT/ALERT® (bioMérieux, Nürtingen, Germany) and BacTec (Becton Dickinson, Franklin Lakes, USA) are currently the most frequently used devices by BE [55]. Both systems analyse cell growth via detection of CO₂ as a by-product of the metabolism of bacteria in the culture bottle. The release of CO₂ into the medium leads to a colorimetric (BacT/ALERT®) or fluorescent (BacTec) signal, which is continuously monitored in the process of cultivation [56].

Culture-based test methods such as the BacT/ALERT® system have been reported to detect bacteria at initial concentrations as low as 1-10 CFU/ml [57–59] and technically can detect less than 10 CFU per test bottle [60]. However, due to the usual very low initial microbial concentration in contaminated PC and the time needed for bacterial proliferation, the detection of pathogens within the first 24 h bears a risk of false-negative results due to sampling errors [31,61,62]. Notably, the required time to detection of pathogens using culture methods can take several days, especially for slow growing bacteria and low initial bacterial loads. Even very high bacterial loads of >10⁸ CFU/ml of gram-negative bacteria, such as *K. pneumoniae* or *Escherichia coli* in PC samples, require a minimum of 4 h to generate a positive alarm signal in aerobic and anaerobic culture bottles, using the BacT/ALERT® system. Similar time-to-detection results were observed with gram-positive bacteria, such as *Staphylococcus aureus* or *Bacillus spp.*, with bacterial loads of >10⁶ CFU/ml [63].

Currently PC are released using the negative-to-date release concept [64,65] and apart from shelf-life elongation, microbiological testing of PC in Germany is only performed as a routine quality control on sentinels, although the above-mentioned methods are approved for bacterial screening [52,66]. The negative-to-date release concept is problematic in particular, as cases of transfusion-related infections are most likely caused by slow-growing skin microbiota derived bacteria [67]. Although these species are generally considered as apathogenic, they can lead to considerable inflammatory responses and bear the risk of life-threatening infections in the recipient after transfusion [31].

Sampling directly after blood donation or blood processing can result in a sterile test culture due to too few or no organisms in the sample (sampling error) taken at this time point. Even if a test is

performed, the time it takes to get a final result implicates the risk of PC being released while microbiological testing is still in progress and culture-based systems may not detect bacterial contamination until PC have already been transfused [62,67]. One possibility to reduce sampling errors is the increase in sample volume. The maximum sample volume for the semi-automated culture detection methods BacTec and BacT/ALERT® is 10 ml per culture bottle (each aerobic and anaerobic culture), according to the manufacturer's specifications. Additionally, using a sample volume of 20 ml in total of a common PC (200 - 400 ml) [27], leads to a notable loss of 5-10 % of the total product volume per tested PC.

Another approach to ensure the sterility of PC are pathogen inactivation (PI) systems, which offer the possibility of reducing bacterial contaminations directly after blood processing and PC production, potentially waving or delaying the requirement for microbiological testing. The methods are mainly based on the irreversible damage to the bacterial DNA, preventing replication and survival [68].

PI technologies have the main advantage of simultaneously inactivating different pathogens including bacteria, many viruses, and parasites [55]. Furthermore, PI methods are capable of inactivating residual donor leukocytes, which protect recipients from developing transfusion-associated graft-versus-host disease [69], prevent the transmission of CMV [70] and reduce Febrile Non-Hemolytic Transfusion Reactions as well as allergic reactions [71]. Several countries implemented PI treatment for PC. In Belgium, a bill was passed in 2009, mandating nationwide PI for all PC distributed to hospitals for transfusion [72]. A similar situation is found in Switzerland, where the INTERCEPT™ system (Cerus, Concord, USA) was generally introduced in 2011, resulting in a reliable prevention of septic transfusion reactions with no reports of bacterial infections from PI-treated PC between 2011 and 2016, in contrast to 2-4 septic reactions per year before introduction of PI-treatment [73]. France introduced PI-treatment in 2017 after a five-year regional trial period. A related study in France reported that the introduction of PI-treatment had significantly reduced acute transfusion reactions in a regional BE [74].

Currently, there are three PI systems commercially available, utilizing UV in the presence or absence of a photosensitizer substrate and all three systems received the CE mark approval for treatment of platelets [55,75] (Tab. 1). Despite the benefits, there is the possibility of bacterial contaminations evading the inactivation capacity of PI systems, leading to a breakthrough of bacteria [76–78] (Tab. 1). Furthermore, biofilm-forming isolates or spores can display increased resistance towards PI [79,80]. Sterility after PI treatment is essential, otherwise the risk of residual

viable bacteria expanding to clinical-relevant concentrations during storage remains [81]. Even if a successful elimination of all bacteria was achieved, remaining pyrogenic cell wall components from gram-negative bacteria or exotoxins may constitute a threat for recipients. Therefore, PI needs to be executed as soon as possible after donation, which is cost intensive and time critical. The application of PI technology furthermore requires a complex logistic system and the establishment of a comprehensive quality assurance procedure, including proficiency testing [55].

Table 1: Overview of commercially available PI systems

| Device | Manufacturer | PI technology | Observed breakthrough |
|-------------------------------|------------------------------|--|--|
| INTERCEPT™ PI system | Cerus, Concord, USA | UVA illumination in the presence of Amotosalen [79,82] | <i>K. pneumoniae</i> and <i>B. cereus</i> [76] |
| Mirasol® PRT system | Terumo BCT, Lakewood, USA | Broad spectrum UV illumination in the presence of Riboflavin [83,84] | <i>K. pneumoniae</i> [77] |
| THERAFLEX UV-platelets system | Maco Pharma, Langen, Germany | UVC illumination and platelet bag agitation [85,86] | <i>E. coli</i> and <i>S. pyogenes</i> [78] |

To overcome the time dependency of cultural testing and the challenging logistics of PI treatment, rapid microbiological methods (RMM) are the current focus of interest for bacterial screening for PC. RMM methods comprise of flow cytometric techniques [87–91], such as the BactiFlow® system and nucleic acid testing (NAT) [92–94]. Furthermore, it is possible to detect bacterial compounds such as peptidoglycan (PGN), lipopolysaccharides (LPS) and lipoteichoic acid (LTA) by immunoassays [66]. The PGD_{prime} test (Verax Biomedical, Marlborough, USA) is one such rapid, qualitative immunoassay for the detection of aerobic and anaerobic gram-positive and gram-negative bacteria that detects the presence of bacterial antigens including LTA and LPS in PC and provides a LOD of 10⁴-10⁶ CFU/ml. This assay is approved by the FDA in the United States [95]. Transfusion of PC must occur within 4-24 h of testing. For certain PC products, testing may be performed only after prior screening by a culture method or in combination with a primary PC

culture in accordance with FDA recommendations to extend PC shelf life from 5 to 7 days in the United States [96].

In conclusion, RMM for the detection of bacterial contaminations in PC have to be performed at an adequate time point after donation, to guarantee their effectiveness. The respective RMM may be performed earliest 48 h after donation when using a nucleic acid test such as polymerase chain reaction (PCR), or earliest 72 h after donation when using a flow cytometric method, such as the BactiFlow® system, or a short-term culture method, to provide reliable detection of bacterial contaminations [19]. However, RMM are not legally required in Germany, but are only approved test methods that can be used to extend the shelf life of PC [53,97–99].

Postponing of sample withdrawal can considerably minimize the sampling error of RMMs [31]. The analytical sensitivity of late sampling rapid bacterial detection methods is lower than for culturing methods and requires a cell count of approximately 10^2 – 10^5 CFU/ml. In this regard, RMMs are best performed as close as possible before transfusion, as opposed to culturing methods and PI [100].

1.1.2 Transfusion-relevant bacteria reference strains

Microbiological contaminations of PC are caused only by a restricted spectrum of bacterial species [101,102]. Furthermore, Kuehnert *et al.* [103] observed that the majority of transfusion fatalities were associated with gram-negative organisms and PC transfusion within 3 days of storage, whereas PC associated with nonfatal transfusion complications were more often related to gram-positive organisms and PC transfusion after 5 days of storage [103]. By contrast, Reading and Brecher [104] observed, that fatalities show a tendency to be equally divided between gram-positive and gram-negative organisms [104]. Apart from this, studies by the Paul-Ehrlich-Institute (PEI, Federal Institute for Vaccines and Biomedicines, Germany) as well as several other reports have shown that not all bacteria, which were identified in blood and blood components, including established bacterial reference strains, are suitable for proficiency testing of transfusion-related bacterial detection and PI methods. This is due to the fact, that bacterial contaminants are not always able to multiply in blood components [105–109].

To decide which bacterial pathogens might pose the greatest threat to recipients of substances of human origin (SoHO) in the European Union, the European Centre for Disease Prevention and Control (ECDC) has established a priority list of bacterial pathogens most commonly transmitted by SoHO, such as blood and blood components, tissues and cells, and organs [42].

Bacterial strains were ranked into four risk tiers, based on frequency of transmission, probability of fatality, antimicrobial resistance and enhancement of the magnitude in threat of the respective

pathogen within the next five years (Fig. 1). By using this priority ranking, it is possible to focus and optimize the development of microbiological detection methods for relevant bacterial contaminants.

To validate and assess methods for microbiological testing and PI of PC in a consistent and standardized manner, a list of bacterial reference strains was compiled, consisting of representative species specifically involved in contaminations of PC. For this reason, ready-to-use, deep frozen bacterial suspensions of platelet transfusion-relevant bacteria reference strains (PTRBR) with known cell count and the ability to grow in PC have been developed at PEI (Tab. 2). PTRBR can be used for low spiking of blood components in correspondence to the potential bacterial load present after blood donation [105].

The bacteria panel includes *Staphylococcus epidermidis* (PEI-B-06), *Streptococcus pyogenes* (PEI-B-20), *Klebsiella pneumoniae* (PEI-B-08) and *Escherichia coli* (PEI-B-19), which were the first four strains, that were approved as internal controls for PTRBR by the WHO Expert Committee of Biological Standardisation [4] (Tab. 2). Afterwards the panel was enlarged with further strains, which were derived from isolates, cultured from contaminated PC. *Enterobacter cloacae* (PEI-B-P-43), *Staphylococcus aureus* (PEI-B-P-63), *Streptococcus dysgalactiae* (PEI-B-P-71) and *Streptococcus bovis* (PEI-B-P-61) were involved in non-fatal septic transfusion reactions whilst *Klebsiella pneumonia* (PEI-B-P-08) and *Serratia marcescens* (PEI-B-P-56), were implicated in fatal transfusion events [100].

| Tier | Ranking | Pathogen | (A) Probability of Transmission | (B) Severity of disease | (C) Antimicrobial resistance | (D) Threat evolution |
|------|---------|---|---------------------------------------|-------------------------------|------------------------------------|----------------------------|
| 1 | 1 | <i>S. aureus</i> | Moderately high | very high | Moderately high | Moderately High |
| | 2 | <i>β-hemolytic streptococci</i> | Moderately high | very high | Very low | Very low |
| 2 | 3 | <i>Klebsiella</i> | Moderately high | Moderately high | Moderately high | Very high |
| | 4 | <i>E. coli</i> | Moderately high | Moderately high | Moderately high | Moderately high |
| | 5 | <i>Pseudomonas spp.</i> | Moderately high | Moderately high | Moderately high | Moderately high |
| | 6 | <i>Enterobacter</i> | Moderately high | Moderately high | Moderately Low | Moderately Low |
| | 7 | <i>Yersinia spp.</i> | Moderately high | Moderately high | Very Low | Very Low |
| 3 | 8 | <i>Acinetobacter</i> | Moderately low | Moderately high | Moderately high | Moderately high |
| | 9 | <i>Staphylococcus spp. (non-aureus)</i> | Moderately high | Moderately low | Moderately high | Moderately high |
| | 10 | <i>Serratia spp.</i> | Moderately low | Moderately high | Moderately low | Moderately low |
| | 11 | <i>Clostridium</i> | Moderately low | Moderately high | very low | very low |
| 4 | 12 | <i>Enterococcus</i> | Moderately low | Moderately low | Moderately high | Moderately high |
| | 13 | <i>M. tuberculosis</i> | very low | Moderately high | Moderately low | Moderately high |
| | 14 | <i>Bacillus spp.</i> | Moderately high | very low | very low | very low |

Figure 1: Bacterial species involved in transfusion-transmitted blood and blood product infections [42] (modified)

Bacterial strains were ranked by their probability of transmission by transfusion (A), severity of disease, if transfused into the bloodstream of the patient (B), antimicrobial resistance against common antibiotics (C) and probability of threat evolution in the next 5 years (D). The values for each risk category corresponded to four possible assignment levels, with each level representing one order of magnitude higher than the previous level labelled with the following qualitative descriptors: very low, moderately low, moderately high and very high.

Table 2: Platelet Transfusion-Relevant Bacteria Reference Strains

| Bacterial strain | Reference |
|--------------------------------------|------------------|
| First WHO repository PTRBR | |
| <i>Klebsiella pneumoniae</i> | PEI-B-P-08 |
| <i>Streptococcus pyogenes</i> | PEI-B-P-20 |
| <i>Escherichia coli</i> | PEI-B-P-19 |
| <i>Staphylococcus epidermidis</i> | PEI-B-P-06 |
| Enlarged WHO Repository PTRBR | |
| <i>Staphylococcus aureus</i> | PEI-B-P-63 |
| <i>Enterobacter cloacae</i> | PEI-B-P-43 |
| <i>Pseudomonas fluorescens</i> | PEI-B-P-77 |
| <i>Serratia marcescens</i> | PEI-B-P-56 |
| <i>Morganella morganii</i> | PEI-B-P-91 |
| <i>Proteus mirabilis</i> | PEI-B-P-55 |
| <i>Bacillus cereus</i> | PEI-B-P-57 |
| <i>Bacillus thuringiensis</i> | PEI-B-P-07 |
| <i>Streptococcus dysgalactiae</i> | PEI-B-P-71 |
| <i>Streptococcus gallolyticus</i> | PEI-B-P-61 |

1.1.3 Selection of representative reference strains for the detection of bacteria in PC

In this thesis, four representative bacterial strains were selected from the PTRBR panel (Tab. 2) for the development and evaluation of new bacteria detection methods in PC: *K. pneumoniae*, *B. cereus*, *S. aureus* and *S. epidermidis*. These strains were selected on the basis of their gram staining, their growth behaviour, their frequency of transmission and the severity of a resulting transfusion transmitted infectious disease (TTID), as well as their threat potential in the future.

1.1.3.1 *S. aureus*

S. aureus are gram-positive, coagulase-positive staphylococci, a major human pathogen, causing mild to severe infections in many tissues, organs and, occasionally, deep-seated infections, which can spread through the blood stream exhibiting a significant morbidity and mortality [110–112].

The high prevalence of *S. aureus* infections is linked to the finding, that approximately 20-30 % of non-hospitalized individuals are permanently colonized with this organism and 30-60 % are intermittently colonized [113–116], implying *S. aureus* may be considered a component of the normal human skin microbiota [117].

The ability of the pathogen to cause diseases in otherwise healthy individuals is likely attributed to *S. aureus* being able to evade immune attacks by utilizing a number of strategies, resulting in a high pathogenicity of the bacterium [118,119]. More importantly, the emergence of methicillin-resistant *S. aureus* (MRSA) has resulted in serious public health concerns [120,121]. Community-acquired MRSA strains (CA-MRSA) are a special concern to clinicians and investigators, as it can cause persistent and aggressive infection that can spread systemically and provoke life-threatening complications [122].

Contaminations of PC with *S. aureus* is one of the most significant ongoing transfusion safety risk in developed countries [123] and has been involved in severe TTIDs and fatalities [50,124–127]. Even after PC were tested with semiautomated microbiological culture systems prior to transfusion, bacterial transmission of *S. aureus* was reported [128,129]. Biofilm and/or aggregate formation of *S. aureus* by direct or indirect interaction with platelets [130–133] can lead to the adhesion of bacterial cells to the PC bag surface. This results in sampling errors, due to an uneven distribution of bacteria in the PC and false-negative results of detection methods. In many cases, transfusion of *S. aureus* contaminated PC was prevented only due to visual anomalies, e.g. clot formation, lack of swirling or change in product colour [50,123,128,129]. Therefore, visual inspection of PC prior to release, issue and administration remains an important part of the routine quality control.

S. aureus was classified into risk tier 1 of transfusion-transmitted bacteria of blood and blood components [42] based on anticipated high severity of disease after transfusion, as well as a moderately high probability of transmission, antimicrobial resistance and threat evolution (Fig. 1).

1.1.3.2 *K. pneumoniae*

K. pneumoniae is a prevailing gram-negative enterobacterium. In humans, *K. pneumoniae* is present as a human commensal and opportunistic pathogen in the nasopharynx, in the intestinal tract and on the skin [134]. *Klebsiella spp.* are more commonly found to be skin contaminants, than other gram-negative organisms [135–139] and are therefore frequently detected in outbreaks at health care institutions, in particular in neonatal units [140]. Bacterial contaminations of *K. pneumoniae* in blood components, especially in PC, can cause severe sepsis and death in recipients [141,142]. Defining features of *K. pneumoniae* infections are metastatic spread, as well as their significant morbidity and mortality [143]. *Klebsiella spp.* were the most commonly reported gram-negative organisms in fatalities [142], but rarely associated with non-fatal cases of sepsis [43]. *K. pneumoniae* was responsible for 17.3 % of all PC transfusion fatalities in the United States from 1976 to 1998 [104] and fatality rates for patients with *Klebsiella* bacteraemia have ranged from 20% to 54% [144–147].

K. pneumoniae was classified into risk tier 2 of transfusion-transmitted bacteria on the ECDC list [42], as probability of transmission, severity of disease and antimicrobial resistance were determined as moderately high (Fig. 1). Threat evolution was classified as very high, as the emergence of hyper-virulent and multidrug-resistant strains of *K. pneumoniae* was determined being a considerable threat within the next 5 years.

K. pneumoniae should be therefore under special observation. *K. pneumoniae* is a known reservoir for antibiotic resistant genes, which can spread to other gram-negative bacteria and very few therapeutic options are left for patients infected with multidrug-resistant *K. pneumoniae* [148]. Recent studies have reported that several virulent and multidrug-resistant *K. pneumoniae* clones have access to a mobile pool of virulence and antimicrobial resistance genes [149–151], potentially resulting in the emergence of a multidrug-resistant, hypervirulent *K. pneumoniae* strain, causing untreatable infections in healthy individuals. Isolations of such strains have already been reported [152–154].

1.1.3.3 *S. epidermidis*

S. epidermidis is a gram-positive, coagulase-negative staphylococci and a normal inhabitant of the human skin microbiota and mucous membranes [155]. Normal human skin microbiota typically predominate TTDI caused by contaminated PC [67]. *S. epidermidis* is one of the most common contaminants that rarely causes a fatal outcome, but can contribute to serious complications, if transfused [1,25,43]. Despite *S. epidermidis* rarely causing life-threatening sepsis, failed detection of *S. epidermidis* in PC by culture systems followed by fatal transfusion reactions have been reported worldwide [7,156–160].

Compared to other bacteria, *S. epidermidis* grows only slowly in PC and growth is characterized by a lag phase of up to 48 h after spiking [161] with minimal growth after up to 3 days of storage [63].

Kou *et al.* [7] have observed, that the storage conditions of PC, for so far unknown reasons, triggers the conversion of *S. epidermidis* from a biofilm-negative into a biofilm-positive phenotype [162,163], which might be the cause of failed detection during PC screening. The pathogenicity of *S. epidermidis* can be enhanced by the PC storage conditions, as it triggers the formation of surface-attached aggregates, increasing its virulence by significantly decreasing its metabolism and growth rate, resulting in increased resistance to antibiotics and immune clearance by the infected host [164].

S. epidermidis was classified into risk tier 3 of transfusion-transmitted bacteria of blood and blood components [42], as the severity of disease, if transfused, is usually moderately low (Fig. 1). Nevertheless, probability of transmission, antimicrobial resistance and threat evolution were determined as moderately high and as one of the most common contaminants in PC, *S. epidermidis* should be under special observation.

1.1.3.4 *B. cereus*

B. cereus is a spore-forming, aerobic to facultative anaerobic, gram-positive, motile rod and a normal commensal of the human skin microbiota. Along with *S. epidermidis*, *B. cereus* is one of most commonly implicated species in bacterial contamination of PC, that may enter the PC bag during phlebotomy [1].

B. cereus produces spores rapidly under normal growing conditions [165], which makes it interesting as a reference strain for bacteria capable of sporulation. These bacteria generally represent a major problem in transfusion medicine [166], as bacterial spores are highly resistant to pathogen inactivation measures [167]. They can enter the vegetative phase after the sterilization step to proliferate in the respective product afterwards. Furthermore, spores can

enter the PC bag during blood donation, because they are not inactivated by some disinfectants, such as 70% isopropyl alcohol [168]. In a former study, spores of *B. cereus* were able to enter the vegetative phase under PC storage conditions, where they showed strong growth [169].

Contaminations of PC with *B. cereus* were reported in the past [1,170] and a breakthrough of high concentrations of *B. cereus* after PI treatment was observed with the subsequent speculation, that isolated spores in the bacterial cell population might be responsible [76].

B. cereus was classified into risk tier 4 of transfusion-transmitted bacteria of blood and blood components [42], as severity of disease, antimicrobial resistance and threat evolution were determined as very low. Nevertheless, probability of transmission was classified as moderately high, as *Bacillus* spp. are one of the most frequently isolated bacteria from contaminated PC. Furthermore, *B. cereus* is a threatening danger in PI-treated PC, as *B. cereus* is a spore-forming organism, which can survive PI treatment in its spore form and then can grow into clinically relevant concentrations of vegetative cells during the shelf life of PC.

1.2 Flow cytometry

1.2.1 Basics of flow cytometry

Flow cytometry is a common application in virology, molecular biology, cancer biology and infectious disease monitoring and is widely accepted as a mature technology, with the method becoming established in diagnostics over the past decades [171,172]. Flow cytometry is particularly interesting and versatile applicable for biological investigations, as it allows a qualitative and quantitative examination of whole cells and cellular constituents [173].

Flow cytometry is a technology, which rapidly analyses single cells or particles, which are suspended in a diluent, also known as sheath fluid. Typically, a sheath fluid, such as phosphate-buffered saline is used and is directed by air pressure into the flow chamber [173,174]. The underlying principle of flow cytometry is, that light is scattered and fluorescence emitted when light from an excitation source impinges on the moving particles. Light scattering and fluorescence are measured constantly for each individual particle passing the excitation source [175].

To perform flow cytometry measurements, cells are hydro-dynamically focused and guided via laminar flow through a confined analysis space with a scalable throughput rate. If the distance between particles in a flow chamber is, due to high particle concentration, too small during acquisition, the cytometer is unable to resolve particles as individual events. Furthermore, a coincidence occurs, if two or more non-adherent particles exit the flow nozzle in such a manner that they are resolved as a single event [173]. For this reason, the pressure of the sheath fluid against the suspended cells has to separate them to prevent coincidence and to allow each cell being acquired individually.

Each cell, which hits the laser light is analysed for visible light scatter and single or multiple fluorescence analytes [172]. The light emitted from each cell is then quantified by the optical and electronics system to collect and display data, which is interpretable by the user. Light scattering is directly related to structural and morphological cell features and fluorescence detects cells that are fluorescently labelled or have an intrinsic fluorescence property [173]. By using flow cytometry, even high counts of cells can be analysed and statistical information about large populations of cells can be obtained in a short period of time.

Cells, which do not exhibit intrinsic fluorescence can be stained by using fluorescence dyes. To perform fluorescence-based flow cytometry, cells or cellular structures are labelled specifically using a variety of different molecules, such as fluorescently conjugated antibodies, nucleic acid

binding dyes, viability dyes, ion indicator dyes or fluorescent expression proteins. The possibility of conducting highly specific fluorescence-labelling allows the measurement of a wide range of parameters in the respective investigated cells. Flow cytometry allows the investigation of the general cell properties (size, diameter, surface area, and volume), the physiological properties, integrity and vitality of cells, as well as presence, location and quantities of DNA, RNA, cytokines, surface and nuclear antigens, enzymes and proteins of the cell [174].

The point where the laser beam intersects with the stream of flowing cells is called the analysis point (Fig. 2) [176]. Two lenses, one in the forward direction along the path of the laser beam and one at a 90 °angle to the direction of the laser beam, collect the light signals emitted by each cell passing the analysis point. The scattered light hitting the photodetector of the first lens is called forward scatter light (FSC) and indicates, for example, the relative size of the cell. A so-called obscuration bar prevents the laser light from hitting the forward scatter detector itself (Fig 2).

The second lens at 90° to the direction of the laser beam (orthogonal) collects light that has been scattered from the original direction and is called side scatter light (SSC). The SSC indicates the internal complexity or granularity on the surface or in the cytoplasm of the cell and reveals (in combination with the FSC) information on the overall physical characteristics of a cell. In addition, the cell can be characterized by its intrinsic fluorescence or by specific fluorescence labelling. Detecting fluorescent light works similar to side-scatter light detection, but with the implementation of wavelength-specific mirrors and filters for each fluorescence channel [177]. After the detected light scattering and fluorescence signals are converted into electrical signals, all information is converted into a digital data format. [172].

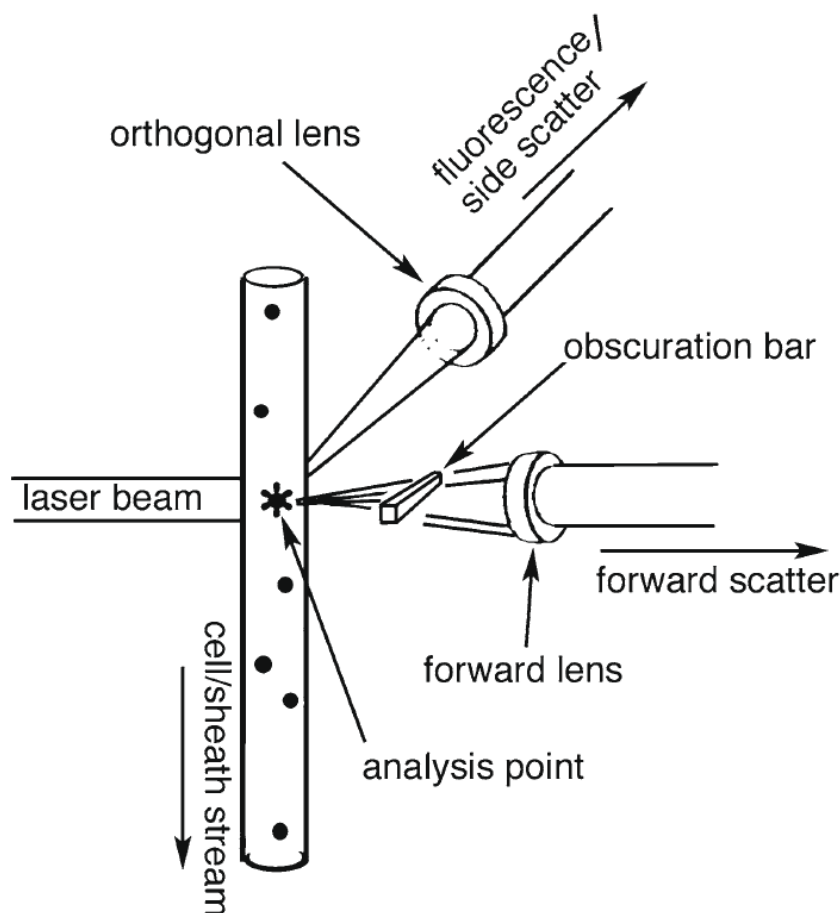


Figure 2: Scheme of the analysis point of a flow cytometer [176]

The analysis point of a flow cytometer displaying the laser beam, the sheath stream and the lenses for collection of FSC, SSC and fluorescence light.

1.2.2 The flow cytometry based BactiFlow® system

The BactiFlow® (bioMérieux, Nürtingen, Germany) is a flow cytometry device, which is detecting viable bacterial cells, based on their esterase activity. The BactiFlow® technology is well established as a routine analyses tool in the cosmetics, pharmaceutical and food manufacturing industry for real-time testing of non-filterable products [178]. Furthermore, the BactiFlow® system was accepted as a method by the German authorities to overcome the limitation of vote 38 of the German Blood Working Party to elongate the shelf life of PC from 4 to 5 days [51].

The detection method is based on a non-fluorescent fluorochrome esterase substrate, which passes through the intact membrane of viable cells and is cleaved by intracellular esterase activity, inducing the fluorescence activity of the fluorochrome. As previously reported, the protocol for the microbiological screening of PC with the BactiFlow® system combines an enzymatic digestion

with subsequent removal of the cell debris by filtration, which is intended to eliminate the background fluorescence [87].

In the process of BactiFlow® analysis the cleaved fluorochrome is excited by an argon-ion laser at 488 nm wavelength and emits light with 540 nm (FL1, green channel) and 590 nm (FL2, red channel). Labelled microorganisms exhibit a specific FL1/FL2 ratio of approximately 1.0 (range 0.8–1.2) and detected fluorescence events are specified as counts/ml [87]. This cytometric-based assay has a distinctive detection limit for routine application in transfusion facilities. Samples are defined as positive, if they exhibit more than 300 specific fluorescence counts/ml [87].

The flow cytometry-based BactiFlow® system was most frequently used by German BE [55]. Since its approval for shelf-life elongation, BactiFlow® was introduced as a routine in-process control in 3 BEs and transfusion facilities [52–54,179], but was discontinued in the year of 2017 [180]. One of the main components of the BactiFlow® assay could temporarily no longer be supplied in an adequate quality [181]. This presumably caused the malfunction of platelet lysis in the samples, resulting in the staining of platelets and obscuration of the detection results, as platelets also express an esterase activity [182]. As a consequence, an alternative flow cytometry method to the BactiFlow® system for microbiological control of PC would be worthwhile.

1.2.3 Application of flow cytometry for the detection of bacteria in PC- status quo

In the last decade, flow cytometry was already been introduced as a sterility test for PC and has proven to be a viable approach for the detection of bacteria in PC, as it can provide rapid, accurate, and quantitative information about bacterial contamination in PC.

However, with the exception of the BactiFlow® system [87], previous methods required a pre-culture step to improve sensitivity of the method, which increased time-to-detection by 1-2 h [12,88]. Without a pre-culture period, a reliable detection between 10^3 to 10^5 CFU/ml were reported [89,90]. In both studies, a pre-culture period at 37 °C was discussed as a way to increase sensitivity as well, reaching from 2-8 h [90] to 20-24 h or 24-48 h for slow-growing bacteria [89]. Sireis *et al.* [52] compared the detection of bacteria spiked and grown in pooled platelets or apheresis platelets until day 3, 4 and 5 using an in-house developed flow cytometry method, the BacT/ALERT® system, the BactiFlow® system and PCR. For three bacterial strains (*S. epidermidis*, *S. aureus*, *S. pyogenes*) analytical sensitivity was reduced, when using the in-house flow cytometry method, as CD61 positive cells (platelet antigen) were gated out to reduce the background noise, which led to the exclusion of bacteria aggregated with platelets. Taken together, previous studies showed that a rapid method based on flow cytometry can prevent the transfusion of highly

contaminated blood components, which would lead to acute septic shock or even death of the patient. However, except for the BactiFlow[®] system, all previously reported methods were highly dependent on the growth behavior of the bacteria, which meant that a time-consuming pre-culture period had to be implemented into the methods. In addition, the analytical quality and sensitivity of the detection of bacteria in PC depended heavily on the accurate detection of the fluorescence signals generated by the bacteria and clear differentiation between platelets, cell debris and bacteria, which has been a major challenge so far.

1.3 The Raman effect

When monochromatic light of a defined frequency (ω_0) impinges on a molecular system, the induced electrical dipole moment oscillates at the same frequency (ω_0) as the incident light. This elastic light scattering process without change of frequency is called Rayleigh scattering (Fig. 3 A). By stimulation of additional natural vibrations of the molecule, the induced electrical dipole moment is modulated in its frequency and the impinging light induces inelastic photon scattering processes, which lead to a shift in the emitted photon's frequency, that is called Raman scattering, named after its discoverer C.V. Raman [183]. In the process, a molecule is stimulated from an energetically lower self-state to a virtual state in the time frame of a few femtoseconds and changes to a final self-state, depending on the scattering process (Fig. 3, [184], modified). A virtual level is a non-stationary and unobservable quantum state, which is only present during the interaction between the molecule and electromagnetic radiation.

This Raman scattering effect is typically a weak process, as only a very small fraction (1 in 1×10^8) of photons are inelastically scattered to a different frequency from the incident light [184]. In the spectrum of the scattered radiation, frequencies less than the impinging frequency are referred to as Stokes scattering ($\omega_0 - \omega$) (Fig. 3 B) and those at frequencies greater than the impinging frequency as anti-Stokes scattering ($\omega_0 + \omega$) (Fig. 3 C). The anti-Stokes spectrum is symmetric to the Stokes spectrum relative to the Rayleigh scattering line. According to the Boltzmann distribution, fewer molecules are in an excited vibrational state, than in ground state at average measurement temperatures [185]. The anti-Stokes-Raman scattering therefore is less pronounced than the Stokes-Raman scattering, of which the latter is then considered for spontaneous Raman spectroscopy measurements. All of the emerging shifts in the emitted photon's frequency summarized are termed the Raman lines or bands and collectively form the Raman spectrum [183].

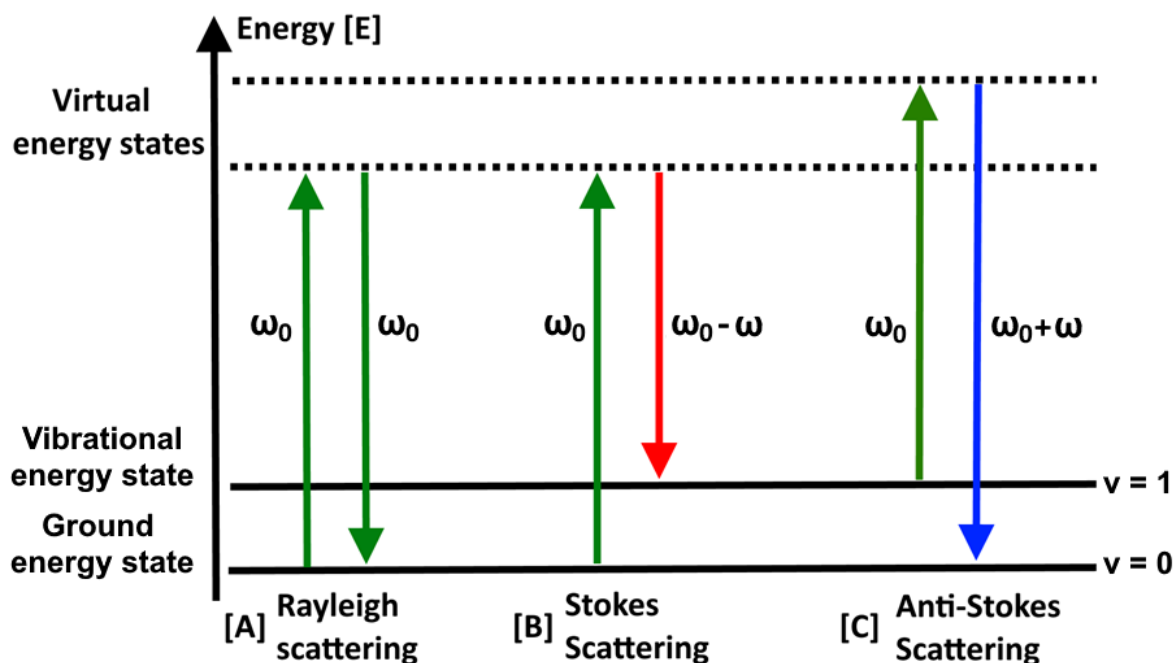


Figure 3: Jablonski diagram of Quantum Energy Transitions for Rayleigh and Raman Scattering [184], modified

ω = frequency: (unit: rad s^{-1}); $\omega = 2\pi/T$; T = period of the oscillation; E = energy; v = vibrational quantum number

During the energy transfer between the incident photons and the molecules, the amount of transferred energy corresponds to specific molecule vibrations. Raman peaks are spectrally narrow and can be associated with the vibration of a particular chemical bond or a single functional group in a molecule. Thereby it is possible to display the molecular composition of the examined sample, which makes the Raman spectroscopy a valuable method in a variety of research areas [186]. The intensity of the Raman bands depends on several factors, which have to be considered for the development of an analytical application (Fig. 4) [187].

$$I_{Stokes} \propto N * \left(\frac{\partial \alpha}{\partial q} \right)_{q_0}^2 * (\omega_0 - \omega)^4 * I_0$$

Figure 4: Dependence of the intensity in spontaneous Raman Scattering [187]

\propto : proportional to

N : number of scattering molecules

$\partial \alpha / \partial q$: Change of polarizability along the normal coordinate

ω_0 : Frequency of the incident photons

ω : Frequency of the molecular vibration

I_0 : Intensity of the incident photons

The intensity of the vibrational bands is dependent on the number of scattering molecules in the laser focus and the intensity of the incident photons, which is shown here exemplary for Stokes-Raman scattering (Fig. 4). At the same time, the intensity of the vibrational bands increases in proportion to the fourth power of the emerging frequencies through the Stokes scattering of the laser. Accordingly, a higher excitation wavelength in the near infrared range leads to a significantly lower signal. However, the energy transfer to the sample is also reduced, which in turn reduces the likelihood of phototoxic reactions, which is essential for the analysis of biological samples [187,188].

1.3.1 Raman spectroscopy of biological samples

Raman Spectroscopy allows a rapid, non-invasive and high spatial resolution acquisition of biochemical and structural information. Although the method has been primarily used for analytical chemistry applications, the use of this technique in biological studies has increased significantly as it has become a viable tool for biomedical applications and is making progress in the area of clinical evaluation.

As water is a weak Raman scatterer and only shows minimal interferences with the sample's spectra [189], Raman spectroscopy allows measurements of samples in aqueous solutions. It is therefore predestined for use *in vitro* and *ex vivo* studies of biological components and cells. Lipids, carbohydrates and proteins, as well as DNA and RNA are the main components of biological specimens and the significant regions of their Raman spectra can be divided into two areas. The low wavenumber region, also called the Raman fingerprint region, lies between the wavenumbers of 600 to 1800 cm^{-1} and exhibits a variety of sharp, localized spectral features, originating from the skeletal vibrations of organic molecules [190].

The fingerprint region is associated with, among other things, C-O-C vibrations of the glycosidic bonds and sugar rings of carbohydrates (800-1,100 cm^{-1}). The most prominent peaks in this region are associated with the secondary structure of proteins and are corresponding to the amide III (1200-1300 cm^{-1}) and amide I (1660-1670 cm^{-1}) vibrations [191]. A further prominent peak in the fingerprint region is characterized by CH_2 and CH_3 deformation vibrations, mainly originating from lipids and proteins (1440 cm^{-1}) [192].

DNA and RNA peaks are characterized by their nucleotides and sugar-phosphate backbone vibrations in this region (788, 782, 813, 1095 and 1578 cm^{-1}) [191]. The second significant Raman area of biological samples is in the so-called high wavenumber region and ranges between 2500 to 3400 cm^{-1} . This region is associated with CH , CH_2 and CH_3 stretching vibrations (2846-3010 cm^{-1}) [193], which are most prominent in lipids due to the number of CH bonds of fatty acid chains. A

so-called "silent" wavenumber region lies between the fingerprint and the high wavenumber regions, where almost no excitable biological molecules are found [190]. The example of a Raman spectrum of a biological specimen (human platelet cell), recorded in this thesis, is shown below and described with the most prominent peaks of the corresponding Raman spectrum. The intensity of the Raman scattering is plotted against the wavenumber in the spectra (Fig. 5).

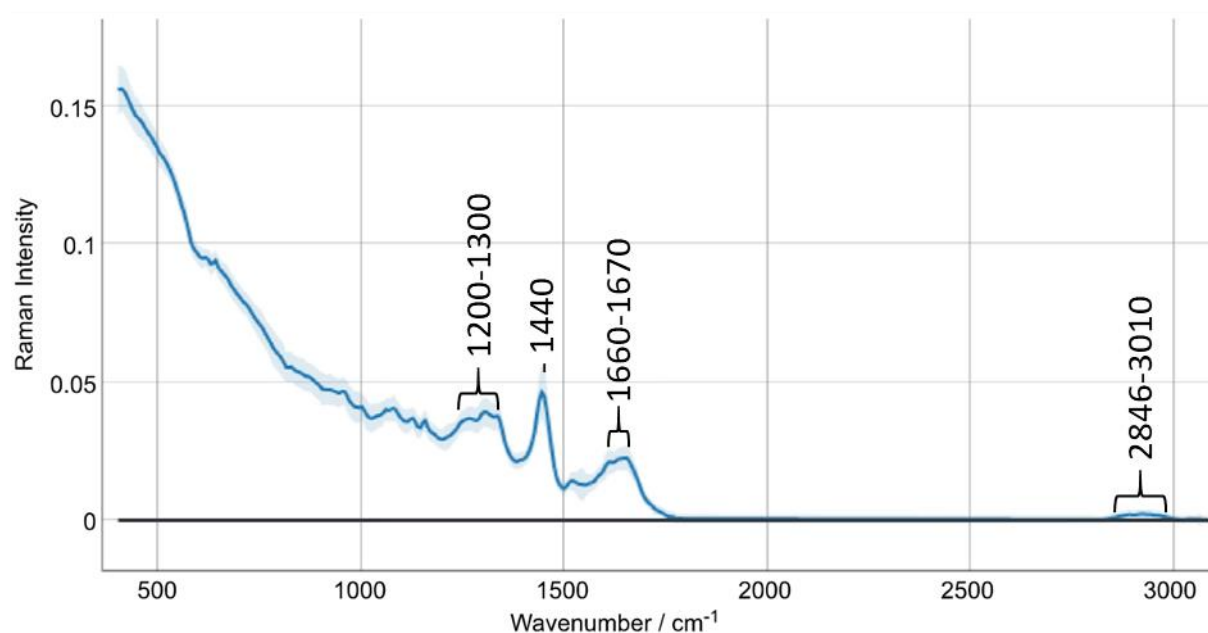


Figure 5: Raman spectrum of a human platelet; important biological peaks and regions:

1200-1300 cm^{-1} : Amide III [191]

1440 cm^{-1} : CH₂ and CH₃ deformation vibrations [192]

1660-1670 cm^{-1} : Amide I [191]

2846-3010 cm^{-1} CH, CH₂ and CH₃ stretching vibrations [193]

1.3.2 Raman microspectroscopy

The combination of optical microscopy with Raman spectroscopy is becoming more and more important for microbiological and clinical applications, as Raman microspectroscopy offers direct information about the molecular composition of biological samples. In a Raman microspectroscope, the combination of an optical microscope and a charge-coupled device (CCD) camera. The development of microspectrometers that combine the power of optical magnification and direct visualization of samples enables the generation of highly informative Raman images of biological samples with improved interpretability [194].

To obtain valuable information on biological samples, a Raman microspectroscope must meet certain characteristics. In general, biological samples consist of low scattering materials that can be damaged by the radiation. The total laser intensity (power/area) with which the sample is

illuminated, is, thus, a key factor when it comes to obtaining high quality results from biological samples. This is important to note because the laser intensity depends on the size of the laser spot (sampling area) and the magnification selected. These factors can have a large impact on the potential laser exposure time of the sample. In addition, Rayleigh scattering is much more intense than Raman scattering and can easily overwhelm the more informative signal if not filtered. Therefore, a Rayleigh filter is required for Raman spectroscopy to block the Rayleigh scattered radiation and transmit only the Raman signals [188].

1.3.3 Design of a Raman experiment

It has been shown that a large noise background in Raman measurements can result from scatterings of the sample itself, which enters the spectrometer as stray light. The optical window of biological tissues exists at longer wavelengths within the near infrared (NIR) region (700–900 nm), where the absorption of light within the tissue sample is minimal [195,196]. Therefore, NIR laser have been extensively applied in biological studies of fixed and live cells. Additionally, NIR laser have a relatively low photon energy and generally do not cause substantial photo damage to biological samples, which is crucial in order to not induce biochemical alterations in the samples and distort the spectra [197].

The choice of a fitting substrate, also known as the carrier, on which the sample is prepared and measured is crucial for the experimental design and depends on the desired experimental outputs and sample characteristics. The matrix on which a sample is supported contributes to physical stability and therefore directly affects the spectral quality, by keeping the sample in focus for the duration of the experiment. The most important properties of the substrate to consider are the spectral background signals, as well as the substrate cost, availability and composition [188].

Fused silica glass slides typically used in optical microscopy are exceptionally cost effective, but have very high background fluorescence at the wavelength of 785 nm, which is utilized in the Raman microspectroscope for this thesis (BioRam®, CellTool GmbH, Tutzing, Germany). Here, a feasible substrate can be found in Raman-grade calcium fluoride (CaF₂), which is rather expensive, but in contrast only shows minimal background interference at the respective wavelength. Furthermore, CaF₂ is biocompatible and nontoxic for cells and tissues placed on them [198].

1.4 Raman data analysis

A typical Raman study can rapidly accumulate a large and information-rich spectral data set. For this reason, multivariate data analysis can be used to investigate Raman microspectroscopy samples [199]. Since Raman spectra of biological cells exhibit all very similar Raman spectra,

special methods are in need to properly analyse the data. Analysis usually includes a pre-processing pipeline, as well as a noise or dimension-reduction step like principal component analysis (PCA) [200]. This information can then be fed into unsupervised or supervised classification tools to differentiate individual spectra, which can then identify relevant biological information.

1.4.1 Raman spectra pre-processing

Unprocessed Raman spectra typically consist of various components including the Raman signals, the background signals (e.g., from fluorescence) and noise. The background signals and the noise have to be reduced in the recorded spectra using pre-processing techniques before further analysis. The Raman signals associated with biological samples are often obscured by a broad slowly-varying background signal caused by fluorescent signals or stray light due to Mie scattering [196]. These signals can originate from a number of sources, including the sample itself, the sample substrate and the optical elements in the system that are common to both the delivery path and the collection path, especially the microscope objective [201]. Another source of background noise are cosmic rays, which are sporadic background artifacts recognized by sensitive detectors, which manifest in Raman spectra as narrow-bandwidth spikes [202]. The presence of this background can compromise the ability to extract reliable and reproducible compositional information from biological Raman spectra.

Most of the instrument software packages contain cosmic ray removal algorithms that allow the user to selectively eliminate spectral artifacts from cosmic rays, as well as algorithms in processing packages for automated cosmic ray removal [203]. The quality of the spectral data sets should be assessed, and pre-processing should be applied to improve the accuracy of the results by minimizing insignificant variability.

Raman spectra are particularly prone to noise and data may require noise reduction to enhance spectral quality by smoothing and despiking of the spectra in the course of pre-processing. Sample and background fluorescence, as well as thermal fluctuations of the CCD, can markedly affect the spectral baseline, and therefore baseline correction is necessary. Raman spectra require normalization to correct for sample and experimental variables, such as thickness and density of samples, which is especially important for biological samples as they can be subject to strong fluctuations. Biological spectral data sets can often present a significant computational burden, because of the many absorbance intensities contained in a single spectrum. By truncating the spectrum to a shorter wavenumber range, this burden can be reduced [188].

Furthermore, model overfitting is a common problem in the classification of complex datasets, encountered during the classification of spectroscopic data, due to the "large dimension - small sample size" problem [204,205]. This can lead to a high generalization error problem, when the number of predictor variables under consideration is much larger than the number of observations [206]. Dimension reduction by discarding unwanted data and therein included dimension selection via multivariate data analysis is a possibility to address this problem and plays a vital role in the performance of classification algorithms [207,208]. The Raman fingerprint region of biological samples tends to lie between the wavenumbers 600 and 1800 cm^{-1} cm [190]. In order to reduce the dimensions of Raman data of biological samples, selective scanning of the region of interest of the spectrum is a possibility, to obtain only the pertinent information, while limiting the dimension size [209].

1.4.2 Multivariate data analysis for classification

Principal component analysis (PCA) is an unsupervised learning approach that can effectively reduce Raman spectra into a defined number of principal components that account for major spectral variance [210]. This technique can be used to examine spectra using only leading principal components, to extract the key variables describing the largest variance within a data set. This makes it possible to retain only the most important spectral data, while removing background noise without requiring prior knowledge of the sample in question [211].

Classification tasks can be supported by supervised machine learning techniques. Different from unsupervised techniques, knowledge of class membership is used to train a classification model. An example for machine learning based on a linear model is linear discriminant analysis (LDA), which is widely used for the classification of Raman spectra. LDA computes linear combinations of variables, to determine directions in the spectral space, which maximize the variance between groups on a subset of the full data set. referred to as the training data set. Another independent subset of data (test data) is subsequently used for model validation. Different validation schemes may be implemented. Cross-validation may be an appropriate solution for smaller data sets, both to avoid overfitting and because resampling approaches can repeat or iterate different training and test data sets for a defined number of times, effectively using as much of the data set as possible [212].

For LDA the number of features used as input for a LDA model should be smaller than the total number of Raman spectra in the training data set, to avoid overfitting. Therefore, entire Raman spectra cannot be analysed directly, because the number of wavelength positions (features) is

usually far larger than the number of cells analysed. To reduce the dimensionality of the spectral data set, PCA is therefore executed prior to LDA

1.5 Aim of the thesis

In Germany, the current strategy for prevention of bacterial contamination in PC is limited to the restriction of PC shelf life to 4 days with a possible extension to 5 days upon microbiological testing. As a result, there is a risk of highly contaminated PCs being released without testing. The current gold standard for the detection of bacteria in PC are culture-based methods. These methods are sensitive, but entail, due to the “negative-to-date” product release concept for PC, a certain risk of TTID for patients. The aim of this thesis was to develop a culture-independent RMM (rapid microbial method), which requires no longer than 2 h time-to-detection, while being cost-effective, vendor-independent and simple in its application with an LOD of at least 10^5 CFU/ml, as required for a clinically relevant detection method [156].

To this end, Raman microspectroscopy and flow cytometry were selected as potential candidates for culture-independent RMM and were evaluated for their suitability for sensitive detection of bacterial contamination in PC.

2 Material

2.1 Bacterial strains

Table 3: PEI PTRBR strains

| Organism | Source | Reference |
|-----------------------------------|---------------------------|------------|
| <i>Bacillus cereus</i> | PEI, WHO Repository PTRBR | PEI-B-P-57 |
| <i>Bacillus thuringiensis</i> | PEI, WHO Repository PTRBR | PEI-B-P-07 |
| <i>Enterobacter cloacae</i> | PEI, WHO Repository PTRBR | PEI-B-P-43 |
| <i>Escherichia coli</i> | PEI, WHO Repository PTRBR | PEI-B-P-19 |
| <i>Klebsiella pneumoniae</i> | PEI, WHO Repository PTRBR | PEI-B-P-08 |
| <i>Morganella morganii</i> | PEI, WHO Repository PTRBR | PEI-B-P-91 |
| <i>Pseudomonas fluorescens</i> | PEI, WHO Repository PTRBR | PEI-B-P-77 |
| <i>Proteus mirabilis</i> | PEI, WHO Repository PTRBR | PEI-B-P-55 |
| <i>Staphylococcus aureus</i> | PEI, WHO Repository PTRBR | PEI-B-P-63 |
| <i>Staphylococcus epidermidis</i> | PEI, WHO Repository PTRBR | PEI-B-P-06 |
| <i>Serratia marcescens</i> | PEI, WHO Repository PTRBR | PEI-B-P-56 |
| <i>Streptococcus pyogenes</i> | PEI, WHO Repository PTRBR | PEI-B-P-20 |

2.2 Culture media and stock solutions

All chemicals and solvents were obtained from HLS GmbH (Übach-Palenberg, Germany), Sigma Aldrich (Darmstadt, Germany), bioMérieux (Nürtingen, Germany), Merck Millipore (Darmstadt, Germany) and Thermo-Scientific (Karlsruhe, Germany), unless otherwise specified.

Table 4: Culture medium

| Description | Manufacturer |
|---|--|
| BacT/ALERT® SA (standard aerobic) culture bottle | bioMérieux, Nürtingen, Germany |
| BacT/ALERT® SN (standard anaerobic) culture bottle | bioMérieux, Nürtingen, Germany |
| Caso-Bouillon EP+USP | Merck Millipore, Darmstadt, Germany |
| Standard Nutrient Agar I (STD-I) plates | Solution laboratory PEI (recipe see appendix Tab. 30) |

Table 5: General Solutions

| Description | Manufacturer |
|---|---|
| 0.85 % NaCl | PEI inhouse production (recipe see appendix Tab. 27) |
| BD FACS™ Clean | Becton Dickinson, Franklin Lakes, USA |
| BD FACS™ Rinse | Becton Dickinson, Franklin Lakes, USA |
| H ₂ O dest. | PEI inhouse production |
| Phosphate buffered saline (PBS) without Ca and Mg pH 7.1 | PEI inhouse production (recipe see appendix Tab. 28) |
| Phosphate buffered saline (PBS) without Ca and Mg pH 7.1, + 1mM EDTA | PEI inhouse production (recipe see appendix Tab. 29) |

Table 6: BactiFlow® Solutions and reagents

| Name | Manufacturer | Application |
|-------------|------------------------------------|--|
| Buffer 1B | HLS GmbH, Übach-Palenberg, Germany | Labelling buffer |
| Buffer 2C | HLS GmbH, Übach-Palenberg, Germany | Counterstain |
| Buffer 2D | HLS GmbH, Übach-Palenberg, Germany | Reducing agent |
| Buffer 3A | HLS GmbH, Übach-Palenberg, Germany | Dissolution buffer |
| Buffer E2 | HLS GmbH, Übach-Palenberg, Germany | Staining substrate |
| Chemsol M1 | bioMérieux, Nürtingen, Germany | Enzymatic digestion reagent |
| Chemsol M2 | bioMérieux, Nürtingen, Germany | Enzymatic digestion reagent |
| ChemSol M3 | bioMérieux, Nürtingen, Germany | Enzymatic digestion reagent |
| Cleaning 10 | HLS GmbH, Übach-Palenberg, Germany | Cleaning solution |
| Diluent M | bioMérieux, Nürtingen, Germany | Dissolution buffer for enzymatic digestion |
| Rinsing 25 | HLS GmbH, Übach-Palenberg, Germany | System solution |
| Standard C | HLS GmbH, Übach-Palenberg, Germany | Measuring cell calibration standard |
| Standard G | HLS GmbH, Übach-Palenberg, Germany | Daily calibration standard |

Table 7: general reagents and chemicals

| Description | Manufacturer |
|--|--|
| Acetaminophen (USP reference standard) | Sigma-Aldrich, Darmstadt, Germany |
| DRAQ5™ (5 mM) | Thermo Scientific, Karlsruhe, Germany |
| Ethanol | PEI inhouse storage |
| Isopropanol | PEI inhouse storage |
| Protein detachment solution Tergazym | Sigma-Aldrich, Darmstadt, Germany |
| Tirofiban (> 98.5 %, HPLC) | Sigma-Aldrich, Darmstadt, Germany |

2.3 Consumables and devices

All consumables were purchased from Eppendorf (Hamburg, Germany), Greiner Bio one GmbH (Frickenhausen, Germany) and Sarstedt (Nümbrecht, Germany), if not specified otherwise.

Table 8: General consumables and blood products

| Description | Manufacturer |
|---|--|
| CaF ₂ microscope slides (Raman grade [VUV]) 1 mm x 76 mm x 26 mm (+/- 0.1 mm) | Crystal GmbH, Berlin, Germany |
| CaF ₂ microscope slides (Raman grade [VUV]) 1 mm x 75 mm x 25 mm (+/- 0.1 mm) | Crystal GmbH, Berlin, Germany |
| Chemfilter 25 | HLS GmbH, Übach-Palenberg, Germany |
| Corning Falcon with cell sieve | Thermo-Fisher Scientific, Karlsruhe, Germany |
| Disposable sample tubes and syringes for Eddy Eddy Jet 2W | I&L Biosystems GmbH, Königswinter, Germany |
| Eppendorf tubes (1,5 ml, 2ml) | Sarstedt; Nümbrecht, Germany |
| Expired and fresh platelet concentrates (PC) | DRK-Blutspendedienst, Baden-Württemberg/Hessen gemeinnützige GmbH, Germany |
| Falcon tubes (15 ml, 50 ml) | Greiner Bio-one GmbH, Frickenhausen, Germany |
| Pipette tips | Starlab GmbH, Hamburg, Germany |
| Flexiperm micro 12 silicone attachment | Sigma-Aldrich, Darmstadt, Germany |

| | |
|--|---------------------------------------|
| In Line Filter | HLS GmbH, Übach-Palenberg, Germany |
| Parafilm | Bemis, Neenah, USA |
| PC transfer bags (with luer connection) | Baxter Fenwal, Deerfield, USA |
| Precision wipes | Carl Roth, Karlsruhe, Germany |
| Si ₂ Standard (monocrystalline) | CellTool GmbH, Tutzing, Germany |
| Sterile platelet storage bags (450 ml) | Macopharma, Langen, Germany |
| Tube caps (20 ml) | Sarstedt, Nümbrecht, Germany |
| Tubes (20 ml) | Sarstedt, Nümbrecht, Germany |
| Tubes (3 ml) | Sarstedt, Nümbrecht, Germany |

Table 9: Devices

| Description | Manufacturer |
|--------------------------------|--|
| BactiFlow® | bioMérieux, Nürtingen, Germany |
| BD LSRFortessa™ flow cytometer | Becton Dickinson, Franklin Lakes, USA |
| Centrifuge 5418 | Eppendorf, Hamburg, Germany |
| Centrifuge 5424 R | Eppendorf, Hamburg, Germany |
| Centrifuge 5427 R | Eppendorf, Hamburg, Germany |
| Centrifuge 5810 R | Eppendorf, Hamburg, Germany |
| Centrifuge Multifuge X3R | Heraeus, Hanau, Germany |
| Fisherbrand cell density meter | FisherScientific, Karlsruhe, Germany |

| | |
|---|--|
| Flow bench Safe2020 | FisherScientific, Karlsruhe, Germany |
| Horizontal shaking device for PC (TI-0) | Sarstedt, Nümbrecht, Germany |
| IBS Fireboy Plus | Integra Biosciences, Zizers, Switzerland |
| Ice machine | Ziegra, Isernhagen, Germany |
| Incubator Galaxy 170 | Eppendorf, Hamburg, Germany |
| Incubator Heracell 150i | FisherScientific, Karlsruhe, Germany |
| Incubator shaker Innova® 44 | Eppendorf, Hamburg, Germany |
| Kelvitron®+ | Heraeus, Hanau, Germany |
| Pipette set Research Plus | Eppendorf, Hamburg, Germany |
| Plate reader SphereFlash® | I&L Biosystems GmbH, Königswinter, Germany |
| Precision scale | Sartorius, Göttingen, Germany |
| Raman microspectroscope BioRam® | CellTool GmbH, Tutzing, Germany |
| Scale PCB 3500-2 | Kern, Balingen-Frommern, Germany |
| Spiral plater Eddy Jet 2W | I&L Biosystems GmbH, Königswinter, Germany |
| Thermo block for BactiFlow® | DITABIS AG - Digital Biomedical Imaging Systems AG, Pforzheim, Germany |
| Thermo block shaker PCMT | Grant Instruments, Cambridge, UK |
| Thermomixer 5436 | Eppendorf, Hamburg, Germany |

| | |
|---------------------|--------------------------------|
| Thermomixer Comfort | Eppendorf, Hamburg, Germany |
| Thermomixer Compact | Eppendorf, Hamburg, Germany |
| Tube welder TSCD-II | Terumo BCT, Lakewood, USA |
| Vortexer | neoLab, Heidelberg, Germany |
| Vortexer Vornado | Cole-Parmer, Wertheim, Germany |

Table 10: Software

| Description | Manufacturer |
|---|---------------------------------------|
| GraphPad PRISM 8 | GraphPad Software Inc, San-Diego, USA |
| Kaluza flow cytometry analysis software version 2.1.1 | Beckman Coulter, Brea, USA |
| Raman Analyst Software version 0.2.0.0 | Leibniz-IPHT, Jena, Germany |

3 Methods

3.1 Procurement and handling of PC

3.1.1 PC transfusion bags

PC consisted of leukocyte-depleted, pooled human platelets derived from four buffy coat bags, resuspended in 220-400 ml Platelet-Additive-Solution (PAS) and CPD-plasma (0.1 L/L). One transfusion bag of PC contained $2-4.5 \times 10^{11}$ platelets. Fresh or expired PC were purchased from DRK Süd (Deutsches Rotes Kreuz e.V. Frankfurt, Germany). The PC obtained for research purposes were either used after expiration (day 5-7 of shelf life) or fresh (day 4 of shelf life), when expired bags weren't available. Platelet bags were inspected visually for clumping, turbidity and change in colour before storage and use, and were additionally tested for sterility using the Bact/ALERT® 3D-System (chapter 3.1.4).

3.1.2 Storage of PC

All obtained and prepared PC were stored at 22 ± 2 °C under constant agitation in their gas-permeable bags, by using a horizontal shaking device for PC (Sarstedt, Nümbrecht, Germany).

3.1.3 Welding of Luer-connection with sterile bag joint for PC sample collection

PC storage bags or empty storage bags for sample splitting (Macopharma, Langen, Germany) and transfer bags (Baxter Fenwal, Deerfield, USA) were connected aseptically by using a tubing welder (Terumo BCT, Lakewood, USA).

3.1.4 Base sterility test of PC using the BacT/ALERT® 3D automated culturing method

Every PC obtained from the DRK Süd (Deutsches Rotes Kreuz e.V. Frankfurt, Germany) was tested for base sterility using the BacT/ALERT® 3D (bioMérieux, Nürtingen Germany) automatic liquid culture system.

The BacT/ALERT® (bioMérieux, Nürtingen Germany) is an FDA-approved system for the detection of bacterial contamination in PC and relies on the detection of CO₂ production resulting from the growth of bacteria. For base sterility testing samples were processed under sterile conditions in a laminar air flow bench. Two 10 ml samples of PC were removed from the transfusion bag over the welded luer connection, using 10 ml syringes. The samples were injected into a BacT/ALERT® aerobic and an anaerobic culture bottle (bioMérieux, Nürtingen Germany). The bottles were incubated and constantly monitored for microbial growth in the BacT/ALERT® 3D system at 32.5 °C for up to 14 days or until CO₂ sensors of the system indicated the presence of microbial

contaminants. In the case of a positive signal, the respective bottle was removed from the system. A sample was drawn from the bottle and was used to inoculate three standard I agar plates (Tab. 30, chapter 7.1) with 1 ml of sample each, to test for microbial growth at aerobic and anaerobic conditions at 37 °C. Positive results led to the disposal of the respective PC. If no bacteria could be detected, the respective bottle was marked as false positive.

3.2 Sample preparations for PC spiked with bacterial strains

3.2.1 Bacterial reference strains for PC spiking

Bacterial reference strains from the WHO international repository for platelet transfusion-relevant bacteria [100] were provided by PEI (chapter 1.1.2, Tab. 2) as cryopreserved stocks with a defined CFU/ml, stored in a 20 % Albumin solution. Stocks were made from bacterial strains, harvested during their logarithmic growth phase and frozen using a validated procedure to ensure defined counts of viable cells [4].

3.2.2 Preparation of cryopreserved bacterial strains

cryopreserved stocks of all reference strains were tested for stability of viable cell counts and batch consistency at PEI every 3-4 months for up to 3 years [100]. A cryo-vial of the respective bacterial species (chapter 1.1.2, Tab. 2) was thawed and vortexed for 10 s before use. The exact bacterial count (CFU/ml) was given per batch and strain used. Depending on the required working concentration, dilution series of the respective bacterial strain (Falcon tubes with 9 ml cold saline, NaCl 0.85%, 4 °C) in log-dilution steps was prepared, to obtain working concentrations for spiking and growth experiments.

3.2.3 Cultivation of bacteria for PC spiking

B. cereus and *B. thuringiensis* were provided by PEI as spore-enriched solution (chapter 1.1.2, Tab. 2) and had to be cultivated into their vegetative cell form, before use. The cryo-vials were prepared, according to the PEI protocol for spore-forming bacteria, derived from [213]. Furthermore, *S. aureus*, *S. epidermidis* and *K. pneumoniae* were cultivated from cryovials, for the comparative experiments with the BactiFlow® system (chapter 4.2.5.2, chapter 4.3, chapter 4.4).

One cryo-vial of the respective bacterial species was thawed in the incubator (37 °C) for 10 min, vortexed for 10 s and afterwards cultivated in 45 ml sterile CASO-Bouillon (Merck Millipore, Darmstadt, Germany) over night at 37 °C and 120 rpm. The following day, the optical density (OD₆₀₀) of the culture was measured using a photometer (Thermo Fisher Scientific, Karlsruhe, Germany). A new culture with 45 ml of CASO-Bouillon was inoculated with the overnight culture

at $OD_{600} = 0.1$ and was incubated at 37 °C and 120 rpm until the exponential phase of the bacterial strain ($OD_{600} = 0.5-0.8$) was reached.

Afterwards bacteria were harvested by centrifugation for 10 min at 6000 rpm and the cell pellet was resuspended in 25 ml PBS + 1 mM EDTA pH=7.1. Plating of the bacterial solution on agar plates was used for evaluation of the bacterial concentration corresponding to $OD_{600}=0.5$. For *B. cereus* $OD_{600}=0.5$ corresponded to 2.19×10^7 CFU/ml. For *B. thuringiensis* $OD_{600}=0.5$ corresponded to 1.27×10^7 CFU/ml. For *S. aureus* $OD_{600}=0.5$ corresponded to 3.45×10^7 CFU/ml. For *K. pneumoniae* $OD_{600}=0.5$ corresponded to 1.24×10^8 CFU/ml. For *S. epidermidis* $OD_{600}=0.5$ corresponded to 7.95×10^6 CFU/ml. The respective culture was diluted with PBS + 1 mM EDTA pH= 7.1 to obtain working concentrations of 1×10^6 CFU/ml - 1×10^7 CFU/ml.

3.2.4 Spiking of PC with defined contamination levels of bacteria

Bacterial working solutions with defined concentrations of 10^2 , 10^3 , 10^4 , 10^5 and 10^6 CFU/ml were generated as described in chapter 3.2.2.

For the spiking procedure, 5 ml of PC were extracted out of the transfusion bag with a 5-ml syringe. These 5 ml were retained in the sterile syringe, while with a second sterile 20- or 50-ml syringe the required amount of PC was taken from the bag for the respective experiments. The obtained PC was split into 900 μ l aliquots and filled into sterile reaction tubes. The 5 ml of PC were injected back into the bag to flush the withdrawal tube. Depending on the experimental layout, the 900 μ l PC samples were inoculated with 100 μ l of the respective bacterial working solution, to achieve the desired contamination level in each sample. Furthermore, non-contaminated PC (negative controls) were spiked with the same amount of sterile saline, to create a full sample set per PC bag used (Tab. 11). All samples were analysed directly after spiking with either the new flow cytometry method (chapter 3.6) or the BactiFlow® system (chapter 3.7).

Table 11: Layout for BactiFlow® and Flow cytometry analysis experiments

| Tube | Sample |
|------|---|
| 1 | PC (non-contaminated) |
| 2 | PC (contaminated with 10^5 CFU/ml bacteria) |
| 3 | PC (contaminated with 10^4 CFU/ml bacteria) |
| 4 | PC (contaminated with 10^3 CFU/ml bacteria) |
| 5 | PC (contaminated with 10^2 CFU/ml bacteria) |

3.2.5 Enumeration of bacteria

Bacterial solutions and bacteria spiked or grown in PC samples were verified by preparing a dilution series (in NaCl 0.85%, 4 °C). The dilution series were plated out in triplicate on Standard I Nutrient Agar (Merck Millipore, Darmstadt, Germany) using the Eddy Jet 2W spiral plater (I&L Biosystems GmbH, Königswinter, Germany). Plates were incubated at 37 °C or 30 °C, depending on the respective organism and counted using the SphereFlash® automatic colony counter (I&L Biosystems GmbH, Königswinter, Germany).

3.3 Sample preparation for bacterial growth assays in PC

3.3.1 Transfer and splitting of PC into storage bags

A setup of a Raman or a flow cytometry growth experiment consisted of two 50 ml PC samples, which were transferred from the transfusion bag obtained from DRK Süd into small sterile, oxygen-permeable storage bags (Macopharma, Langen, Germany). 2 sterile 50-ml syringes were used to withdraw 50 ml of PC out of the transfusion bag to transfer PC into the respective storage bags. The residual volume of PC in the transfusion bag was stored until the final negative or positive result of the BacT/ALERT® 3D system was available.

3.3.2 Preparation of the spiking solution for bacterial growth assays in PC

A dilution series of the respective bacterial spiking solution (in NaCl 0.85 %, 4 °C) was prepared, to obtain a working concentration of 2-5 CFU/ml for bacterial growth experiments in PC. Bacteria were cultivated as described in chapter 3.2.3.

Every dilution was thoroughly vortexed for 10 s, prior to each dilution step. 100 µl of each dilution was plated on Standard I agar, using the spiral plater Eddy Jet 2W (I&L Biosystems GmbH, Königswinter, Germany) in log mode 100 in triplicates per dilution step, to verify the concentration of the inoculum.

3.3.3 Spiking of PC bags for bacterial growth assays

The small sterile storage bags containing 50 ml PC were spiked with 2-5 CFUs (corresponding to a low initial contamination between 0.03-0.3 CFU/ml) of *K. pneumoniae* (PEI-B-P-08), *B. cereus* (PEI-B-P-57) or *S. epidermidis* (PEI-B-P-06) per bag, respectively. For this, 5 ml of PC were taken out of each storage bag with a 5-ml syringe and were stored. With a 1 ml syringe, 1 ml of bacterial working stock solution (2-5 CFU/ml) was injected into one of the bags. The other bag was injected with 1 ml of sterile Saline (NaCl 0.85%) to act as negative control. The retained 5 ml of PC were injected back into the respective bags to flush the withdrawal tube. The bags were thoroughly mixed for 20 s and were then incubated at 22.4 °C on a horizontal shaker.

3.3.4 Sample collection of bacterial growth assays in PC

Before sample collection, the platelet storage bags were mixed thoroughly for 20 s. 5 ml of PC were taken out with a 5-ml syringe of the respective bag and were stored. With a second syringe the required amount of sample was collected and the initially removed 5 ml of PC were injected back into the bag to flush the withdrawal tube. After use the PC bags were immediately transferred to the horizontal shaker again, to minimize inequalities in bacterial growth. At the selected time-points, aliquots of 1 ml of non-contaminated or spiked PC (chapter 3.3.5, chapter 4.4) were analysed using Raman microspectroscopy (chapter 3.4) or the new flow cytometry method (chapter 3.6) and the BactiFlow[®] system (chapter 3.7). For each chosen time point a dilution series was plated out in triplicate on Standard I Nutrient Agar (Merck Millipore, Darmstadt, Germany) (chapter 3.2.5).

3.3.5 Evaluation of growth of *K. pneumoniae* in PC for Raman microspectroscopy measurements

Growth kinetics of *K. pneumoniae* in PC were analysed (Fig. 6) by spiking 2-5 CFU into a 50 ml storage bags (see chapter 3.3.3). The first time point was taken directly after inoculation of the platelet storage bag as a baseline reference (t=0). The next time point was collected during exponential phase of the bacterial culture at an approximate bacterial concentration of 10³ CFU/ml after 14 h of incubation. The next time point was chosen around a 10 log higher CFU/ml than the previous one. Bacterial growth in PC was evaluated, as described above (chapter 3.2.5).

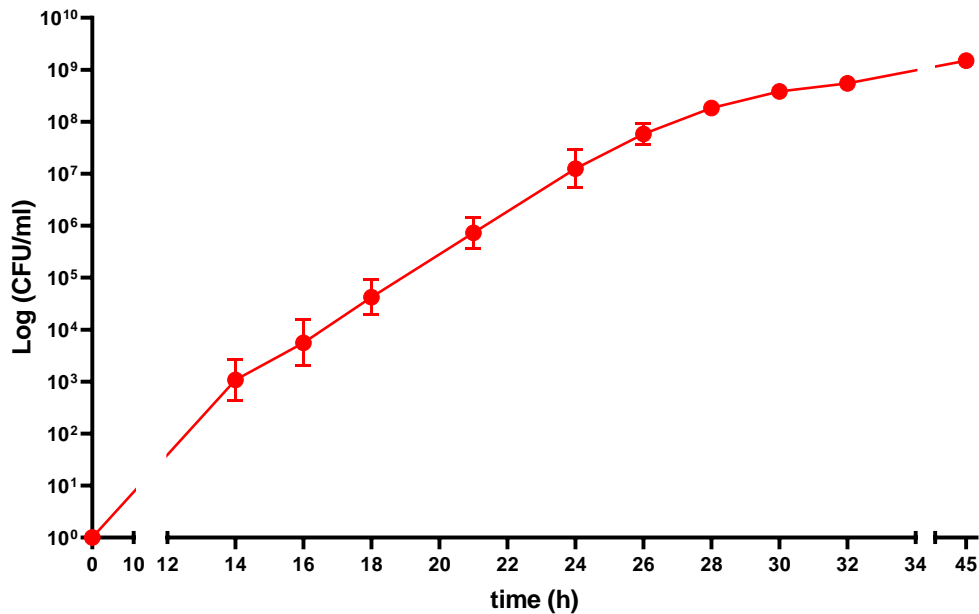


Figure 6: Growth curve of *K. pneumoniae* in PC at 20 °C (log₁₀)

Samples of contaminated PC were taken 14, 16, 18, 22, 24, 26, 28, 30, 32 and 45 h after spiking to measure the bacterial growth inside the PC bag. At each time point, a sample of 1 ml was collected from the bag and samples were diluted and plated in triplicates on Standard I Nutrient Agar plates for colony counting. (Mean CFU/ml \pm 1 SD; n = 3).

3.4 Detection of bacteria in PC using Raman microspectroscopy

3.4.1 Preparation of Calcium fluoride (CaF₂) microscopy slides

Preparation of CaF₂ microscopy slides was always performed under sterile conditions. flexiPERM[®] (Sigma-Aldrich, Darmstadt, Germany) are re-usable silicone attachments here used for liquid sample separation on the microscopy slides. flexiPERM[®] silicone attachments were stored in containers with 70 % EtOH, dried before use, placed on the CaF₂ slide and softly pressed on it for attachment. Slides and silicone attachments for contaminated and non-contaminated samples were stored separately to avoid the contamination of negative reference samples with bacterial components.

3.4.2 Raman measurements using the BioRam[®] Raman microspectroscope

After the start of the setup software, the laser, microscope, camera and Raman spectrometer of the device were started. Laser voltage was set in default to 80 mW. The device was started 30 min before the first Raman measurements, to heat up the internal laser and ensure its reliable functionality.

3.4.3 Calibration measurements for Raman spectra

To create a calibration data set, a tiny amount of Raman-grade pure Acetaminophen (Sigma-Aldrich, Darmstadt, Germany) was transferred to a sterile CaF₂ slide. The object stage was navigated using the 4x magnification objective and switched to 60x magnification (NA = 1.0) to focus on a planar Acetaminophen crystal structure to start measurements with the BioRam[®] software. For the measurement of the Acetaminophen standard, a recording time of 10 s and 1 accumulation was selected. A grid of 50 measurement points was generated using the navigation software followed by Raman measurement.

To test the stability of the Raman intensity signal, a thin slice of monocrystalline Silicon (Si₂) was added to a Borosilicate microscopy slide. The sample was navigated using the 4x magnification objective, then switched to 60x magnification (NA = 1.0) magnification to focus in close proximity to the Si₂ slide around z= 40.6. A single measurement with a recording time of 10 s and 3 accumulations was performed. The stability of the Raman intensity signal was approved, when the intensity of the signal showed at least a value above 100,000 (arb. u. = arbitrary units). To calibrate day dependent differences of the Raman microspectroscope, daily sets of standard spectra of Acetaminophen and Si₂ were acquired.

3.4.4 Raman measurements of PC samples

Samples of prepared PC (chapter 3.3.4) were vortexed for 10 s and triplicates of 200 µl per time point (chapter 3.3.5) were transferred to flexiPERM[®] attachments on CaF₂ slides.

60x (NA = 1.0) magnification was used to focus on sedimented platelets. Measurements were taken near the CaF₂ slides surface around z= 40.6. 30 spectra (10 per triplicate) with a recording time of 10 s and 3 accumulations for each condition and time point were acquired.

Measurements of contaminated samples were performed first to prevent a further growth of bacteria in the samples. Non-contaminated PC samples were collected and prepared only after measurements of contaminated samples were executed. With this method, the time of samples on the CaF₂ plate was kept constant to prevent further activation of platelets.

3.5 Analysis of Raman spectra

3.5.1 Structuring Raman data for reading into the software

Spectral analysis was executed using the Raman Analyst Software version 0.2.0.0 (Leibniz-IPHT; Jena, Germany). Raman data was exported as .csv file, using the export manager function of the BioRam® software and was reorganized in a given data folder structure, in order to read them into the program. Data was structured based on metadata (date, bacterial strain, ID of experiment, status of contamination) both for test and training data sets (Fig. 7).

A “parameters” folder (1) was created, in which all relevant parameters for pre-processing were saved as a .txt file (chapter 7.8, Fig. 65). These were imported into the program before each data analysis to ensure constant analysis. A Raman data set folder (2) was created, in which all measurement spectra were collected.

The data was displayed either as test data set (3) or training data set (7). Data sets consisted of all Raman spectra of a defined measurement time point and were sorted and summarized by respective bacterial count of the spiked PC sample (chapter 3.5.3, Tab. 12). Data sets were split manually into k subsets, resulting in k-1 training data sets and one test data set for k-fold cross validation (chapter 3.5.3). Each test and training data subset consisted of 30 Raman spectra of a single measurement time point of a contaminated PC sample (4) and 30 Raman spectra of a non-contaminated PC negative control from a single experiment (5), as well as an associated Acetaminophen calibration spectrum (6). All data was saved as .csv files in the respective parent folder and were imported into the software as .zip files.

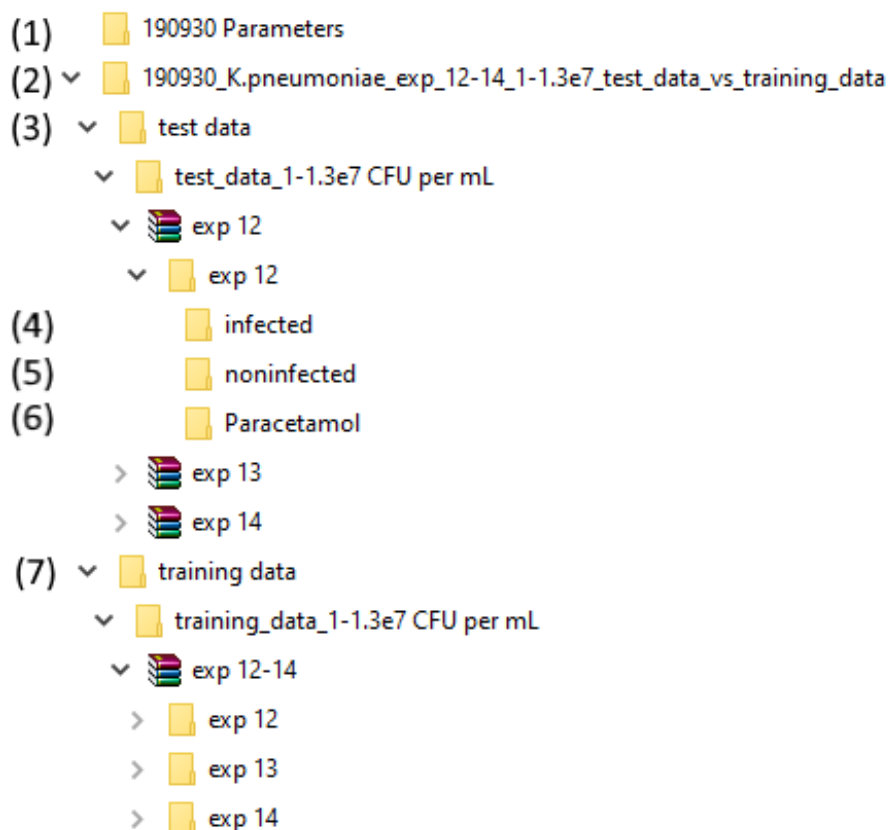


Figure 7: Data structure of Raman measurements

Parameters (1); Total data set folder with ID (2); Test data set (3); Raman spectra of infected PC (4); Raman spectra of noninfected PC (5); Acetaminophen reference spectrum (6); Training data set (7)

3.5.2 Pre-processing of raw spectra with the Raman Analyst Software

Raman raw data was analysed using the Raman Analyst Software version 0.2.0.0 (Leibniz-IPHT; Jena, Germany) with a given data pre-processing pipeline (Fig. 8-14). The parameters and calculation models of the pre-processing pipeline were set in the parameters folder (chapter 7.8, Fig. 65) of each Raman data-set, to ensure the comparability of each processed data-set. After the start of the pre-processing pipeline, the software gave out a report for every processed data-set in the form of an XPS-Document (.xps). A mean spectrum of all measured spectra prior pre-processing was displayed (Fig. 8), allowing for plotting of stratified spectra with respect to pre-assigned classes: “infected” (contaminated) and “non-infected” (non-contaminated) (Fig. 9). Pre-processing of the whole raw spectra data started by despiking of spectra, in order to remove the cosmic spike background (Fig. 10). After despiking, the wavenumber axis was calibrated, using the prominent peaks of the respective Acetaminophen reference spectrum data set (Fig. 11) and background was corrected, using a baseline-correction algorithm (Fig. 12). In the final step, data

was normalized, using vector normalization (Fig. 13). After completion of the data pre-processing, the data sets were ready to be used for further data analysis (Fig. 14).

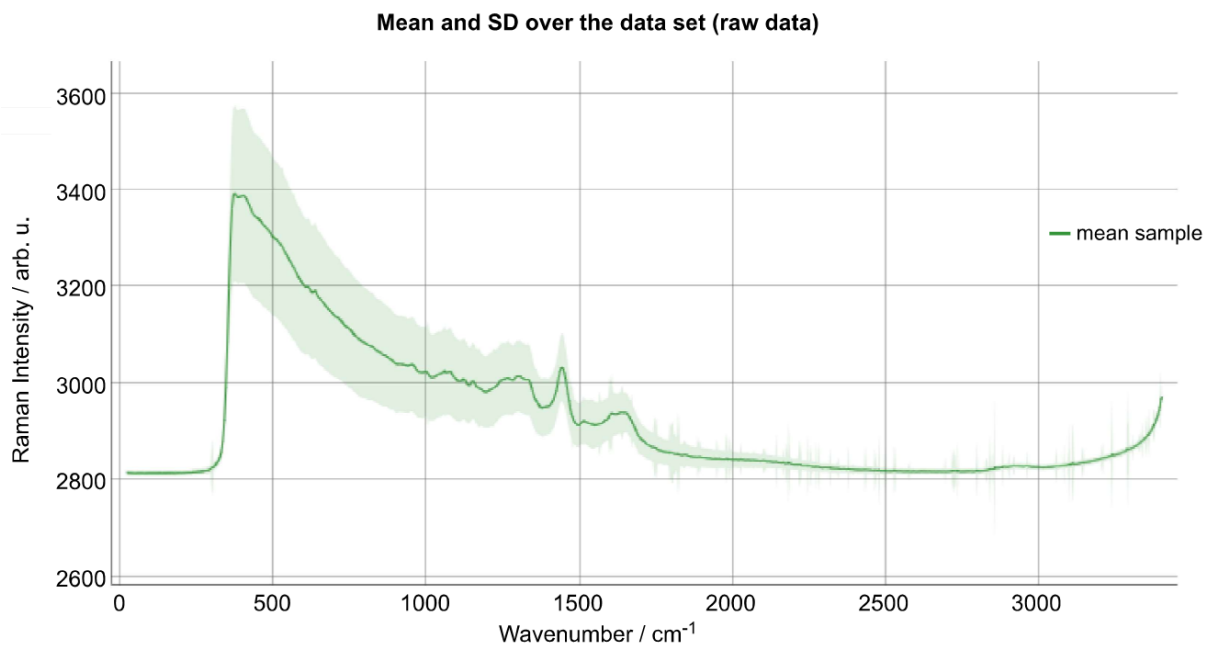


Figure 8: Mean plot of all sample spectra of the data set

Mean spectrum of all measured spectra prior pre-processing. x-axis: Wavenumber (cm^{-1}), y-axis: Raman intensity (arb. u.).

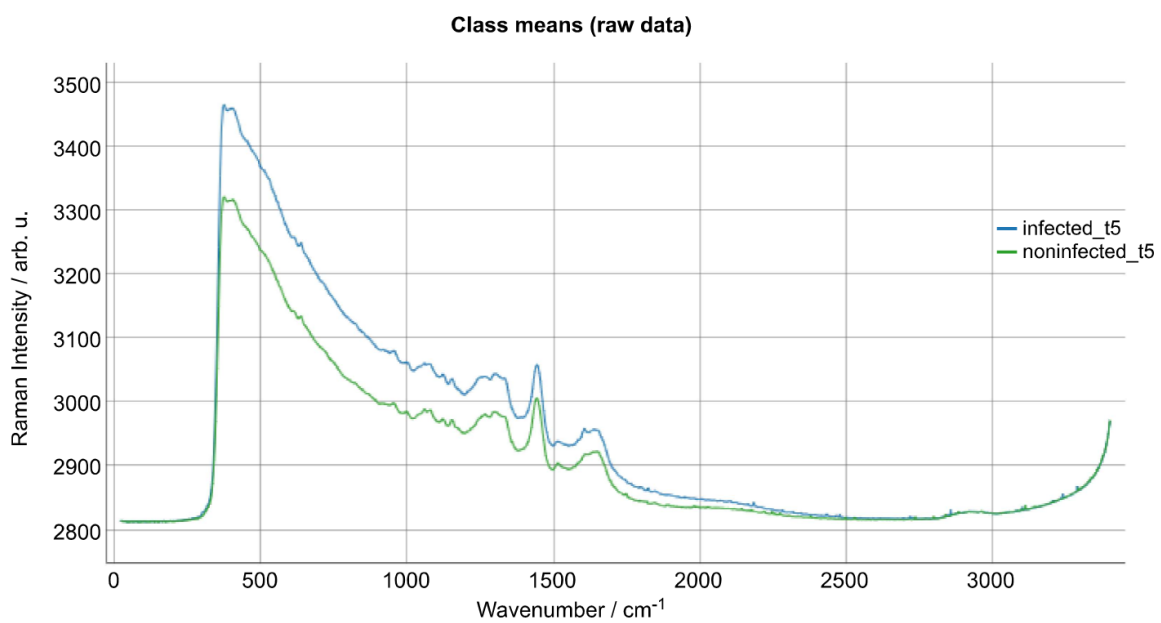


Figure 9: Mean plot of each defined class

spectra with pre-assigned classes “infected” and “non-infected”. x-axis: Wavenumber (cm^{-1}), y-axis: Raman intensity (arb. u.).

Applied parameters for despiking step

Two spectra presence false

Threshold for despiking 10

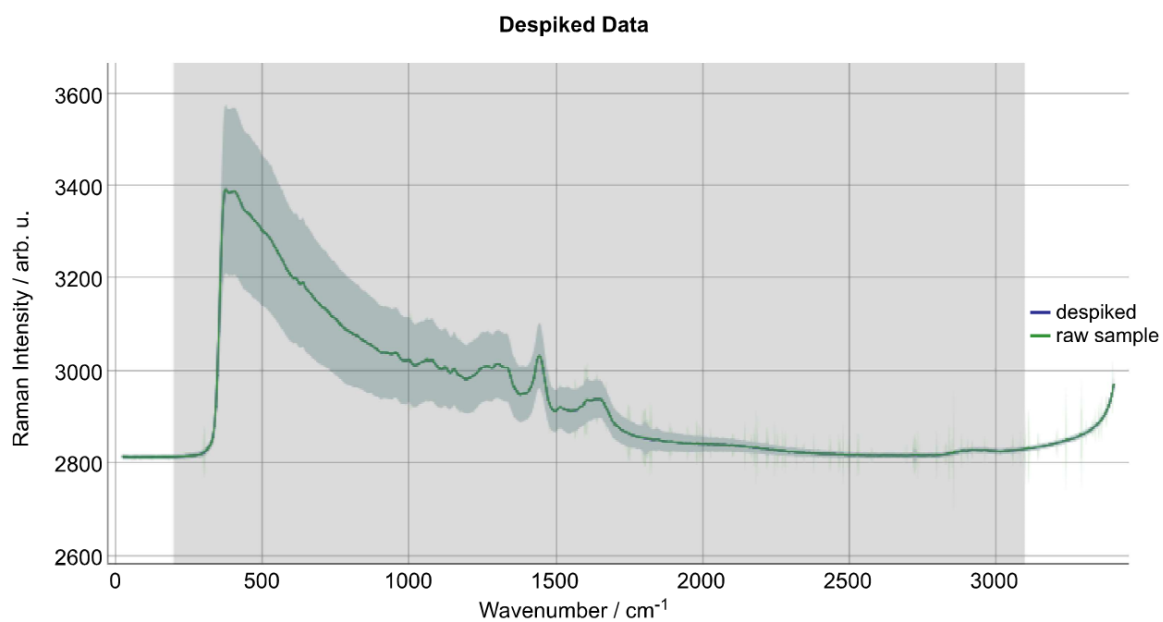


Figure 10: Data Pre-processing: Despiking

Display of raw spectral data and despiked data. x-axis: Wavenumber (cm⁻¹), y-axis: Raman intensity (arb. u.).

Applied parameters for calibration step

| | |
|-----------------------------|---|
| Peak fitting method | gauss |
| Standard peaks | [213.3, 329.2, 390.9, 465.1, 651.6, 710.8, 797.2, 857.9, 1168.5, 1236.8, 1278.5, 1323.9, 1371.5, 1515.1, 1561.5, 1648.4, 2931.1, 3064.6, 3102.4] cm^{-1} |
| Degree of polynomial | 3 |
| Resolution | 6 cm^{-1} |
| Wavenumber area | [200, 3100] cm^{-1} |

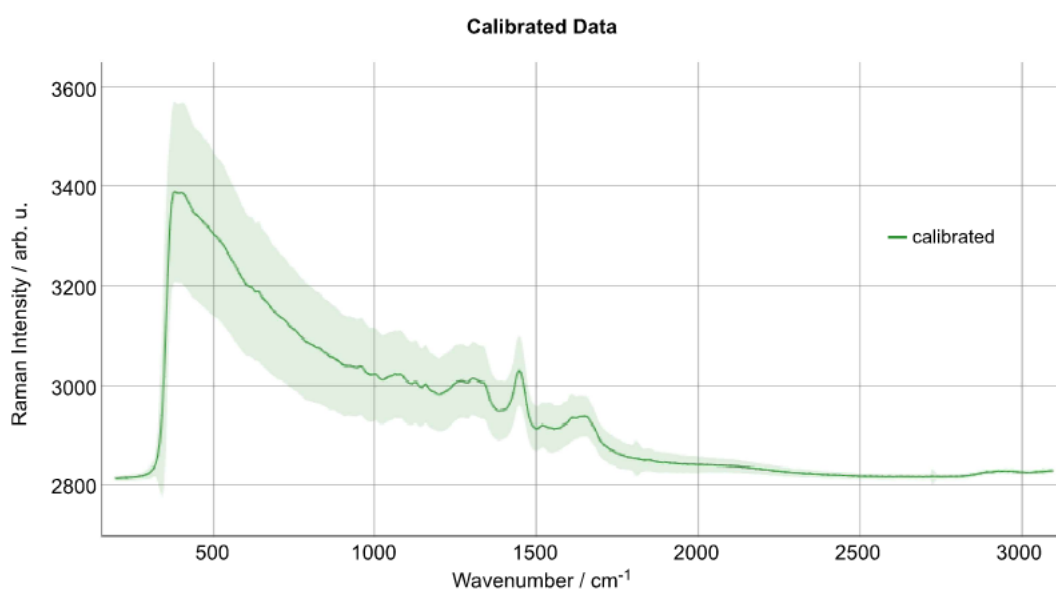
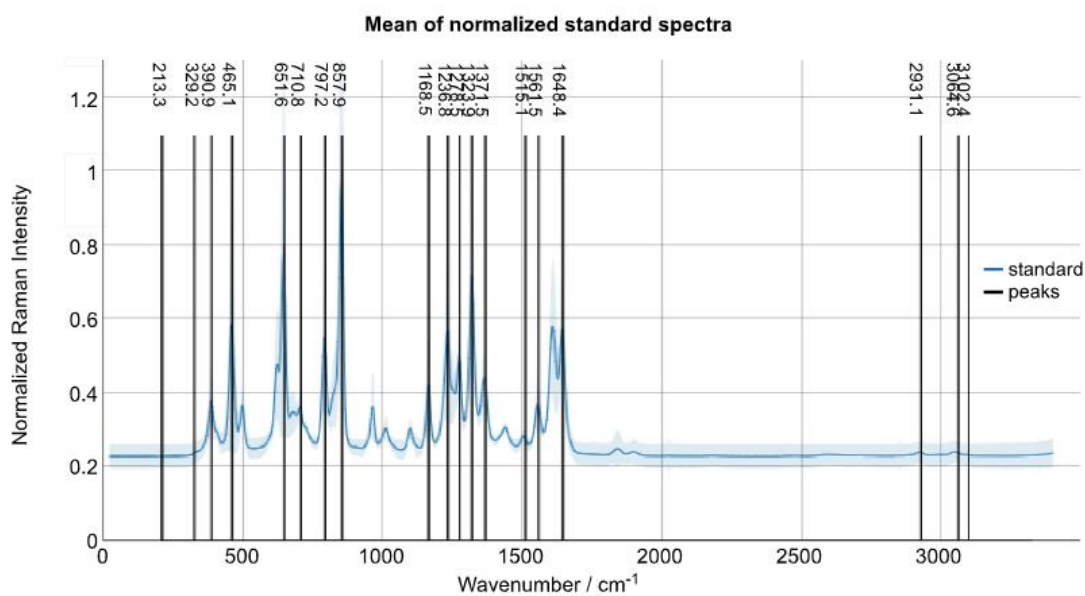


Figure 11: Data Pre-processing: Wavenumber axis calibration

Calibration of the wavenumber axis using an Acetaminophen standard reference spectrum. x-axis: Wavenumber (cm^{-1}), y-axis: Raman intensity (arb. u.).

Applied parameters for background corrections step

Baseline correction algorithm snip

Baseline Iteration 40

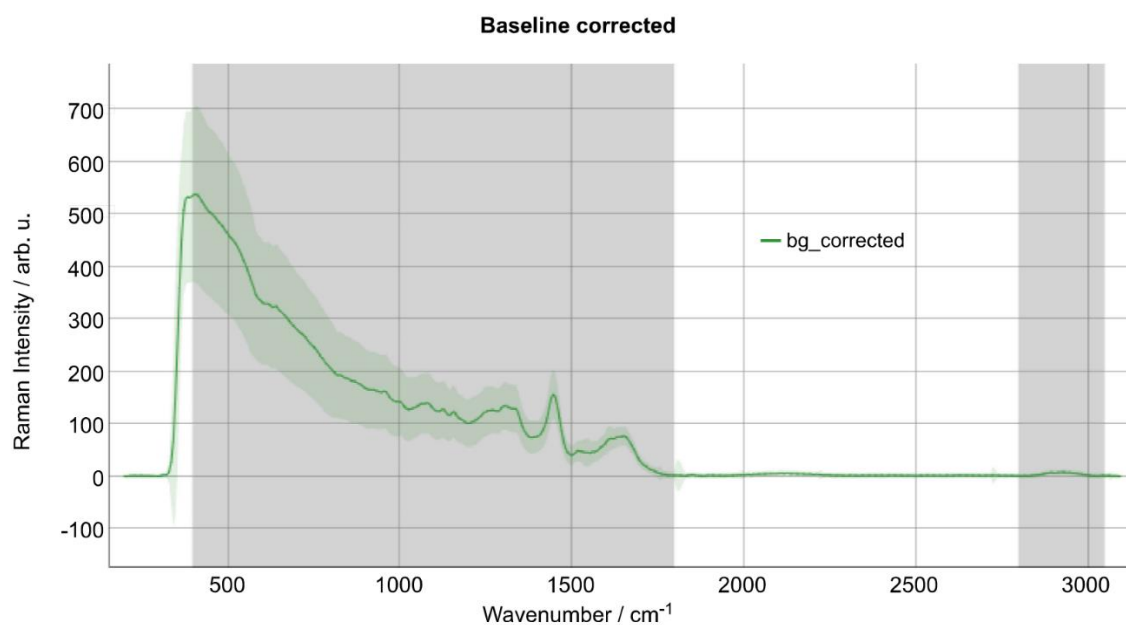


Figure 12: Data-Pre-processing: Background correction

Background of the selected wavenumber regions were corrected, by using a baseline-correction algorithm. x-axis: Wavenumber (cm⁻¹), y-axis: Raman intensity (arb. u.).

Applied parameters for normalization step

| | |
|---------------------------|-------------------------------|
| Normalization type | vector |
| Used area | [400, 400] cm^{-1} |
| Excluded area | [1800, 2800] cm^{-1} |

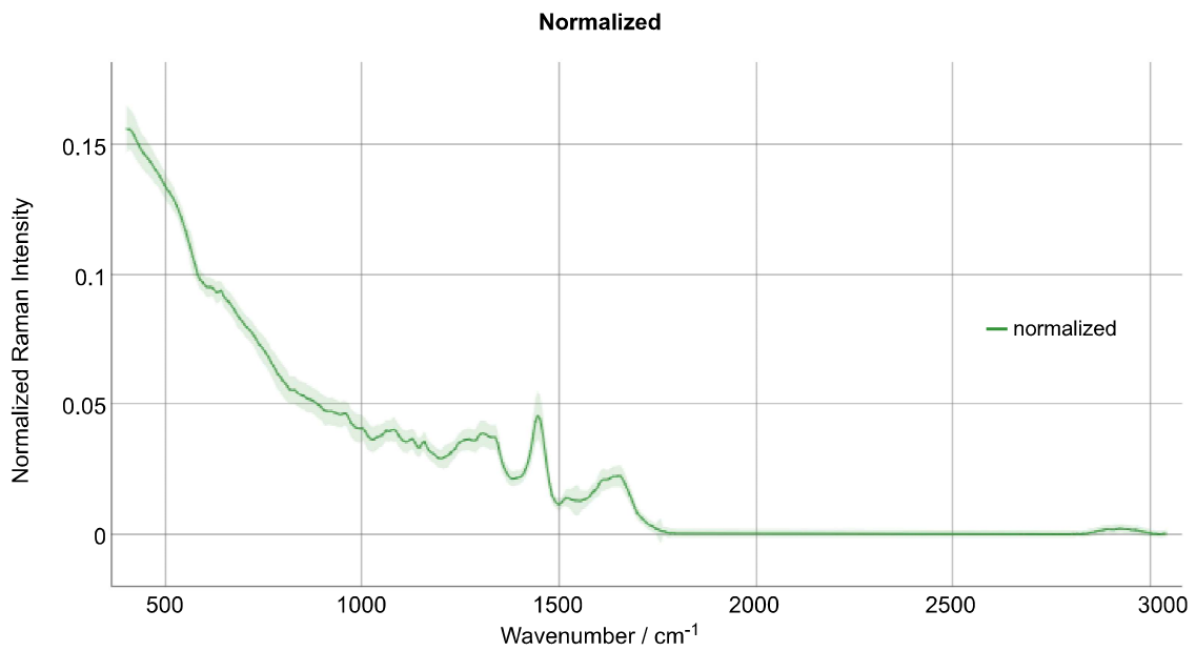


Figure 13: Data Pre-processing: Normalization

Normalization of spectral data by using a vector normalization. x-axis: Wavenumber (cm^{-1}), y-axis: Raman intensity (arb. u.).

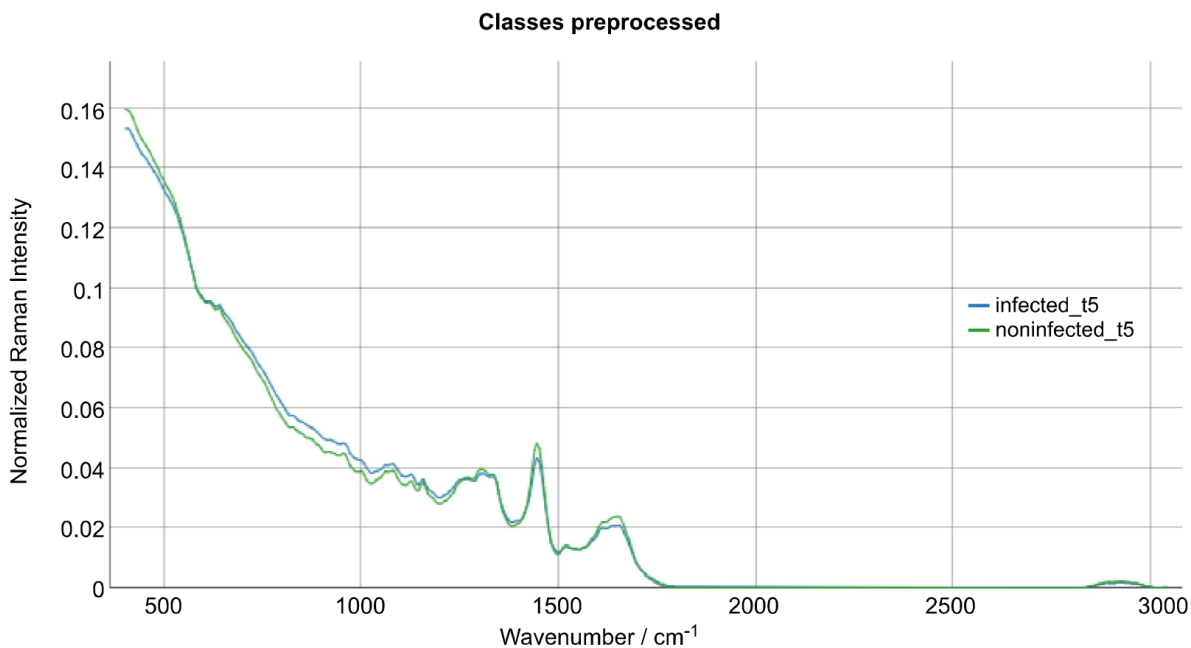


Figure 14: Data Pre-processing: Processed classes of data

Display of pre-processed classes of data for further analysis modelling. x-axis: Wavenumber (cm^{-1}), y-axis: Raman intensity (arb. u.).

3.5.3 Model cross-validation

Analysis was executed consisting of a combination of PCA and LDA modelling of contaminated and non-contaminated classes, utilizing the wavenumber region between 600 to 1800 cm^{-1} , where the most relevant, biological spectral information is located (chapter 1.3.1). Models based on each data set were analysed via k-fold cross-validation to evaluate, if the classifier can separate and match contaminated and non-contaminated references at the respective contamination level appropriately (Tab. 12).

Table 12: Overview of the recorded Raman spectra summarized in data sets

| h after spiking | Contamination level (CFU/ml) | Number of experiments | Number of spectra Pos. control/neg. control | Splitting of overall data-sets into test data and training data sets |
|-----------------|------------------------------|-----------------------|---|--|
| 18 | 2.10-7.42x10 ⁵ | 5 | 150/150 | 5 x 30/30; 5 x 120/120 |
| 21 | 0,84-1.74x10 ⁶ | 5 | 150/150 | 5 x 30/30; 5 x 120/120 |
| 24 | 1.00-8.10x10 ⁷ | 7 | 210/210 | 7 x 30/30; 7 x 180/180 |
| 28-32 | 1.56-7.29x10 ⁸ | 12 | 360/360 | 12 x 30/30; 12 x 330/330 |
| 45 | 1.16-1.78x10 ⁹ | 5 | 150/150 | 5 x 30/30; 5 x 120/120 |

To implement a cross validated prediction model, each data set representing one contamination level was split into k subsets, depending on the number of experiments included in the data set. One data subset was used for validation as a test data set, while the remaining k-1 data sets were merged into a training data set for the model (Fig. 15). A test data-set always consisted of one biological replicate tested with a defined concentration of bacteria (1 PC bag; 30 spectra: 10 per triplicate) and corresponding 30 Raman spectra of a non-contaminated PC negative-reference (chapter 3.4.4).

Each training data set was read into the Raman Analyst software version 0.2.0.0, pre-processed and validated by 10-fold cross validation. After that, the corresponding test data set was read into the software, pre-processed and used to test the model estimated on the basis of the training-

data set, to generate a single model performance measure. This was repeated k times, depending on the number of experiments for each contamination level (table 11). Classification results for individual spectra were displayed in data prediction tables by the Raman Analyst software version 0.2.0.0 (Fig. 16). The decision whether the respective sample was “infected” (contaminated) or “noninfected” (non-contaminated), was based on a manually performed two-thirds majority vote according to the classification of individual spectra.

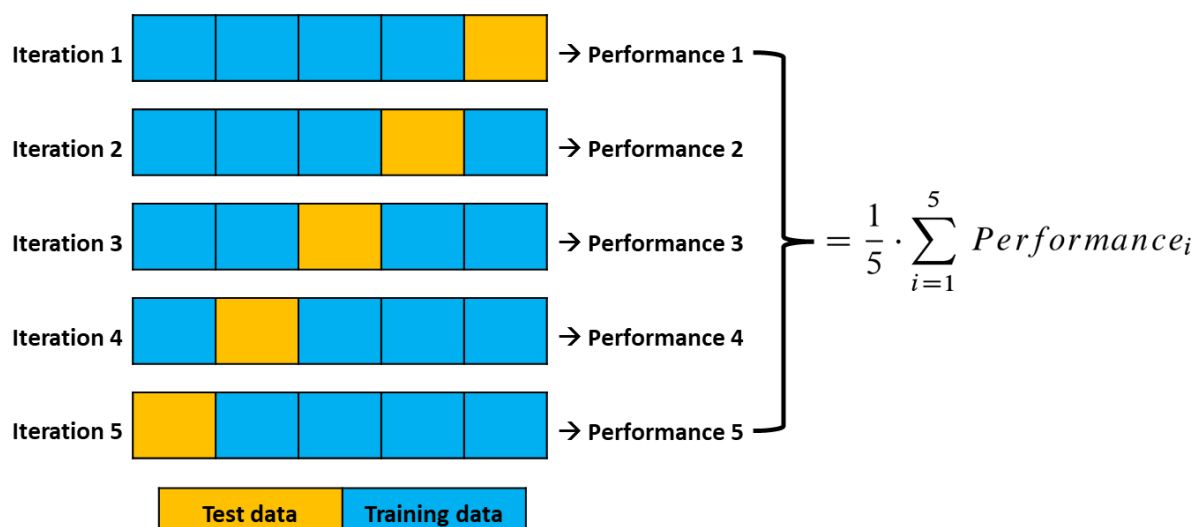


Figure 15: k-fold cross validation

k-Fold Cross Validation is performed by training a model using $k-1$ of the partitions as training data. The resulting model was validated with the prior subtracted data set, which was used as a test data set to compute a single performance measure. All performance measures reported by k -fold cross-validation were then calculated into the average of the performance of all iterations.

Performance of Iteration 1 (test data set 1)**Accuracy: 0.983 Mean sensitivity: 0.983**

Test data prediction

| True \ Predicted | [1] | [2] | sens | spec |
|------------------|--------|-----|-------|-------|
| infected_t5 | [1] 30 | 0 | 1 | 0.967 |
| noninfected_t5 | [2] 1 | 29 | 0.967 | 1 |

Performance of Iteration 2 (test data set 2)**Accuracy: 0.983 Mean sensitivity: 0.983**

Test data prediction

| True \ Predicted | [1] | [2] | sens | spec |
|------------------|--------|-----|-------|-------|
| infected_t5 | [1] 29 | 1 | 0.967 | 1 |
| noninfected_t5 | [2] 0 | 30 | 1 | 0.967 |

Performance of Iteration 3 (test data set 3)**Accuracy: 0.983 Mean sensitivity: 0.983**

Test data prediction

| True \ Predicted | [1] | [2] | sens | spec |
|------------------|--------|-----|-------|-------|
| infected_t5 | [1] 29 | 1 | 0.967 | 1 |
| noninfected_t5 | [2] 0 | 30 | 1 | 0.967 |

Performance of Iteration 4 (test data set 4)**Accuracy: 0.883 Mean sensitivity: 0.883**

Test data prediction

| True \ Predicted | [1] | [2] | sens | spec |
|------------------|--------|-----|-------|-------|
| infected_t5 | [1] 23 | 7 | 0.767 | 1 |
| noninfected_t5 | [2] 0 | 30 | 1 | 0.767 |

Performance of Iteration 5 (test data set 5)**Accuracy: 1 Mean sensitivity: 1**

Test data prediction

| True \ Predicted | [1] | [2] | sens | spec |
|------------------|--------|-----|------|------|
| infected_t5 | [1] 30 | 0 | 1 | 1 |
| noninfected_t5 | [2] 0 | 30 | 1 | 1 |

Figure 16: Representative illustration of k-fold cross validated test data sets (

PC contaminated with $1.16\text{-}1.78 \times 10^9$ CFU/ml *K. pneumoniae*, 45 h after contamination ($k = 5$). A data-set (table 12) was split manually into test and training data-sets according to the principle of a k-fold cross validation. The overall data set consisted of 5 experiments and was therefore divided into 5 subsets. For each iteration, one experimental data set acting as the test data set was tested on the model trained on the basis of the 4 remaining data sets. Prediction tables were created by the Raman Analyst software version 0.2.0.0. The calculated prediction tables were evaluated using the manually determined 2/3 majority vote and displayed in a corresponding confusion table for each iteration.

3.6 Detection of bacteria in PC using flow cytometry**3.6.1 New flow cytometry method: Staining protocol for the detection of bacteria in PC**

PC samples of 1 ml with defined bacterial contamination levels (chapter 3.2.4) or low spiked PC storage bags to study bacterial growth under real PC storage conditions (chapter 3.3.4) were prepared for flow cytometry measurements. Samples were either incubated with a Tirofiban solution (10 μM Tirofiban in 0.85 % NaCl) for 10 min at 37 °C to inhibit platelet aggregation or lysed directly without Tirofiban incubation. For platelet lysis, a series of tests with lysis incubation steps

for 30 min at room temperature using solutions containing between 0.5 % and 0.01 % Triton X-100 was conducted, to titrate the optimal concentration for the platelet lysis step (chapter 7.9, Fig. 66).

A lysis step with a solution of 0.2 % Triton X-100 in PBS + 1 mM EDTA (pH= 7.1) gave the best results, with platelets largely lysed but bacteria mostly intact. Samples were centrifuged at 13000 rpm for 1 min. The supernatant was discarded and the pellet was resuspended in 1 ml lysis solution (PBS + 1 mM EDTA pH= 7.1 + 0.2 % Triton X-100) to lyse platelets for 30 min at RT.

Samples specifically contaminated with *S. aureus* were not centrifuged prior to platelet lysis with Triton X-100, to prevent clumping of bacteria and platelets. For platelet lysis, 100 µl of lysis solution (PBS + 1 mM EDTA pH 7.1 + 2 % Triton X-100) was added directly to the samples, without removing the supernatant to ensure a final concentration of around 0.2 % Triton X-100 in the samples in order to lyse the platelets for 30 min at RT.

After the lysis of platelets, all samples regardless of bacterial contaminant were centrifuged for 1 min at 13000 rpm afterwards. Supernatant was discarded and pellets were resuspended in 100 µl of 4% Paraformaldehyde (pFA) in PBS + 1 mM EDTA pH= 7.1 to fix the cells. Samples were incubated at room temperature (20-22 °C) for 20 min and centrifuged for 1 min at 13000 rpm afterwards. Supernatant was discarded and pellets were resuspended in 200 µl of PBS + 1 mM EDTA pH= 7.1. Samples were stained with DRAQ5™ (Thermo Fisher Scientific, Karlsruhe, Germany), a membrane-permeable DNA-intercalating fluorescent dye. DRAQ5™ was diluted to a working concentration of 0.5 mM (Tab. 13) with PBS + 1 mM EDTA pH 7.1. Samples were incubated with the staining solution (final concentration 5 µM) for 30 min at 37 °C and filtered through a cell strainer (mesh size = 35 µM) prior to flow cytometry measurement to prevent blockage of the flow cytometer nozzle.

The flow cytometer (BD LSRFortessa™ flow cytometer, Becton Dickinson, Franklin Lakes, USA) was equipped with a blue argon laser (488 nm). A fluorescence filter set for APC-Alexa Fluor 700 (dichroic filter (690LP), and a bandpass filter (710/50) was used to collect the fluorescence emission from DRAQ5™ complexed with nucleic acids for detection of bacterial contamination. Data analysis was performed using the Kaluza flow cytometry analysis software version 2.1.1 (Beckman Coulter, Brea, USA). After use, the flow cytometer was cleaned by placing a tube filled with BD FACS™ Clean solution (Becton Dickinson, Franklin Lakes, USA) on the sample injection port. The instrument was then switched to "high" flow mode for 5 minutes. This step was repeated with BD FACS™ Rinse (Becton Dickinson, Franklin Lakes, USA) for 10 min and H₂O dest. for 5 min. The instrument was then set to "standby" mode and a tube of H₂O dest. was placed on the sample injection port.

Table 13: Fluorescence dye for flow cytometry

| Thermo Scientific™ DRAQ5™ Fluorescent Probe Solution | |
|---|---|
| Stock concentration | 5 mM |
| Working concentration | 0.5 mM |
| Staining concentration | 5 μ M |
| DNA-intercalation | A-T of dsDNA |
| Excitation (nm) | 488 nm (For flow cytometric applications) |
| Emission (nm) | 665 nm to 681 nm / 697 nm (intercalated with dsDNA) |
| Fluorescence channel | APC-Alexa Fluor 700 |
| Dichroic filter (nm) | 690 LP |
| Bandpass filter (nm) | 710/50 |

3.6.2 Validation of the LOD of flow cytometry for detection of bacteria in PC

Samples were measured under low flow conditions regarding the high number of events in the samples. Samples were measured for 5 min or until 1 million events were counted by the device. Samples were saved as .csv data using the export function of the software. Data was analysed using the Kaluza flow cytometry analysis software version 2.1.1 (Beckman Coulter, Brea, USA).

3.6.3 Gating strategy for detection of bacteria in PC using the Kaluza flow cytometry analysis software version 2.1.1

The gating strategy to detect bacterial contaminations in PC was defined in the course of this project. The development of the method is shown in detail in chapter 4.2.1.

3.6.4 Analysis of flow cytometry data

Analytical accuracy of the flow cytometric detection method was determined using area under the receiver operating characteristic curve (AUROC) analyses. Non-contaminated PC samples served as negative control references and were compared to contaminated PC samples. Based on this data, samples were classified as non-contaminated, when their bacteria-specific events came

below the discrimination threshold, whereas samples were considered contaminated when the bacteria-specific counts exceeded the calculated discrimination threshold (chapter 4.2.4). Statistical analysis was performed using GraphPad Prism8 (GraphPad Software Inc., San-Diego, USA).

3.7 Detection of bacteria in PC using the BactiFlow® system

3.7.1 Preparation of the BactiFlow® device before measurements

Calibration of the BactiFlow® device (bioMérieux, Nürtingen Germany) took place after the laser was preheated (10 min) and a system rinse step. 1 ml of Standard G was shaken thoroughly and transferred into a 3 ml tube and calibration was performed by placing the tube in the BactiFlow® holder. Analysis was starting automatically after placing the tube. After calibration, the BactiFlow® device was ready for analysis.

3.7.2 Preparation of working solutions for BactiFlow® Analysis

All required reagents were purchased ready-to-use from bioMérieux (Nürtingen, Germany) and HLS GMBH, Übach-Palenberg, Germany (chapter 2.1.1, Tab. 6). The exact required amounts of the respective chemicals for the lysis and staining solution were calculated depending on the number of samples of the respective experiment from table 13 for the enzymatic lysis solution and table 14 for the staining solution.

To prepare the enzymatic lysis solution, Chemsol M2 was thawed at room temperature. In the meantime, the required amount of Chemsol M1 was weighed and mixed with Diluent M in a glass beaker with a magnetic stirrer for 15 min, while foaming was avoided. The solution was sterile filtered to remove clumps of non-dissolved Chemsol M1. In a 50 ml Falcon tube, Chemsol M2 and Chemsol M3 were added to Chemsol M1 and the enzymatic lysis solution was stored at 4 °C until use. To prepare the staining solution, Buffer B1 and Buffer E2 were mixed in a glass beaker and stored under the exclusion of light at 4 °C until use.

Table 14: Enzymatic lysis solution for BactiFlow®

| Product | Required amount per sample | storage |
|------------|----------------------------|---------|
| Chemsol M1 | 1 ml | RT |

| | | |
|------------|--------------|--------|
| Diluent M | 0.1 g | RT |
| ChemSol M2 | 69.5 μ l | -20 °C |
| ChemSol M3 | 28 μ l | RT |

Table 15: Staining solution for BactiFlow®

| Product | Required amount per sample | storage |
|-----------|----------------------------|---------|
| Buffer 1B | 3 ml | RT |
| Buffer E2 | 30 μ l | 4 °C |

3.7.3 Sample processing for BactiFlow® analysis

For each sample, 1 ml of PC (PC samples spiked with defined concentrations of bacteria, chapter 3.2.4; bacteria grown in PC bags and sampled at specific time-points, chapter 4.4) was transferred into a 20 ml tube according to the respective experimental setup (Tab. 11). 432 μ l of enzymatic lysis solution (Tab. 14) was added to each sample. Samples were vortexed for 5 s and incubated for 15 min at 37 °C. Afterwards 7 ml of buffer 3A was added to each tube and mixed thoroughly. Each sample was filtered using a Chemfilter 25 and transferred into fresh 20 ml tube. Samples were transferred into a 15 ml Falcon tube and centrifuged for 8 min at 2000 rpm. After centrifugation, the supernatant was discarded and the pellet was resuspended with 3 ml of staining solution (Tab. 15). The resuspended samples were transferred into a new 20 ml tube and incubated, under the exclusion of light for 12 min at 30 °C in a heat block.

After the incubation step, 140 μ l of buffer 2C was added to the samples by gentle swirling, whereby foaming was avoided. Approximately one spatula tip of buffer 2D powder was added to each sample and dissolved by gentle swirling. 700 μ l of each sample was then transferred into a test tube to start the BactiFlow® Analysis.

3.7.4 Performing BactiFlow® Analysis

The BactiFlow® cytometer is equipped with a blue argon ion laser (488 nm) and fluorescence filter sets for FL1 (540 nm) and FL2 (590 nm) with a distinct positive/negative discrimination (reactive:

≥ 300 counts/ml, negative: < 300 counts/ml). The BactiFlow® software has a fixed bacteria detection region, that exhibits a specific FL1/FL2 ratio of approximately 1.0 (range 0.8 –1.2).

After calibration the option “Analysis” was chosen in the BactiFlow® software. For each experiment, a new session data file was created. After choosing the number of samples and the respective application, analysis was performed by placing the tube in the BactiFlow® holder, when the command “PLEASE LOAD SAMPLE” appeared. Analysis was starting automatically after placing the tube.

After analysis the BactiFlow® device was cleaned choosing the option “Clean system” and “Daily Rinse” in the BactiFlow® software. A 1-liter bottle of cleaning solution (Cleaning 10, 1:10 diluted in dest. H₂O) was connected to the device via the system fluid adapter and cleaning was executed.

3.7.5 Comparison of BactiFlow® measurements with flow cytometric measurements

To compare the BactiFlow® analysis with the new flow cytometry method, all samples of the PC spiked with defined bacterial counts (chapter 3.2.4, Tab. 11) and samples taken at specific time-points of bacterial growth in PC bags (chapter 4.4) were prepared as a duplicate. One sample set was prepared for the new flow cytometry method analysis (chapter 3.6). The other sample set was prepared for BactiFlow® measurements according to chapter 3.7.

4 Results

4.1 Detection of bacterial contaminations in PC using Raman microspectroscopy

4.1.1 Evaluation of the Raman data sets and confusion table results

To evaluate the differences in Raman spectral profiles of non-contaminated and contaminated PC over time, the respective transfusion bag was previously split into two storage bags (chapter 3.3.1). One bag was spiked with an initial inoculum of 2-5 CFU of *K. pneumoniae*, whilst the other bag was kept sterile. Time points for sample collection were selected based on a previously created standard growth curve of *K. pneumoniae* in PC (chapter 3.3.5, Fig. 6). At these time points, samples were taken from both bags, as described in chapter 3.2.4 and measured accordingly to chapter 3.4.4. The Raman spectral data at each sample collection time point was combined in overall data sets for each bacteria contamination level from 10^5 to 10^9 CFU/ml (chapter 3.5.3, Tab. 12). A PCA and LDA-based model was trained and cross-validated to predict the contamination status of PC based on individual Raman spectra. Following a 2/3 majority vote among 30 predictions derived from the 30 measured spectra per sample (chapter 3.5.3), discrimination between contaminated and non-contaminated samples was possible.

Table 16: PC contaminated with $2.10-7.42 \times 10^5$ CFU/ml *K. pneumoniae*

| | Prediction Contaminated | Prediction Non-contaminated |
|------------------|-------------------------|-----------------------------|
| Contaminated | 3 | 2 |
| Non-contaminated | 2 | 3 |

Incubation time: 18 h

Table 17: PC contaminated with $0.84-1.74 \times 10^6$ CFU/ml *K. pneumoniae*

| | Prediction Contaminated | Prediction Non-contaminated |
|------------------|-------------------------|-----------------------------|
| Contaminated | 1 | 4 |
| Non-contaminated | 3 | 2 |

Incubation time: 21 h

Table 18: PC contaminated with $1.00-8.10 \times 10^7$ CFU/ml *K. pneumoniae*

| | Prediction Contaminated | Prediction Non-contaminated |
|------------------|-------------------------|-----------------------------|
| Contaminated | 3 | 4 |
| Non-contaminated | 4 | 3 |

Incubation time: 24 h + 26 h

Table 19: PC contaminated with $1.56-7.29 \times 10^8$ CFU/ml *K. pneumoniae*

| | Prediction Contaminated | Prediction Non-contaminated |
|------------------|-------------------------|-----------------------------|
| Contaminated | 10 | 2 |
| Non-contaminated | 1 | 11 |

Incubation time: 28 h, 30 h, 32 h

Table 20: PC contaminated with $1.16-1.78 \times 10^9$ CFU/ml *K. pneumoniae*

| | Prediction Contaminated | Prediction Non-contaminated |
|------------------|-------------------------|-----------------------------|
| Contaminated | 5 | 0 |
| Non-contaminated | 0 | 5 |

Incubation time: 45 h

Growth of *K. pneumoniae* in PC resulting in a concentration between 10^5-10^7 CFU/ml (18h-26h after contamination) could not be reliably detected by Raman microspectroscopy (Tab. 16-18). A discrimination between non-contaminated PC and PC contaminated with *K. pneumoniae* was possible, starting at a concentration of approximately 1×10^8 CFU/ml after 28-32 h of incubation with 87.5 % reliability (Tab. 19) and was 100% reliable at 1×10^9 CFU/ml after 45 h (Tab. 20).

4.2 Detection of bacterial contaminations in PC using flow cytometry

4.2.1 Definition of a universal gating strategy for the detection of bacteria in PC by flow cytometry

Bacteria from the WHO repository of PTRBR (chapter 1.1.2, Tab. 2) were measured alone or within PC matrix (chapter 3.6.1). Bacterial cells were identified by granularity (SSC) and DNA content using DRAQ5™. During sample preparation, platelets were lysed to specifically stain and identify bacterial cells.

WHO bacterial reference strains (in the absence of PC) were used to create a reference population gate for the detection of bacterial contaminations: 10^6 CFU of *K. pneumonia* (Fig. 17 A), *B. cereus* (Fig. 18 A), *S. epidermidis* (Fig. 19 A), *S. aureus* (Fig. 20 A), *E. coli* (chapter 7.2, Fig. 37 A), *E. cloacae* (chapter 7.2, Fig. 38 A), *P. fluorescens* (chapter 7.2, Fig. 39 A), *P. mirabilis* (chapter 7.2, Fig. 40 A), *S. marcescens* (chapter 7.2, Fig. 41 A), *M. morgani* (chapter 7.2, Fig. 42 A), *S. pyogenes* (chapter 7.2, Fig. 43 A) and *B. thuringiensis* (chapter 7.2, Fig. 44 A) were analysed using the BD LSRFortessa™ flow cytometer (Becton Dickinson, Franklin Lakes , USA). *S. pyogenes* was analysed as a representative of the genus *Streptococcus*.

Based on granularity (SSC) and DNA content (DRAQ5™ fluorescence intensity), a reference population gate for the detection of bacterial contaminations within PC was created (Fig. 17-20 B; chapter 7.2, Fig. 37-44 B). After measurement of selected bacterial strains in PC, the bacterial population gate was adjusted to exclude the PC background signal (Fig. 17-20 C; chapter 7.2, Fig. 37-44 C). Based on this defined bacteria gate, further adjustments for exclusion of non-specifically stained cell remnants and cell debris were carried out (Fig. 21). The final bacterial detection gate was defined to enable the detection of stained nucleoids of all examined WHO PTRBR strains.

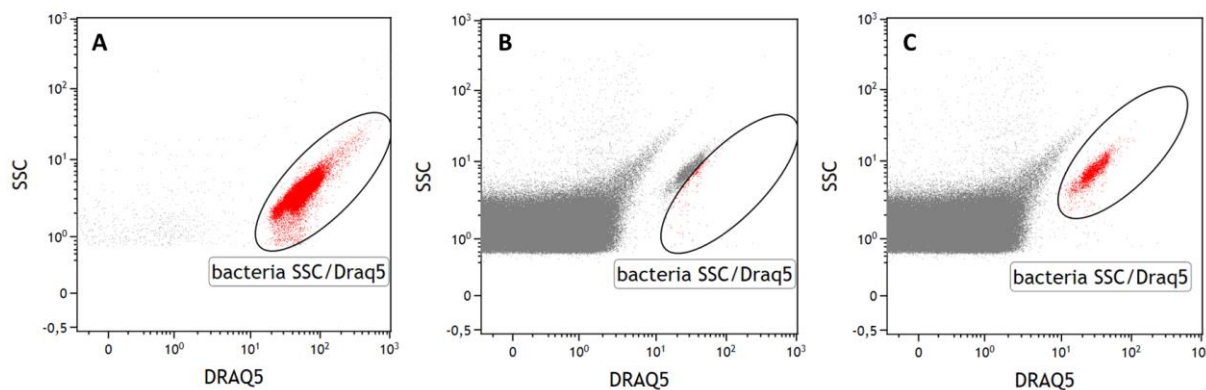


Figure 17: Flow cytometric detection gate for *K. pneumoniae* in PC samples

(A) Representative dot plot of DRAQ5-positive *K. pneumoniae* (10^6 CFU) without PC measured by the established flow cytometry method. Gating of bacterial fluorescence events without the influence of PC based on granularity (SSC) and DNA content (DRAQ5™ fluorescence intensity) ($n = 3$). (B) To determine and confirm the position of the bacteria detection gate in presence of PC, 10^6 CFU/ml of *K. pneumoniae* were spiked in PC and samples were measured by using the new flow cytometry method. (C) The detection gate for bacteria in PC was adjusted based on the granularity (SSC) and DRAQ5™ staining intensity of the bacteria within the PC sample. ($n = 3$).

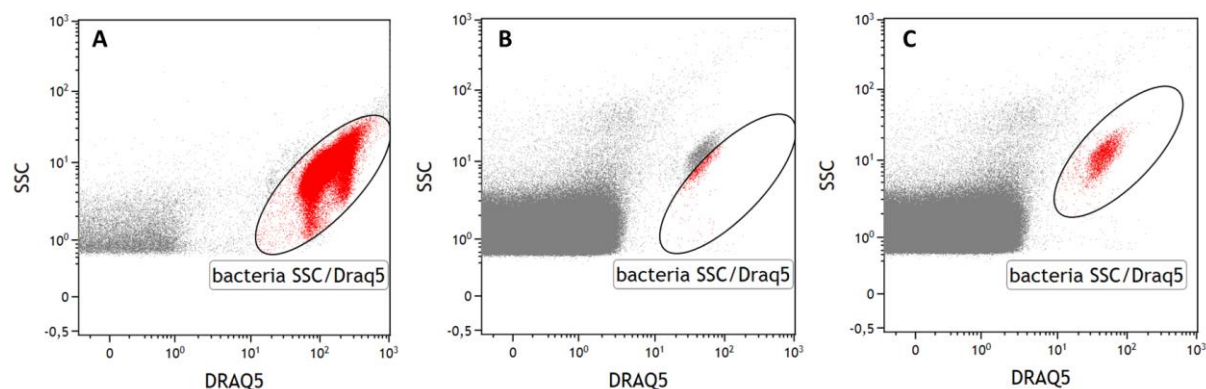


Figure 18: Flow cytometric detection gate for *B. cereus* in PC samples

(A) Representative dot plot of DRAQ5-positive *B. cereus* (10^6 CFU) without PC measured by the established flow cytometry method. Gating of bacterial fluorescence events without the influence of PC based on granularity (SSC) and DNA content (DRAQ5™ fluorescence intensity) ($n = 3$). (B) To determine and confirm the position of the bacteria detection gate in presence of PC, 10^6 CFU/ml of *B. cereus* were spiked in PC and samples were measured by using the new flow cytometry method. (C) The detection gate for bacteria in PC was adjusted based on the granularity (SSC) and DRAQ5™ staining intensity of the bacteria within the PC sample. ($n = 3$).

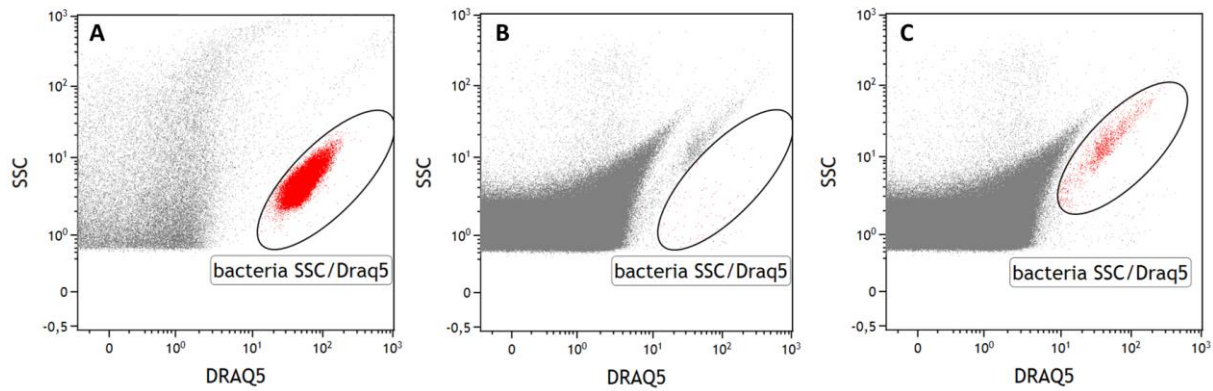


Figure 19: Flow cytometric detection gate for *S. epidermidis* in PC samples

(A) Representative dot plot of DRAQ5-positive *S. epidermidis* (10^6 CFU) without PC measured by the established flow cytometry method. Gating of bacterial fluorescence events without the influence of PC based on granularity (SSC) and DNA content (DRAQ5™ fluorescence intensity) ($n = 3$). (B) To determine and confirm the position of the bacteria detection gate in presence of PC, 10^6 CFU/ml of *S. epidermidis* were spiked in PC and samples were measured by using the new flow cytometry method. (C) The detection gate for bacteria in PC was adjusted based on the granularity (SSC) and DRAQ5™ staining intensity of the bacteria within the PC sample. ($n = 3$).

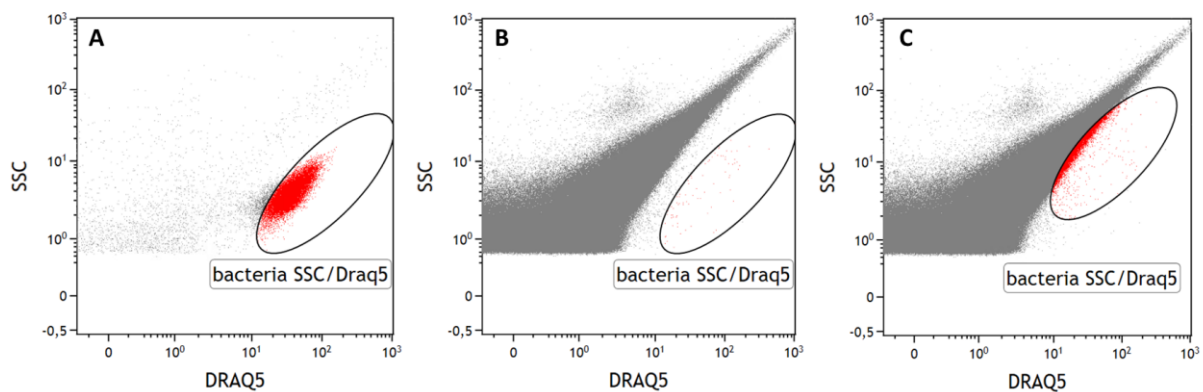


Figure 20: Flow cytometric detection gate for *S. aureus* in PC samples

(A) Representative dot plot of DRAQ5-positive *S. aureus* (10^6 CFU) without PC measured by the established flow cytometry method. Gating of bacterial fluorescence events without the influence of PC based on granularity (SSC) and DNA content (DRAQ5™ fluorescence intensity) ($n = 3$). (B) To determine and confirm the position of the bacteria detection gate in presence of PC, 10^6 CFU/ml of *S. aureus* were spiked in PC and samples were measured by using the new flow cytometry method. (C) The detection gate for bacteria in PC was adjusted based on the granularity (SSC) and DRAQ5™ staining intensity of the bacteria within the PC sample. ($n = 3$).

To improve the sensitivity of the established flow cytometry method, the previously defined detection gate for bacterial contaminants in PC (chapter 4.2.1, Fig. 17-20 C; chapter 7.2, Fig. 37-44 C) was further adjusted to minimize the acquisition of non-specifically stained sample components, such as cell debris (grey) or remaining non-lysed platelets (blue) (Fig. 21 A).

The resulting bacterial population (green) within the PC sample formed a coherent event population and could be separated from the surrounding individual events, which were characterized as intact, non-specifically stained platelets (blue) (Fig. 21 B).

Due to their similar size and granularity, remaining intact platelets after the specific staining step (chapter 3.6.1) partially overlapped with the bacteria population regarding their SSC and FSC parameters. Therefore, non-specifically stained platelets (blue) had to be further separated from stained bacteria (red) by gating based on their DNA content (DRAQ5™ staining intensity), resulting in a defined bacteria SSC/DRAQ5™ gate. All events outside this specific bacterial detection gate (green) were excluded. The events outside of the defined bacteria SSC/DRAQ5™ gate were categorized as residual stained, intact platelet events and non-specific stained cell debris (Fig. 21, C). Fluorescent events from PC samples with different concentrations of bacteria were measured in the bacteria SSC/DRAQ5™ gate and compared with non-contaminated PC samples. Analytical sensitivity of the flow cytometry method was determined using area under the receiver operating characteristic curves (AUROCs) analysis (chapter 4.2.4), to define a discrimination threshold between non-contaminated and contaminated PC samples.

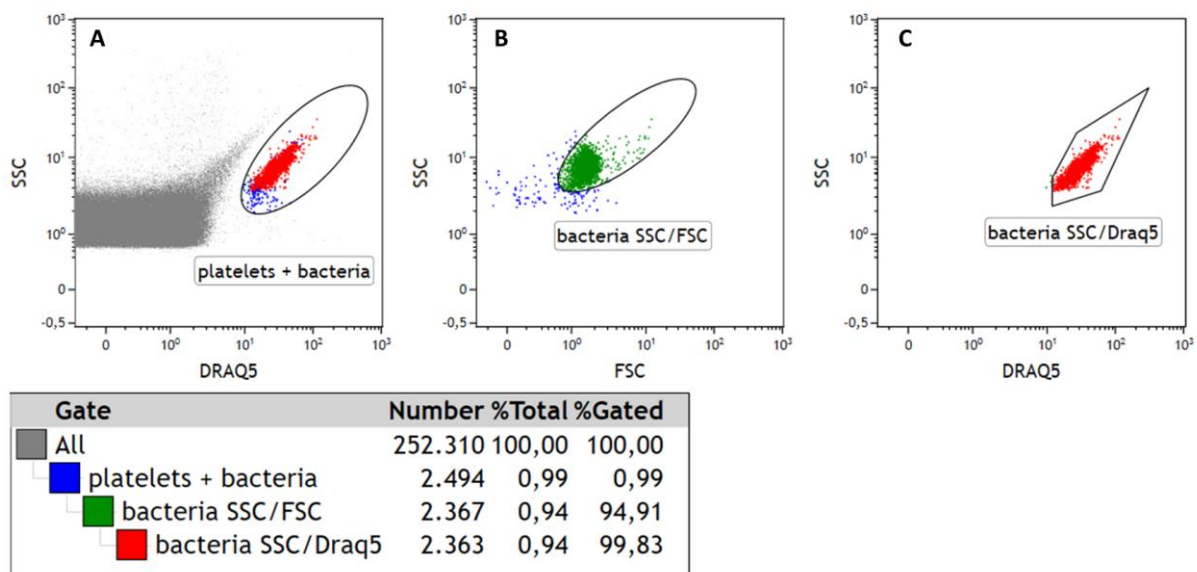


Figure 21: Gating strategy for bacterial detection in contaminated PC

Stained bacteria (red) were identified by granularity (SSC) and DNA content (DRAQ5™ staining intensity) (A). The bacterial population (green) and non-lysed, non-specifically stained platelets (blue) were distinguished based on granularity (SSC) and size (FSC) (B). The bacterial population (red) was differentiated from the remaining non-specifically stained cell debris and platelets (green) based on the intensity of DRAQ5™ staining. Fluorescence events within the defined bacterial detection gate were counted as bacteria (C). The Fig. shows a representative PC sample spiked with 10^5 CFU/ml *K. pneumoniae*.

4.2.2 Comparison of flow cytometric bacteria detection in PC before and after the use of the platelet aggregation inhibitor Tirofiban during sample preparation

To further reduce non-specific fluorescence events originating from cell debris and platelets in the SSC/DRAQ5™ bacteria detection gate (Fig. 21 C), an incubation step with Tirofiban was introduced into the flow cytometry method (chapter 3.6.1) to reduce the aggregation of platelets in the samples and thereby increase the lysis efficiency of platelets in the assay.

To study the effects of Tirofiban during sample staining, platelet lysis efficiency and the amount of remaining non-specifically stained cell debris and platelets in the SSC/DRAQ5™ bacteria detection gate, were compared by performing the staining protocol (chapter 3.6.1) with (Fig. 22-25, bottom illustration) or without (Fig. 22-25, upper illustration; chapter 7.3, Fig. 45-47) the Tirofiban incubation step.

Incubation with Tirofiban resulted in the inhibition of cell aggregation, leading to a more efficient platelets lysis and less platelet events in the SSC/DRAQ5™ bacteria detection gate (Fig. 22-25 C, bottom illustration).

Due to the reduction of background events by the Tirofiban incubation step, analysis of PC samples spiked with *K. pneumoniae*, *B. cereus* and *S. epidermidis* allowed an improved differentiation between platelets and bacteria. The flow cytometry method with the addition of Tirofiban, prior to staining was adopted as the final reference method for comparison against the BactiFlow® system (chapter 4.3).

However, it was not possible to detect *S. aureus* in PC independent of Tirofiban incubation (Fig. 25). Therefore, an alternative staining procedure was developed for *S. aureus* in PC (chapter 3.6.1).

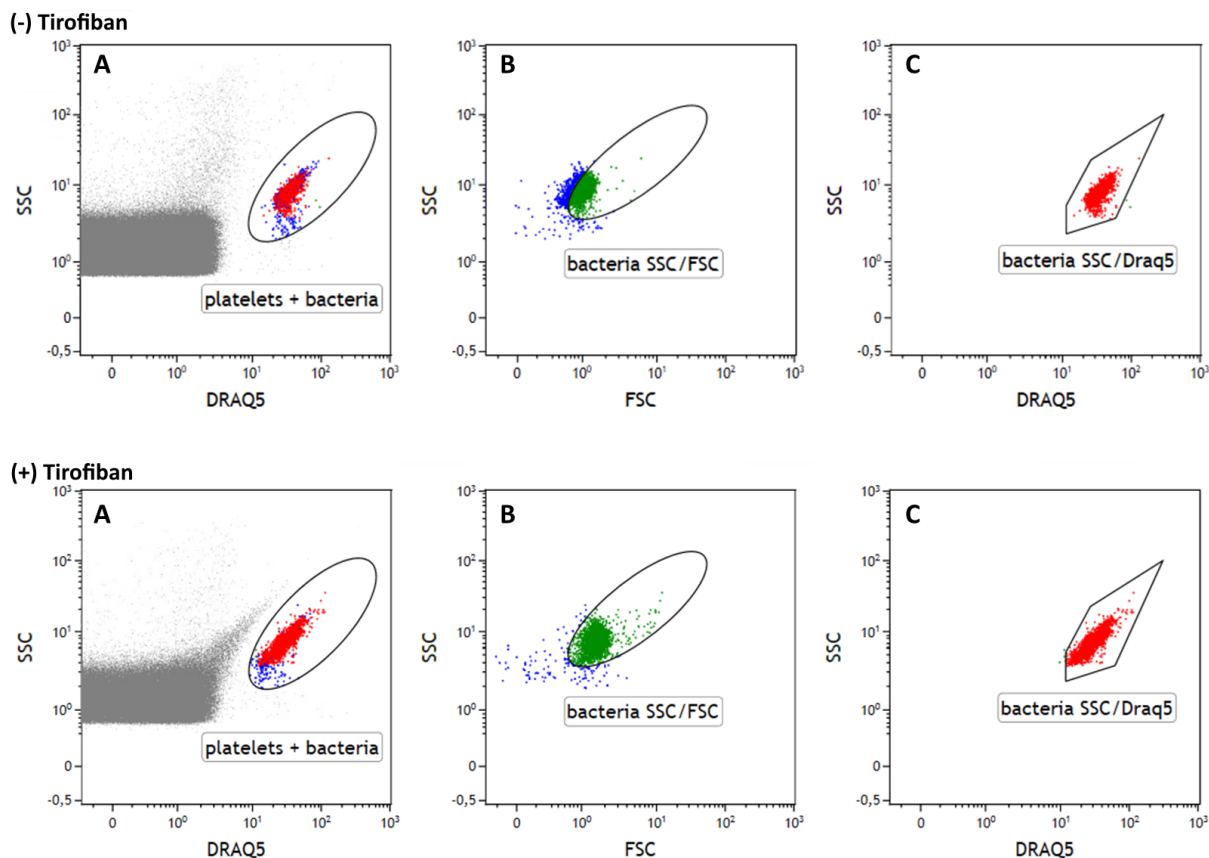


Figure 22: Effects of Tirofiban on the flow cytometric detection of *K. pneumoniae* in PC.

Representative dot plot of PC spiked with 10^5 CFU/ml of *K. pneumoniae*, measured using the new flow cytometry method without Tirofiban treatment (upper row; $n = 3$) or with Tirofiban treatment (lower row; $n = 12$). Platelets (blue) and bacteria (red) were gated based on SSC and DRAQ5™ staining intensity (A). The bacterial population (green) and residual platelets (blue) were discriminated by SSC and FSC (B). Additionally, the bacterial population (red) was discriminated from residual non-specific stained cell debris and platelets (green) based on DRAQ5™ staining intensity. Fluorescence events within the defined bacterial detection gate were counted as bacteria (C).

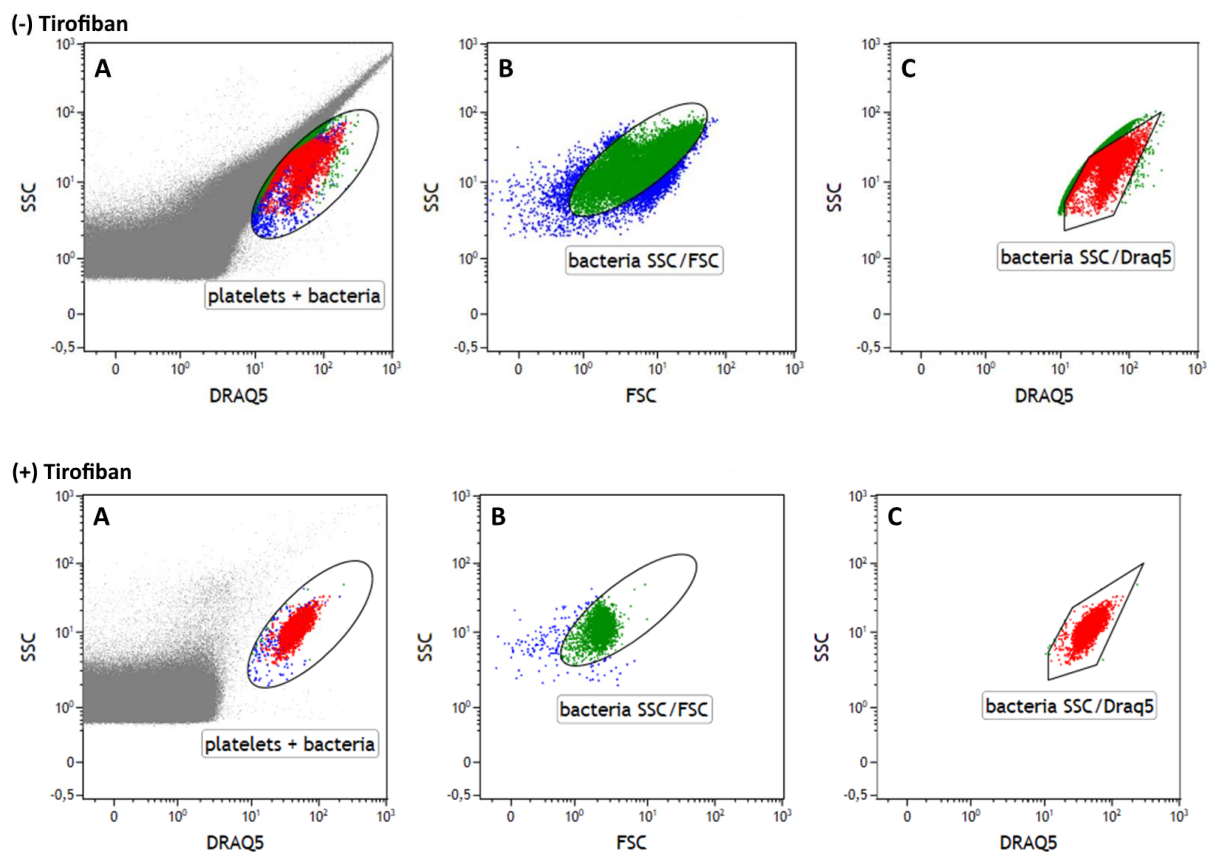


Figure 23: Effects of Tirofiban on the flow cytometric detection of *B. cereus* in PC

Representative dot plot of PC spiked with 10^5 CFU/ml of *B. cereus*, measured using the new flow cytometry method without Tirofiban treatment (upper row; $n = 3$) or with Tirofiban treatment (lower row; $n = 12$). Platelets (blue) and bacteria (red) were gated based on SSC and DRAQ5™ staining intensity (A). The bacterial population (green) and residual platelets (blue) were discriminated by SSC and FSC (B). Additionally, the bacterial population (red) was discriminated from residual non-specific stained cell debris and platelets (green) based on DRAQ5™ staining intensity. Fluorescence events within the defined bacterial detection gate were counted as bacteria (C).

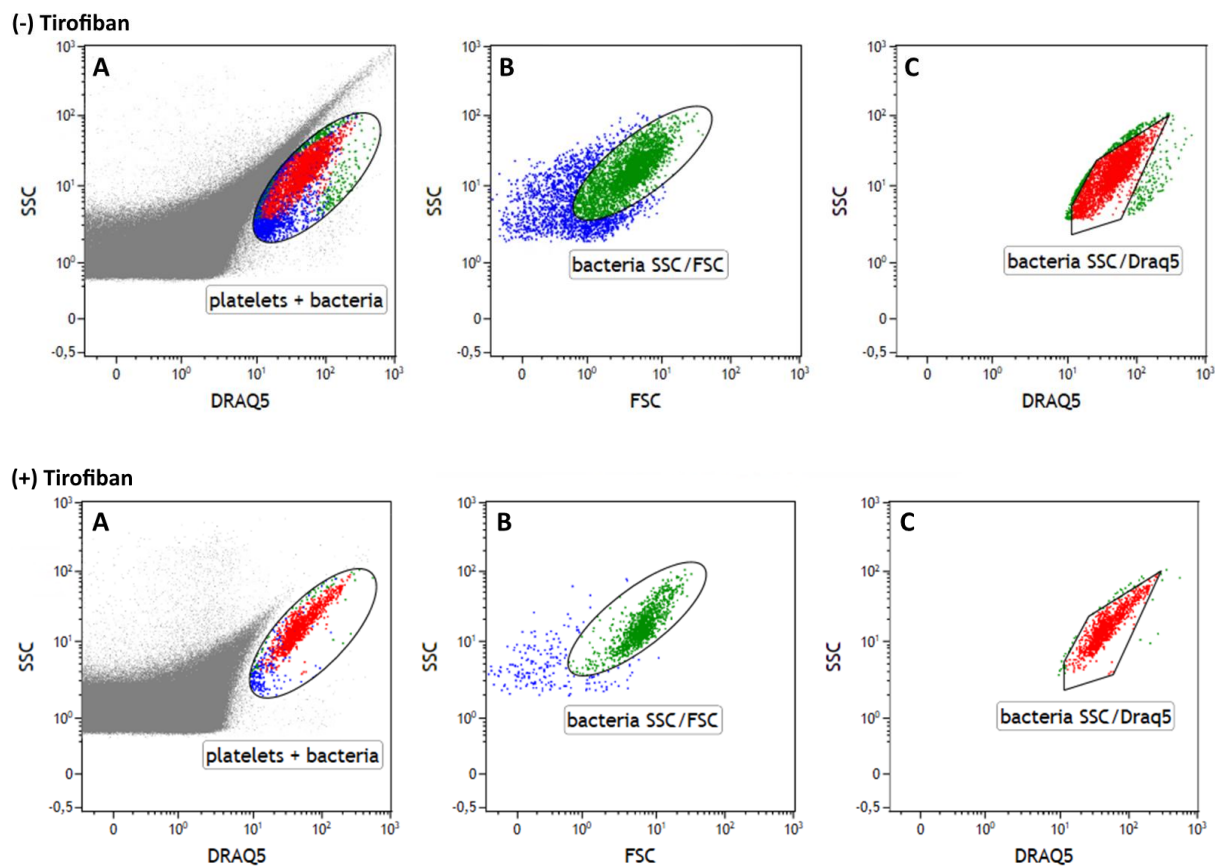


Figure 24: Effects of Tirofiban on the flow cytometric detection of *S. epidermidis* in PC

Representative dot plot of PC spiked with 10^5 CFU/ml of *S. epidermidis*, measured using the new flow cytometry method without Tirofiban treatment (upper row; $n = 3$) or with Tirofiban treatment (lower row; $n = 15$). Platelets (blue) and bacteria (red) were gated based on SSC and DRAQ5™ staining intensity (A). The bacterial population (green) and residual platelets (blue) were discriminated by SSC and FSC (B). Additionally, the bacterial population (red) was discriminated from residual non-specific stained cell debris and platelets (green) based on DRAQ5™ staining intensity. Fluorescence events within the defined bacterial detection gate were counted as bacteria (C).

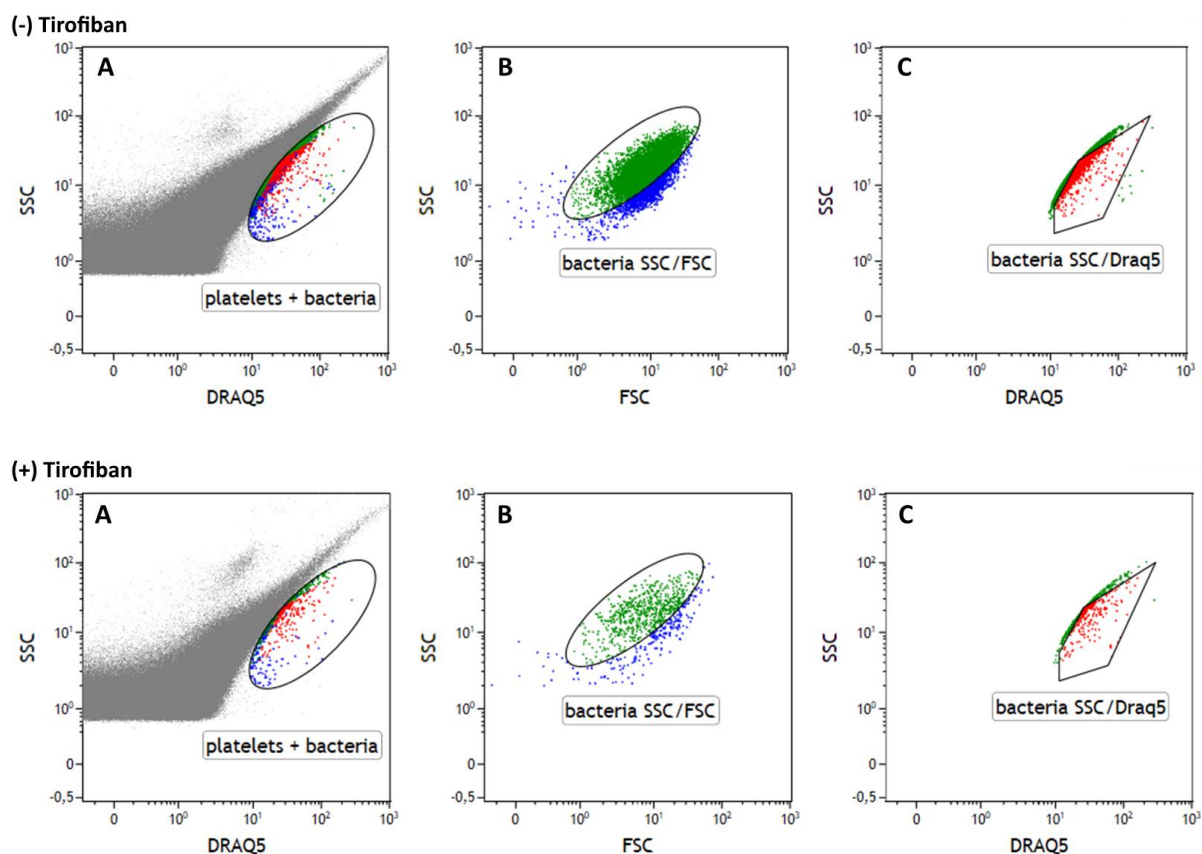


Figure 25: Effects of Tirofiban on the flow cytometric detection of *S. aureus* in PC

Representative dot plot of PC spiked with 10^5 CFU/ml of *S. aureus*, measured using the new flow cytometry method without Tirofiban treatment (upper row; $n = 3$) or with Tirofiban treatment (lower row; $n = 3$). Platelets (blue) and bacteria (red) were gated based on SSC and DRAQ5™ staining intensity (A). The bacterial population (green) and residual platelets (blue) were discriminated by SSC and FSC (B). Additionally, the bacterial population (red) was discriminated from residual non-specific stained cell debris and platelets (green) based on DRAQ5™ staining intensity. Fluorescence events within the defined bacterial detection gate were counted as bacteria (C).

4.2.3 Detection of *S. aureus* in PC using an adjusted method protocol and detection gate

DRAQ5™ –labelled *S. aureus* could not be detected as a defined population in PC samples with or without inhibition of PC aggregation by Tirofiban (Fig. 25). Sample centrifugation prior to the PC lysis step (chapter 3.6.1) impaired resuspension of *S. aureus* spiked PC samples in the lysis solution, which prevented the separation of the *S. aureus* population from lysed platelets during flow cytometric analysis. In comparison, a distinct population of *S. aureus* was visible without PC (chapter 4.2.1, Fig. 20). Hence, the centrifugation step prior to platelet lysis was omitted in order to prevent increased physical contact of platelets with *S. aureus*, resulting in aggregation and deteriorated dissociation of the *S. aureus* population (chapter 3.6.1). With the adjusted flow cytometry method, it was possible to detect *S. aureus* within the PC samples (Fig. 26).

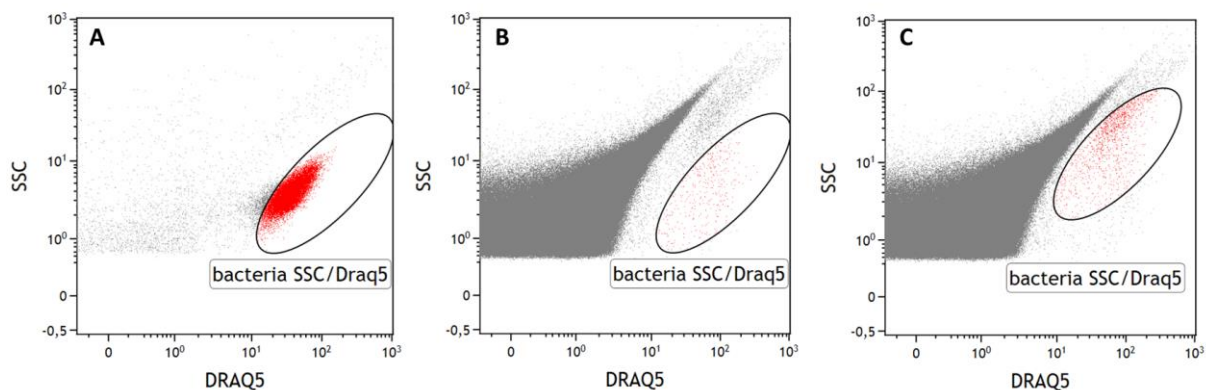


Figure 26: Generation of an *S. aureus*- specific population gate

(A) Representative dot plot of DRAQ5-positive *S. aureus* (10^6 CFU) incubated with Tirofiban without centrifugation prior to platelet lysis, measured by the established flow cytometry method. Gating of bacterial fluorescence events without the influence of PC based on granularity (SSC) and DNA content (DRAQ5™ fluorescence intensity) ($n = 3$). (B) To determine and confirm the position of the bacteria detection gate in presence of PC, 10^6 CFU/ml of *S. aureus* were spiked in PC and samples were measured by using the new flow cytometry method. (C) The detection gate for bacteria in PC was adjusted based on the granularity (SSC) and DRAQ5™ staining intensity of the bacteria within the PC sample. ($n = 3$).

Since the position of *S. aureus* in regard to granularity (SSC) and fluorescence intensity (DRAQ5™) differed greatly from those of the other bacteria studied, a specific bacterial gate was created for *S. aureus*, to reliably detect bacterial contaminations with *S. aureus* in PC samples (Fig. 27).

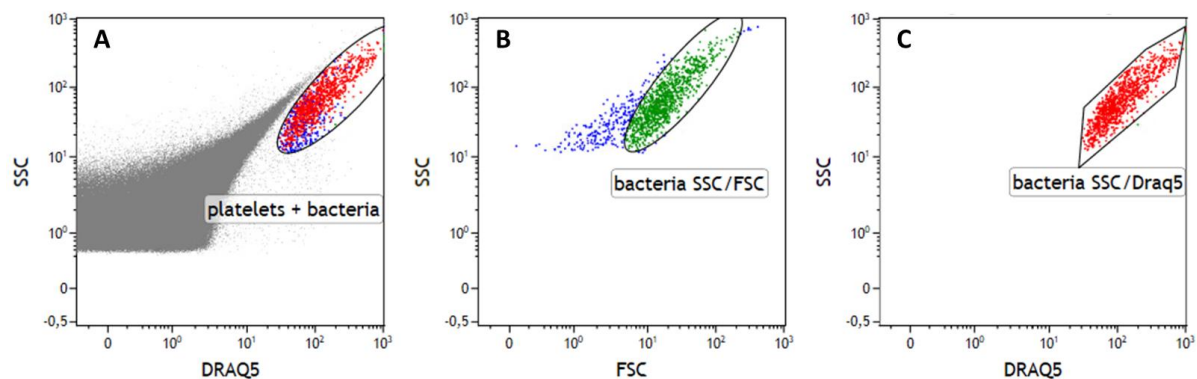


Figure 27: Effect of Tirofiban on *S. aureus* detection in PC without centrifugation prior to platelet lysis and DRAQ5™ staining

Representative dot plot of PC spiked with 10^5 CFU/ml of *S. aureus*, measured using the new flow cytometry method with Tirofiban incubation step without a centrifugation step prior to platelet lysis and DRAQ5™ staining ($n = 3$). Platelets (blue) and bacteria (red) were gated based on SSC and DRAQ5™ staining intensity (A). The bacterial population (green) and residual platelets (blue) were discriminated by SSC and FSC (B). Additionally, the bacterial population (red) was discriminated from residual non-specific stained cell debris and platelets (green) based on DRAQ5™ staining intensity. Fluorescence events within the defined bacterial detection gate were counted as bacteria (C).

4.2.4 Calculation of the analytical accuracy of the flow cytometry method using area under the receiver operating characteristic curves

The analytic accuracy of the detection of bacterial contaminations in PC by the developed flow cytometric detection method was determined using area under the receiver operating characteristic curves (AUROCs) of fluorescence events within the defined bacteria detection gate. For analysis of the flow cytometry data, AUROC binary classifier were used to measure the classification performance between contaminated and non-contaminated PC (Fig. 28-30).

K. pneumoniae, *B. cereus*, *S. epidermidis*, *S. aureus*, *E. coli*, *E. cloacae* and *B. thuringiensis* were spiked into PC samples (3 bags/data set) in concentrations ranging from 10^2 - 10^5 CFU/ml. Afterwards, samples were analysed by using the flow cytometry method without the addition of the platelet aggregation inhibitor Tirofiban. Fluorescent events were measured according to the previously defined gating strategy for bacterial detection (chapter 4.2.1, Fig. 21) and compared to the respective non-contaminated PC samples (chapter 7.4, Fig. 48).

An AUROC classifier was calculated for the discrimination of contaminated and non-contaminated PC samples (Fig. 28 A). AUROC calculated a discrimination threshold of 1072 fluorescent events, resulting in 60 % (95 % CI, 47.3 %–71.0 %) sensitivity and 90.5 % (95 % CI, 71.1 %–98.3 %) specificity for the detection of bacterial contaminations in PC in the range of 10^3 - 10^5 CFU/ml from the non-contaminated PC negative references (Fig. 28 B).

Flow cytometry data corresponding to PC spiked with 10^2 CFU/ml was excluded from the analysis, since the mean events were in the same range as the mean events of the non-contaminated negative control (chapter 7.4, Fig. 48 D). PC samples were tested positive for bacteria, when the bacteria-specific event counts were \geq the calculated discrimination threshold of 1072 fluorescent events.

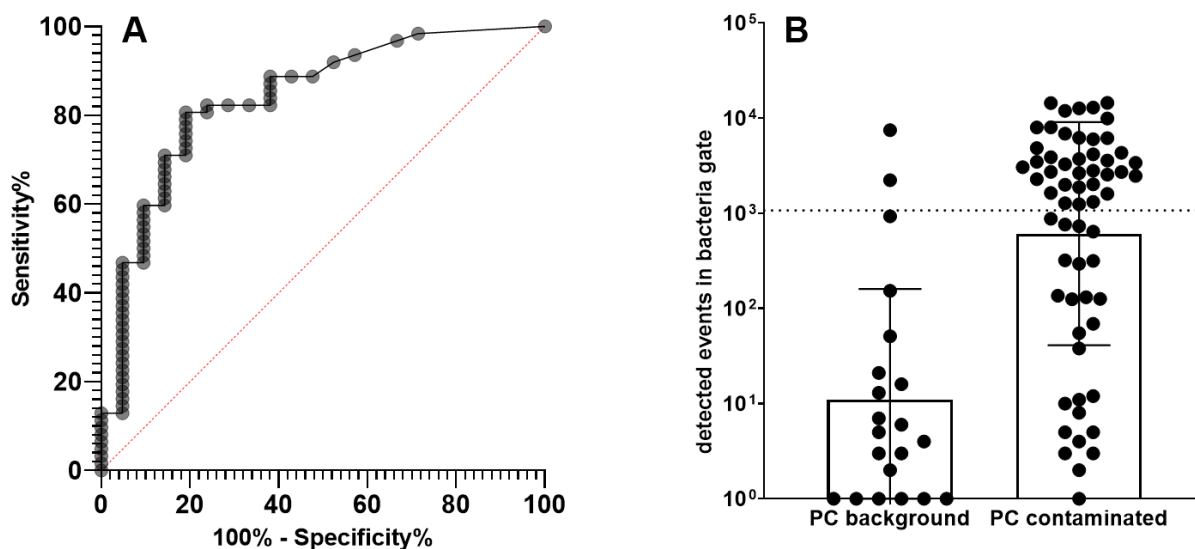


Figure 28: Analysis of the classification performance of the flow cytometric method for contaminated and non-contaminated PC without the platelet aggregation inhibitor Tirofiban

The area under the receiver operating characteristic curve was calculated with the detected fluorescence events from the flow cytometry measurements of spiked PC (10^3 - 10^5 CFU/ml *K. pneumoniae*, *B. cereus*, *S. epidermidis*, *S. aureus*, *E. coli*, *E. cloacae*, *B. thuringiensis*) and non-contaminated PC samples ($n_{\text{negative control}} = 21$; $n_{\text{contaminated}} = 62$; Std. Error = 0.052; 95 % CI = 0.736 -0.941; p value = <0.0001) (A). The calculated discrimination threshold of 1072 fluorescent events was defined as classification limit between the event background of the negative control and contaminated PC (dashed line). Error bars show the mean value of detected events ± 1 SD (B).A

To evaluate the effect of introducing a Tirofiban incubation step on the analytical accuracy of the flow cytometry method, samples from 12 individual PC spiked with *K. pneumoniae* and *B. cereus* and from 15 PC spiked with *S. epidermidis* at concentrations of 10^2 - 10^5 CFU/ml were prepared for analysis by the established flow cytometry method including tirofiban.

Data acquisition was performed according to the previously defined bacteria gating strategy (chapter 4.2.1, Fig. 21) and counted events were compared to the respective negative controls (chapter 7.4, Fig. 49). An AUROC classifier was calculated for contaminated and non-contaminated PC samples (Fig. 29 A). AUROC calculated a discrimination threshold of 19 fluorescent events, resulting in 85 % (95 % CI, 77.2 %–90.4 %) sensitivity and 96.5 % (95 % CI, 91.3 %–98.6 %) specificity for the detection of bacterial contaminations in PC in the range of 10^3 - 10^5 CFU/ml from the non-contaminated PC negative references (Fig. 29 B). Flow cytometry data corresponding to PC spiked with 10^2 CFU/ml was excluded from the analysis, as the mean events were in the same range as the background mean events of the non-contaminated PC negative references, leading to a sensitivity under 50 % (chapter 7.4, Fig. 49 D). PC samples were

considered positive, if their bacteria-specific count was \geq the calculated discrimination threshold of 19 fluorescent events.

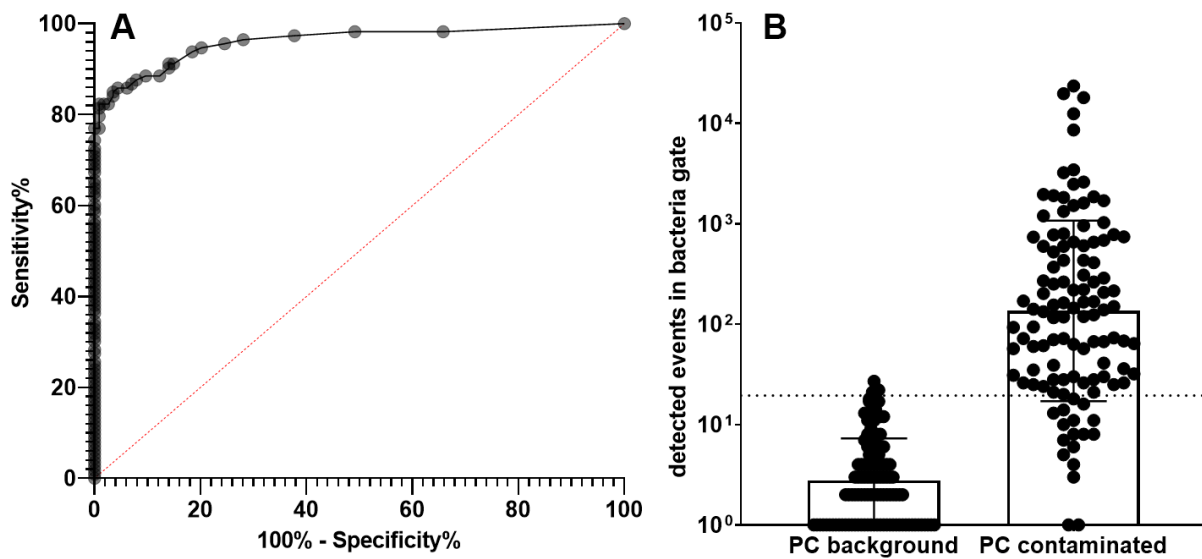


Figure 29: Analysis of the classification performance of the flow cytometric method for contaminated and non-contaminated PC using the platelet aggregation inhibitor Tirofiban

The area under the receiver operating characteristic curve was calculated with the detected fluorescence events from the flow cytometry measurements of spiked PC (10^3 - 10^5 CFU/ml *K. pneumoniae*, *B. cereus* and *S. epidermidis*) and non-contaminated PC samples ($n_{\text{negative control}} = 114$; $n_{\text{contaminated}} = 113$; Std. Error = 0.013; 95 % CI = 0.936 -0.986; p value = <0.0001) (A). The calculated discrimination threshold of 19 fluorescent events was defined as classification limit between the event background of the negative control and contaminated PC (dashed line). Error bars show the mean value of detected events ± 1 SD (B).

S. aureus could not be detected using the default staining protocol (chapter 3.6.1). Due to the adjustment of the method workflow, an AUROC classifier was calculated specifically for *S. aureus* spiked PC samples (Fig. 30 A). The calculated discrimination threshold of 1.562 fluorescent events resulted in 100 % (95 % CI, 75.75 %–100 %) sensitivity and 100 % (95 % CI, 43.85 %–100 %) specificity of bacterial detection in PC at concentrations of 10^2 - 10^5 CFU/ml (Fig. 30 B). PC samples were tested positive for bacteria, when the bacteria-specific event counts were \geq the calculated discrimination threshold of 1.562 fluorescent events.

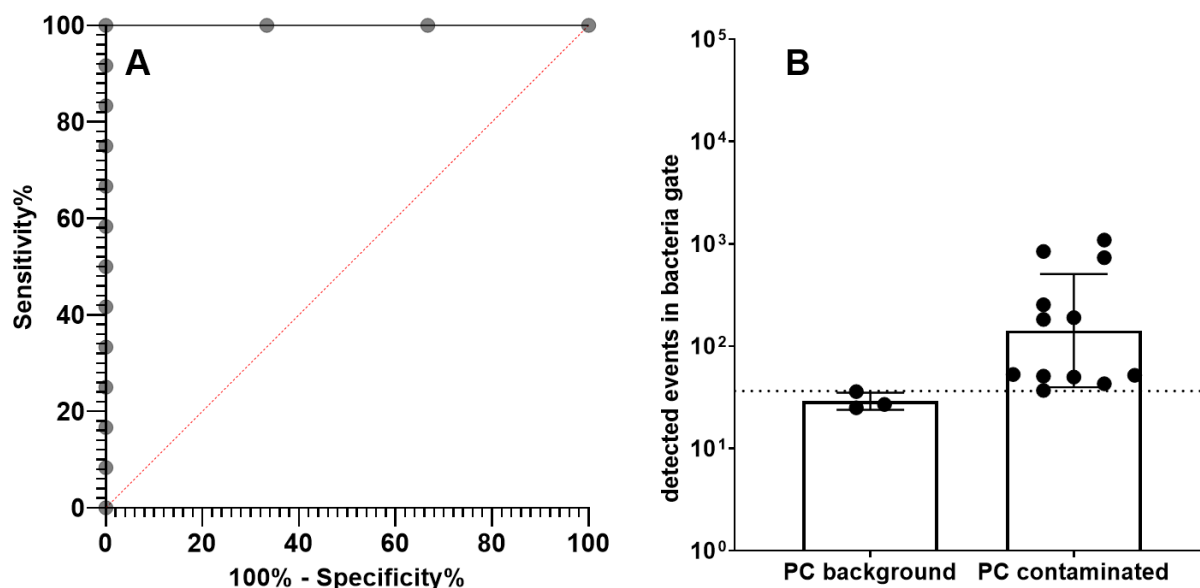


Figure 30: AUROC analysis of *S. aureus* contaminated PC and non-contaminated PC

An area under the receiver operating characteristic curve was calculated with the detected events from the flow cytometry data of *S. aureus* spiked PC in the range of 10^2 - 10^5 CFU/ml and negative references of non-contaminated PC samples ($n_{\text{negative control}} = 3$; $n_{\text{contaminated}} = 12$; Std. Error = 0.000; 95 % CI = 1.000; p value = <0.0094) (A). The calculated discrimination threshold of 34 fluorescent events was defined as classification limit between the event background of the negative control and contaminated PC (dashed line). Error bars indicate mean of detected events ± 1 SD (B).

4.2.5 Screening for bacterial contaminations spiked in PC samples using the flow cytometry method under standardized conditions

The overall detection of bacteria in PC samples depending on contamination level was determined (Tab. 21 + 23), and the specific detection for different transfusion-relevant bacterial strains was evaluated (Tab. 22 + 24) using the previously calculated discrimination thresholds (chapter 4.2.4, Fig. 28-30). The mean bacterial counts spiked in the respective PC samples were verified by preparing dilution series of the corresponding spiking solutions (10^2 - 10^5 CFU/ml) (chapter 7.5, Tab. 31 and chapter 7.6, Tab. 32).

4.2.5.1 Bacterial detection in PC samples by the flow cytometry method is decreased by omitting the Tirofiban incubation step

To determine the overall bacterial detection of the established flow cytometry method dependent on contamination level and examined bacterial strain, PC samples spiked with 10^2 - 10^5 CFU/ml of *K. pneumoniae*, *B. cereus*, *S. epidermidis*, *S. aureus*, *E. coli*, *E. cloacae* and *B. thuringiensis* were analysed with the flow cytometry method without the addition of Tirofiban (according to chapter 3.6.1). Counted bacterial events of the spiked PC and non-contaminated PC negative control were

displayed in a common bar chart (Fig. 31) to calculate the overall detection per contamination level (Tab. 21).

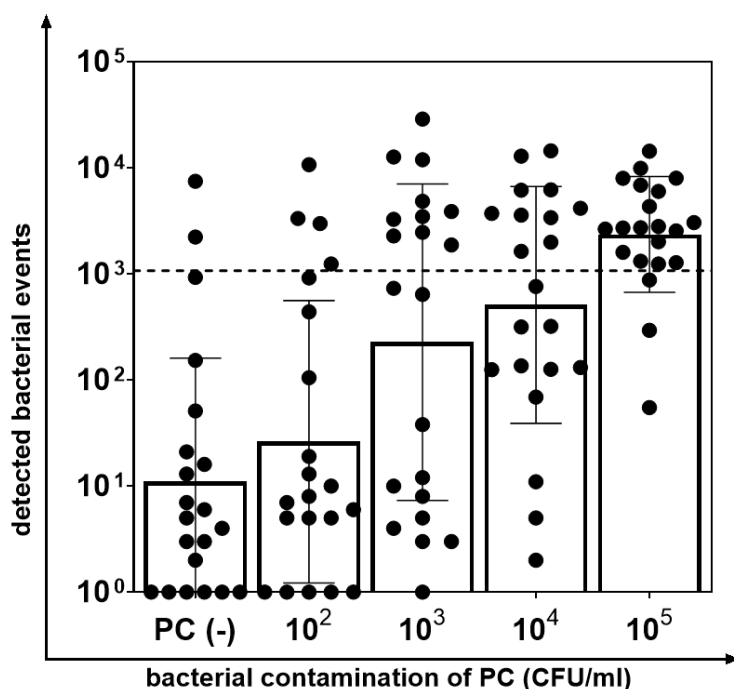


Figure 31: Flow cytometric detection of bacterial events of WHO Repository (PTRBR) strains spiked in PC samples at different concentrations without using Tirofiban

PC samples were spiked with 10^2 - 10^5 CFU/ml of *K. pneumoniae*, *B. cereus*, *S. epidermidis*, *S. aureus*, *B. thuringiensis*, *E. coli* and *E. cloacae* and analysed using the flow cytometry method without the Tirofiban incubation step. Events detected in the bacteria SSC/DRAQ5™ gate (chapter 4.2.1, Fig. 21) were counted and displayed as one data point. The calculated discrimination threshold of 1072 fluorescence events (chapter 4.2.4, Fig. 28) was defined as classification limit between the event background of the negative control and contaminated PC (dashed line). Error bars indicate mean of detected events \pm 1 SD. n= 3 (independent PC bags).

Without Tirofiban incubation step, it was possible to detect 19 % of all PC samples spiked with *K. pneumoniae*, *B. cereus*, *S. epidermidis*, *S. aureus*, *E. coli*, *E. cloacae* and *B. thuringiensis* at a contamination level of 10^2 CFU/ml. At a contamination level of 10^3 and 10^4 CFU/ml it was possible to detect 48 % and at 10^5 CFU/ml it was possible to detect 86 % of all PC samples spiked with the respective bacterial strains (Tab. 21).

Table 21: Overall detection of contaminated PC samples using the new flow cytometry method (without Tirofiban)

| | |
|---|------|
| Investigated PC samples* | 21 |
| Positive detected samples at 10 ² CFU/ml | 19 % |
| Positive detected samples at 10 ³ CFU/ml | 48 % |
| Positive detected samples at 10 ⁴ CFU/ml | 48 % |
| Positive detected samples at 10 ⁵ CFU/ml | 86 % |

*Biological replicates from one PC bag each.

After evaluation of the overall detection, data was subdivided into strain specific detection (Tab. 22; chapter 7.5, Fig. 50-56). At a contamination level of 10² CFU/ml PC samples contaminated with *K. pneumoniae*, *B. cereus* and *S. aureus* could not be detected. *S. epidermidis* and *B. thuringiensis* were detected positive for presence of bacteria in 33% of the PC samples, while it was possible to detect bacteria in 66 % of samples spiked with *E. coli*.

At a contamination level of 10³ CFU/ml per PC sample, *S. aureus* could not be detected by the flow cytometric method. *K. pneumoniae* and *E. cloacae* showed a detection of 33 % and *B. cereus* of 66 %. Furthermore, it was possible to detect all replicates (100 %) contaminated with *B. thuringiensis* and *E. coli*.

33 % of all PC samples spiked with 10⁴ CFU/ml of *S. aureus* or *B. cereus* were detected positive for presence of bacteria. PC samples spiked with *E. coli* and *E. cloacae* were identified positive with a detection of 66 % each, whilst all PC bags (100 %) spiked with *B. thuringiensis* were detected. At this contamination level, the mean bacterial events of *K. pneumoniae* were below the discrimination threshold and hence could not be detected (chapter 7.5, Fig. 51).

At a contamination level of 10⁵ CFU/ml it was possible to detect *S. aureus*, *S. epidermidis* and *E. cloacae* at a detection of 66 % each, whereas all PC bags spiked with *K. pneumoniae*, *B. cereus*, *B. thuringiensis* and *E. coli* were detected as positive for presence of bacteria (Tab. 22).

Table 22: Strain specific detection of contaminated PC samples using the new flow cytometry method (without Tirofiban)

| Bacterial strain | <i>K. pneumoniae</i> | <i>B. cereus</i> | <i>S. epidermidis</i> | <i>S. aureus</i> |
|---|----------------------|------------------|-----------------------|------------------|
| Investigated PC samples* | 3 | 3 | 3 | 3 |
| Positive detected samples at 10 ² CFU/ml | 0 % | 0 % | 33 % | 0 % |
| Positive detected samples at 10 ³ CFU/ml | 33 % | 66 % | 0 % | 0 % |
| Positive detected samples at 10 ⁴ CFU/ml | 0 % | 33 % | 0 % | 33 % |
| Positive detected samples at 10 ⁵ CFU/ml | 100 % | 100 % | 66 % | 66 % |

| Bacterial strain | <i>B. thuringiensis</i> | <i>E. coli</i> | <i>E. cloacae</i> |
|---|-------------------------|----------------|-------------------|
| Investigated PC samples* | 3 | 3 | 3 |
| Positive detected samples at 10 ² CFU/ml | 33 % | 66 % | 0 % |
| Positive detected samples at 10 ³ CFU/ml | 100 % | 100 % | 33 % |
| Positive detected samples at 10 ⁴ CFU/ml | 100 % | 66 % | 66 % |
| Positive detected samples at 10 ⁵ CFU/ml | 100 % | 100 % | 66 % |

*Biological replicates from one PC bag each.

4.2.5.2 Introduction of a Tirofiban incubation step leads to improved results in bacterial screening of PC by flow cytometry

12 PC samples contaminated with 10^2 - 10^5 CFU/ml *K. pneumoniae* or *B. cereus* and 15 PC samples contaminated with 10^2 - 10^5 CFU/ml *S. epidermidis* were measured and analysed using the new flow cytometry method with the Tirofiban incubation step (chapter 3.6.1). Counted events of the contaminated PC and non-contaminated PC negative references were displayed in a common bar chart (Fig. 32), to calculate the overall detection per contamination level (Tab. 23).

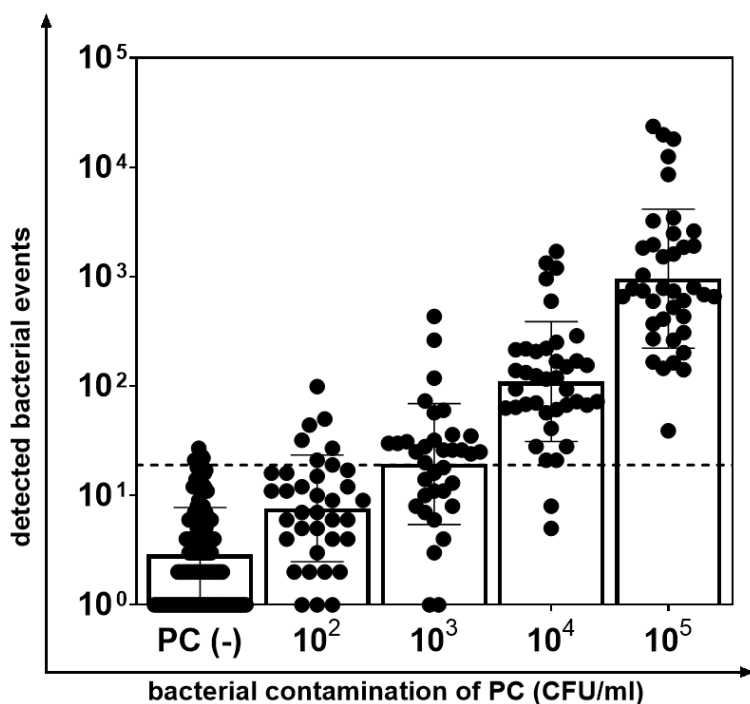


Figure 32: Flow cytometric detection of bacterial events of WHO Repository (PTRBR) strains spiked in PC samples at different concentrations with Tirofiban

PC samples were spiked with 10^2 - 10^5 CFU/ml of *K. pneumoniae* (n= 12), *B. cereus* (n= 12) and *S. epidermidis* (n= 15) and analysed using the flow cytometry method with the Tirofiban incubation step (independent PC bags). Data points with exceptionally high event numbers and visibly incomplete lysis were excluded from the data set and the corresponding bags were excluded in the calculation of the detection (Tab. 25) and are not shown in the illustration (chapter 7.6, Fig. 57-59). Events detected in the bacteria SSC/DRAQ5™ gate (chapter 4.2.1, Fig. 21) were counted and displayed as one data point. The calculated discrimination threshold of 19 fluorescence events (chapter 4.2.4, Fig. 29) was defined as classification limit between the event background of the negative control and contaminated PC (dashed line). Error bars indicate mean of detected events \pm 1 SD.

It was possible to detect 19 % of PC samples contaminated with *K. pneumoniae*, *B. cereus* and *S. epidermidis* at a contamination level of 10^2 CFU/ml with the new flow cytometry method including the Tirofiban incubation step. At a contamination level of 10^3 CFU/ml it was possible to detect 57

% of contaminated PC samples. At a contamination of 10^4 CFU/ml it was possible to detect 95 % of contaminated samples and at 10^5 CFU/ml, 100 % of all samples were detected (Tab. 23).

Table 23: Overall detection of contaminated PC samples using the new flow cytometry method (with Tirofiban)

| | |
|--|-----------------|
| Investigated PC samples* | 39 ⁺ |
| Positive detected samples at 10^2 CFU/ml | 19 % |
| Positive detected samples at 10^3 CFU/ml | 57 % |
| Positive detected samples at 10^4 CFU/ml | 95 % |
| Positive detected samples at 10^5 CFU/ml | 100 % |

⁺ Data points with exceptionally high event number and visibly incomplete lysis were excluded from the data set the corresponding bags were excluded in the calculation of the detection (chapter 7.6, Fig. 57-59). *Biological replicates from one PC bag each.

After evaluation of the overall detection, data was separated into strain specific detection (Tab. 24; chapter 7.6, Fig. 57-60). At a concentration of 10^2 CFU/ml *B. cereus* in PC samples, bacteria were not detectable with the new flow cytometry method. *S. epidermidis* was detected in 33% of the spiked PC samples and *K. pneumoniae* was detected at a rate of 18 %.

The detection of *K. pneumoniae* in PC samples at a contamination level of 10^3 CFU/ml was 73 %, *S. epidermidis* could be detected in 57% and *B. cereus* in 40 % of the tested samples at this contamination level.

At a contamination level of 10^4 CFU/ml, it was possible to detect 100 % of all spiked PC samples independent of the bacterial strain. Only samples contaminated with *B. cereus* were detected in only 83 % of the tested samples. At a contamination level of 10^5 CFU/ml all bacteria were detected in PC samples, independently from the tested bacterial strain (Tab. 24). As *S. aureus* could not be detected using the default staining protocol, a specific discrimination threshold for the detection of *S. aureus* in PC was calculated for the data analysis (chapter 4.2.4, Fig. 30). 3 PC bags were contaminated with 10^2 - 10^5 CFU/ml *S. aureus* and analysed by flow cytometry, using the adjusted flow cytometry workflow (chapter 3.6.1). Results were displayed in a bar chart (chapter 7.6, Fig. 60). By using the adjusted flow cytometry method specified for *S. aureus*, it was possible to detect

S. aureus in 100% of the spiked PC samples independent of the examined contamination level (Tab. 24).

Table 24: Strain specific detection of contaminated PC samples using the new flow cytometry method (with) Tirofiban)

| Bacteria strain | <i>K. pneumoniae</i> | <i>B. cereus</i> | <i>S. epidermidis</i> | <i>S. aureus</i> ⁺ |
|--|----------------------|------------------|-----------------------|-------------------------------|
| Investigated PC samples* | 12 ⁺ | 12 ⁺ | 15 ⁺ | 3 |
| Positive detected samples at 10 ² CFU/ml | 18 % | 0 % | 33 % | 100 % |
| Positive detected samples at 10 ³ CFU/ml | 73 % | 40 % | 57 % | 100 % |
| Positive detected samples at 10 ⁴ CFU/ml | 100 % | 83 % | 100 % | 100 % |
| Positive detected samples at 10 ⁵ CFU/ml | 100 % | 100 % | 100 % | 100 % |

⁺ Data points with exceptionally high event number and visibly incomplete lysis were excluded from the data set the corresponding bags were excluded in the calculation of the detection (chapter 7.6, Fig. 57-59). ^{*}Calculated with the discrimination threshold for the detection of *S. aureus* in PC (chapter 4.2.4, Fig. 30). ^{*}Biological replicates from one PC bag each.

Overall, the introduction of Tirofiban into the assay led to a lower discrimination threshold between non-contaminated and contaminated samples when incubated with Tirofiban. The background events of the negative references treated with Tirofiban were more constant and lower (chapter 4.2.4, Fig. 29), than the background events of the untreated samples, which had higher overall background events and a high variation in the number of events (chapter 4.2.4, Fig. 28). Similar to non-contaminated samples without Tirofiban incubation step, untreated contaminated PC samples showed significantly higher event counts in the bacteria detection gate (chapter 4.2.5.1, Fig. 31) than comparable samples with Tirofiban treatment (chapter 4.2.5.2, Fig. 32). However, after direct comparison of the untreated samples with Tirofiban-treated samples (chapter 4.2.2, Fig. 22-25), it became clear that the increased event count of the former was caused by non-specifically stained platelets and cell debris.

With the new flow cytometry method with inhibition of platelet aggregation by Tirofiban it was possible to reliably detect WHO Repository (PTRBR) bacterial strains in PC. In the following, this method will be compared with the detection of bacterial contamination in PC using the commercially available, Ph. Eur.-compliant RMM; the BactiFlow® system.

4.3 Detection of bacterial contaminations in PC samples using the BactiFlow® system

To compare the newly developed staining protocol with the Ph. Eur.-compliant BactiFlow® analysis system, all spiked PC samples were prepared in duplicates with identical bacterial concentrations (chapter 7.5, Tab. 31 and chapter 7.6, Tab. 32) and were analysed simultaneously with both methods (according to chapter 3.6.1 [Flow cytometry method] and 3.7.4 [BactiFlow®]). The BactiFlow® system has a defined threshold for the detection of bacteria, which is 300 counts/ml. Counted bacterial events of the spiked PC and non-contaminated PC were displayed in a bar chart (Fig. 33) to determine the detection rate of contaminated PC per investigated contamination level (Tab. 25).

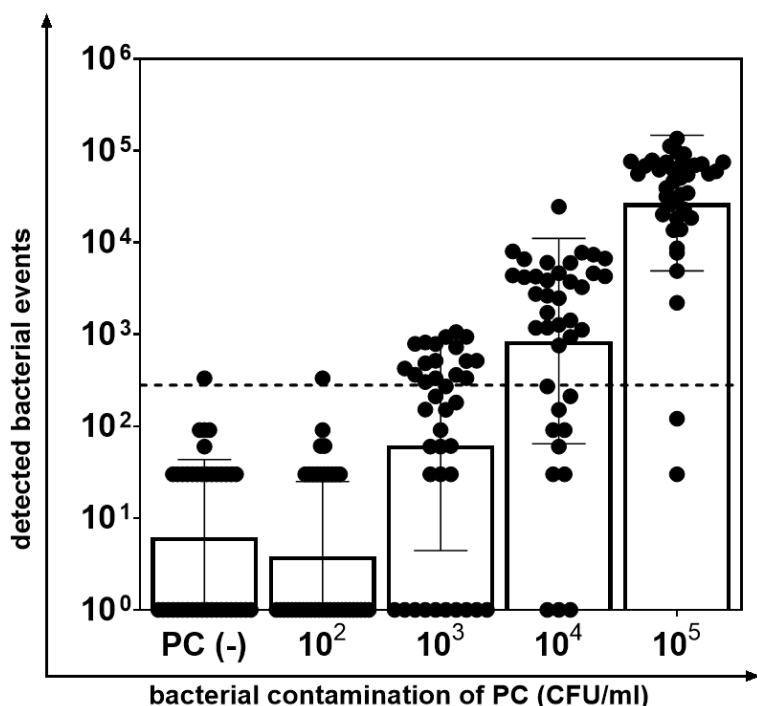


Figure 33: Detected bacterial events of WHO Repository (PTRBR) strains spiked in PC samples at different contamination levels analysed with the BactiFlow® system

PC samples were spiked with 10^2 - 10^5 CFU/ml of *K. pneumoniae*, *B. cereus*, *S. epidermidis* and *S. aureus* and analysed using the BactiFlow® system. Classification of non-contaminated PC and contaminated PC was performed by the BactiFlow® system based on the defined LOD of 300 counts/ml (dashed line). Error bars indicate mean of detected events \pm 1 SD. (n=39)

With the BactiFlow® system, it was possible to reach an overall detection of 3 % of all PC samples spiked with *K. pneumoniae*, *B. cereus*, *S. epidermidis* and *S. aureus* at a contamination level of 10^2 CFU/ml. At a contamination level of 10^3 CFU/ml 44 % of PC samples spiked with those bacteria were detectable. At a contamination level of 10^4 CFU/ml it was possible to detect 72 % of the spiked PC samples and at 10^5 CFU/ml, 95 % of all spiked PC samples were detected (Tab. 25).

Table 25: Overall detection of contaminated PC samples using the BactiFlow® system

| | |
|--|------|
| Investigated PC samples* | 39 |
| Positive detected samples at 10^2 CFU/ml | 3 % |
| Positive detected samples at 10^3 CFU/ml | 44 % |
| Positive detected samples at 10^4 CFU/ml | 72 % |
| Positive detected samples at 10^5 CFU/ml | 95 % |

*Biological replicates from one PC bag each.

Furthermore, the detection of each examined bacterial strain (chapter 7.7, Fig. 61-64) were calculated from the BactiFlow® bacterial event counts at the indicated contamination levels (Tab. 26). At a contamination level of 10^2 CFU/ml, 8 % of *K. pneumoniae* spiked PC samples were detected, while samples spiked with *B. cereus*, *S. epidermidis* and *S. aureus* were not detected.

The BactiFlow® system allowed for the detection of all investigated bacteria in PC, starting at a contamination level of 10^3 CFU/ml. At this contamination level, 17 % of *K. pneumoniae* spiked PC samples were detected and it was possible to detect 50 % of samples contaminated with *B. cereus* and *S. epidermidis*, respectively. Furthermore, the BactiFlow® system detected all samples spiked with *S. aureus* beginning at the contamination level of 10^3 CFU/ml.

At a contamination level of 10^4 CFU/ml, 100 % of samples spiked with *B. cereus* were detectable by BactiFlow®, while only 42 % of samples spiked with *K. pneumoniae* and 67 % of samples spiked with *S. epidermidis* were detected as positive for the presence of bacteria in the PC sample.

At a contamination level of 10^5 CFU/ml, 83 % of PC samples spiked with *K. pneumoniae* were detected, while all samples spiked with *B. cereus* and *S. epidermidis* were detectable with the BactiFlow® system (Tab. 26).

Table 26: Detection of indicated bacterial strains spiked in PC samples using the BactiFlow® system

| Bacterial strain | <i>K. pneumoniae</i> | <i>B. cereus</i> | <i>S. epidermidis</i> | <i>S. aureus</i> |
|---|----------------------|------------------|-----------------------|------------------|
| Investigated PC samples | 12 | 12 | 12 | 3 |
| Positive detected samples at 10^2 CFU/ml | 8 % | 0 % | 0 % | 0 % |
| Positive detected samples at 10^3 CFU/ml | 17 % | 50 % | 50 % | 100 % |
| Positive detected samples at 10^4 CFU/ml | 42 % | 100 % | 67 % | 100 % |
| Positive detected samples at 10^5 CFU/ml | 83 % | 100 % | 100 % | 100 % |

*Biological replicates from one PC bag each.

4.4 Bacterial screening of bacteria grown in PC bags

To detect bacteria grown in PC bags under real life storage conditions with either the new flow cytometry method or the BactiFlow® system, PC bags were inoculated with a low number of bacteria, according to the spiking protocol of chapter 3.3.3. PC bags were stored under standard storing conditions and samples of contaminated and non-contaminated PC negative references were taken after 12, 14, 16, 18 and 21 h of incubation time, respectively 48, 52, 55, 60, 70, 82 and 101 h for samples contaminated with *S. epidermidis*. Samples were analysed with the new flow cytometry method including the Tirofiban incubation step and the BactiFlow® system.

4.4.1 Bacterial growth detection of transfusion-relevant bacteria in PC bags by the new flow cytometry method in comparison to BactiFlow®

The BactiFlow® system enabled the detection of 56 % of PC bags spiked with *K. pneumoniae* after 12 h and of 78 % after 15 h. After 18 h and 21 h of incubation, 100 % of the samples were tested positive for bacterial contamination (Fig. 34 A).

For *K. pneumoniae*, the mean bacterial concentration was 7.9×10^2 CFU/ml (1×10^2 - 2×10^3 CFU/ml) after 12 h of incubation. After 15 h of incubation, the mean bacteria concentration was 7.5×10^3 CFU/ml (2.5×10^3 - 1.5×10^4 CFU/ml), 5.6×10^4 CFU/ml (2.3×10^4 CFU/ml – 9.6×10^4 CFU/ml) after 18 h and 6.3×10^5 CFU/ml (1.8×10^5 CFU/ml – 1.4×10^6) after 21 h (Fig 34 B).

The new flow cytometry method (including Tirofiban) detected 33 % of PC bags contaminated with *K. pneumoniae* after 12 h of incubation mean bacterial concentration was 7.9×10^2 CFU/ml (1×10^2 - 2×10^3 CFU/ml)]. After 15 h of incubation 44 % of samples and after 18 and 21 h 100% of the samples were tested positive for the presence of bacteria (Fig. 34 A).

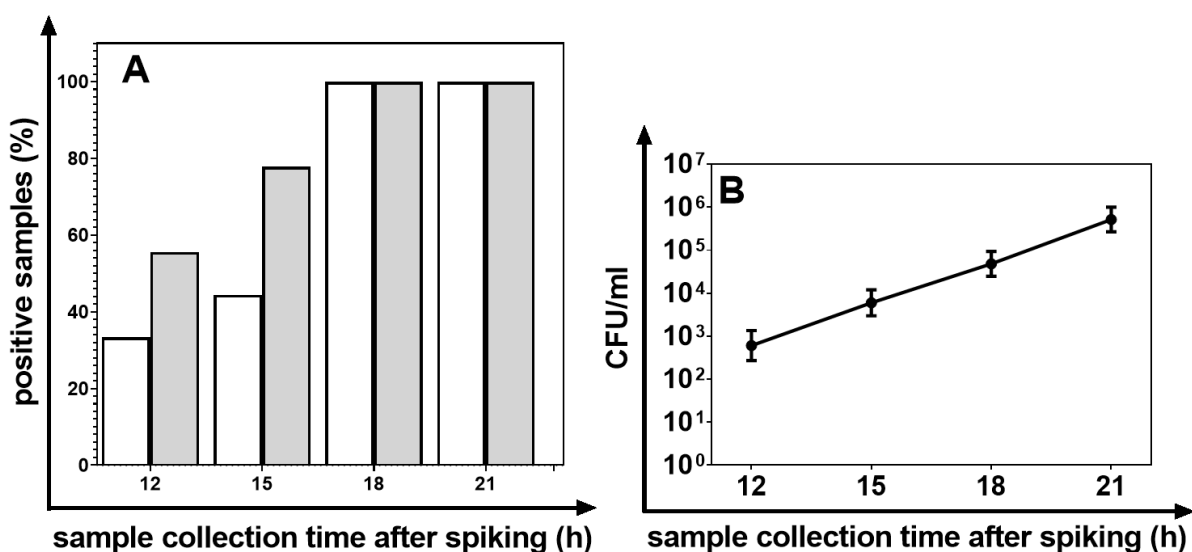


Figure 34: Growth of *K. pneumoniae* spiked in PC bags

Samples from PC bags spiked with 2-5 CFU/bag (n= 9) were collected after 12, 15, 18 and 21 h and analysed with the flow cytometric method (white) as well as the BactiFlow® system (grey) (A). At each time point a sample of 3 ml was collected from each PC bag. 1 ml each was processed according to the respective method protocol. Additionally, 1ml of the sample was used to prepare a dilution series and was plated out in triplicates on Standard I Nutrient Agar plates to determine the number of bacteria per PC bag at the respective time point. Error bars indicate mean CFU/ml \pm 1 SD (B).

After 12 h of incubation, PC bags spiked with *B. cereus* were not detected as positive for bacteria by the BactiFlow® system. After 15 h, 11 % of samples were tested positive and after 18 and 21 h 33 % of samples were detected positive for *B. cereus* (Fig. 35 A).

For *B. cereus*, the mean bacteria concentration was 1.3×10^3 CFU/ml (8×10^1 - 3.7×10^3 CFU/ml) after 12 h of incubation. After 15 h of incubation, the mean bacteria concentration was 9.5×10^3 CFU/ml (1.5×10^3 - 1.9^4 CFU/ml), 3.6×10^4 CFU/ml (1.3×10^4 CFU/ml – 7.4×10^4 CFU/ml) after 18 h and 2.9×10^6 CFU/ml (1.5×10^5 CFU/ml – 8.1×10^6) after 21 h (Fig. 35 B).

The new flow cytometry method was not able to detect any PC samples contaminated with *B. cereus* after 12 h of incubation. After 15 h, 33 % of samples were tested positive for presence of bacteria and after 18 h and 21 h all replicates were tested positive (Fig. 35 A).

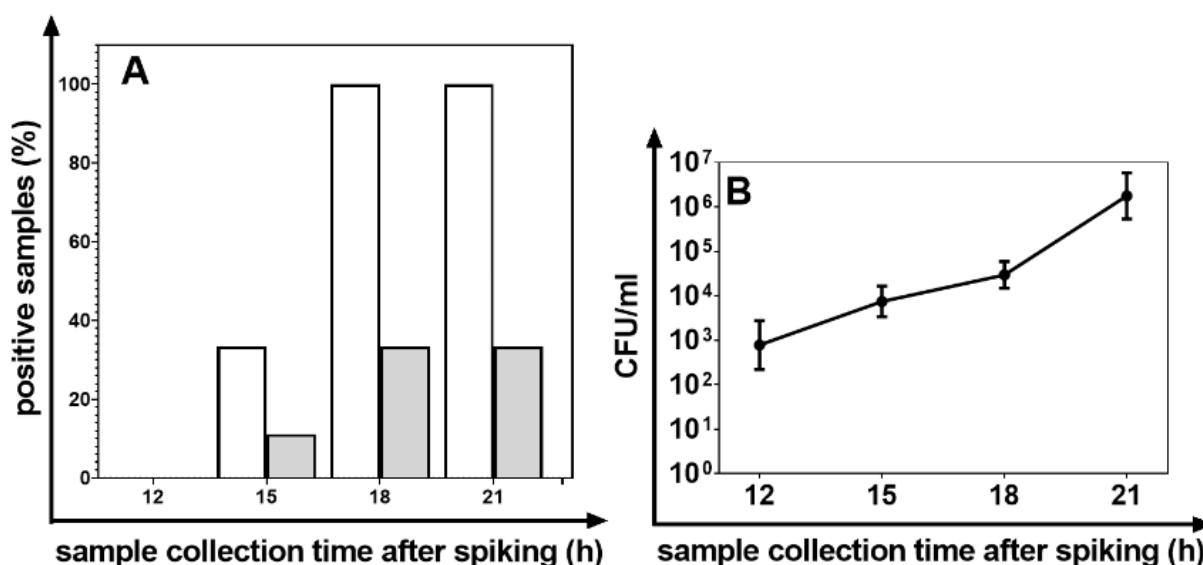


Figure 35: Growth of *B. cereus* spiked in PC bags

Samples from PC bags spiked with 2-5 CFU/bag ($n=9$) were collected after 12, 15, 18 and 21 h and analysed with the flow cytometric method (white) as well as the BactiFlow® system (grey) (A). At each time point a sample of 3 ml was collected from each PC bag. 1 ml each was processed according to the respective method protocol. Additionally, 1ml of the sample was used to prepare a dilution series and was plated out in triplicates on Standard I Nutrient Agar plates to determine the number of bacteria per PC bag at the respective time point. Error bars indicate mean CFU/ml \pm 1 SD (B).

PC bags spiked with *S. epidermidis* were not detected by the BactiFlow® system until 52 h of incubation. After 52 h, 33 % of samples were tested positive for *S. epidermidis* and 66 % after 55 h, 60 h and 70 h of incubation. After 82 h to 101 h of incubation, *S. epidermidis* was detected in all measured samples (Fig. 36 A).

PC samples spiked with *S. epidermidis* could not be detected by the new flow cytometry method until 82 h of incubation. After 82 h, 66 % of samples and after 101 h of incubation all samples were detected positive (Fig. 36 A).

PC contaminated with *S. epidermidis* could not be detected with either method in the time between 12 to 21 h of incubation. After 21 h of incubation, *S. epidermidis* could not be detected by culture either, due to very slow growth of the organism in PC samples. After 48 h of incubation, *S. epidermidis* showed a mean bacterial concentration in the PC samples of 5.9×10^1 CFU/ml (0 - 1.2×10^2 CFU/ml). After 52 h, *S. epidermidis* showed a mean bacterial concentration in PC of 1.2×10^2 CFU/ml (0 - 2.5×10^2 CFU/ml). After 55 h the mean bacterial concentration in PC was 1.87×10^2 CFU/ml (0 - 3.9×10^2 CFU/ml). After 60 h the mean bacterial concentration in PC was 3.87×10^2 CFU/ml (1.0×10^1 - 7.8×10^2 CFU/ml). After 70 h the mean bacterial concentration in PC was 2.3×10^3 CFU/ml (3.0×10^1 - 3.8×10^3 CFU/ml). After 82 h the mean bacterial concentration in PC was 1.4×10^4 CFU/ml (1.8×10^2 - 2.3×10^4 CFU/ml) and at after 101 h of incubation the mean bacterial concentration in PC was 2.68×10^5 CFU/ml (1.8×10^3 CFU/ml - 5.0×10^5) (Fig. 36 B).

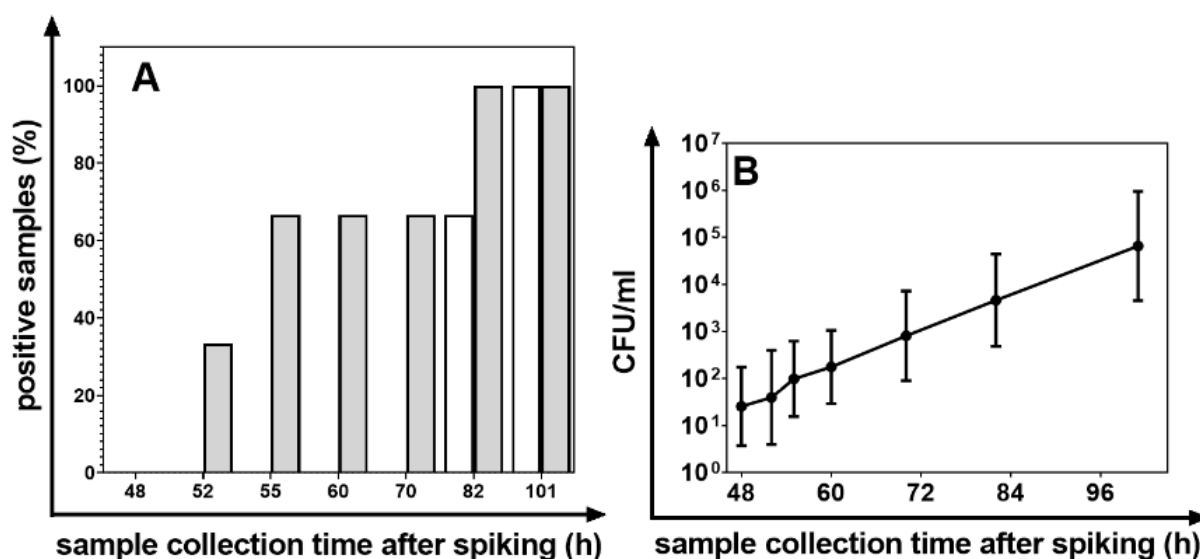


Figure 36: Growth of *S. epidermidis* spiked in PC with 2-5 CFU/bag

Samples from PC bags spiked with 2-5 CFU/bag (n= 2) were taken after 48, 52, 55, 60, 70, 82 and 101 h and analysed with the new flow cytometric method (white) as well as the BactiFlow® system (grey) (A). For each time point, a sample of 3 ml was collected from each PC bag. 1 ml each was processed according to the respective method protocol. Additionally, 1ml of the sample was used to prepare a dilution series and was plated out in triplicates on Standard I Nutrient Agar plates to determine the number of bacteria per PC bag at the respective time point. Error bars indicate mean CFU/ml \pm 1 SD (B).

5 Discussion

5.1 Raman microspectroscopy

5.1.1 Challenges of bacterial contaminant detection in PC using Raman microspectroscopy

The aim of this thesis was to determine whether Raman microspectroscopy is a suitable RMM for the detection of bacteria in PC. Current culture-based methods, although sensitive, take considerable time to detect, require significant sample volumes and are not mandatory, but are only performed for routine quality control [52,66]. In addition, due to the "negative-to-date" product release concept of PC, patients continue to be at risk of a TTID [64,65].

Raman microspectroscopy is a non-invasive method to analyse biological samples on a molecular level without complex sample preparation and labelling of biomolecules. In this thesis, the detection of bacterial contaminations in PC by Raman microspectroscopy measurements were technically feasible in less than 30 min, requiring only a sample volume of 200 μ l and no further sample preparation before measurement. Our results indicated that *K. pneumoniae* contaminations in PC were reliably detected at approximately 1×10^8 CFU/ml, 28-32 h after spiking (see chapter 4.1.1, Tab. 19).

One of the reasons for the low sensitivity of the Raman microspectroscopy method used, is the variety of spectral signals due to the complex composition of biological matrices, such as proteins, nucleic acids, lipids and carbohydrates, which overlap with the spectra of interest and create a high level of complexity during data analysis [214]. Also, PC not only consist of platelets, but also contain residual corpouscular cells, e.g., erythrocytes and leukocytes, as well as immunoglobulines and other plasma compounds and PAS, each contributing to the Raman spectra of the examined sample. Here, the biological variability between PC units plays a minor role, because although the general complex composition of PC leads to a complex Raman spectrum, it only reflects the general chemical composition of the blood product and cannot depict the biological variance within blood donors without further specific analysis of the data. Therefore, it is challenging to distinguish the subtle changes in the Raman spectra of contaminated versus non-contaminated PC.

Key features of the contaminants have to be identified and extracted, to differentiate the spectral information of interest from the surrounding matrix. As mentioned above, PC are a particularly challenging material regarding Raman microspectroscopic measurements due to a highly complex background signal, which makes the classification of non-contaminated and contaminated PC

samples considerably more difficult. The complex background signal results from sample specific properties described in the following. One PC contains at least 2×10^{11} platelets in a volume of 200 - 400 ml [23]. Even for PC contaminations with very high bacterial loads, the number of platelets in the transfusion bag is by several log levels higher in relation to the bacterial contaminant. This results in a fundamentally stronger intensity of platelet related Raman signals in comparison to the Raman signals of the contaminant. Furthermore, PC can contain up to 3×10^9 of residual erythrocytes per bag and a small number of leukocytes ($< 1 \times 10^6$ /bag) after preparation [23]. Erythrocytes contain Hemoglobin, which makes up $>95\%$ of the dried weight of these cells and is a very strong Raman scatterer, due to its highly conjugated heme sub-units [215]. We assume that Hemoglobin could be a relevant disruptive factor for Raman measurements of bacterial contaminants in PC, as its major Raman spectrum peak regions ($1300\text{-}1450\text{ cm}^{-1}$; $1500\text{-}1650\text{ cm}^{-1}$) overlap with the common wavenumber region of biological samples [216].

In this thesis, PC samples were investigated using a low energy near-infrared wavelength laser (785 nm) for excitation. This choice was based on the observation that biological systems are prone to auto-fluorescence and other effects, such as thermal decomposition or organic impurities, which may deteriorate or even completely mask a spectrum [217]. Therefore, low energy lasers are necessary to ensure that biological samples are not biochemically altered by the laser energy, thus falsifying the results by photo-induced destruction. However, the low energy laser combined with the measurement of a biological sample, whose molecular density is comparatively low, results in a very low intensity of the recorded Raman signals from the PC samples, leading to an unfavourable SNR between non-specific background Raman signals and the Raman signals of interest.

To conduct microbiological testing of PC without any further sample processing and a minimal hands-on-time, samples were measured directly in their aqueous storage solution (PAS). With spontaneous Raman scattering, the relatively low bacterial concentration in the PC solution results in the reduction of bacteria-specific Raman signals, and a low detection sensitivity for bacteria in PC. Therefore, our results indicate the need for refinement of the pre-analytical sample processing and/or modification of the Raman measurement technique used. For example, by further improvement of the SNR between Raman background signals and Raman signals of interest. In the current experiments the whole fingerprint region of biological samples ($600\text{ and }1800\text{ cm}^{-1}$) was measured and used for multivariate analysis. Here could lie a potential to further reduce the data to only the pertinent information, while limiting the dimension size by targeting only the most prominent peaks and further exclude interfering Raman signals of no interest.

5.1.2 Improvement of bacterial detection in PC by Raman spectroscopy

The spontaneous Raman scattering used in this thesis can be a powerful analytical tool for analysis of the chemical composition of biological samples. However, spectroscopic studies based on spontaneous Raman scattering involve serious drawbacks as the conversion efficiency of the Raman effect is fairly poor. Only a small number (1 in 1×10^8) of the laser photons are scattered inelastically [184], severely limiting the detection sensitivity of sample components with a very low concentration, such as bacteria in PC.

Platelets can be activated by bacteria via direct interaction or indirectly through bridging molecules or secreted bacterial products [218–220]. The changes in metabolism and phenotype (platelet activation/aggregation) can lead to specific chemical alterations in the PC matrix, which could be detectable in their respective Raman spectrum. These changes, if they can be defined, could be used as key spectral features for a more specific and sensitive detection of bacteria in PC, overcoming the limited detection sensitivity.

In addition, the identification of the bacteria themselves in the sample matrix could potentially be improved by defining contaminant-specific spectral features. For instance, Raman bands at 1027 and 1078 cm^{-1} were found to be key features in the Raman spectrum of *K. pneumoniae*. The first band is assigned to C–H in-plane bending of Phenylalanine. Chain C–C stretching of lipids as well as C–O and C–C stretching of carbohydrates can be assigned for the second band corresponding to lipid bilayers, lipopolysaccharides and the slime capsular polysaccharide (CPS) of *K. pneumoniae* [194]. However, these key features would have to be identified and defined in advance for each potential contaminant. These chemical changes in the sample, in turn, would have to be distinct enough to be reliably detectable within the PC matrix, while providing reproducible results. Here, the creation of a key-feature-panel would be conceivable, whereby all possible chemical differences must first be defined by the metabolic activity and or presence of all potential contaminants in the sample matrix.

The low sensitivity of the spontaneous Raman scattering measurements may be increased by pre-analytic bacterial enrichment, which results in an amplified Raman signal of potential bacterial contaminants in the sample. Selective enhancement of bacteria characteristic key components in the Raman spectra of samples would be possible by drying PC sample lysate drops on a suitable substrate. This method would be possible by using the so-called drop coating deposition Raman (DCDR). This would make it possible to reposition the plate in the device by turning the plate upside

down with the sample facing the laser, instead of measuring through the CaF₂ object carrier. The evaporation of the liquid allows the measurement of the concentrated sample components.

When using DCDR, a small volume in the range of μl to nl of an aqueous solution is concentrated through drying (coffee-ring drying pattern) on a special hydrophobic plate prior to Raman analysis [221]. DCDR facilitates the segregation and independent spectral characterization of mixture components. The quality of the spontaneous (non-enhanced) Raman spectra are significantly improved, because of reduced spectral interference from fluorescent impurities and liquid compounds of the respective solution [222].

With this method, the bacterial components of interest would first need to be characterized and then localized in the dried droplet. This could prove difficult as the remnants of lysed PC would be highly concentrated in the cellular components of the sample matrix as well. Therefore, the cellular components of the matrix would need to be separated from the potential bacteria prior to lysis to avoid overlap of components of interest with the matrix components. The small sample size would further increase the measurement error and decrease the amount of potentially detectable bacterial components, thus decreasing the overall sensitivity of the method.

Separation of bacteria suspended in PC by filtration would increase the potentially detectable bacterial components in the sample prior to Raman measurement. However, this would be a difficult procedure because the particle sizes of bacteria and platelets do not differ significantly, as bacteria (0.5 - 5 μm) [186] are approximately about the same size as the diameter of platelets (2 - 4 μm) [223]. The pliability of platelets would allow them to fit through 2-3 μm filter pores, which are required to allow rod-shaped enteric bacteria to pass unhindered. Further separation of bacteria and platelets might also be possible by developing a specific gradient centrifugation technique. Again, the separation of bacteria and platelets would be a major challenge, in this case because of similar sedimentation rates [224]. The development of a separation method of bacteria from a PC matrix requires more in-depth work and method validation experiments. Ultimately, elaborate protocols for pre-analysis would contradict the advantages of Raman microspectroscopy as a non-invasive RMM.

Special Raman techniques, such as resonance Raman spectroscopy (RRS) and surface-enhanced Raman scattering (SERS) can enhance the intensity of Raman signals by several orders of magnitude [217]. Resonance Raman spectroscopy (RRS) is based on the Resonance Raman effect (RRE) and involves the excitation with a laser energy that results in an electron transfer in the target molecule. This approach improves the scattering cross-section and can selectively enhance

spectral features [225]. For utilizing the RRE no special equipment, other than used for conventional Raman spectroscopy, is necessary. However, it may be suitable to use an adjustable laser, which allows the delivery of an appropriate excitation energy within the electronic absorption. For resonance Raman investigations, laser lines in the ultraviolet are often necessary, since many molecules absorb in the ultraviolet. However, the high costs of lasers and optics for this spectral region limits the usage of UV resonance Raman spectroscopy to a small number of specialists [217].

Surface-enhanced Raman spectroscopy (SERS) can enhance Raman scattering using metallic surfaces or nanoparticles, resulting in an improvement in detection sensitivity due to a combination of electromagnetic enhancement associated with plasmon excitation in the metallic particles and chemical enhancement due to the target molecules being able to transfer electrons to/from the metallic SERS substrate [213]. This technique can be performed either without labeling, in which case the observed bands are associated with the analytes themselves, or with indirect labeling using SERS labels capable of selectively identifying target molecules or binding sites. The characteristic spectrum of the SERS label changes in the presence of the analyte of interest, which can then be detected and analysed further [215].

SERS could be used in the context of bacterial contamination detection in PC to enhance the specific Raman signals from known cellular components of the contaminants, thereby lowering their detection limit. In a previous study, SERS was used for the detection and quantification of LPS adsorbed on the surface of gold nanoparticles. This resulted in an increase in a Raman signal intensity of about 6-7 orders of magnitude compared to LPS alone, which allowed a sensitive detection and quantification of LPS [226]. For the detection of contaminations in PC it would be required to investigate, whether the addition of nanoparticles to the PC samples and the subsequent Raman measurements can be performed directly or whether the sample needs to be pre-processed beforehand to minimize any interference between the nanoparticles and the sample matrix and to maximize sensitivity of the assay. If nanoparticles are used, which have to adsorb LPS before the Raman measurements, it would be useful to lyse the samples beforehand to maximize the amount of potential LPS in the sample and introduce an incubation step.

A SERS experiment consists of essentially the same components as conventional Raman spectroscopy. However, to optimize the electromagnetic surface-enhancement effect, the laser frequency used must match the frequency of a plasmon resonance [217].

Since the Raman microspectroscope Bioram® (CellTool GmbH, Tutzing, Germany) used in this thesis, has a fixed laser with a wavelength of 785 nm, it was not possible to install a tunable laser

to optimize the instrument for RRS investigations. SERS experiments could not be conducted either, regarding the requirement of a tunable laser. Since the Raman device measures samples through a laser light permeable substrate (CaF_2) which carries the sample material, SERS measurement designs based on a metallic surface were not possible either, since the sample would have to be measured upside down due to the construction type of the Bioram[®] device I. This setup was necessary to measure samples in aqueous solution. Therefore, these Raman techniques were not suitable for the further development of a rapid bacteria detection method in PC in the course of this thesis. In summary, it was possible to use spontaneous Raman microspectroscopy as a RMM for the detection of bacteria in PC in this thesis, while only using minimal sample volumes and without further sample preparation. However, the current technique did not achieve the sensitivity appropriate for a rapid test method characterized by a LOD of at least 10^5 CFU/ml bacteria [156].

Cell identification by Raman spectroscopy in general has been recognized to be an attractive diagnostic tool, because of its potential to provide comprehensive cellular phenotypic information at the single cell level. Although Raman spectroscopy is an established technique in various fields such as analytical chemistry and material science, it is still considered as an emerging tool in biomedical research and clinical settings. Most Raman studies regarding bacterial pathogens are based on pure bacterial isolates, which heavily rely on medium culture, while Raman spectra from actual clinical samples are still underrepresented [227,228].

As changes in Raman spectra are generally small and might even be affected by batch-to-batch variations of samples and/or daily variations of the instrument itself, standardization and comparability of measurements are the biggest challenges in Raman spectroscopy. Therefore, Raman cell studies should be performed preferably at the batch level rather than the cell level. If Raman data is collected over a period of several days, each cell type studied should be investigated on every day and a standardized instrument calibration procedure should be performed daily to ensure reproducible results and a robust classification model [229].

For clinical practice, databases with Raman spectra would be a crucial requirement to identify bacterial pathogens reliably and reproducibly using generally applicable Raman libraries. For these databases to work under clinical conditions, generally valid Raman spectra of environmental and patient derived samples are required, as current Raman databases are mainly instrument specific. [186].

The reason for the lack of generalized Raman libraries for biological samples is that they currently consist of tailor-made, workgroup-specific spectral databases with Raman spectra of samples measured with different technical parameters, calculated using subsequent statistical data evaluation steps with proprietary mathematical models. This greatly hinders the definition of standardized methods, which would be indispensable for comparability of results [228]. Raman spectroscopy has enormous potential in the field of medical diagnostics, but there is still a great need for research to integrate these methods into a clinical setting.

5.2 Flow Cytometry

5.2.1 Development of the new flow cytometry method for the detection of bacteria in PC

The prevention of TTIDs is an ongoing challenge, especially for blood products like PC, as there is currently no mandatory microbiological testing prior to PC transfusion in Germany [52,66]. PC are released based on the “negative-to-date” concept, which includes microbiological culture methods. This carries the risk of severe or even fatal transfusion reactions, as PC are released before a final test result is available [64,65]. When a PC tested positive for bacterial contamination using semi-automated blood culture systems, such as the Bact/ALERT®, a product recall must be performed. Since culture-based methods need up to several days until pathogen detection, the PC may have already been transfused and the recipient must be clinically monitored [168].

A RMM with a late sampling strategy shortly before transfusion and without a cultivation step could extend the shelf-life of PC and detect transfusion-relevant concentrations of pathogens in PC, while overcoming the drawbacks of culture-based assays. This approach would also minimize sampling errors, observed with early sampling strategies, as sampling within the first 24 h of PC storage can result in false negative results, because there are too few contaminants in the sample at that time [31,61,62]. Furthermore, semi-automated blood culture systems are only capable of detecting viable, culturable bacteria in PC, because these systems are based on the detection of CO₂, which is a by-product of the metabolism of bacteria [56].

Our goal was to develop a new rapid method based on flow cytometry without a culturing step, that would allow for testing shortly before transfusion to prevent severe sepsis and fatal adverse events.

Flow cytometric detection of bacterial DNA in PC may provide a solution for detecting contaminations with viable, but non-culturable as well as dead bacteria. In blood products such as

PC, any bacterial contamination is undesirable and potentially harmful, as blood components containing large amounts of normally apathogenic bacteria can also lead to life-threatening infections after transfusion [31]. In this thesis, a vendor independent, low-cost flow cytometry method for rapid detection of bacterial contaminations in PC was developed.

In order to detect bacteria in a difficult matrix such as PC, pathogens have to be reliably distinguished from the blood product components. After processing, a standard PC unit consists mainly of platelets (at least 2×10^{11} /bag), residual erythrocytes (up to 3×10^9 /bag) and a small fraction of leukocytes ($< 1 \times 10^6$ /bag) [23]. PC are generally poor in nucleated cells and thus contain a relatively low amount of DNA. This can be exploited to detect bacteria in this matrix by staining the nucleoids of the pathogens with a DNA binding dye.

In this thesis, DRAQ5™ was selected to enable a staining procedure compatible with common flow cytometry devices and easy to implement into the respective lab setting of BEs. DRAQ5™ can be excited with a 488 nm argon-ion laser, which is the most common laser in commercially available flow cytometry devices [230]. DRAQ5™ (deep red-fluorescing bisalkylaminoanthraquinone number five) is a far-red cell-permeable high affinity DNA-labelling dye, which combines a high capacity to permeate cell membranes and rapid staining of the DNA content of live and fixed cells [231], while showing a low rate of unspecific RNA or mitochondrial DNA staining [232]. So far, DRAQ5™ has been mostly used in eukaryotes [231,233,234]. Only few DRAQ5™ staining protocols for prokaryotes have been published, but those have shown that DRAQ5™ is a good choice for bacterial DNA staining. It was possible to label and to detect different physiological states of gram-positive lactic acid bacteria using DRAQ5™ [235,236], as well as staining gram-negative bacteria [237].

In this thesis, both gram-negative as well as gram-positive bacteria, which were involved in reported fatal and non-fatal septic transfusion reactions, were selected from the PTRBR panel (chapter 1.1.2, Tab. 2). This bacterial reference material consisted of ready-to-use bacterial suspensions of platelet transfusion-relevant strains with known bacterial counts and ability to grow in blood components such as PC [100]. The suitability of DRAQ5™ for distinguishing these bacterial reference strains from cell debris and non-specifically stained platelets was tested in this thesis (chapter 4.2.1, Fig. 21). since DRAQ5™ was reported to have no significant interaction with mitochondrial DNA or RNA [232], our results from non-contaminated PC samples suggest, that DRAQ5™ led to unspecific staining of intact platelets and cell debris. Due to the high number of co-stained platelets in the samples, the fluorescence intensity of the bacterial populations

were shifted and the specific DRAQ5™ staining of the bacterial nucleoids in PC samples was less distinct in comparison to bacteria without PC (chapter 4.2.1, Fig. 17-20; chapter 7.2, Fig. 37-44).

It has been reported in previous studies that bacterial quantification in PC by flow cytometry, especially at lower bacteria concentrations, was negatively influenced by the high background signals derived from platelet debris [89].

This background presents one of the greatest challenges in detecting bacteria in PC, as the platelet count is several log levels higher than the number of potentially contaminating bacteria, even at very high contamination levels, as discussed earlier in chapter 5.1.1. Unspecific fluorescence derived from PC debris leads to incorrect detection of bacterial contaminations or a considerable loss of detection sensitivity. The clear separation of the bacteria population from the platelet debris is complicated, as fluorescence signals from bacteria partially overlap those from platelets [88]. For this reason, the reduction of the platelet concentration in the sample without sample dilution is crucial to improve the sensitivity of the detection method. In the case of PC, it was reasonable to introduce a PC lysis step prior to DRAQ5 staining, to lyse the platelets in the sample, while leaving the bacteria largely intact.

The non-ionic surfactant Triton X-100 is one of the most commonly used detergents for cell lysis, protein and cellular organelles extraction and cell permeabilization in general [238–242]. In this thesis, Triton X-100 was selected for cell lysis due to its common and easy use. By performing a lysis step, it was possible to improve differentiation between bacteria and the remaining, non-specifically stained cells and cell debris in the PC based on their staining intensity (chapter 4.2.2, Fig. 22-24; chapter 4.2.3, Fig. 27).

In addition, platelet aggregation resulted in non-lysable cell aggregates and masking of bacterial events, reducing the staining efficiency of the assay. This made it difficult to distinguish between bacteria and platelets during flow cytometry analysis (chapter 4.2.2, Fig. 22-24, top illustration; chapter 7.3, Fig. 45-47). Resuspension of centrifuged cell pellets prior to platelet lysis was more difficult for samples contaminated with bacteria, compared to cell pellets consisting of platelets alone. To solve this problem, platelet clumping due to activation and evasion of effective lysis had to be prevented.

One way to inhibit platelet aggregation is to block platelet membrane glycoproteins (GP), such as the GPIIb/IIIa receptor. Platelet GPs not only ensure their usual function in hemostasis, but also play a role in adherence to bacteria [130].

A common GPIIb/IIIa receptor inhibitor is Tirofiban, which is a potent and specific fibrinogen receptor antagonist, which mimics the binding sequence of the fibrinogen ligand [243]. It prevents fibrinogen cross-linking and thereby platelet aggregation by prothrombinase inhibition [244–246]. To prevent aggregation of platelets and clumping with bacterial contaminants, reduction of shearing forces by centrifugation and a Tirofiban treatment were introduced in the final flow cytometry method (chapter 3.6.1).

Overall, the measurements did not show a correlation between the bacterial contamination level of the examined PC sample and the final detected fluorescent events. However, after the introduction of Tirofiban (chapter 4.2.5.2, Fig. 32), a trend between the bacterial load and measured fluorescent events became apparent, which was not visible before the introduction of Tirofiban (chapter 4.2.5.1, Fig. 31). The new flow cytometric RMM should be considered as a qualitative, non-quantitative test, indicating “contaminated” or “not contaminated” as final test result, but not indicating the exact total bacterial load. Since any contamination in blood products, such as PC is undesirable and potentially harmful for the transfusion patient, this statement is sufficient for deciding whether the tested PC bag can be used or must be discarded.

In the context of microbiological testing of PC, the use of a platelet aggregation inhibitor is a novel and promising approach. Lysis of platelets has already been introduced with the BactiFlow® system, combining enzymatic digestion of platelets with the removal of cell debris by filtration to minimize background fluorescence [87]. The introduction of Triton X-100 into the newly developed assay has the advantage of using a well-known, common and easy-to-use detergent without the need for a subsequent filter step. The combination of inhibition of platelet aggregation during sample preparation and lysis of platelets allowed reliable discrimination between DRAQ5™-stained bacteria and non-specifically stained residual platelets and cell debris using the new flow cytometric method.

5.2.2 Adaptation of the new flow cytometry protocol for the detection of *S. aureus* in PC

Despite incubation with the fibrinogen receptor antagonist Tirofiban, complete inhibition of platelet aggregation was not achieved in *S. aureus*-contaminated PC samples. Hence, it was not possible to detect a distinctive population of *S. aureus* in contaminated PC samples using the previously established pre-analytic procedure of the flow cytometry method (chapter 4.2.2, Fig. 25).

In the investigated samples, activation of platelet aggregation caused by *S. aureus* most likely occurred during sample preparation prior to lysis of platelets. Induction of platelet aggregation by *S. aureus* is mediated by bacterial cell wall-associated proteins known as MSCRAMMs (microbial

surface components recognizing adhesive matrix molecules) [247]. These protein receptors on the surface of *S. aureus* enable the interaction with platelet integrins [248,249]. The major MSCRAMMs of *S. aureus* surface proteins include ClfA and ClfB (clumping factors A and B), which bind fibrinogen and induce the activation and cell aggregation of platelets [250,251].

Platelet aggregation induced by ClfA and ClfB can be inhibited by GPIIb/IIIa antagonists [219]. Hannachi *et al.* [252] and Herrmann *et al.* [253] have reported that inhibition of *S. aureus* induced platelet activation and aggregation can be achieved by the use of Tirofiban. Although treatment of *S. aureus* contaminated samples with Tirofiban led to the absence of bacterial clusters and a decrease of the fibrin network of cell aggregates, complete absence of such aggregates could not be achieved in this study. This might be due to a very persistent filamentous network between cell aggregates in *S. aureus* contaminated samples of platelet rich plasma [252]. *S. aureus* is able to trigger coagulation via its two coagulases: staphylo-coagulase (Coa) and von Willebrand factor binding protein (VWbp) [254,255], which results in the formation of a fibrin network [256] despite platelet aggregation inhibitors [252].

This was confirmed by the persistence of platelet cell aggregation even when the two fibrinogen-binding sites on GPIIb–IIIa were blocked by a monoclonal antibody or by blocking of the RGD (Arginylglycylaspartic acid) and dodecapeptide recognition sites on the GP IIb/IIIa receptor by synthetic RGD and Dodecapeptide [133]. This supports the assumption, that treatment of PC with Tirofiban is not sufficient to suppress cell aggregation in samples contaminated with *S. aureus*, because Tirofiban mediated inhibition of platelet aggregation is circumvented by GPIIb-IIIa antagonist independent activation. Therefore, it proved difficult to detect *S. aureus* with the new flow cytometry method.

In PC samples contaminated with *S. aureus*, no distinct bacterial population could be detected in untreated PC samples (chapter 4.2.2, Fig. 25, upper illustration) or in samples treated with Tirofiban before platelet lysis (chapter 4.2.2, Fig. 25, bottom illustration), regardless of the bacterial count. One of the most critical steps regarding potential platelet activation is the centrifugation step prior to lysis of platelets, as platelets and bacteria are pressed together by the centrifugal force, which may increase cell aggregation in the process. A concentration dependency between bacterial contamination of samples and difficulty of resuspension of centrifuged cell pellets was found.

To test the influence of the centrifugation step on PC samples contaminated with *S. aureus*, the centrifugation step prior to lysis of platelets was omitted for samples spiked with *S. aureus*, which otherwise could only be resuspended with great difficulty or hardly at all after centrifugation. We

hypothesize that during centrifugation of samples contaminated with *S. aureus*, the bacteria and platelets irreversibly clump with the forming fibrin network

By avoiding the centrifugation step and adjusting the subsequent platelet lysis step (chapter 3.6.1), it was possible to detect *S. aureus* in PC samples (chapter 4.2.3, Fig. 26). The adaptation of the flow cytometry method altered the properties of *S. aureus* in terms of light scattering and fluorescence intensity compared to the other bacterial species examined. This resulted in a very poor detection of *S. aureus* in PC, when the previously established common bacterial detection gate was applied (chapter 4.2.3, Fig. 27, upper illustration). Therefore, the gating strategy was optimized for *S. aureus* (chapter 4.2.3, Fig. 27, bottom illustration). It was possible to create a detection gate specifically for the detection of *S. aureus* in PC, which allowed the detection of *S. aureus* with a high sensitivity, starting at a bacterial count of 10^2 CFU/ml (chapter 4.2.5.1, Tab. 24). Furthermore, background events of non-contaminated PC samples were measured using the *S. aureus* adapted method and a specific discrimination threshold for *S. aureus* contaminated PC samples was calculated (chapter 4.2.4, Fig. 30).

For the specific detection of all transfusion-relevant bacterial species in PC using the new flow-through analysis method, it is useful to collect two 1-ml samples from a potentially contaminated PC. Here, one of the samples is processed by Tirofiban treatment followed by centrifugation prior to platelet lysis and the second sample is processed by Tirofiban treatment and platelet lysis without prior centrifugation.

Other bacteria from the PTRBR panel (chapter 1.1.2, Tab. 2), which have not yet been tested in the current experimental setup, could possibly cause similar problems in regard to platelet aggregation. Here, *β -hemolytic streptococci* are particularly worthy of mention, including, for example, *S. sanguinis*. This bacterium, like *S. aureus*, has been categorized into risk tier 1 of transfusion-transmitted bacteria of blood and blood components. However, in comparison to *S. aureus*, *S. sanguinis* only has a low antimicrobial resistance and very low threat evolution [42].

S. sanguinis can directly interact with platelets, resulting in activation and aggregate formation, the latter of which is dependent on GPIIb/IIIa and thromboxane [218]. A recent study reported, that Tirofiban completely inhibits platelet aggregation induced by *S. sanguinis* [252]. However, platelets can also directly bind to *S. sanguinis*, which was not inhibited by GPIIb/IIIa antagonists. In the case of *S. sanguinis*, antibodies to GPIb could inhibit both platelet aggregation and platelet adhesion to bacteria, suggesting a direct interaction between GPIb of platelets and *S. sanguinis* [218].

In the current experimental setup, we can assume that treatment with Tirofiban will also have a positive effect on the detection of PC contaminated with *β-hemolytic streptococci*, such as *S. sanguinis*. During sample preparation, it is particularly important that platelets do not aggregate before the platelets are lysed, in order to ensure the most effective lysis and resuspension of the sample in the staining buffer. Activation of platelets can already be assumed during bacterial growth in the corresponding blood product and therefore cannot be prevented. The final method consisted of the inactivation of platelet aggregation by Tirofiban treatment, lysis of the platelets by using a Triton X-100 solution, fixation of samples with pFA and a subsequent staining with DRAQ5™ of bacterial contaminants in PC samples. Finally, the performance of the flow cytometric method was compared to the commercially available, regulatory accepted flow cytometry-based BactiFlow® system (chapter 4.3) regarding sensitivity, hands-on-time and time-to-detection.

5.2.3 Comparison of BactiFlow® and the new flow cytometric detection method

Some German BEs have implemented a rapid bacterial detection method (BactiFlow® system) with a late sampling strategy to identify contaminated PC on day 3 or 4 of shelf life and shelf-life extension to 5 days [52–54,179]. In 2017 one of the main reagents of the BactiFlow® assay (M1) could temporarily no longer be supplied in an adequate quality and was discontinued in German BEs [180,181]. This incident once again highlights the importance of the development of an alternative RMM. A vendor independent detection method based on flow cytometry combined with a late sampling strategy would be of great value for patient safety. The flow cytometric method developed in this thesis can be combined with a late-sampling strategy and performed shortly prior transfusion and could be used as a replacement for the BactiFlow® assay.

Compared to the new flow cytometry method, the overall sensitivity of the BactiFlow® system was lower for each bacterial concentration measured, and in this work the BactiFlow® system detection limit of 300 counts/ml was not reproducible (chapter 4.3, Tab. 25).

In addition of the spiking experiments under standardized conditions with defined bacterial concentrations in PC (chapter 4.2.5, chapter 4.3), the detection of a selection of transfusion-relevant bacteria (*K. pneumoniae*, *S. epidermidis* and *B. cereus*) grown in PC bags from typical low initial contamination levels (0.03-0.3 CFU/ml) [31] were investigated to validate detection of bacteria under real life PC storage conditions. Both methods were finally compared in terms of time-to-detection of bacterial growth in PC (chapter 4.4.1).

With the new flow cytometry method, a detection of 33 % of all *K. pneumoniae* contaminations in PC after 12 h and 44 % after 15 h of incubation was achieved. Compared to the new flow cytometry method, the BactiFlow® system showed a higher detection for *K. pneumoniae* after 12 and 15 h of incubation (12 h = 56 %; 15 h = 78 %). After 18 h of incubation at a contamination level between 10^4 and 10^5 CFU/ml, both methods detected 100 % of all contaminations (chapter 4.4.1, Fig. 34). Overall, the BactiFlow® performed slightly better than the new flow cytometry method in detecting *K. pneumoniae* grown in PC on a percentage basis after 12 and 15 hours of incubation. However, both methods were equally fast in detecting 100 % of all contaminated samples as positive after 18 hours of storage.

S. epidermidis was not detectable by either the BactiFlow® system or the new flow cytometry method between 12 to 21 h of incubation in the PC bags. In previous studies, *S. epidermidis* showed slow growth in PC, characterized by a lag phase of up to 48 h after spiking [161] and only minimal growth after 3 days of PC storage [63]. In this thesis, we observed a similar growth behaviour characterized by slow and irregular growth leading to large fluctuations in the number of CFU/ml detected per measurement time point (chapter 4.4.1, Fig. 36 B).

The BactiFlow® system detected 100 % of *S. epidermidis* contaminated samples after 82 h of incubation, while the new flow cytometry detected 66 % of samples after 82 h and all samples (100%) were detected after 101 h of incubation (chapter 4.4.1; Fig. 36). The BactiFlow® system was able to detect all *S. epidermidis* contaminated PC 1 day faster, than the new flow cytometry method. However, severe or life-threatening transfusion reactions caused by *S. epidermidis* have been reported only at concentrations greater than 10^5 CFU/ml [156], which only occurred after 101 h of incubation at the earliest (chapter 4.4.1; Fig. 36). Both methods were able to detect transfusion-relevant contamination of *S. epidermidis* at this concentration, demonstrating that a late sampling strategy combined with a RMM, is the ideal approach to detect slow growing as well as fast growing bacteria, as bacterial loads leading to moderate and severe transfusion reactions can be reliably detected.

The observed variation in detection sensitivity of the new flow cytometry method and the BactiFlow® system for *K. pneumoniae* and *S. epidermidis*, when grown in PC bags compared to bacteria spiked in PC, may be due in part to the ability to form biofilms, particularly on indwelling medical devices and abiotic surfaces [257]. In a study of Taha *et al.* [258], bacterial adhesion to the inner surface of platelet bags was evaluated on day 7 of storage. Scanning electron microscopy showed, that *K. pneumoniae*, as well as *S. epidermidis* formed surface-attached aggregates or

biofilms on PC container surfaces. The formation of bacterial clusters during growth in PC bags prevents an even distribution of bacteria in the bag and can lead to high sampling errors, which can influence the measurement result of the RMM performed.

The reliable detection of *B. cereus* grown in PC bags by the BactiFlow® system was not possible regardless of the bacterial load. Even after 21 h of incubation at a concentration of approximately 10^6 CFU/ml (chapter 4.4.1, Fig. 35), only 33 % of the PC bags were detected as contaminated. This was also reflected by the fluorescent events detected by the BactiFlow® software. Fluorescence emission from bacteria, cell debris, and viable platelets was indistinguishable because the cells visibly clumped together, producing measurement results that could not be accurately evaluated. In a previous study, exposure of human whole blood in an in vitro flow chamber assay to clusters of *B. cereus* initiated a rapid coagulation of the blood. Furthermore *B. cereus* was capable of directly activating coagulation factors such as prothrombin (factor II) and factor X [259]. The effect of aggregation may be attributed to the difference in contact time between *B. cereus* and platelets when grown in bags compared to *B. cereus* when spiked in PC samples, as in the latter only a few minutes elapse between the addition of *B. cereus* to the PC sample and the subsequent lysis of platelets. The underlying differences in detection sensitivity between the BactiFlow® assay and the new flow cytometry method in the detecting PC-grown *B. cereus* may be due to inhibition of further platelet activation by Tirofiban treatment in the latter method prior to subsequent sample preparation. Tirofiban most likely prevented further clustering by contact activation of platelets due to non-physiological surfaces [260] and resulted in improved detection of *B. cereus* by the new flow cytometry method, as all replicates of the contaminated PC samples tested positive after 18 hours.

The BactiFlow® assay was discontinued in the year of 2017, because one of the main components, Chemsol M1 (naturally derived saponin from tree bark), could temporarily no longer be supplied in sufficient quality [180,181], which led to insufficient lysis quality of the enzymatic lysis step. In this thesis we report similar observations with respect to the Chemsol M1 reagent (chapter 2.1.1, Tab. 6), resulting in a significantly increased detection limit of the BactiFlow® assay, compared to the manufacturers specifications. At irregular intervals, it was no longer possible to distinguish platelets from bacteria based on their fluorescence activity.

Altogether the BactiFlow® assay had a prolonged hands-on-time, while offering a similar time-to-detection in comparison to the new flow cytometry method, developed in this thesis. An equally notable drawback of the BactiFlow® assay is that it only measures viable cells with enzyme activity and membrane integrity [87]. In contrast, the DRAQ5™ based DNA staining of the new flow

cytometry method allows for measurement of viable as well as dead bacterial contaminants, which can be a potential threat for the recipient after transfusion [33]. In summary, the developed flow cytometry method offers a reliable detection of transfusion-relevant bacterial contaminations in PC, as well as significant advantages in handling and processing time.

5.3 Conclusions and Perspectives

Early detection of bacterial pathogens is an important principle in the prevention of infection and transmission, both in the clinical setting and in the processing of substances of human origin (SoHO). Systemic infection caused by bacterial contamination of blood products remains the greatest risk in transfusion medicine. The severity is of course also due to the fact that the direct access to the blood circulation provides an ideal way for the bacterium to spread throughout the body. Due to their specific storage conditions, in which bacteria can proliferate rapidly, PC are the most frequently affected blood product [1–4]. Despite this, there is no obligation for microbiological testing of PC in Germany [52,66]. This approach entails the risk of transfusing highly contaminated PC, which can lead to severe or even fatal sepsis. In this thesis, we investigated the potential of a combination of Raman spectroscopy and confocal microscopy as well as a new flow cytometry method as culture-independent, minimal-invasive and rapid detection methods for bacterial contaminations in PC.

Reliable Raman microspectroscopic detection of bacterial contamination in PC was only achieved at high bacterial concentrations ($>10^8$ CFU/ml), falling below the required sensitivity of a clinical relevant detection method with an LOD of at least 10^5 CFU/ml [156]. To develop a suitable method based on Raman microspectroscopy, sample preparation and pre-processing of acquired Raman spectral data would need further improvement. In addition, it would make sense to switch to a signal-amplifying Raman technique, to further increase the quality and intensity of the Raman bands of the pathogen compounds to be detected in the PC matrix.

A suitable RMM alternative to spontaneous Raman microspectroscopy are molecular biologic techniques, such as NAT testing of PC, based on real-time PCR. Universal bacterial detection can be performed targeting the 16S or 23S ribosomal genes [261,262]. In 2011, A NAT method based on real-time PCR of the 16S-rRNA gene for bacterial detection in PC was approved by PEI and accepted as a release test for individual donations, mini-pools of 5, or mini-pools of 10 samples in Germany [52].

In a clinical context, real-time PCR is one of the most promising molecular methods for diagnosing infectious diseases with high specificity and sensitivity using only a small sample volume (< 1 ml). Real-time PCR screening methods of PC currently have an approximate LOD of 10-50 CFU/mL, depending on the contaminating bacterial species [97].

Theoretically, PCR-based assays are capable of detecting single molecules of 16S rRNA, but this potential has generally not been realised because contamination of most 16S PCR reagents with minor impurities of bacterial genome fragments from the manufacturing process is a known problem [263]. Because PCR can amplify low amounts of DNA, co-amplification of trace amounts of contaminating DNA can occur, causing non-specific background noise and producing false-positive results. Several different approaches have been described to eliminate or reduce PCR reagent contamination, such as physical, chemical and enzymatic treatments, where treatment of PCR master mixes with ethidium monoazide (EMA) followed by photoactivation is considered to be the most reliable and effective means of eliminating residual contaminating DNA without compromising the sensitivity of the assay [264].

Furthermore, regarding NAT-based methods, it should be noted that there is no direct correlation between the detected gene copy number and the actual bacterial load, as the quantification of bacteria is influenced by the variation of gene copies in a given bacterial species. These variations in copy number of the gene of interest between species and also within species, depending among other things on the current metabolic state, complicate the use of standard curves for quantifying the bacterial load and make it difficult to determine the overall LOD of the assay. [265,266]. To measure the efficiency and yield of the nucleic acid released during lysis of bacteria, defined bacterial suspensions (as been provided by PEI [chapter 1.1.2, Tab. 2]) should be used, cultivated under standardized conditions and characterized regarding overall cell count (via flow cytometry) and bacterial titer (CFU). Using the correlation between bacterial count and resulting nucleic acid molecule count after sample preparation, the performance and detection limit of the method can be evaluated more successfully and reproducibly [266].

Limitations of NAT assays for PC screening are related regarding their feasibility for routine implementation, comparability and cost of the assays. NAT assays are highly specific and sensitive; however, these methods require robust validation and pose difficulties for routine implementation due to requirements of special equipment and trained specialist personnel. At present, there are no commercial generic bacterial NAT assays available to the blood community and comparisons of different methods or laboratory findings remain difficult [180].

Further validation studies and definitions of standardization of NAT assays for the broad-range detection of bacteria, internal amplification controls, reagent controls, and the processing of negative and positive controls (run controls) are needed to improve the applicability of NAT for routine contamination screening by transfusion services [266,267]. In addition to their complexity and the necessity of pre-processing samples and reagents, NAT assays have a time-to-detection of approximately 4 h, which is comparably time-consuming for a RMM [87,97].

In comparison, flow cytometry for the detection of bacterial contaminations in PC has been demonstrated to be a more rapid and feasible approach in previous studies [88–91] and in this thesis. We present a new bacterial detection method based on flow cytometry, which offers a rapid, cost-effective and vendor-independent alternative to current RMM. With a time-to-detection under 2 h, a very short hands-on-time and the possibility to detect PTRBRs in PC at a concentration between 10^3 to 10^5 CFU/ml without any pre-cultivation step. This method enables the reliable detection of clinically relevant bacterial contaminations in PC prior to transfusion and thereby prevention of moderate to severe sepsis and fatal outcomes. This flow cytometric method furthermore enables the safe bridging of supply shortages by shelf-life extension and reduced discard of older PC.

For further validation of the developed method, the entire set of WHO transfusion relevant Reference strains (PTRBR panel chapter 1.1.2, Tab. 2) may be analysed to ensure a reliable detection of all common bacterial species, which are able to replicate in PC. To further increase the sensitivity of the detection method by possibly one log level, the sample volume might be increased up to 10 ml. This approach would still be less invasive than the automated culture method (BacT/ALERT® system), which requires twice the PC volume [55]. In perspective, the developed flow cytometry method could be relatively easily introduced into BE workflows.

6 Literature

- [1] Brecher ME, Hay SN. Bacterial Contamination of Blood Components. *Clin Microbiol Rev* 2005; 18: 195–204. doi:10.1128/CMR.18.1.195-204.2005
- [2] Hong H, Xiao W, Lazarus HM, et al. Detection of septic transfusion reactions to platelet transfusions by active and passive surveillance. *Blood* 2016; 127: 496–502. doi:10.1182/blood-2015-07-655944
- [3] Stainsby D, Jones H, Asher D, et al. Serious Hazards of Transfusion: A Decade of Hemovigilance in the UK. *Transfusion Medicine Reviews* 2006; 20: 273–282. doi:10.1016/j.tmr.2006.05.002
- [4] Störmer M, Arroyo A, Brachert J, et al. Establishment of the first International Repository for Transfusion-Relevant Bacteria Reference Strains: ISBT Working Party Transfusion-Transmitted Infectious Diseases (WP-TTID), Subgroup on Bacteria: International Repository for Transfusion-Relevant Bacteria References. *Vox Sanguinis* 2012; 102: 22–31. doi:10.1111/j.1423-0410.2011.01510.x
- [5] Haass KA, Sapiano MRP, Savinkina A, et al. Transfusion-Transmitted Infections Reported to the National Healthcare Safety Network Hemovigilance Module. *Transfusion Medicine Reviews* 2019; 33: 84–91. doi:10.1016/j.tmr.2019.01.001
- [6] Horth RZ, Jones JM, Kim JJ, et al. Fatal Sepsis Associated with Bacterial Contamination of Platelets — Utah and California, August 2017. *MMWR Morb Mortal Wkly Rep* 2018; 67: 718–722. doi:10.15585/mmwr.mm6725a4
- [7] Kou Y, Pagotto F, Hannach B, et al. Fatal false-negative transfusion infection involving a buffy coat platelet pool contaminated with biofilm-positive *Staphylococcus epidermidis* : a case report: Fatal Transfusion-Associated *S. Epidermidis* Infection. *Transfusion* 2015; 55: 2384–2389. doi:10.1111/trf.13154
- [8] Nevala-Plagemann C, Powers P, Mir-Kasimov M, et al. A Fatal Case of Septic Shock Secondary to *Acinetobacter* Bacteremia Acquired from a Platelet Transfusion. *Case Reports in Medicine* 2019; 2019: 1–4. doi:10.1155/2019/3136493
- [9] Hourfar MK, Jork C, Schottstedt V, et al. Experience of German Red Cross blood donor services with nucleic acid testing: results of screening more than 30 million blood donations for human immunodeficiency virus-1, hepatitis C virus, and hepatitis B virus. *Transfusion* 2008; 48: 1558–1566. doi:10.1111/j.1537-2995.2008.01718.x
- [10] Roth WK, Busch MP, Schuller A, et al. International survey on NAT testing of blood donations: expanding implementation and yield from 1999 to 2009: International Forum. *Vox Sanguinis* 2012; 102: 82–90. doi:10.1111/j.1423-0410.2011.01506.x
- [11] Funk MB, Heiden M, Volkens P, et al. Evaluation of Risk Minimisation Measures for Blood Components – Based on Reporting Rates of Transfusion-Transmitted Reactions (1997-2013). *Transfus Med Hemother* 2015; 42: 240–246. doi:10.1159/000381996
- [12] Schmidt M, Hourfar MK, Nicol S-B, et al. A comparison of three rapid bacterial detection methods under simulated real-life conditions. *Transfusion* 2006; 46: 1367–1373. doi:10.1111/j.1537-2995.2006.00904.x

-
- [13] Thyer J, Perkowska-Guse Z, Ismay SL, et al. Bacterial testing of platelets - has it prevented transfusion-transmitted bacterial infections in Australia? *Vox Sang* 2018; 113: 13–20. doi:10.1111/vox.12561
- [14] Ramirez-Arcos S, DiFranco C, McIntyre T, et al. Residual risk of bacterial contamination of platelets: six years of experience with sterility testing: STERILITY TESTING OF OUTDATED PLATELETS. *Transfusion* 2017; 57: 2174–2181. doi:10.1111/trf.14202
- [15] Katus MC, Szczepiorkowski ZM, Dumont LJ, et al. Safety of platelet transfusion: past, present and future. *Vox Sang* 2014; 107: 103–113. doi:10.1111/vox.12146
- [16] Schrezenmeier H, Walther-Wenke G, Müller TH, et al. Bacterial contamination of platelet concentrates: results of a prospective multicenter study comparing pooled whole blood-derived platelets and apheresis platelets. *Transfusion* 2007; 47: 644–652. doi:10.1111/j.1537-2995.2007.01166.x
- [17] Blajchman M, Beckers E, Dickmeiss E, et al. Bacterial Detection of Platelets: Current Problems and Possible Resolutions. *Transfusion Medicine Reviews* 2005; 19: 259–272. doi:10.1016/j.tmr.2005.05.002
- [18] Hillyer CD, Josephson CD, Blajchman MA, et al. Bacterial Contamination of Blood Components: Risks, Strategies, and Regulation. *Hematology* 2003; 2003: 575–589. doi:10.1182/asheducation-2003.1.575
- [19] Janetzko K, Schmidt M. Verlängerung der Haltbarkeitsdauer von Thrombozytenkonzentraten von 4 auf 5 Tage. *Transfusionsmedizin* 2015; 5: 27–30. doi:10.1055/s-0034-1396188
- [20] Stramer SL. Current risks of transfusion-transmitted agents: a review. *Arch Pathol Lab Med* 2007; 131: 702–707. doi:10.5858/2007-131-702-CROTAA
- [21] Dodd RY. Current risk for transfusion transmitted infections: Current Opinion in Internal Medicine 2007; 7: 45–50. doi:10.1097/MOH.0b013e3282e38e8a
- [22] Funk MB, Lohmann A, Guenay S, et al. Transfusion-Transmitted Bacterial Infections – Haemovigilance Data of German Blood Establishments (1997–2010). *Transfus Med Hemother* 2011; 38: 266–271. doi:10.1159/000330372
- [23] Bundesärztekammer (2017): Richtlinie zur Gewinnung von Blut und Blutbestandteilen und zur Anwendung von Blutprodukten (Richtlinie Hämotherapie). Aufgestellt gemäß §§ 12a und 18 Transfusionsgesetz von der Bundesärztekammer im Einvernehmen mit dem Paul-Ehrlich-Institut. Bundesärztekammer. Deutscher Ärzteverlag GmbH 2017; Im Internet: <https://shop.aerzteverlag.de/gesundheitswesen/2211-richtlinie-blut-9783769136562.html>; Stand: 17.10.2021
- [24] Russell AD. Bacterial spores and chemical sporicidal agents. *Clin Microbiol Rev* 1990; 3: 99–119
- [25] Knutson F, Alfonso R, Dupuis K, et al. Photochemical inactivation of bacteria and HIV in buffy-coat-derived platelet concentrates under conditions that preserve in vitro platelet function. *Vox Sang* 2000; 78: 209–216. doi:10.1159/000031183

-
- [26] Allain JP, Bianco C, Blajchman MA, et al. Protecting the Blood Supply From Emerging Pathogens: The Role of Pathogen Inactivation. *Transfus Med Rev* 2005; 19: 110–126. doi:10.1016/j.tmr.2004.11.005
- [27] 2 Platelet Concentrates. *Transfus Med Hemother* 2009; 36: 372–382
- [28] van der Meer PF, de Korte D. Platelet Additive Solutions: A Review of the Latest Developments and Their Clinical Implications. *Transfus Med Hemother* 2018; 45: 98–102. doi:10.1159/000487513
- [29] Klinger MHF, Josch M, Klüter H. Platelets Stored in a Glucose-Free Additive Solution or in Autologous Plasma - An Ultrastructural and Morphometric Evaluation. *Vox Sanguinis* 1996; 71: 13–20. doi:10.1046/j.1423-0410.1996.7110013.x
- [30] Greco CA, Zhang JG, Kalab M, et al. Effect of platelet additive solution on bacterial dynamics and their influence on platelet quality in stored platelet concentrates: BACTERIAL DYNAMICS IN PCs PRODUCED IN PAS. *Transfusion* 2010; 50: 2344–2352. doi:10.1111/j.1537-2995.2010.02726.x
- [31] Montag T. Strategies of bacteria screening in cellular blood components. *Clinical Chemistry and Laboratory Medicine* 2008; 46. doi:10.1515/CCLM.2008.176
- [32] Palavecino EL, Yomtovian RA, Jacobs MR. Bacterial contamination of platelets. *Transfusion and Apheresis Science* 2010; 42: 71–82. doi:10.1016/j.transci.2009.10.009
- [33] Pearce S, Rowe GP, Field SP. Screening of platelets for bacterial contamination at the Welsh Blood Service. *Transfusion Medicine* 2011; 21: 25–32. doi:10.1111/j.1365-3148.2010.01037.x
- [34] Murphy WG, Foley M, Doherty C, et al. Screening platelet concentrates for bacterial contamination: low numbers of bacteria and slow growth in contaminated units mandate an alternative approach to product safety. *Vox Sang* 2008; 95: 13–19. doi:10.1111/j.1423-0410.2008.01051.x
- [35] European Parliament and the Council of the European Union: Directive 2002/98/EC of the European Parliament and of the Council of 27 January 2003 setting standards of quality and safety for the collection, testing, processing, storage and distribution of human blood and blood components and amending Directive 2001/83/EC. Official J L 033, 08/02/2003 P. 0030–0040.
- [36] European Parliament and the Council of the European Union: Commission Directive 2004/33/EC of 22 March 2004 implementing Directive 2002/98/EC of the European Parliament and of the Council as regards certain technical requirements for blood and blood components. Official J L 091, 30/03/2004 P. 0025–0039. 2004
- [37] European Directorate for the Quality of Medicines & HealthCare (EDQM). Guide to the preparation, use and quality assurance of blood components, 19th ed. Strassbourg: EDQM; 2017.
- [38] Funk MB, Günay S, Lohmann A, et al. Bewertung der Maßnahmen zur Reduktion schwerwiegender Transfusionsreaktionen (Hämovigilanzdaten von 1997 bis 2008). *Bundesgesundheitsbl* 2010; 53: 347–356. doi:10.1007/s00103-010-1037-8

- [39] Puckett A, Davison G, Entwistle CC, et al. Post transfusion septicaemia 1980-1989: importance of donor arm cleansing. *Journal of Clinical Pathology* 1992; 45: 155–157. doi:10.1136/jcp.45.2.155
- [40] McDonald CP. Interventions Implemented to Reduce the Risk of Transmission of Bacteria by Transfusion in the English National Blood Service. *Transfus Med Hemother* 2011; 38: 255–258. doi:10.1159/000330474
- [41] Gibson T, Norris W. SKIN FRAGMENTS REMOVED BY INJECTION NEEDLES. *The Lancet* 1958; 272: 983–985. doi:10.1016/S0140-6736(58)90475-6
- [42] Domanović D, Cassini A, Bekeredjian-Ding I, et al. Prioritizing of bacterial infections transmitted through substances of human origin in Europe: PRIORITIZED SoHO-TRANSMITTED BACTERIA. EDITORIAL 2017; 57: 1311–1317. doi:10.1111/trf.14036
- [43] Wagner SJ. Transfusion-transmitted bacterial infection: risks, sources and interventions. *Vox Sang* 2004; 86: 157–163. doi:10.1111/j.0042-9007.2004.00410.x
- [44] McDonald CP. Bacterial risk reduction by improved donor arm disinfection, diversion and bacterial screening. *Transfus Med* 2006; 16: 381–396. doi:10.1111/j.1365-3148.2006.00697.x
- [45] Goldman M, Roy G, Fréchette N, et al. Evaluation of donor skin disinfection methods. *Transfusion* 1997; 37: 309–312. doi:10.1046/j.1537-2995.1997.37397240214.x
- [46] McDonald CP, Lowe P, Roy A, et al. Evaluation of donor arm disinfection techniques: Donor arm disinfection techniques. *Vox Sanguinis* 2001; 80: 135–141. doi:10.1046/j.1423-0410.2001.00029.x
- [47] Wagner SJ, Robinette D, Friedman LI, et al. Diversion of initial blood flow to prevent whole-blood contamination by skin surface bacteria: an in vitro model. *Transfusion* 2000; 40: 335–338. doi:10.1046/j.1537-2995.2000.40030335.x
- [48] Liunbruno GM, Catalano L, Piccinini V, et al. Reduction of the risk of bacterial contamination of blood components through diversion of the first part of the donation of blood and blood components. *Blood Transfusion* 2009; doi:10.2450/2008.0026-08
- [49] Satake M, Mitani T, Oikawa S, et al. Frequency of bacterial contamination of platelet concentrates before and after introduction of diversion method in Japan. *Transfusion* 2009; 49: 2152–2157. doi:10.1111/j.1537-2995.2009.02243.x
- [50] McDonald C, Allen J, Brailsford S, et al. Bacterial screening of platelet components by National Health Service Blood and Transplant, an effective risk reduction measure: BACTERIAL SCREENING. EDITORIAL 2017; 57: 1122–1131. doi:10.1111/trf.14085
- [51] Festlegung der Haltbarkeitsfrist von Thrombozytenkonzentraten mit dem Ziel der Reduktion lebensbedrohlicher septischer Transfusionsreaktionen durch bakterielle Kontamination: Bei der 66. Sitzung des Arbeitskreises Blut am 9. Juni 2008 wurde folgendes Votum (V 38) verabschiedet: *Bundesgesundheitsbl* 2008; 51: 1484–1484. doi:10.1007/s00103-008-0723-2

- [52] Sireis W, Rüster B, Daiss C, et al. Extension of platelet shelf life from 4 to 5 days by implementation of a new screening strategy in Germany: Bacterial detection by BacT/ALERT and Bactiflow. *Vox Sanguinis* 2011; 101: 191–199. doi:10.1111/j.1423-0410.2011.01485.x
- [53] Vollmer T, Schottstedt V, Bux J, et al. Bacterial screening of platelet concentrates on day 2 and 3 with flow cytometry: the optimal sampling time point? *Blood Transfus* 2014; 12: 388–395. doi:10.2450/2014.0175-13
- [54] Vollmer T, Engemann J, Kleesiek K, et al. Bacterial screening by flow cytometry offers potential for extension of platelet storage: results of 14 months of active surveillance. *Transfusion Medicine* 2011; 21: 175–182. doi:10.1111/j.1365-3148.2011.01070.x
- [55] Prax M, Bekeredjian-Ding I, Krut O. Microbiological Screening of Platelet Concentrates in Europe. *Transfus Med Hemother* 2019; 46: 76–86. doi:10.1159/000499349
- [56] Dunne WmM, Case LK, Isgriggs L, et al. In-house validation of the BACTEC 9240 blood culture system for detection of bacterial contamination in platelet concentrates. *Transfusion* 2005; 45: 1138–1142. doi:10.1111/j.1537-2995.2005.04343.x
- [57] Brecher ME, Means N, Jere CS, et al. Evaluation of an automated culture system for detecting bacterial contamination of platelets: an analysis with 15 contaminating organisms. *Transfusion* 2001; 41: 477–482. doi:10.1046/j.1537-2995.2001.41040477.x
- [58] McDonald CP, Rogers A, Cox M, et al. Evaluation of the 3D BacT/ALERT automated culture system for the detection of microbial contamination of platelet concentrates. *Transfus Med* 2002; 12: 303–309. doi:10.1046/j.1365-3148.2002.00390.x
- [59] Brecher ME, Hay SN, Rose AD, et al. Evaluation of BacT/ALERT plastic culture bottles for use in testing pooled whole blood-derived leukoreduced platelet-rich plasma platelets with a single contaminated unit. *Transfusion* 2005; 45: 1512–1517. doi:10.1111/j.1537-2995.2005.00563.x
- [60] Totty H, Ullery M, Spontak J, et al. A controlled comparison of the BacT/ALERT® 3D and VIRTUO™ microbial detection systems. *Eur J Clin Microbiol Infect Dis* 2017; 36: 1795–1800. doi:10.1007/s10096-017-2994-8
- [61] Benjamin RJ, Wagner SJ. The residual risk of sepsis: modeling the effect of concentration on bacterial detection in two-bottle culture systems and an estimation of false-negative culture rates. *Transfusion* 2007; 47: 1381–1389. doi:10.1111/j.1537-2995.2007.01326.x
- [62] te Boekhorst PAW, Beckers EAM, Vos MC, et al. Clinical significance of bacteriologic screening in platelet concentrates. *Transfusion* 2005; 45: 514–519. doi:10.1111/j.0041-1132.2005.04270.x
- [63] Vollmer T, Dabisch-Ruthe M, Weinstock M, et al. Late sampling for automated culture to extend the platelet shelf life to 5 days in Germany. *Transfusion* 2018; 58: 1654–1664. doi:10.1111/trf.14617
- [64] Schurig U, Karo J-O, Sicker U, et al. Aktuelles Konzept zur mikrobiologischen Sicherheit von zellbasierten Arzneimitteln. *Bundesgesundheitsbl* 2015; 58: 1225–1232. doi:10.1007/s00103-015-2237-z

-
- [65] Koopman MMW, van't Ende E, Lieshout-Krikke R, et al. Bacterial screening of platelet concentrates: results of 2 years active surveillance of transfused positive cultured units released as negative to date. *Vox Sanguinis* 2009; 97: 355–357. doi:10.1111/j.1423-0410.2009.01221.x
- [66] Störmer M, Vollmer T. Diagnostic Methods for Platelet Bacteria Screening: Current Status and Developments. *Transfus Med Hemother* 2014; 41: 5–5. doi:10.1159/000357651
- [67] Fang CT, Chambers LA, Kennedy J, et al. Detection of bacterial contamination in apheresis platelet products: American Red Cross experience, 2004. *Transfusion* 2005; 45: 1845–1852. doi:10.1111/j.1537-2995.2005.00650.x
- [68] Cid J, Lozano M. Pathogen inactivation of platelets for transfusion. *Platelets* 2021; 1–4. doi:10.1080/09537104.2021.1935838
- [69] Cid J. Prevention of transfusion-associated graft-versus-host disease with pathogen-reduced platelets with amotosalen and ultraviolet A light: a review. *Vox Sang* 2017; 112: 607–613. doi:10.1111/vox.12558
- [70] Schlenke P, Hagenah W, Irsch J, et al. Safety and clinical efficacy of platelet components prepared with pathogen inactivation in routine use for thrombocytopenic patients. *Ann Hematol* 2011; 90: 1457–1465. doi:10.1007/s00277-011-1222-3
- [71] Jimenez-Marco T, Garcia-Recio M, Girona-Llobera E. Our experience in riboflavin and ultraviolet light pathogen reduction technology for platelets: from platelet production to patient care: RIBOFLAVIN UV LIGHT-TREATED PLTs. *Transfusion* 2018; 58: 1881–1889. doi:10.1111/trf.14797
- [72] Feys HB, Van Aelst B, Compennolle V. Biomolecular Consequences of Platelet Pathogen Inactivation Methods. *Transfusion Medicine Reviews* 2019; 33: 29–34. doi:10.1016/j.tmr.2018.06.002
- [73] Jutzi M, Mansouri Taleghani B, Rueesch M, et al. Nationwide Implementation of Pathogen Inactivation for All Platelet Concentrates in Switzerland. *Transfus Med Hemother* 2018; 45: 151–156. doi:10.1159/000489900
- [74] Cazenave J-P, Isola H, Waller C, et al. Use of additive solutions and pathogen inactivation treatment of platelet components in a regional blood center: impact on patient outcomes and component utilization during a 3-year period: ROUTINE USE OF PATHOGEN-INACTIVATED PLT COMPONENTS. *Transfusion* 2011; 51: 622–629. doi:10.1111/j.1537-2995.2010.02873.x
- [75] Schubert P, Johnson L, Marks DC, et al. Ultraviolet-Based Pathogen Inactivation Systems: Untangling the Molecular Targets Activated in Platelets. *Front Med* 2018; 5: 129. doi:10.3389/fmed.2018.00129
- [76] Schmidt M, Hourfar MK, Sireis W, et al. Evaluation of the effectiveness of a pathogen inactivation technology against clinically relevant transfusion-transmitted bacterial strains: EFFICIENCY OF PATHOGEN INACTIVATION. *Transfusion* 2015; 55: 2104–2112. doi:10.1111/trf.13171

- [77] Alabdullatif M, Osman IE, Alrasheed M, et al. Evaluation of riboflavin and ultraviolet light treatment against *KLEBSIELLA PNEUMONIAE* in whole blood-derived platelets: A pilot study. *Transfusion* 2021; 61: 1562–1569. doi:10.1111/trf.16347
- [78] Gravemann U, Handke W, Müller TH, et al. Bacterial inactivation of platelet concentrates with the THERAFLEX UV-Platelets pathogen inactivation system: INACTIVATION OF BACTERIA WITH UVC. *Transfusion* 2019; 59: 1324–1332. doi:10.1111/trf.15119
- [79] Irsch J, Lin L. Pathogen Inactivation of Platelet and Plasma Blood Components for Transfusion Using the INTERCEPT Blood System™. *Transfus Med Hemother* 2011; 38: 19–31. doi:10.1159/000323937
- [80] Taha M, Culibrk B, Kalab M, et al. Efficiency of riboflavin and ultraviolet light treatment against high levels of biofilm-derived *Staphylococcus epidermidis* in buffy coat platelet concentrates. *Vox Sang* 2017; 112: 408–416. doi:10.1111/vox.12519
- [81] Benjamin RJ. Bacterial contamination. *VOXS* 2014; 9: 37–43. doi:10.1111/voxs.12067
- [82] Irsch J, Seghatchian J. Update on pathogen inactivation treatment of plasma, with the INTERCEPT Blood System: Current position on methodological, clinical and regulatory aspects. *Transfusion and Apheresis Science* 2015; 52: 240–244. doi:10.1016/j.transci.2015.02.013
- [83] Goodrich RP, Edrich RA, Li J, et al. The Mirasol™ PRT system for pathogen reduction of platelets and plasma: An overview of current status and future trends. *Transfusion and Apheresis Science* 2006; 35: 5–17. doi:10.1016/j.transci.2006.01.007
- [84] Marschner S, Goodrich R. Pathogen Reduction Technology Treatment of Platelets, Plasma and Whole Blood Using Riboflavin and UV Light. *Transfus Med Hemother* 2011; 38: 8–18. doi:10.1159/000324160
- [85] Seltsam A, Müller TH. UVC Irradiation for Pathogen Reduction of Platelet Concentrates and Plasma. *Transfus Med Hemother* 2011; 38: 43–54. doi:10.1159/000323845
- [86] Seghatchian J, Tolksdorf F. Characteristics of the THERAFLEX UV-Platelets pathogen inactivation system – An update. *Transfusion and Apheresis Science* 2012; 46: 221–229. doi:10.1016/j.transci.2012.01.008
- [87] Dreier J, Vollmer T, Kleesiek K. Novel Flow Cytometry–Based Screening for Bacterial Contamination of Donor Platelet Preparations Compared with Other Rapid Screening Methods. *Clinical Chemistry* 2009; 55: 1492–1502. doi:10.1373/clinchem.2008.122515
- [88] Karo O, Wahl A, Nicol S-B, et al. Bacteria detection by flow cytometry. *Clinical Chemistry and Laboratory Medicine* 2008; 46. doi:10.1515/CCLM.2008.156
- [89] Mohr H, Lambrecht B, Bayer A, et al. Basics of flow cytometry-based sterility testing of platelet concentrates. *Transfusion* 2006; 46: 41–49. doi:10.1111/j.1537-2995.2005.00668.x
- [90] Schmidt M, Hourfar MK, Nicol S-B, et al. FACS technology used in a new rapid bacterial detection method. *Transfus Med* 2006; 16: 355–361. doi:10.1111/j.1365-3148.2006.00686.x

- [91] Schmidt M, Karakassopoulos A, Burkhart J, et al. Comparison of three bacterial detection methods under routine conditions. *Vox Sang* 2007; 92: 15–21. doi:10.1111/j.1423-0410.2006.00850.x
- [92] Dreier J, Störmer M, Pichl L, et al. Sterility screening of platelet concentrates: questioning the optimal test strategy. *Vox Sang* 2008; 95: 181–188. doi:10.1111/j.1423-0410.2008.01087.x
- [93] Mohammadi T, Savelkoul PHM, Pietersz RNI, et al. Applications of real-time PCR in the screening of platelet concentrates for bacterial contamination. *Expert Rev Mol Diagn* 2006; 6: 865–872. doi:10.1586/14737159.6.6.865
- [94] Rood IGH, Koppelman MHGM, Pettersson A, et al. Development of an internally controlled PCR assay for broad range detection of bacteria in platelet concentrates. *J Microbiol Methods* 2008; 75: 64–69. doi:10.1016/j.mimet.2008.05.007
- [95] Mintz PD, Vallejo RP. The PGD prime immunoassay for detection of bacterial contamination in platelet concentrates: sensitivity and specificity. *Annals of Blood* 2021; 6. doi:10.21037/aob-2020-bcpc-01
- [96] Bacterial Risk Control Strategies for Blood Collection Establishments and Transfusion Services to Enhance the Safety and Availability of Platelets for Transfusion. Guidance for Industry. Silver Spring, MD: U.S. Department of Health and Human Services, Food and Drug Administration, Center for Biologics Evaluation and Research. September 2019, updated December 2020. [cited 2023 January 6]. Available online: <https://www.fda.gov/media/123448/download>.
- [97] Schmidt M, Sireis W, Seifried E. Implementation of Bacterial Detection Methods into Blood Donor Screening – Overview of Different Technologies. *Transfus Med Hemother* 2011; 38: 259–265. doi:10.1159/000330305
- [98] Vollmer T, Dreier J, Schottstedt V, et al. Detection of bacterial contamination in platelet concentrates by a sensitive flow cytometric assay (BactiFlow): a multicentre validation study: BactiFlow multicentre study. *Transfusion Med* 2012; 22: 262–271. doi:10.1111/j.1365-3148.2012.01166.x
- [99] Vollmer T, Knabbe C, Geilenkeuser W-J, et al. Bench Test for the Detection of Bacterial Contamination in Platelet Concentrates Using Rapid and Cultural Detection Methods with a Standardized Proficiency Panel. *Transfus Med Hemother* 2015; 42: 220–225. doi:10.1159/000437396
- [100] Spindler-Raffel E, Benjamin RJ, McDonald CP, et al. Enlargement of the WHO international repository for platelet transfusion-relevant bacteria reference strains. *Vox Sang* 2017; 112: 713–722. doi:10.1111/vox.12548
- [101] Païssé S, Valle C, Servant F, et al. Comprehensive description of blood microbiome from healthy donors assessed by 16S targeted metagenomic sequencing: BLOOD MICROBIOME 16S METAGENOMIC SEQUENCING. *Transfusion* 2016; 56: 1138–1147. doi:10.1111/trf.13477
- [102] Oberbach A, Schlichting N, Feder S, et al. New insights into valve-related intramural and intracellular bacterial diversity in infective endocarditis. *PLoS ONE* 2017; 12: e0175569. doi:10.1371/journal.pone.0175569

- [103] Kuehnert MJ, Roth VR, Haley NR, et al. Transfusion-transmitted bacterial infection in the United States, 1998 through 2000. *Transfusion* 2001; 41: 1493–1499. doi:10.1046/j.1537-2995.2001.41121493.x
- [104] Reading FC, Brecher ME. Transfusion-related bacterial sepsis. *Curr Opin Hematol* 2001; 8: 380–386. doi:10.1097/00062752-200111000-00011
- [105] Müller TH, Mohr H, Montag T. Methods for the detection of bacterial contamination in blood products. *Clinical Chemistry and Laboratory Medicine* 2008; 46. doi:10.1515/CCLM.2008.154
- [106] Mohr H, Lambrecht B, Bayer A, et al. Sterility testing of platelet concentrates prepared from deliberately infected blood donations. *Transfusion* 2006; 46: 486–491. doi:10.1111/j.1537-2995.2006.00747.x
- [107] Mohr H, Bayer A, Gravemann U, et al. Elimination and multiplication of bacteria during preparation and storage of buffy coat-derived platelet concentrates. *Transfusion* 2006; 46: 949–955. doi:10.1111/j.1537-2995.2006.00827.x
- [108] Ezuki S, Kawabata K, Kanno T, et al. Culture-based bacterial detection systems for platelets: the effect of time prior to sampling and duration of incubation required for detection with aerobic culture. *Transfusion* 2007; 47: 2044–2049. doi:10.1111/j.1537-2995.2007.01428.x
- [109] Störmer M, Kleesiek K, Dreier J. *Propionibacterium acnes* lacks the capability to proliferate in platelet concentrates. *Vox Sang* 2008; 94: 193–201. doi:10.1111/j.1423-0410.2007.01019.x
- [110] Miller LS, Cho JS. Immunity against *Staphylococcus aureus* cutaneous infections. *Nat Rev Immunol* 2011; 11: 505–518. doi:10.1038/nri3010
- [111] Lowy FD. *Staphylococcus aureus* infections. *N Engl J Med* 1998; 339: 520–532. doi:10.1056/NEJM199808203390806
- [112] Corey GR. *Staphylococcus aureus* bloodstream infections: definitions and treatment. *Clin Infect Dis* 2009; 48 Suppl 4: S254–259. doi:10.1086/598186
- [113] Gorwitz RJ, Kruszon-Moran D, McAllister SK, et al. Changes in the prevalence of nasal colonization with *Staphylococcus aureus* in the United States, 2001–2004. *J Infect Dis* 2008; 197: 1226–1234. doi:10.1086/533494
- [114] Graham PL, Lin SX, Larson EL. A U.S. population-based survey of *Staphylococcus aureus* colonization. *Ann Intern Med* 2006; 144: 318–325. doi:10.7326/0003-4819-144-5-200603070-00006
- [115] Gordon RJ, Lowy FD. Pathogenesis of Methicillin-Resistant *Staphylococcus aureus* Infection. *Clin Infect Dis* 2008; 46: S350–S359. doi:10.1086/533591
- [116] Kluytmans J, van Belkum A, Verbrugh H. Nasal carriage of *Staphylococcus aureus*: epidemiology, underlying mechanisms, and associated risks. *Clin Microbiol Rev* 1997; 10: 505–520

- [117] von Eiff C, Becker K, Machka K, et al. Nasal carriage as a source of *Staphylococcus aureus* bacteremia. Study Group. *N Engl J Med* 2001; 344: 11–16. doi:10.1056/NEJM200101043440102
- [118] Foster TJ. Immune evasion by staphylococci. *Nat Rev Microbiol* 2005; 3: 948–958. doi:10.1038/nrmicro1289
- [119] Graves SF, Kobayashi SD, DeLeo FR. Community-associated methicillin-resistant *Staphylococcus aureus* immune evasion and virulence. *J Mol Med (Berl)* 2010; 88: 109–114. doi:10.1007/s00109-009-0573-x
- [120] Daum RS. Clinical practice. Skin and soft-tissue infections caused by methicillin-resistant *Staphylococcus aureus*. *N Engl J Med* 2007; 357: 380–390. doi:10.1056/NEJMcp070747
- [121] DeLeo FR, Otto M, Kreiswirth BN, et al. Community-associated methicillin-resistant *Staphylococcus aureus*. *Lancet* 2010; 375: 1557–1568. doi:10.1016/S0140-6736(09)61999-1
- [122] Chambers HF, Deleo FR. Waves of resistance: *Staphylococcus aureus* in the antibiotic era. *Nat Rev Microbiol* 2009; 7: 629–641. doi:10.1038/nrmicro2200
- [123] Loza-Correa M, Kou Y, Taha M, et al. Septic transfusion case caused by a platelet pool with visible clotting due to contamination with *Staphylococcus aureus*. *Transfusion* 2017; 57: 1299–1303. doi:10.1111/trf.14049
- [124] Perpoint T, Lina G, Poyart C, et al. Two Cases of Fatal Shock after Transfusion of Platelets Contaminated by *Staphylococcus aureus*: Role of Superantigenic Toxins. *Clinical Infectious Diseases* 2004; 39: e106–e109. doi:10.1086/425499
- [125] Kaufman RM, Savage WJ. *Staphylococcus aureus* sepsis from one cocomponent of a „triple“ apheresis platelet donation. *Transfusion* 2014; 54: 1704. doi:10.1111/trf.12593
- [126] Coutinho H, Galloway A, Ajdukiewicz K, et al. A case of *Staphylococcus aureus* septicaemia following platelet transfusion. *J Clin Pathol* 2010; 63: 262–263. doi:10.1136/jcp.2007.050492
- [127] Klevens RM, Morrison MA, Nadle J, et al. Invasive methicillin-resistant *Staphylococcus aureus* infections in the United States. *JAMA* 2007; 298: 1763–1771. doi:10.1001/jama.298.15.1763
- [128] Abela MA, Fenning S, Maguire KA, et al. Bacterial contamination of platelet components not detected by BacT/ALERT®. *Transfus Med* 2018; 28: 65–70. doi:10.1111/tme.12458
- [129] Brailsford SR, Tossell J, Morrison R, et al. Failure of bacterial screening to detect *Staphylococcus aureus*: the English experience of donor follow-up. *Vox Sang* 2018; doi:10.1111/vox.12670
- [130] Hamzeh-Cognasse H, Damien P, Chabert A, et al. Platelets and Infections - Complex Interactions with Bacteria. *Front Immunol* 2015; 6. doi:10.3389/fimmu.2015.00082
- [131] Herrmann M, Lai QJ, Albrecht RM, et al. Adhesion of *Staphylococcus aureus* to Surface-Bound Platelets: Role of Fibrinogen/Fibrin and Platelet Integrins. *J Infect Dis* 1993; 167: 312–322. doi:10.1093/infdis/167.2.312

- [132] Fitzgerald JR, Foster TJ, Cox D. The interaction of bacterial pathogens with platelets. *Nat Rev Microbiol* 2006; 4: 445–457. doi:10.1038/nrmicro1425
- [133] Bayer AS, Sullam PM, Ramos M, et al. Staphylococcus aureus induces platelet aggregation via a fibrinogen-dependent mechanism which is independent of principal platelet glycoprotein IIb/IIIa fibrinogen-binding domains. *Infect Immun* 1995; 63: 3634–3641. doi:10.1128/iai.63.9.3634-3641.1995
- [134] Montgomerie JZ. Epidemiology of Klebsiella and hospital-associated infections. *Rev Infect Dis* 1979; 1: 736–753. doi:10.1093/clinids/1.5.736
- [135] Cichon MJ, Craig CP, Sargent J, et al. Nosocomial Klebsiella infections in an intensive care nursery. *South Med J* 1977; 70: 33–35. doi:10.1097/00007611-197701000-00016
- [136] Cooke EM, Edmondson AS, Starkey W. The ability of strains of Klebsiella aerogenes to survive on the hands. *J Med Microbiol* 1981; 14: 443–450. doi:10.1099/00222615-14-4-443
- [137] Knittle MA, Eitzman DV, Baer H. Role of hand contamination of personnel in the epidemiology of gram-negative nosocomial infections. *J Pediatr* 1975; 86: 433–437. doi:10.1016/s0022-3476(75)80980-2
- [138] Hart CA, Gibson MF, Buckles AM. Variation in skin and environmental survival of hospital gentamicin-resistant enterobacteria. *J Hyg (Lond)* 1981; 87: 277–285
- [139] Casewell MW, Phillips I. Epidemiological patterns of Klebsiella colonization and infection in an intensive care ward. *J Hyg (Lond)* 1978; 80: 295–300. doi:10.1017/s0022172400053651
- [140] Hart CA. Klebsiellae and neonates. *J Hosp Infect* 1993; 23: 83–86. doi:10.1016/0195-6701(93)90013-p
- [141] Adjei AA, Kuma GK, Tettey Y, et al. Bacterial contamination of blood and blood components in three major blood transfusion centers, Accra, Ghana. *Jpn J Infect Dis* 2009; 62: 265–269
- [142] Niu M, Knippen M, Simmons L, et al. Transfusion-Transmitted Klebsiella pneumoniae Fatalities, 1995 to 2004. *Transfusion medicine reviews* 2006; 20: 149–157. doi:10.1016/j.tmr.2005.11.007
- [143] Paczosa MK, Mecsas J. Klebsiella pneumoniae: Going on the Offense with a Strong Defense. *Microbiol Mol Biol Rev* 2016; 80: 629–661. doi:10.1128/MMBR.00078-15
- [144] Yinnon AM, Butnaru A, Raveh D, et al. Klebsiella bacteraemia: community versus nosocomial infection. *QJM* 1996; 89: 933–941. doi:10.1093/qjmed/89.12.933
- [145] García de la Torre M, Romero-Vivas J, Martínez-Beltrán J, et al. Klebsiella bacteremia: an analysis of 100 episodes. *Rev Infect Dis* 1985; 7: 143–150. doi:10.1093/clinids/7.2.143
- [146] Watanakunakorn C, Jura J. Klebsiella bacteremia: a review of 196 episodes during a decade (1980-1989). *Scand J Infect Dis* 1991; 23: 399–405. doi:10.3109/00365549109075086
- [147] Paganin F, Lilienthal F, Bourdin A, et al. Severe community-acquired pneumonia: assessment of microbial aetiology as mortality factor. *European Respiratory Journal* 2004; 24: 779–785. doi:10.1183/09031936.04.00119503

- [148] Bengoechea JA, Sa Pessoa J. *Klebsiella pneumoniae* infection biology: living to counteract host defences. *FEMS Microbiol Rev* 2019; 43: 123–144. doi:10.1093/femsre/fuy043
- [149] Holt KE, Wertheim H, Zadoks RN, et al. Genomic analysis of diversity, population structure, virulence, and antimicrobial resistance in *Klebsiella pneumoniae*, an urgent threat to public health. *Proc Natl Acad Sci U S A* 2015; 112: E3574-3581. doi:10.1073/pnas.1501049112
- [150] Lam MMC, Wick RR, Wyres KL, et al. Genetic diversity, mobilisation and spread of the yersiniabactin-encoding mobile element ICEKp in *Klebsiella pneumoniae* populations. *Microb Genom* 2018; 4. doi:10.1099/mgen.0.000196
- [151] Lam MMC, Wyres KL, Duchêne S, et al. Population genomics of hypervirulent *Klebsiella pneumoniae* clonal-group 23 reveals early emergence and rapid global dissemination. *Nat Commun* 2018; 9: 2703. doi:10.1038/s41467-018-05114-7
- [152] Zhang Y, Zeng J, Liu W, et al. Emergence of a hypervirulent carbapenem-resistant *Klebsiella pneumoniae* isolate from clinical infections in China. *J Infect* 2015; 71: 553–560. doi:10.1016/j.jinf.2015.07.010
- [153] Gu D, Dong N, Zheng Z, et al. A fatal outbreak of ST11 carbapenem-resistant hypervirulent *Klebsiella pneumoniae* in a Chinese hospital: a molecular epidemiological study. *Lancet Infect Dis* 2018; 18: 37–46. doi:10.1016/S1473-3099(17)30489-9
- [154] Yao H, Qin S, Chen S, et al. Emergence of carbapenem-resistant hypervirulent *Klebsiella pneumoniae*. *Lancet Infect Dis* 2018; 18: 25. doi:10.1016/S1473-3099(17)30628-X
- [155] von Eiff C, Peters G, Heilmann C. Pathogenesis of infections due to coagulase-negative staphylococci. *Lancet Infect Dis* 2002; 2: 677–685. doi:10.1016/s1473-3099(02)00438-3
- [156] Jacobs MR, Good CE, Lazarus HM, et al. Relationship between Bacterial Load, Species Virulence, and Transfusion Reaction with Transfusion of Bacterially Contaminated Platelets. *CLIN INFECT DIS* 2008; 46: 1214–1220. doi:10.1086/529143
- [157] Yomtovian RA, Palavecino EL, Dysktra AH, et al. Evolution of surveillance methods for detection of bacterial contamination of platelets in a university hospital, 1991 through 2004. *Transfusion* 2006; 46: 719–730. doi:10.1111/j.1537-2995.2006.00790.x
- [158] Hsueh JC, Ho CF, Chang SH, et al. Blood surveillance and detection on platelet bacterial contamination associated with septic events. *Transfus Med* 2009; 19: 350–356. doi:10.1111/j.1365-3148.2009.00949.x
- [159] Martini R, Horner R, Rodrigues M de A, et al. Bacteriological analysis of platelets and cases of septic reactions associated with transfusion of contaminated samples. *Transfus Apher Sci* 2012; 47: 313–318. doi:10.1016/j.transci.2012.06.011
- [160] Walther-Wenke G, Schrezenmeier H, Deitenbeck R, et al. Screening of platelet concentrates for bacterial contamination: spectrum of bacteria detected, proportion of transfused units, and clinical follow-up. *Ann Hematol* 2010; 89: 83–91. doi:10.1007/s00277-009-0762-2
- [161] Motoyama Y, Yamaguchi N, Matsumoto M, et al. Staphylococcus epidermidis Forms Floating Micro-colonies in Platelet Concentrates at the Early Stage of Contamination. *JOURNAL OF HEALTH SCIENCE* 2009; 55: 726–731. doi:10.1248/jhs.55.726

- [162] Greco C, Martincic I, Gusinjac A, et al. Staphylococcus epidermidis forms biofilms under simulated platelet storage conditions. *Transfusion* 2007; 47: 1143–1153. doi:10.1111/j.1537-2995.2007.01249.x
- [163] Ali H, Greco-Stewart VS, Jacobs MR, et al. Characterization of the growth dynamics and biofilm formation of Staphylococcus epidermidis strains isolated from contaminated platelet units. *J Med Microbiol* 2014; 63: 884–891. doi:10.1099/jmm.0.071449-0
- [164] Hodgson SD, Greco-Stewart V, Jimenez CS, et al. Enhanced pathogenicity of biofilm-negative Staphylococcus epidermidis isolated from platelet preparations. *Transfusion* 2014; 54: 461–470. doi:10.1111/trf.12308
- [165] Kotiranta A, Lounatmaa K, Haapasalo M. Epidemiology and pathogenesis of Bacillus cereus infections. *Microbes and Infection* 2000; 2: 189–198. doi:10.1016/S1286-4579(00)00269-0
- [166] Terpstra FG, van 't Wout AB, Schuitemaker H, et al. Potential and limitation of UVC irradiation for the inactivation of pathogens in platelet concentrates. *Transfusion* 2008; 48: 304–313. doi:10.1111/j.1537-2995.2007.01524.x
- [167] Slieman TA, Nicholson WL. Artificial and solar UV radiation induces strand breaks and cyclobutane pyrimidine dimers in Bacillus subtilis spore DNA. *Appl Environ Microbiol* 2000; 66: 199–205. doi:10.1128/AEM.66.1.199-205.2000
- [168] de Korte D, Curvers J, de Kort WLAM, et al. Effects of skin disinfection method, deviation bag, and bacterial screening on clinical safety of platelet transfusions in the Netherlands. *Transfusion* 2006; 46: 476–485. doi:10.1111/j.1537-2995.2006.00746.x
- [169] Störmer M, Vollmer T, Kleesiek K, et al. Spore-forming organisms in platelet concentrates: a challenge in transfusion bacterial safety. *Transfus Med* 2008; 18: 371–376. doi:10.1111/j.1365-3148.2008.00895.x
- [170] Shimoyama R, Nakase T, Mitani T, et al. Contamination of Bacillus cereus in an apheresis-derived platelet concentrate. *J Clin Apher* 1997; 12: 103. doi:10.1002/(sici)1098-1101(1997)12:2<103::aid-jca9>3.0.co;2-e
- [171] Robinson JP. Overview of Flow Cytometry and Microbiology. *Current Protocols in Cytometry* 2018; 84. doi:10.1002/cpcy.37
- [172] McKinnon KM. Flow Cytometry: An Overview. *Current Protocols in Immunology* 2018; 120. doi:10.1002/cpim.40
- [173] Radcliff G, Jaroszeski MJ. Basics of flow cytometry. *Methods Mol Biol* 1998; 91: 1–24. doi:10.1385/0-89603-354-6:1
- [174] Büscher M. Flow Cytometry Instrumentation - An Overview. *Current Protocols in Cytometry* 2019; 87: e52. doi:10.1002/cpcy.52
- [175] Picot J, Guerin CL, Le Van Kim C, et al. Flow cytometry: retrospective, fundamentals and recent instrumentation. *Cytotechnology* 2012; 64: 109–130. doi:10.1007/s10616-011-9415-0

- [176] Givan AL. Flow Cytometry: An Introduction. In: Hawley TS, Hawley RG, Hrsg. Flow Cytometry Protocols. Totowa, NJ: Humana Press; 2011: 1–29
- [177] Waggoner A. Optical Filter Sets for Multiparameter Flow Cytometry. *Current Protocols in Cytometry* 1997; 00. doi:10.1002/0471142956.cy0105s00
- [178] Flint S, Walker K, Waters B, et al. Description and validation of a rapid (1 h) flow cytometry test for enumerating thermophilic bacteria in milk powders: Rapid enumeration of thermophiles. *Journal of Applied Microbiology* 2007; 102: 909–915. doi:10.1111/j.1365-2672.2006.03167.x
- [179] Müller B, Walther-Wenke G, Kalus M, et al. Routine bacterial screening of platelet concentrates by flow cytometry and its impact on product safety and supply. *Vox Sang* 2015; 108: 209–218. doi:10.1111/vox.12214
- [180] Schmidt M, Ramirez-Arcos S, Stiller L, et al. Current status of rapid bacterial detection methods for platelet components: A 20-year review by the ISBT Transfusion-Transmitted Infectious Diseases Working Party Subgroup on Bacteria. *Vox Sanguinis* 2022; 117: 983–988. doi:10.1111/vox.13283
- [181] Vollmer T, Hinse D, Diekmann J, et al. Extension of the Storage Period of Platelet Concentrates in Germany to 5 Days by Bacterial Testing: Is it Worth the Effort? *Transfus Med Hemother* 2019; 46: 111–113. doi:10.1159/000499543
- [182] Saba SR, Mason RG. Acetylcholine, Cholinesterase Activity, and the Aggregability of Human Platelets. *Experimental Biology and Medicine* 1970; 135: 104–107. doi:10.3181/00379727-135-34998
- [183] Long DA. The Raman effect: a unified treatment of the theory of Raman scattering by molecules. Chichester ; New York: Wiley; 2002
- [184] Gardiner DJ. Introduction to Raman Scattering. In: Gardiner DJ, Graves PR, Hrsg. Practical Raman Spectroscopy. Berlin, Heidelberg: Springer Berlin Heidelberg; 1989: 1–12
- [185] Fujimori H, Kakihana M, Ioku K, et al. Advantage of anti-Stokes Raman scattering for high-temperature measurements. *Appl Phys Lett* 2001; 79: 937–939. doi:10.1063/1.1394174
- [186] Pahlow S, Meisel S, Cialla-May D, et al. Isolation and identification of bacteria by means of Raman spectroscopy. *Advanced Drug Delivery Reviews* 2015; 89: 105–120. doi:10.1016/j.addr.2015.04.006
- [187] Clara Cornelia Stiebing. Visualisierung der intrazellulären Aufnahme und des Metabolismus von Lipiden und Lipoproteinen mittels Raman-Spektroskopie, Diss., Friedrich-Schiller-Universität Jena. 2017
- [188] Butler HJ, Ashton L, Bird B, et al. Using Raman spectroscopy to characterize biological materials. *Nat Protoc* 2016; 11: 664–687. doi:10.1038/nprot.2016.036
- [189] Pandey R, Paidi SK, Valdez TA, et al. Noninvasive Monitoring of Blood Glucose with Raman Spectroscopy. *Acc Chem Res* 2017; 50: 264–272. doi:10.1021/acs.accounts.6b00472

- [190] Shipp DW, Sinjab F, Notingher I. Raman spectroscopy: techniques and applications in the life sciences. *Adv Opt Photon* 2017; 9: 315. doi:10.1364/AOP.9.000315
- [191] Notingher I, Hench LL. Raman microspectroscopy: a noninvasive tool for studies of individual living cells *in vitro*. *Expert Review of Medical Devices* 2006; 3: 215–234. doi:10.1586/17434440.3.2.215
- [192] Hanlon EB, Manoharan R, Koo T-W, et al. Prospects for *in vivo* Raman spectroscopy. *Phys Med Biol* 2000; 45: R1–R59. doi:10.1088/0031-9155/45/2/201
- [193] Borchman D, Tang D, Yappert MC. Lipid composition, membrane structure relationships in lens and muscle sarcoplasmic reticulum membranes. *Biospectroscopy* 1999; 5: 151–167. doi:10.1002/(SICI)1520-6343(1999)5:3<151::AID-BSPY5>3.0.CO;2-D
- [194] M. Yogesha, Chawla K, Bankapur A, et al. A micro-Raman and chemometric study of urinary tract infection-causing bacterial pathogens in mixed cultures. *Anal Bioanal Chem* 2019; 411: 3165–3177. doi:10.1007/s00216-019-01784-4
- [195] Svoboda K, Block SM. Biological Applications of Optical Forces. *Annu Rev Biophys Biomol Struct* 1994; 23: 247–285. doi:10.1146/annurev.bb.23.060194.001335
- [196] Bonnier F, Mehmood A, Knief P, et al. *In vitro* analysis of immersed human tissues by Raman microspectroscopy: *In vitro* analysis of immersed human tissues by Raman microspectroscopy. *J Raman Spectrosc* 2011; 42: 888–896. doi:10.1002/jrs.2825
- [197] Swain RJ, Stevens MM. Raman microspectroscopy for non-invasive biochemical analysis of single cells. *Biochemical Society Transactions* 2007; 35: 544–549. doi:10.1042/BST0350544
- [198] Kerr LT, Byrne HJ, Hennelly BM. Optimal choice of sample substrate and laser wavelength for Raman spectroscopic analysis of biological specimen. *Anal Methods* 2015; 7: 5041–5052. doi:10.1039/C5AY00327J
- [199] Eberhardt K, Stiebing C, Matthäus C, et al. Advantages and limitations of Raman spectroscopy for molecular diagnostics: an update. *Expert Review of Molecular Diagnostics* 2015; 15: 773–787. doi:10.1586/14737159.2015.1036744
- [200] Bocklitz T, Walter A, Hartmann K, et al. How to pre-process Raman spectra for reliable and stable models? *Analytica Chimica Acta* 2011; 704: 47–56. doi:10.1016/j.aca.2011.06.043
- [201] Byrne HJ, Sockalingum GD, Stone N. Chapter 4. Raman Microscopy: Complement or Competitor? In: Moss D, Hrsg. *RSC Analytical Spectroscopy Series*. Cambridge: Royal Society of Chemistry; 2010: 105–143
- [202] Zhang L, Henson MJ. A Practical Algorithm to Remove Cosmic Spikes in Raman Imaging Data for Pharmaceutical Applications. *Appl Spectrosc* 2007; 61: 1015–1020. doi:10.1366/000370207781745847
- [203] Lasch P. Spectral pre-processing for biomedical vibrational spectroscopy and microspectroscopic imaging. *Chemometrics and Intelligent Laboratory Systems* 2012; 117: 100–114. doi:10.1016/j.chemolab.2012.03.011

- [204] Thomas A, Tourassi GD, Elmaghraby AS, et al. Data mining in proteomic mass spectrometry. *Clin Proteom* 2006; 2: 13–32. doi:10.1385/CP:2:1:13
- [205] Li L, Umbach DM, Terry P, et al. Application of the GA/KNN method to SELDI proteomics data. *Bioinformatics* 2004; 20: 1638–1640. doi:10.1093/bioinformatics/bth098
- [206] Subramanian J, Simon R. Overfitting in prediction models – Is it a problem only in high dimensions? *Contemporary Clinical Trials* 2013; 36: 636–641. doi:10.1016/j.cct.2013.06.011
- [207] Hilario M, Kalousis A, Pellegrini C, et al. Processing and classification of protein mass spectra. *Mass Spectrom Rev* 2006; 25: 409–449. doi:10.1002/mas.20072
- [208] Levner I. Feature selection and nearest centroid classification for protein mass spectrometry. *BMC Bioinformatics* 2005; 6: 68. doi:10.1186/1471-2105-6-68
- [209] Mandrell CT, Holland TE, Wheeler JF, et al. Machine Learning Approach to Raman Spectrum Analysis of MIA PaCa-2 Pancreatic Cancer Tumor Repopulating Cells for Classification and Feature Analysis. *Life* 2020; 10: 181. doi:10.3390/life10090181
- [210] Jolliffe I. Principal Component Analysis. In: *Wiley StatsRef: Statistics Reference Online*. American Cancer Society; 2014
- [211] Chen G, Qian S-E. Denoising and dimensionality reduction of hyperspectral imagery using wavelet packets, neighbour shrinking and principal component analysis. *International Journal of Remote Sensing* 2009; 30: 4889–4895. doi:10.1080/01431160802653724
- [212] Esbensen KH, Geladi P. Principles of Proper Validation: use and abuse of re-sampling for validation. *J Chemometrics* 2010; 24: 168–187. doi:10.1002/cem.1310
- [213] Yousten AA, Rogoff MH. Metabolism of *Bacillus thuringiensis* in relation to spore and crystal formation. *J Bacteriol* 1969; 100: 1229–1236. doi:10.1128/jb.100.3.1229-1236.1969
- [214] Krafft C. Bioanalytical applications of Raman spectroscopy. *Analytical and Bioanalytical Chemistry* 2004; 378: 60–62. doi:10.1007/s00216-003-2266-6
- [215] Atkins CG, Buckley K, Blades MW, et al. Raman Spectroscopy of Blood and Blood Components. *Appl Spectrosc* 2017; 71: 767–793. doi:10.1177/0003702816686593
- [216] Kang L-L, Huang Y-X, Liu W-J, et al. Confocal Raman microscopy on single living young and old erythrocytes. *Biopolymers* 2008; 89: 951–959. doi:10.1002/bip.21042
- [217] Petry R, Schmitt M, Popp J. Raman Spectroscopy-A Prospective Tool in the Life Sciences. *ChemPhysChem* 2003; 4: 14–30. doi:10.1002/cphc.200390004
- [218] Kerrigan SW, Douglas I, Wray A, et al. A role for glycoprotein Ib in *Streptococcus sanguis*-induced platelet aggregation. *Blood* 2002; 100: 509–516. doi:10.1182/blood.v100.2.509
- [219] O’Brien L, Kerrigan SW, Kaw G, et al. Multiple mechanisms for the activation of human platelet aggregation by *Staphylococcus aureus*: roles for the clumping factors ClfA and ClfB, the serine-aspartate repeat protein SdrE and protein A: Multiple mechanisms for stimulating platelet aggregation in *S. aureus*. *Molecular Microbiology* 2002; 44: 1033–1044. doi:10.1046/j.1365-2958.2002.02935.x

- [220] Bhakdi S, Muhly M, Mannhardt U, et al. Staphylococcal alpha toxin promotes blood coagulation via attack on human platelets. *J Exp Med* 1988; 168: 527–542. doi:10.1084/jem.168.2.527
- [221] Deegan RD, Bakajin O, Dupont TF, et al. Capillary flow as the cause of ring stains from dried liquid drops. *Nature* 1997; 389: 827–829. doi:10.1038/39827
- [222] Zhang D, Xie Y, Mrozek MF, et al. Raman Detection of Proteomic Analytes. *Anal Chem* 2003; 75: 5703–5709. doi:10.1021/ac0345087
- [223] Frojmovic MM, Milton JG. Human platelet size, shape, and related functions in health and disease. *Physiological Reviews* 1982; doi:10.1152/physrev.1982.62.1.185
- [224] Pitt WG, Alizadeh M, Hussein GA, et al. Rapid Separation of Bacteria from Blood—Review and Outlook. *Biotechnol Prog* 2016; 32: 823–839. doi:10.1002/btpr.2299
- [225] Efremov EV, Ariese F, Gooijer C. Achievements in resonance Raman spectroscopy. *Analytica Chimica Acta* 2008; 606: 119–134. doi:10.1016/j.aca.2007.11.006
- [226] Mangini M, Verde A, Boraschi D, et al. Interaction of nanoparticles with endotoxin Importance in nanosafety testing and exploitation for endotoxin binding. *Nanotoxicology* 2021; 15: 558–576. doi:10.1080/17435390.2021.1898690
- [227] Wang L, Liu W, Tang J-W, et al. Applications of Raman Spectroscopy in Bacterial Infections: Principles, Advantages, and Shortcomings. *Front Microbiol* 2021; 12: 683580. doi:10.3389/fmicb.2021.683580
- [228] Lorenz B, Wichmann C, Stöckel S, et al. Cultivation-Free Raman Spectroscopic Investigations of Bacteria. *Trends Microbiol* 2017; 25: 413–424. doi:10.1016/j.tim.2017.01.002
- [229] Krafft C, Popp J. The many facets of Raman spectroscopy for biomedical analysis. *Anal Bioanal Chem* 2015; 407: 699–717. doi:10.1007/s00216-014-8311-9
- [230] Shapiro HM. Lasers for flow cytometry. *Curr Protoc Cytom* 2004; Chapter 1: Unit 1.9. doi:10.1002/0471142956.cy0109s27
- [231] Smith PJ, Blunt N, Wiltshire M, et al. Characteristics of a novel deep red/infrared fluorescent cell-permeant DNA probe, DRAQ5, in intact human cells analyzed by flow cytometry, confocal and multiphoton microscopy. *Cytometry* 2000; 40: 280–291. doi:10.1002/1097-0320(20000801)40:4<280::AID-CYTO4>3.0.CO;2-7
- [232] van Zandvoort MAMJ, de Grauw CJ, Gerritsen HC, et al. Discrimination of DNA and RNA in cells by a vital fluorescent probe: Lifetime imaging of SYTO13 in healthy and apoptotic cells. *Cytometry* 2002; 47: 226–235. doi:10.1002/cyto.10076
- [233] Allan RW, Ansari-Lari MA, Jordan S. DRAQ5-Based, No-Lyse, No-Wash Bone Marrow Aspirate Evaluation by Flow Cytometry. *Am J Clin Pathol* 2008; 129: 706–713. doi:10.1309/D2M6Q7BYHWAM1FYQ
- [234] Wiltshire M, Patterson LH, Smith PJ. A novel deep red/low infrared fluorescent flow cytometric probe, DRAQ5NO, for the discrimination of intact nucleated cells in apoptotic

- cell populations. *Cytometry* 2000; 39: 217–223. doi:10.1002/(SICI)1097-0320(20000301)39:3<217::AID-CYTO7>3.0.CO;2-M
- [235] Herrero M, Quirós C, García LA, et al. Use of Flow Cytometry To Follow the Physiological States of Microorganisms in Cider Fermentation Processes. *Appl Environ Microbiol* 2006; 72: 6725–6733. doi:10.1128/AEM.01183-06
- [236] Quirós C, Herrero M, García LA, et al. Application of Flow Cytometry to Segregated Kinetic Modeling Based on the Physiological States of Microorganisms. *Appl Environ Microbiol* 2007; 73: 3993–4000. doi:10.1128/AEM.00171-07
- [237] Silva F, Lourenço O, Pina-Vaz C, et al. The Use of DRAQ5 to Monitor Intracellular DNA in *Escherichia coli* by Flow Cytometry. *J Fluoresc* 2010; 20: 907–914. doi:10.1007/s10895-010-0636-y
- [238] Mattei B, Lira RB, Perez KR, et al. Membrane permeabilization induced by Triton X-100: The role of membrane phase state and edge tension. *Chemistry and Physics of Lipids* 2017; 202: 28–37. doi:10.1016/j.chemphyslip.2016.11.009
- [239] Koley D, Bard AJ. Triton X-100 concentration effects on membrane permeability of a single HeLa cell by scanning electrochemical microscopy (SECM). *Proceedings of the National Academy of Sciences* 2010; 107: 16783–16787. doi:10.1073/pnas.1011614107
- [240] Gennuso F, Ferneti C, Tirolo C, et al. Bilirubin protects astrocytes from its own toxicity by inducing up-regulation and translocation of multidrug resistance-associated protein 1 (Mrp1). *Proceedings of the National Academy of Sciences* 2004; 101: 2470–2475. doi:10.1073/pnas.0308452100
- [241] Hipfner DR, Gauldie SD, Deeley RG, et al. Detection of the M(r) 190,000 multidrug resistance protein, MRP, with monoclonal antibodies. *Cancer Res* 1994; 54: 5788–5792
- [242] Benoit J, Cormier M, Wepierre J. Comparative effects of four surfactants on growth, contraction and adhesion of cultured human fibroblasts. *Cell Biol Toxicol* 1988; 4: 111–122. doi:10.1007/BF00141290
- [243] Giordano A, Musumeci G, D'Angelillo A, et al. Effects Of Glycoprotein IIb/IIIa Antagonists: Anti Platelet Aggregation And Beyond. *Curr Drug Metab* 2016; 17: 194–203. doi:10.2174/1389200217666151211121112
- [244] Jagroop IA, Mikhailidis DP. The Effect of Tirofiban on Fibrinogen/Agonist-Induced Platelet Shape Change and Aggregation. *Clin Appl Thromb Hemost* 2008; 14: 295–302. doi:10.1177/1076029608316014
- [245] Li Y, Spencer FA, Ball S, et al. Inhibition of platelet-dependent prothrombinase activity and thrombin generation by glycoprotein IIb/IIIa receptor-directed antagonists: potential contributing mechanism of benefit in acute coronary syndromes. *J Thromb Thrombolysis* 2000; 10: 69–76. doi:10.1023/a:1018754906289
- [246] Ciborowski M, Tomasiak M, Rusak T, et al. The in-vitro effect of tirofiban, glycoprotein IIb/IIIa antagonist, on various responses of porcine blood platelets: *Blood Coagulation & Fibrinolysis* 2008; 19: 557–567. doi:10.1097/MBC.0b013e3283079e29

- [247] Patti JM, Allen BL, McGavin MJ, et al. MSCRAMM-mediated adherence of microorganisms to host tissues. *Annu Rev Microbiol* 1994; 48: 585–617. doi:10.1146/annurev.mi.48.100194.003101
- [248] Hannachi N, Habib G, Camoin-Jau L. Aspirin Effect on *Staphylococcus aureus*—Platelet Interactions During Infectious Endocarditis. *Front Med* 2019; 6: 217. doi:10.3389/fmed.2019.00217
- [249] Zecconi A, Scali F. *Staphylococcus aureus* virulence factors in evasion from innate immune defenses in human and animal diseases. *Immunol Lett* 2013; 150: 12–22. doi:10.1016/j.imlet.2013.01.004
- [250] McDevitt D, Francois P, Vaudaux P, et al. Molecular characterization of the clumping factor (fibrinogen receptor) of *Staphylococcus aureus*. *Mol Microbiol* 1994; 11: 237–248. doi:10.1111/j.1365-2958.1994.tb00304.x
- [251] Ní Eidhin D, Perkins S, Francois P, et al. Clumping factor B (ClfB), a new surface-located fibrinogen-binding adhesin of *Staphylococcus aureus*. *Molecular Microbiology* 1998; 30: 245–257. doi:10.1046/j.1365-2958.1998.01050.x
- [252] Hannachi N, Ogé-Ganaye E, Baudoin J-P, et al. Antiplatelet Agents Have a Distinct Efficacy on Platelet Aggregation Induced by Infectious Bacteria. *Front Pharmacol* 2020; 11: 863. doi:10.3389/fphar.2020.00863
- [253] Herrmann M. Salicylic acid: an old dog, new tricks, and staphylococcal disease. *J Clin Invest* 2003; 112: 149–151. doi:10.1172/JCI19143
- [254] Bjerketorp J, Jacobsson K, Frykberg L. The von Willebrand factor-binding protein (vWbp) of *Staphylococcus aureus* is a coagulase. *FEMS Microbiology Letters* 2004; 234: 309–314. doi:10.1111/j.1574-6968.2004.tb09549.x
- [255] Thomer L, Schneewind O, Missiakas D. Multiple Ligands of von Willebrand Factor-binding Protein (vWbp) Promote *Staphylococcus aureus* Clot Formation in Human Plasma. *Journal of Biological Chemistry* 2013; 288: 28283–28292. doi:10.1074/jbc.M113.493122
- [256] Gersh K, Nagaswami C, Weisel J. Fibrin network structure and clot mechanical properties are altered by incorporation of erythrocytes. *Thromb Haemost* 2009; 102: 1169–1175. doi:10.1160/TH09-03-0199
- [257] Hatt JK, Rather PN. Role of Bacterial Biofilms in Urinary Tract Infections. In: Romeo T, Hrsg. *Bacterial Biofilms*. Berlin, Heidelberg: Springer Berlin Heidelberg; 2008: 163–192
- [258] Taha M, Kalab M, Yi Q-L, et al. Bacterial survival and distribution during buffy coat platelet production. *Vox Sang* 2016; 111: 333–340. doi:10.1111/vox.12427
- [259] Kastrup CJ, Boedicker JQ, Pomerantsev AP, et al. Spatial localization of bacteria controls coagulation of human blood by „quorum acting“. *Nat Chem Biol* 2008; 4: 742–750. doi:10.1038/nchembio.124
- [260] Apte G, Börke J, Rothe H, et al. Modulation of Platelet-Surface Activation: Current State and Future Perspectives. *ACS Appl Bio Mater* 2020; 3: 5574–5589. doi:10.1021/acsabm.0c00822

-
- [261] Mohammadi T, Pietersz RNI, Vandenbroucke-Grauls CMJE, et al. Detection of bacteria in platelet concentrates: comparison of broad-range real-time 16S rDNA polymerase chain reaction and automated culturing. *Transfusion* 2005; 45: 731–736. doi:10.1111/j.1537-2995.2005.04258.x
- [262] Dreier J, Störmer M, Kleesiek K. Two novel real-time reverse transcriptase PCR assays for rapid detection of bacterial contamination in platelet concentrates. *J Clin Microbiol* 2004; 42: 4759–4764. doi:10.1128/JCM.42.10.4759-4764.2004
- [263] Corless CE, Guiver M, Borrow R, et al. Contamination and sensitivity issues with a real-time universal 16S rRNA PCR. *J Clin Microbiol* 2000; 38: 1747–1752. doi:10.1128/JCM.38.5.1747-1752.2000
- [264] Garson JA, Patel P, McDonald C, et al. Evaluation of an ethidium monoazide-enhanced 16S rDNA real-time polymerase chain reaction assay for bacterial screening of platelet concentrates and comparison with automated culture. *Transfusion* 2014; 54: 870–878. doi:10.1111/trf.12256
- [265] Nadkarni MA, Martin FE, Jacques NA, et al. Determination of bacterial load by real-time PCR using a broad-range (universal) probe and primers set. *Microbiology (Reading)* 2002; 148: 257–266. doi:10.1099/00221287-148-1-257
- [266] Dreier J, Störmer M, Kleesiek K. Real-time polymerase chain reaction in transfusion medicine: applications for detection of bacterial contamination in blood products. *Transfus Med Rev* 2007; 21: 237–254. doi:10.1016/j.tmr.2007.03.006
- [267] Espy MJ, Uhl JR, Sloan LM, et al. Real-Time PCR in Clinical Microbiology: Applications for Routine Laboratory Testing. *Clin Microbiol Rev* 2006; 19: 165–256. doi:10.1128/CMR.19.1.165-256.2006

7 Appendix

7.1 Recipes of stock solutions and media

Table 27: Recipe of NaCl 0.85 % (1 l)

| Ingredient | Amount |
|------------------------|--------|
| NaCl | 8.5 g |
| H ₂ O dest. | ad 1 l |

Table 28: Recipe of PBS without Ca and Mg pH 7.1 (1 l)

| Ingredient | Amount |
|----------------------------------|---------|
| H ₂ O dest | 900 ml |
| NaCl | 8 g |
| KCl | 0.2 g |
| KH ₂ PO ₄ | 0.2 g |
| Na ₂ HPO ₄ | 1.15 g |
| HCl 1N for pH adjustment | ~1.4 ml |
| H ₂ O dest | Ad 1 l |

Table 29: Recipe of PBS without Ca and Mg pH 7.1 + 1 mM EDTA (1l)

| Ingredient | Amount |
|----------------------------------|---------|
| PBS without Ca and Mg pH 7.1 x10 | 100 ml |
| H ₂ O dest | 800 ml |
| Titriplex III (EDTA-Na) | 0.372 g |
| HCl 1 N for pH adjustment | ~ x ml |
| H ₂ O dest | Ad 1 l |

Table 30: Recipe of Standard-I-Agar (1 l)

| Ingredient | Amount |
|-----------------------|--------|
| Peptone | 15 g |
| Yeast extract | 3 g |
| NaCl | 6 g |
| D (+) Glucose | 1 g |
| Agar-Agar | 12 g |
| H ₂ O dest | Ad 1 l |

7.2 Result graphs flow cytometry method (WHO bacteria panel)

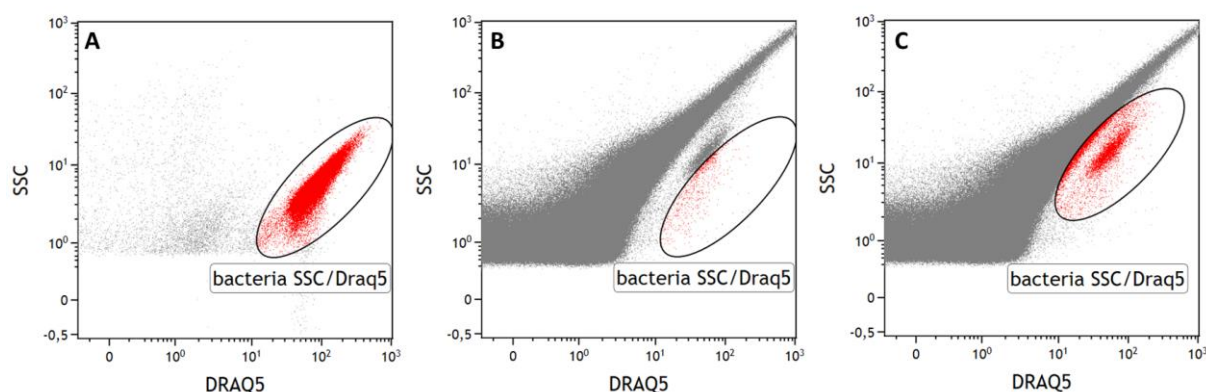


Figure 37: Flow cytometric detection gate for *E. coli* in PC samples

(A) Representative dot plot of DRAQ5-positive *E. coli* (10^6 CFU) without PC measured by the established flow cytometry method. Gating of bacterial fluorescence events without the influence of PC based on granularity (SSC) and DNA content (DRAQ5™ fluorescence intensity) ($n = 3$). (B) To determine and confirm the position of the bacteria detection gate in presence of PC, 10^6 CFU/ml of *E. coli* were spiked in PC and samples were measured by using the new flow cytometry method. (C) The detection gate for bacteria in PC was adjusted based on the granularity (SSC) and DRAQ5™ staining intensity of the bacteria within the PC sample. ($n = 3$).

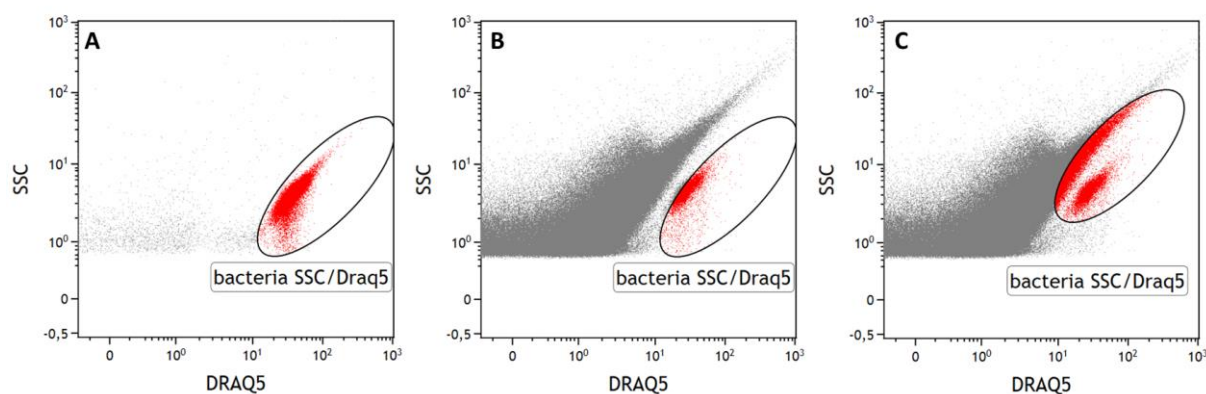


Figure 38: Flow cytometric detection gate for *E. cloacae* in PC samples

(A) Representative dot plot of DRAQ5-positive *E. cloacae* (10^6 CFU) without PC measured by the established flow cytometry method. Gating of bacterial fluorescence events without the influence of PC based on granularity (SSC) and DNA content (DRAQ5™ fluorescence intensity) ($n = 3$). (B) To determine and confirm the position of the bacteria detection gate in presence of PC, 10^6 CFU/ml of *E. cloacae* were spiked in PC and samples were measured by using the new flow cytometry method. (C) The detection gate for bacteria in PC was adjusted based on the granularity (SSC) and DRAQ5™ staining intensity of the bacteria within the PC sample. ($n = 3$).

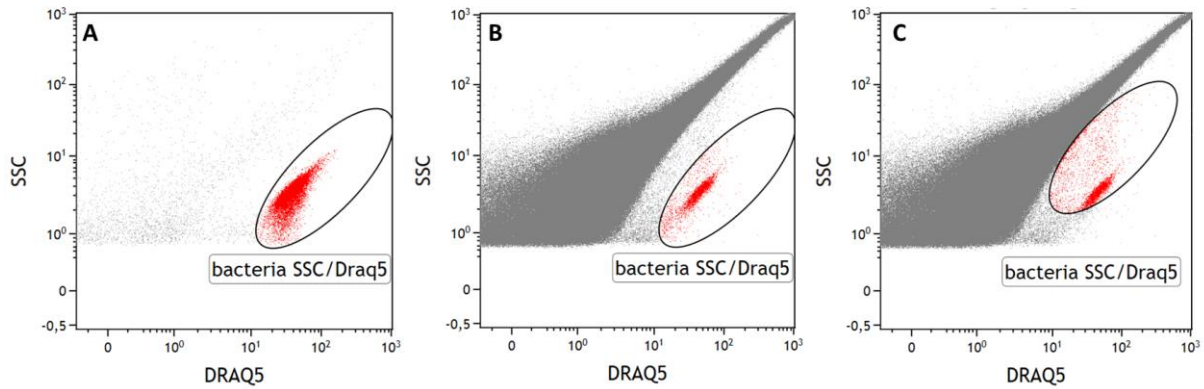


Figure 39: Flow cytometric detection gate for *P. fluorescens* in PC samples

(A) Representative dot plot of DRAQ5-positive *P. fluorescens* (10^6 CFU) without PC measured by the established flow cytometry method. Gating of bacterial fluorescence events without the influence of PC based on granularity (SSC) and DNA content (DRAQ5™ fluorescence intensity) ($n = 3$). (B) To determine and confirm the position of the bacteria detection gate in presence of PC, 10^6 CFU/ml of *P. fluorescens* were spiked in PC and samples were measured by using the new flow cytometry method. (C) The detection gate for bacteria in PC was adjusted based on the granularity (SSC) and DRAQ5™ staining intensity of the bacteria within the PC sample. ($n = 3$).

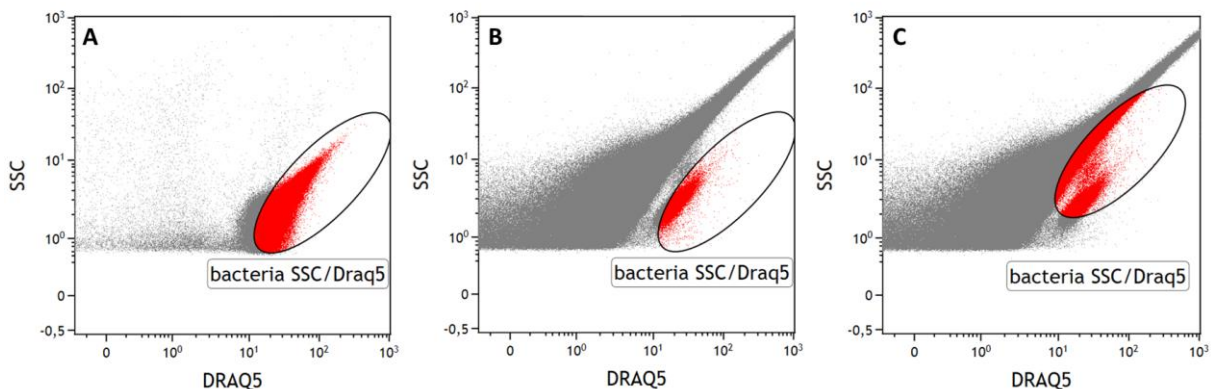


Figure 40: Flow cytometric detection gate for *P. mirabilis* in PC samples

(A) Representative dot plot of DRAQ5-positive *P. mirabilis* (10^6 CFU) without PC measured by the established flow cytometry method. Gating of bacterial fluorescence events without the influence of PC based on granularity (SSC) and DNA content (DRAQ5™ fluorescence intensity) ($n = 3$). (B) To determine and confirm the position of the bacteria detection gate in presence of PC, 10^6 CFU/ml of *P. mirabilis* were spiked in PC and samples were measured by using the new flow cytometry method. (C) The detection gate for bacteria in PC was adjusted based on the granularity (SSC) and DRAQ5™ staining intensity of the bacteria within the PC sample. ($n = 3$).

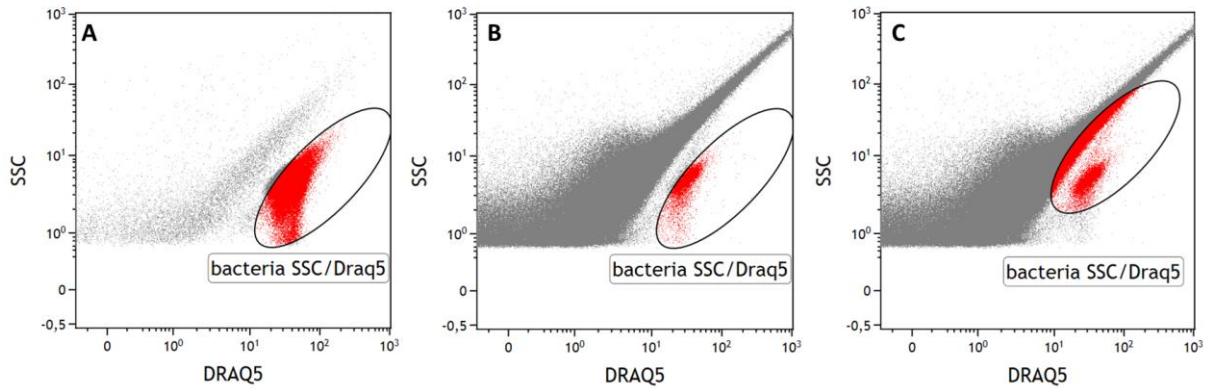


Figure 41: Flow cytometric detection gate for *S. marcescens* in PC samples

(A) Representative dot plot of DRAQ5-positive *S. marcescens* (10^6 CFU) without PC measured by the established flow cytometry method. Gating of bacterial fluorescence events without the influence of PC based on granularity (SSC) and DNA content (DRAQ5™ fluorescence intensity) ($n = 3$). (B) To determine and confirm the position of the bacteria detection gate in presence of PC, 10^6 CFU/ml of *S. marcescens* were spiked in PC and samples were measured by using the new flow cytometry method. (C) The detection gate for bacteria in PC was adjusted based on the granularity (SSC) and DRAQ5™ staining intensity of the bacteria within the PC sample. ($n = 3$).

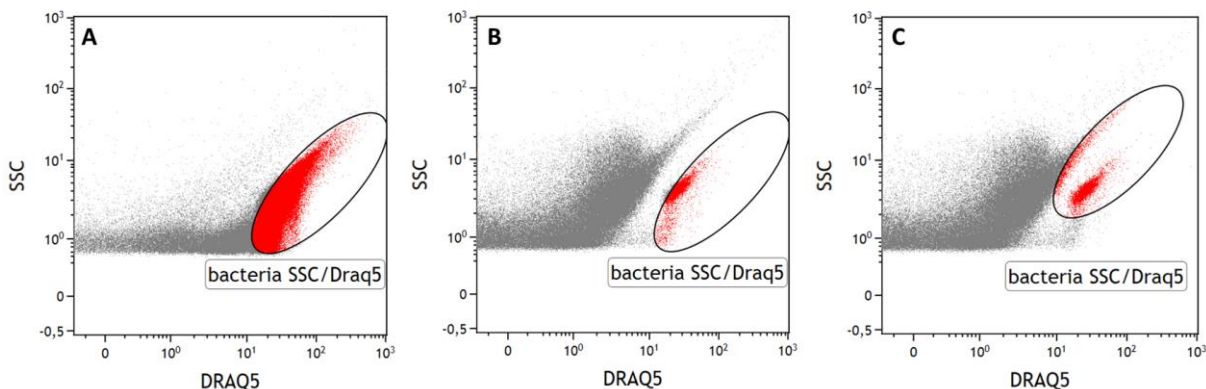


Figure 42: Flow cytometric detection gate for *M. morgani* in PC samples

(A) Representative dot plot of DRAQ5-positive *M. morgani* (10^6 CFU) without PC measured by the established flow cytometry method. Gating of bacterial fluorescence events without the influence of PC based on granularity (SSC) and DNA content (DRAQ5™ fluorescence intensity) ($n = 3$). (B) To determine and confirm the position of the bacteria detection gate in presence of PC, 10^6 CFU/ml of *M. morgani* were spiked in PC and samples were measured by using the new flow cytometry method. (C) The detection gate for bacteria in PC was adjusted based on the granularity (SSC) and DRAQ5™ staining intensity of the bacteria within the PC sample. ($n = 3$).

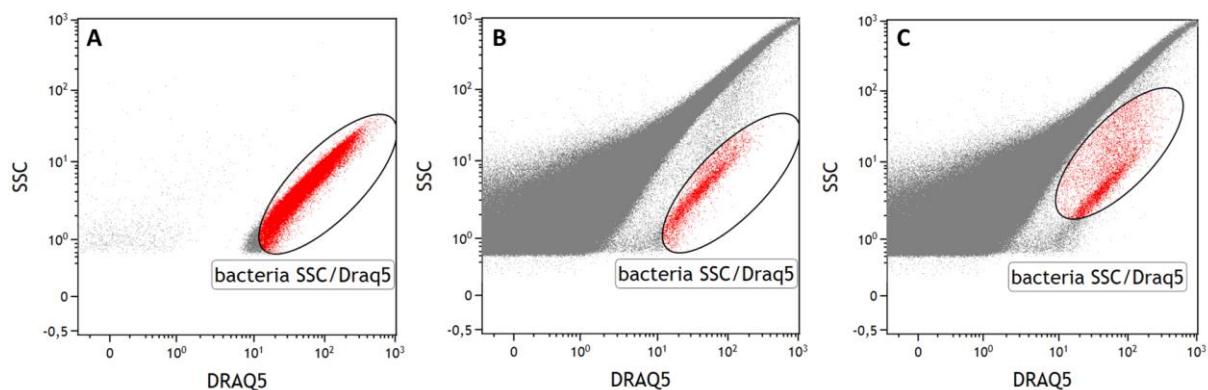


Figure 43: Flow cytometric detection gate for *S. pyogenes* in PC samples

(A) Representative dot plot of DRAQ5-positive *S. pyogenes* (10^6 CFU) without PC measured by the established flow cytometry method. Gating of bacterial fluorescence events without the influence of PC based on granularity (SSC) and DNA content (DRAQ5™ fluorescence intensity) ($n = 3$). (B) To determine and confirm the position of the bacteria detection gate in presence of PC, 10^6 CFU/ml of *S. pyogenes* were spiked in PC and samples were measured by using the new flow cytometry method. (C) The detection gate for bacteria in PC was adjusted based on the granularity (SSC) and DRAQ5™ staining intensity of the bacteria within the PC sample. ($n = 3$).

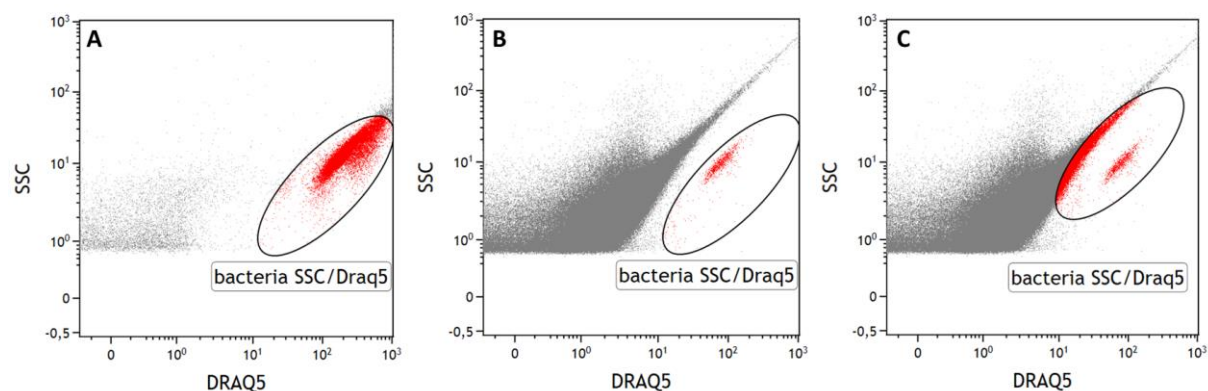


Figure 44: Flow cytometric detection gate for *B. thuringiensis* in PC samples

(A) Representative dot plot of DRAQ5-positive *B. thuringiensis* (10^6 CFU) without PC measured by the established flow cytometry method. Gating of bacterial fluorescence events without the influence of PC based on granularity (SSC) and DNA content (DRAQ5™ fluorescence intensity) ($n = 3$). (B) To determine and confirm the position of the bacteria detection gate in presence of PC, 10^6 CFU/ml of *B. thuringiensis* were spiked in PC and samples were measured by using the new flow cytometry method. (C) The detection gate for bacteria in PC was adjusted based on the granularity (SSC) and DRAQ5™ staining intensity of the bacteria within the PC sample. ($n = 3$).

7.3 Detection of bacteria in PC without Tirofiban incubation step

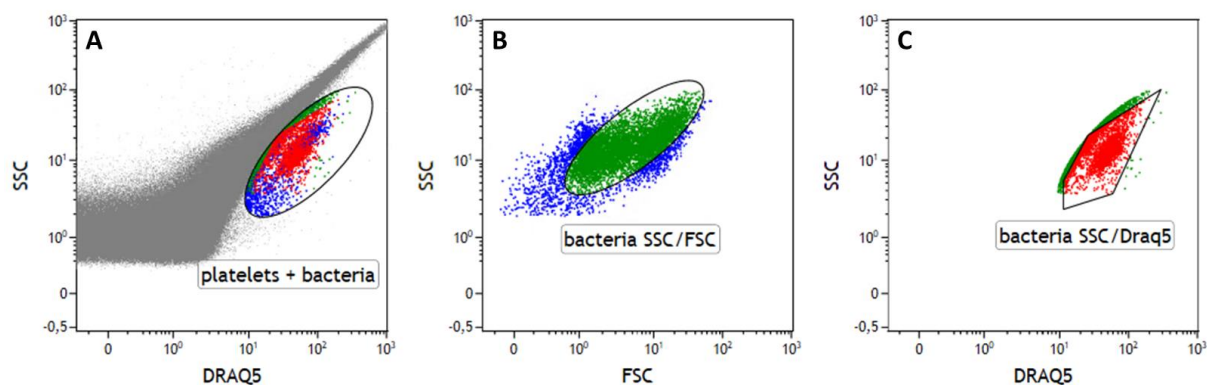


Figure 45: Detection of 10^5 CFU/ml *E. coli* in PC without Tirofiban incubation step

Representative dot plot of PC spiked with 10^5 CFU/ml of *E. coli*, measured using the new flow cytometry method without Tirofiban treatment [n = 3]. Platelets (blue) and bacteria (red) were gated based on SSC and DRAQ5™ staining intensity (A). The bacterial population (green) and residual platelets (blue) were discriminated by SSC and FSC (B). Additionally, the bacterial population (red) was discriminated from residual non-specific stained cell debris and platelets (green) based on DRAQ5™ staining intensity. Fluorescence events within the defined bacterial detection gate were counted as bacteria (C).

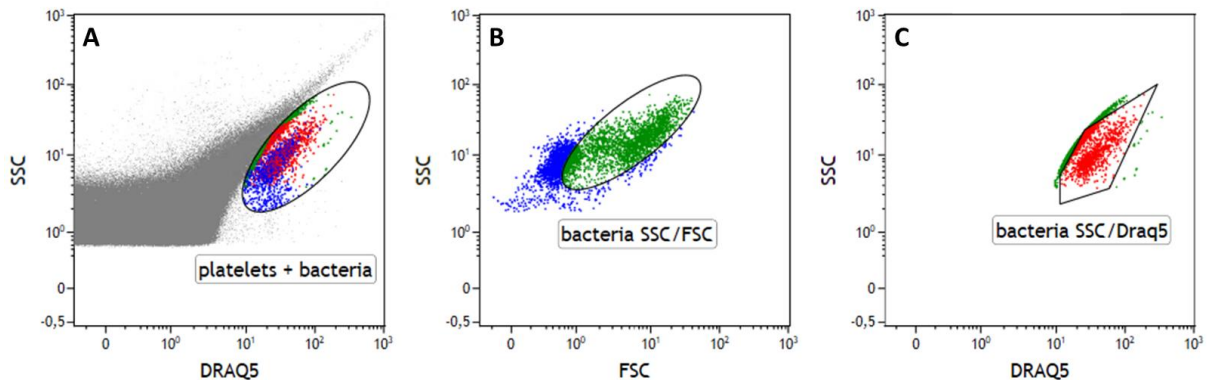


Figure 46: Detection of 10^5 CFU/ml *E. cloacae* in PC without Tirofiban incubation step

Representative dot plot of PC spiked with 10^5 CFU/ml of *E. cloacae*, measured using the new flow cytometry method without Tirofiban treatment [n = 3]. Platelets (blue) and bacteria (red) were gated based on SSC and DRAQ5™ staining intensity (A). The bacterial population (green) and residual platelets (blue) were discriminated by SSC and FSC (B). Additionally, the bacterial population (red) was discriminated from residual non-specific stained cell debris and platelets (green) based on DRAQ5™ staining intensity. Fluorescence events within the defined bacterial detection gate were counted as bacteria (C).

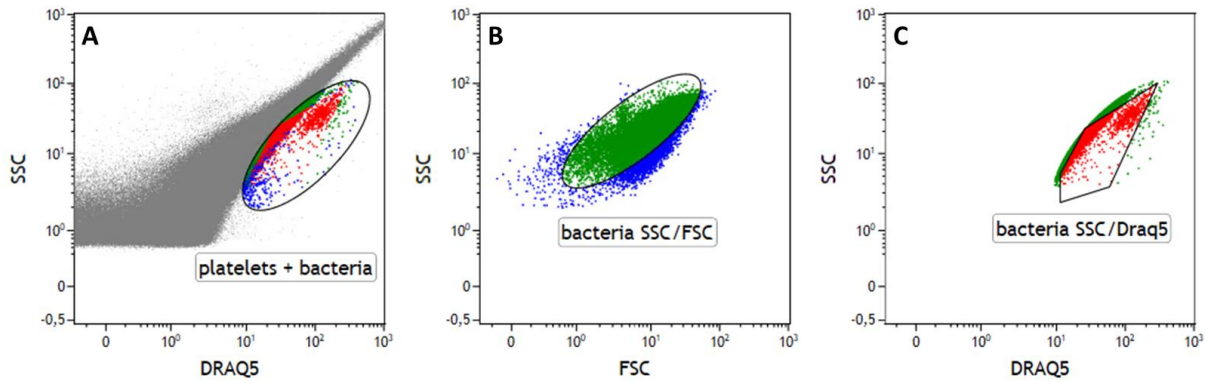


Figure 47: Detection of 10⁵ CFU/ml *B. thuringiensis* in PC without Tirofiban incubation step

Representative dot plot of PC spiked with 10⁵ CFU/ml of *B. thuringiensis*, measured using the new flow cytometry method without Tirofiban treatment [n = 3]. Platelets (blue) and bacteria (red) were gated based on SSC and DRAQ5™ staining intensity (A). The bacterial population (green) and residual platelets (blue) were discriminated by SSC and FSC (B). Additionally, the bacterial population (red) was discriminated from residual non-specific stained cell debris and platelets (green) based on DRAQ5™ staining intensity. Fluorescence events within the defined bacterial detection gate were counted as bacteria (C).

7.4 Result graphs for the discrimination threshold of bacterial contaminations in PC

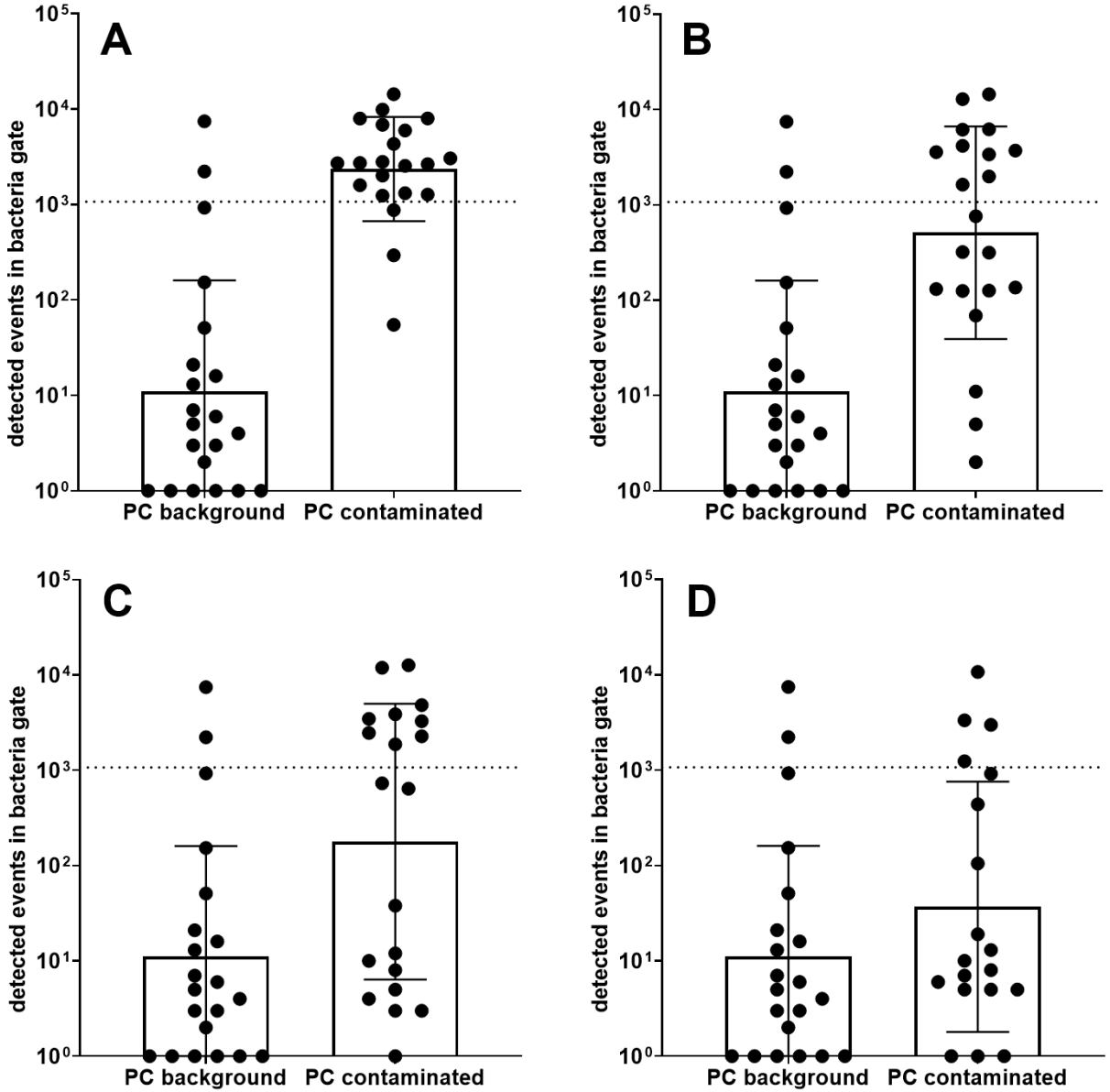


Figure 48: Comparison of detected events of contaminated and non-contaminated PC without Tirofiban

To define a discrimination threshold (dashed line) of contaminated and non-contaminated PC, an area under the receiver operating characteristic curve (AUROC) was performed (chapter 4.2.4, Fig. 28). Non-contaminated PC were analysed as negative control and compared to PC samples contaminated with *K. pneumoniae*, *B. cereus* and *S. epidermidis* as positive control at contamination levels of 10² CFU/ml (A), 10³ CFU/ml (B), 10⁴ CFU/ml (C) and 10⁵ CFU/ml (D). Error bars indicate mean of detected events ± 1 SD.

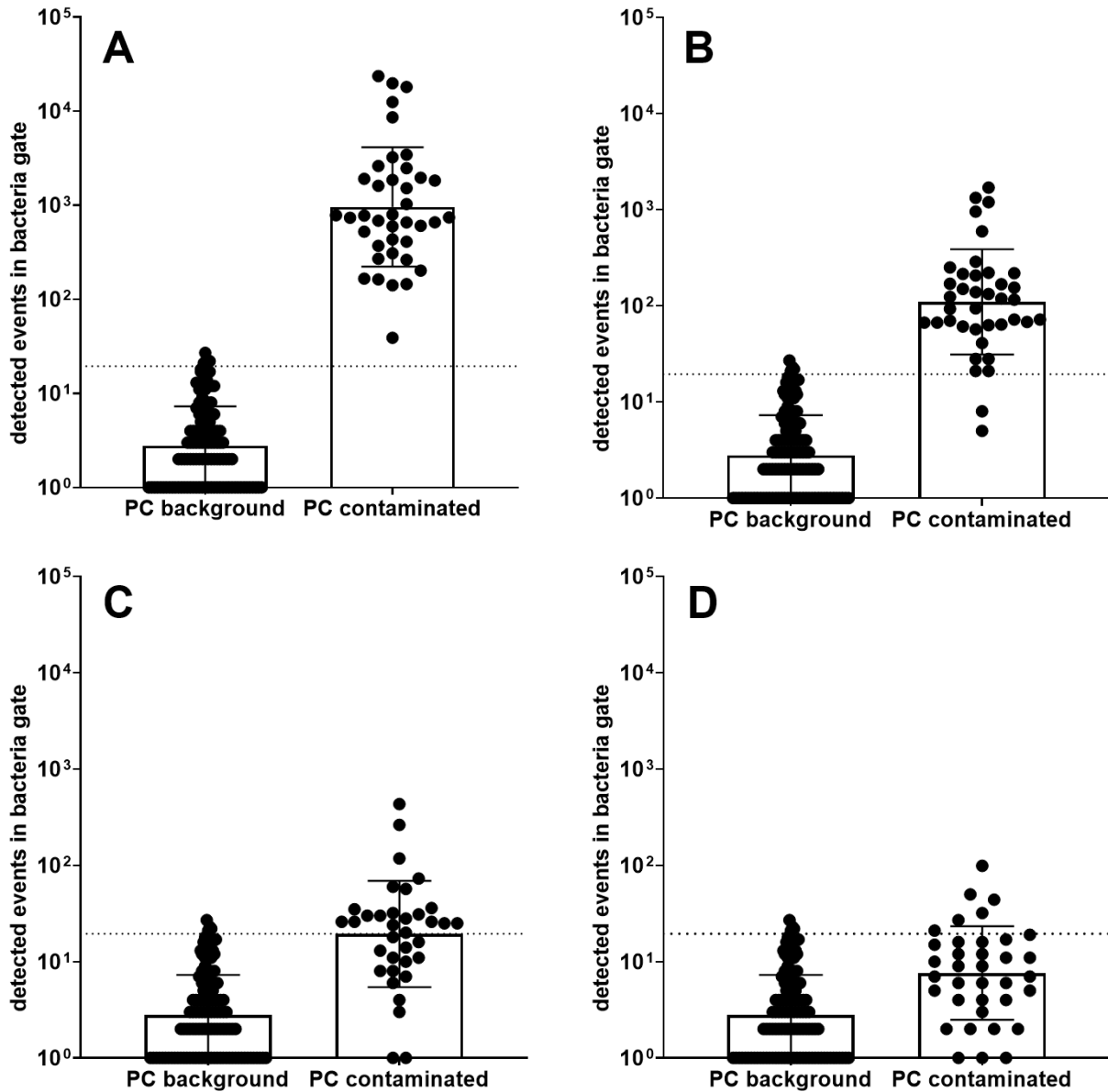


Figure 49: Comparison of detected events of contaminated and non-contaminated PC incubated with Tirofiban

To define a discrimination threshold (dashed line) of contaminated and non-contaminated PC, an area under the receiver operating characteristic curve (AUROC) was performed (chapter 4.2.4, Fig. 29). non-contaminated PC were analysed as negative control and compared to PC samples contaminated with *K. pneumoniae*, *B. cereus* and *S. epidermidis* as positive control at contamination levels of 10^2 CFU/ml (A), 10^3 CFU/ml (B), 10^4 CFU/ml (C) and 10^5 CFU/ml (D). Error bars indicate mean of detected events ± 1 SD.

7.5 Mean number (CFU/ml) of bacteria spiked into PC and result graphs of the new flow cytometry method without Tirofiban

Table 31: Mean number (CFU/ml) of bacteria spiked into PC samples (without Tirofiban)

| Bacteria strain | <i>K. pneumoniae</i> | <i>B. cereus</i> | <i>S. epidermidis</i> | <i>S. aureus</i> |
|--------------------------------------|----------------------|----------------------|-----------------------|----------------------|
| 10 ² CFU/ml (mean count*) | 1.33x10 ² | 2.30x10 ² | 7.67x10 ¹ | 1.83x10 ² |
| 10 ³ CFU/ml (mean count*) | 1.25x10 ³ | 3.10x10 ³ | 7.63x10 ² | 1.71x10 ³ |
| 10 ⁴ CFU/ml (mean count*) | 1.24x10 ⁴ | 4.27x10 ⁴ | 9.09x10 ³ | 1.75x10 ⁴ |
| 10 ⁵ CFU/ml (mean count*) | 1.44x10 ⁵ | 1.98x10 ⁵ | 7.02x10 ⁴ | 1.63x10 ⁵ |

| Bacteria strain | <i>B. thuringiensis</i> | <i>E. coli</i> | <i>E. cloacae</i> |
|--------------------------------------|-------------------------|----------------------|----------------------|
| 10 ² CFU/ml (mean count*) | 2.00x10 ¹ | 9.00x10 ¹ | 6.67x10 ¹ |
| 10 ³ CFU/ml (mean count*) | 2.30x10 ² | 1.47x10 ³ | 5.00x10 ² |
| 10 ⁴ CFU/ml (mean count*) | 4.81x10 ³ | 1.30x10 ⁴ | 3.67x10 ³ |
| 10 ⁵ CFU/ml (mean count*) | 5.02x10 ⁴ | 1.11x10 ⁵ | 4.67x10 ⁴ |

*Mean count corresponds to the respective triplicate per experiment and contamination level (*K. pneumoniae*: n= 3, 9 plates analysed; *B. cereus*: n= 3, 9 plates analysed; *S. epidermidis*: n= 3, 9 plates analysed; *S. aureus*: n= 3, 9 plates analysed, *B. thuringiensis*: n= 3, 9 plates analysed; *E. coli*: n= 3, 9 plates analysed; *E. cloacae*: n= 3, 9 plates analysed).

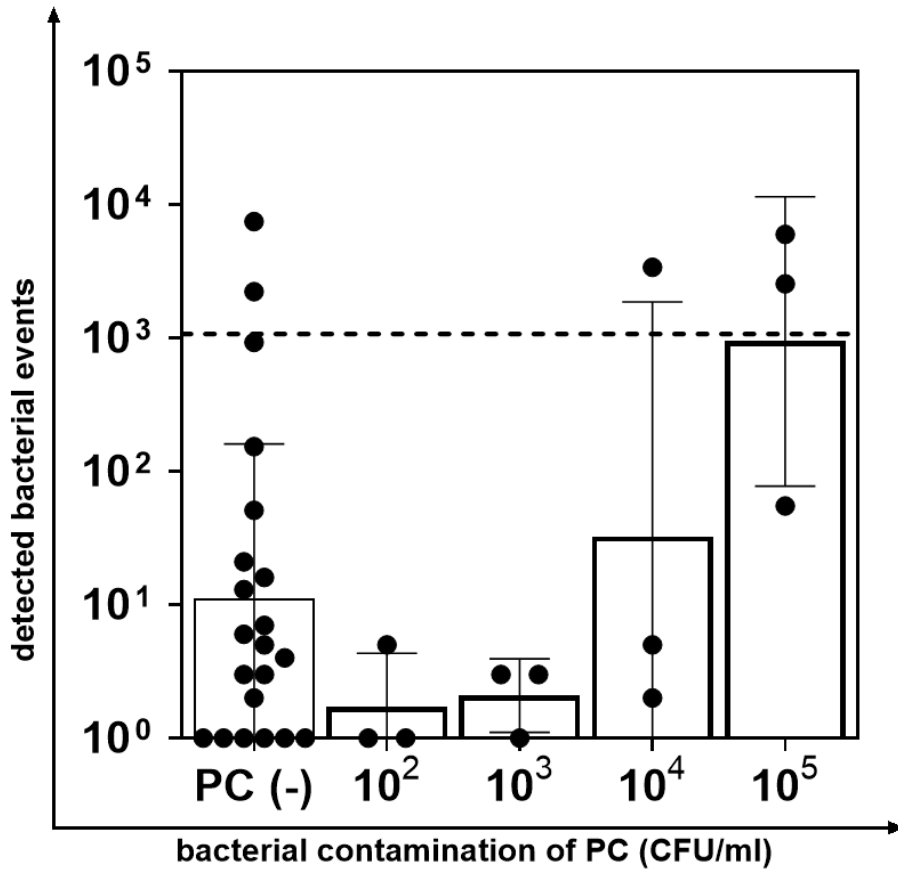


Figure 50: PC spiked with *S. aureus* analysed with the new flow cytometry method without Tirofiban

PC samples were spiked with defined contamination levels of *S. aureus* ranging from 10^2 - 10^5 CFU/ml and analysed using the new flow cytometry method. Non-contaminated PC samples PC (-) were analysed as negative reference to determine the background events. Classification into non-contaminated PC and contaminated PC was performed using the calculated discrimination threshold of 1072 (chapter 4.2.4, Fig. 28) (dashed line). Error bars indicate mean of detected events \pm 1 SD.

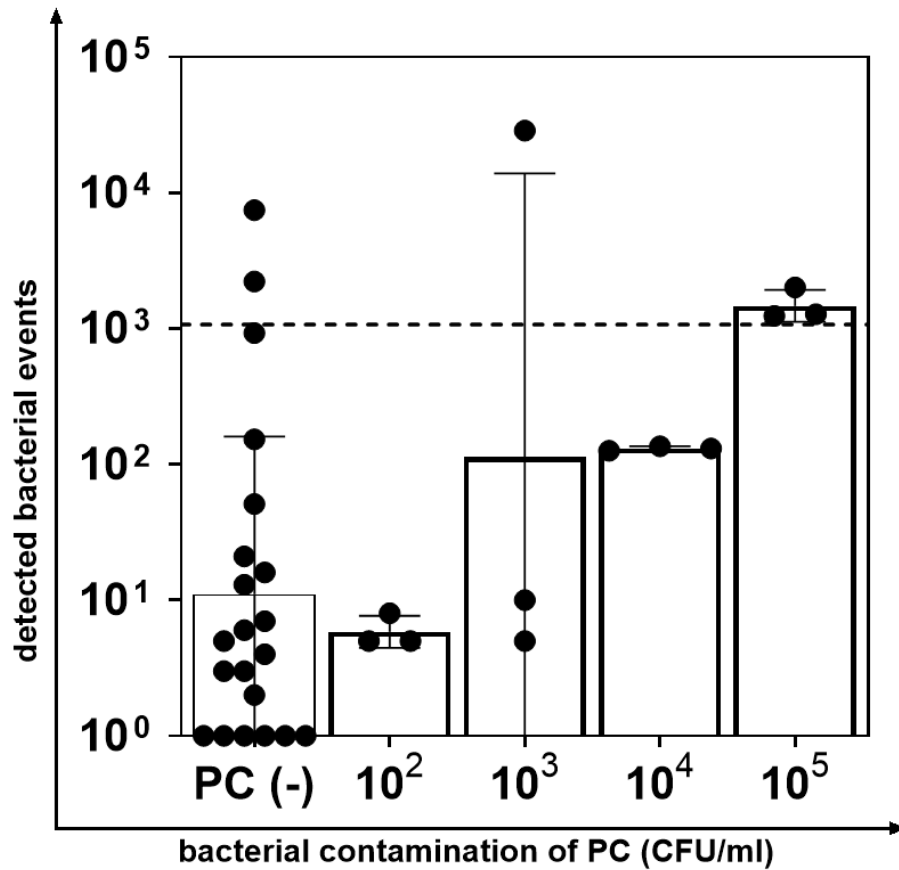


Figure 51: PC spiked with *K. pneumoniae* analysed with the new flow cytometry method without Tirofiban

PC samples were spiked with defined contamination levels of *K. pneumoniae* ranging from 10^2 - 10^5 CFU/ml and analysed using the new flow cytometry method. Non-contaminated PC samples PC (-) were analysed as negative reference to determine the background events. Classification into non-contaminated PC and contaminated PC was performed using the calculated discrimination threshold of 1072 (chapter 4.2.4, Fig. 28) (dashed line). Error bars indicate mean of detected events \pm 1 SD.

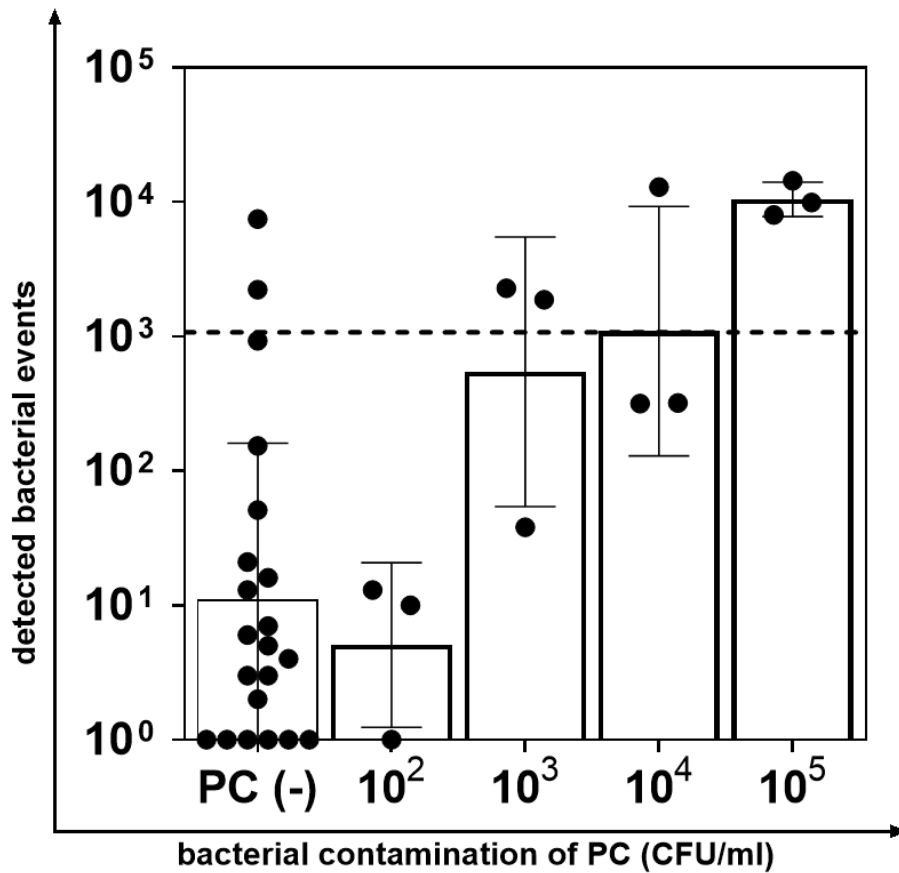


Figure 52: PC spiked with *B. cereus* analysed with the new flow cytometry method without Tirofiban

PC samples were spiked with defined contamination levels of *B. cereus* ranging from 10^2 - 10^5 CFU/ml and analysed using the new flow cytometry method. Non-contaminated PC samples PC (-) were analysed as negative reference to determine the background events. Classification into non-contaminated PC and contaminated PC was performed using the calculated discrimination threshold of 1072 (chapter 4.2.4, Fig. 28) (dashed line). Error bars indicate mean of detected events \pm 1 SD.

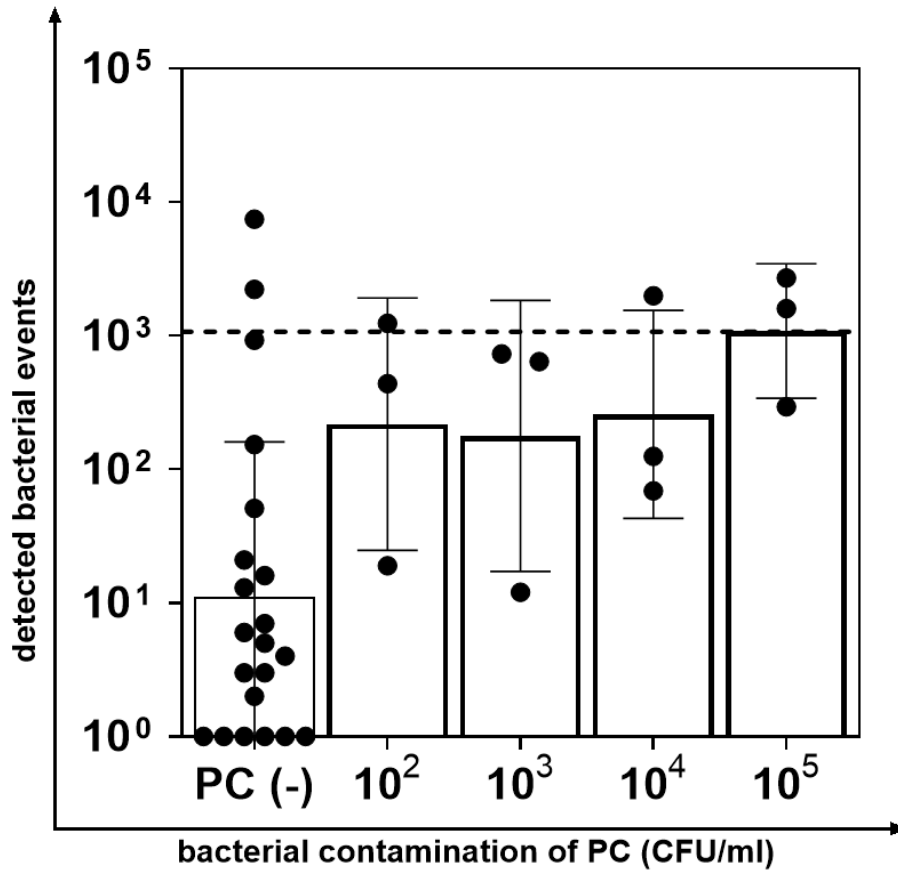


Figure 53: PC spiked with *S. epidermidis* analysed with the new flow cytometry method without Tirofiban

PC samples were spiked with defined contamination levels of *S. epidermidis* ranging from 10^2 - 10^5 CFU/ml and analysed using the new flow cytometry method. Non-contaminated PC samples PC (-) were analysed as negative reference to determine the background events. Classification into non-contaminated PC and contaminated PC was performed using the calculated discrimination threshold of 1072 (chapter 4.2.4, Fig. 28) (dashed line). Error bars indicate mean of detected events \pm 1 SD.

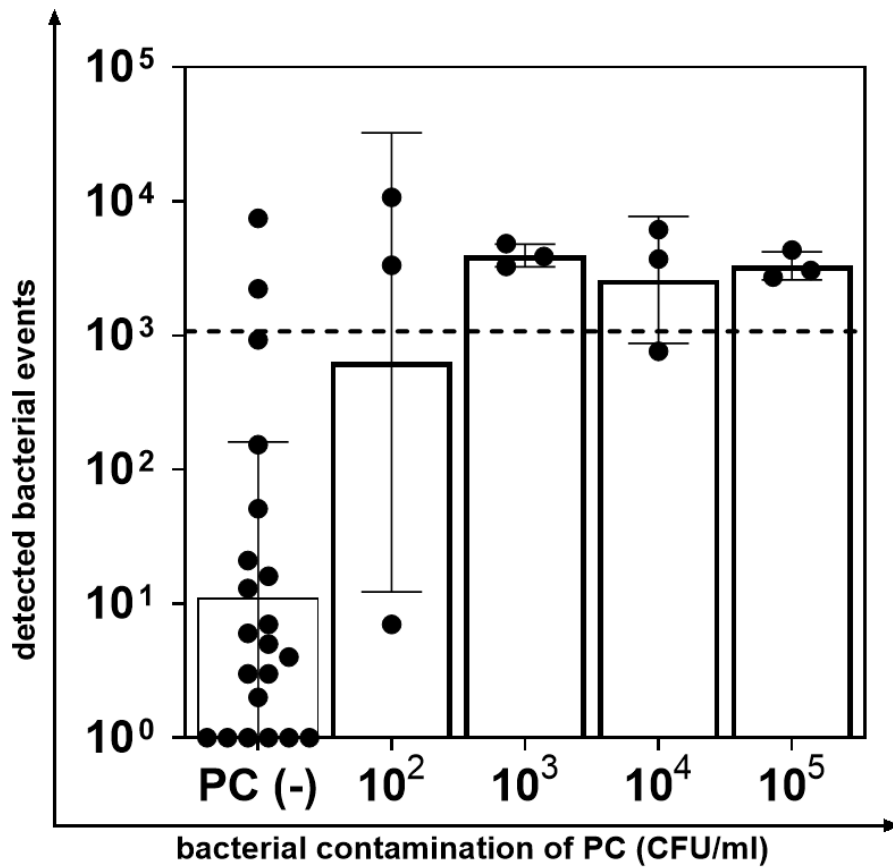


Figure 54: PC spiked with *E. coli* analysed with the new flow cytometry method without Tirofiban

PC samples were spiked with defined contamination levels of *E. coli* ranging from 10^2 - 10^5 CFU/ml and analysed using the new flow cytometry method. Non-contaminated PC samples PC (-) were analysed as negative reference to determine the background events. Classification into non-contaminated PC and contaminated PC was performed using the calculated discrimination threshold of 1072 (chapter 4.2.4, Fig. 28) (dashed line). Error bars indicate mean of detected events \pm 1 SD.

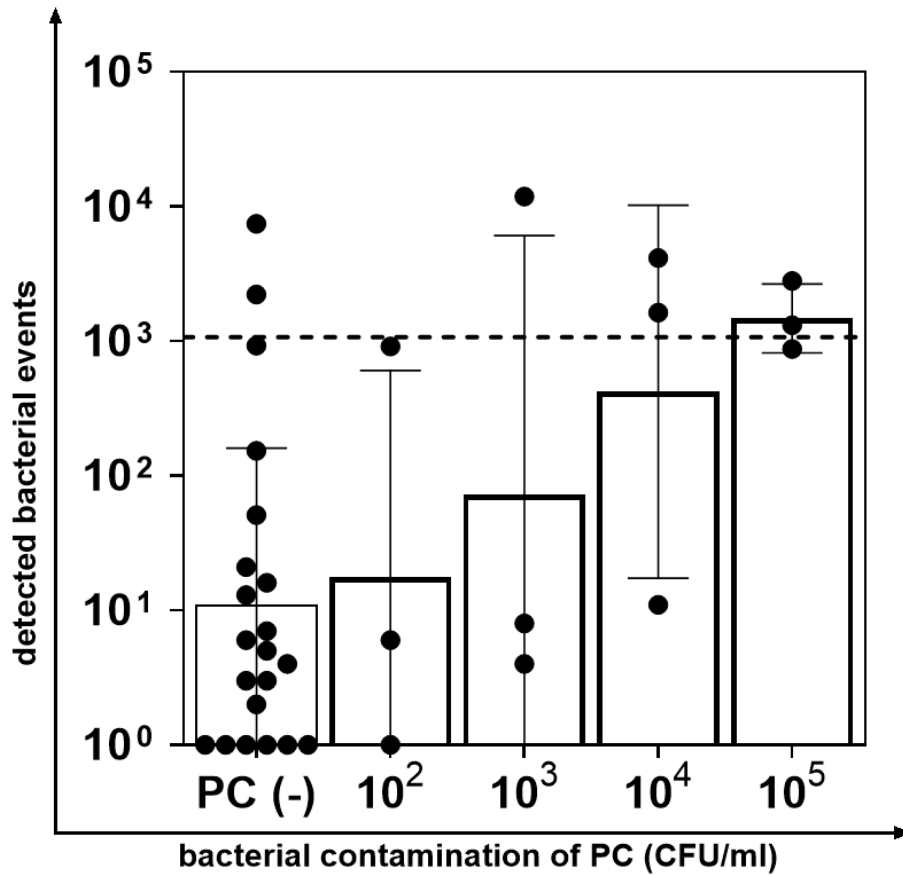


Figure 55: PC spiked with *E. cloacae* analysed with the new flow cytometry method without Tirofiban

PC samples were spiked with defined contamination levels of *E. cloacae* ranging from 10^2 - 10^5 CFU/ml and analysed using the new flow cytometry method. Non-contaminated PC samples PC (-) were analysed as negative reference to determine the background events. Classification into non-contaminated PC and contaminated PC was performed using the calculated discrimination threshold of 1072 (chapter 4.2.4, Fig. 28) (dashed line). Error bars indicate mean of detected events \pm 1 SD.

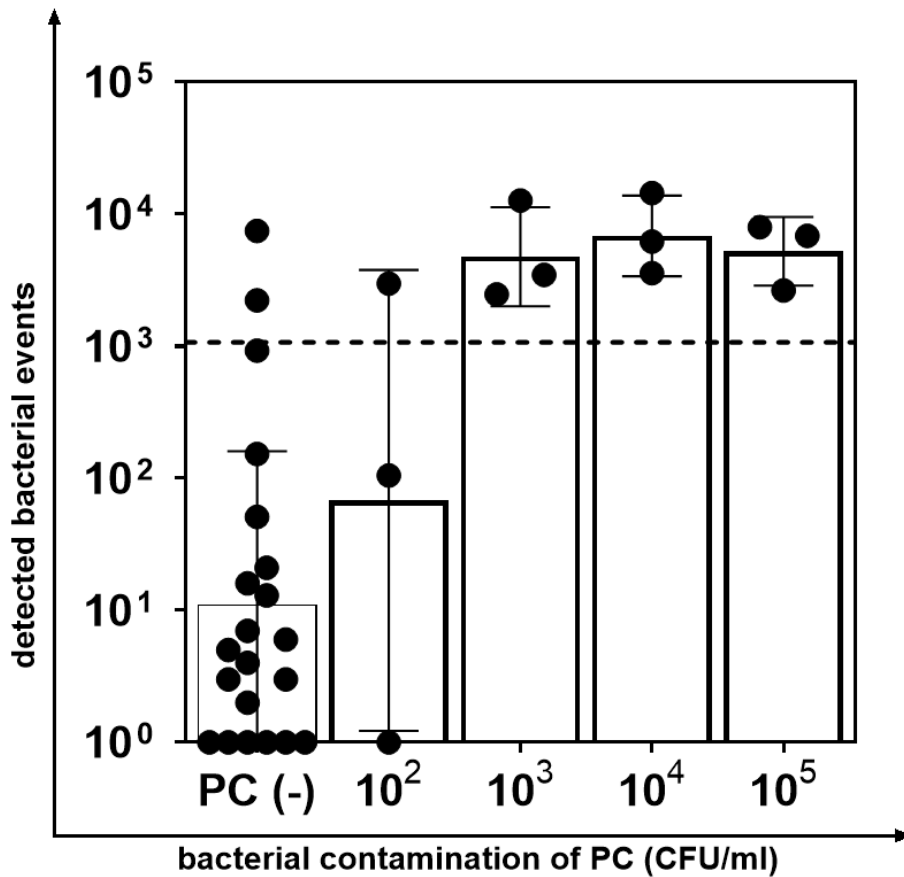


Figure 56: PC spiked with *B. thuringiensis* analysed with the new flow cytometry method without Tirofiban

PC samples were spiked with defined contamination levels of *B. thuringiensis* ranging from 10^2 - 10^5 CFU/ml and analysed using the new flow cytometry method. Non-contaminated PC samples PC (-) were analysed as negative reference to determine the background events. Classification into non-contaminated PC and contaminated PC was performed using the calculated discrimination threshold of 1072 (chapter 4.2.4, Fig. 28) (dashed line). Error bars indicate mean of detected events \pm 1 SD.

7.6 Mean number (CFU/ml) of bacteria spiked into PC and result graphs of the new flow cytometry method with Tirofiban

Table 32: Mean number (CFU/ml) of bacteria spiked into PC samples (+ Tirofiban)

| Bacteria strain | <i>K. pneumoniae</i> | <i>B. cereus</i> | <i>S. epidermidis</i> | <i>S. aureus</i> |
|--------------------------------------|----------------------|----------------------|-----------------------|----------------------|
| 10 ² CFU/ml (mean count*) | 1.10x10 ² | 1.62x10 ² | 1.27x10 ² | 1.17x10 ² |
| 10 ³ CFU/ml (mean count*) | 1.25x10 ³ | 1.52x10 ³ | 1.23x10 ³ | 1.66x10 ³ |
| 10 ⁴ CFU/ml (mean count*) | 1.15x10 ⁴ | 1.49x10 ⁴ | 1.16x10 ⁴ | 1.63x10 ⁴ |
| 10 ⁵ CFU/ml (mean count*) | 1.13x10 ⁵ | 1.42x10 ⁵ | 1.21x10 ⁵ | 1.70x10 ⁵ |

*Mean count corresponds to the respective triplicate per experiment and contamination level (*K. pneumoniae*: n= 12, 36 plates analysed; *B. cereus*: n= 12, 36 plates analysed; *S. epidermidis*: n= 15, 45 plates analysed; *S. aureus*: n= 3, 9 plates analysed).

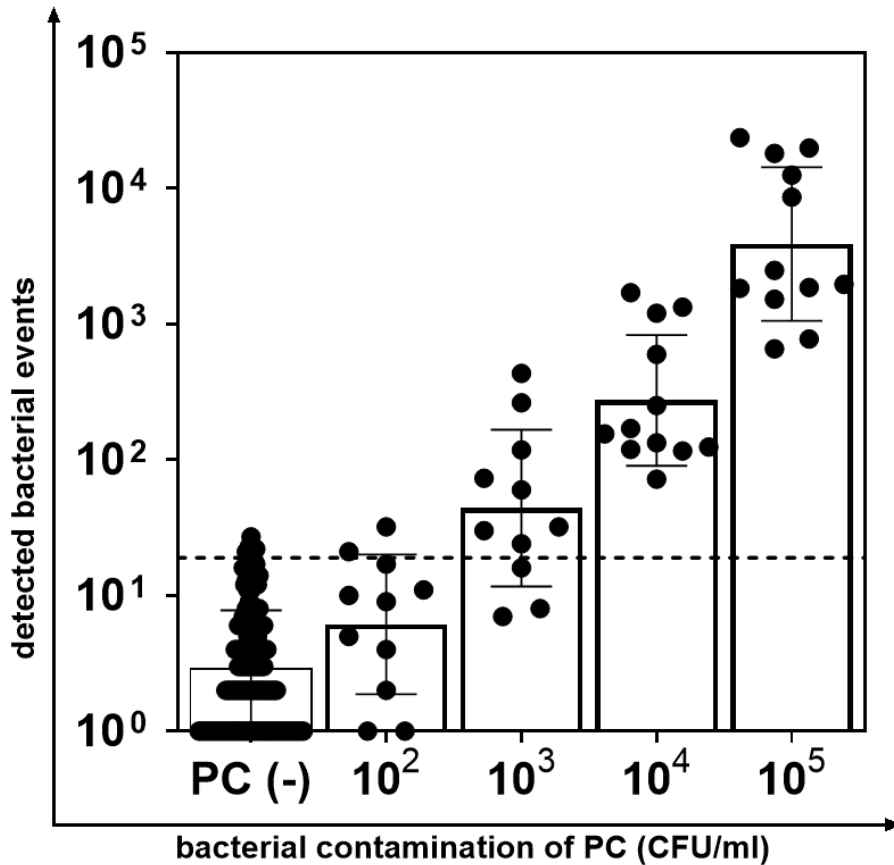


Figure 57: PC spiked with *K. pneumoniae* analysed with the new flow cytometry method with Tirofiban

PC samples were spiked with defined contamination levels of *K. pneumoniae* ranging from 10^2 - 10^5 CFU/ml and analysed using the new flow cytometry method. Non-contaminated PC samples PC (-) were analysed as negative reference to determine the background events. Classification into non-contaminated PC and contaminated PC was performed using the calculated discrimination threshold of 19 (chapter 4.2.4, Fig. 29) (dashed line). Data points with exceptionally high event number and visibly incomplete lysis were excluded from the data set (1 data point at 10^2 , 1 data point at 10^3). Error bars indicate mean of detected events \pm 1 SD.

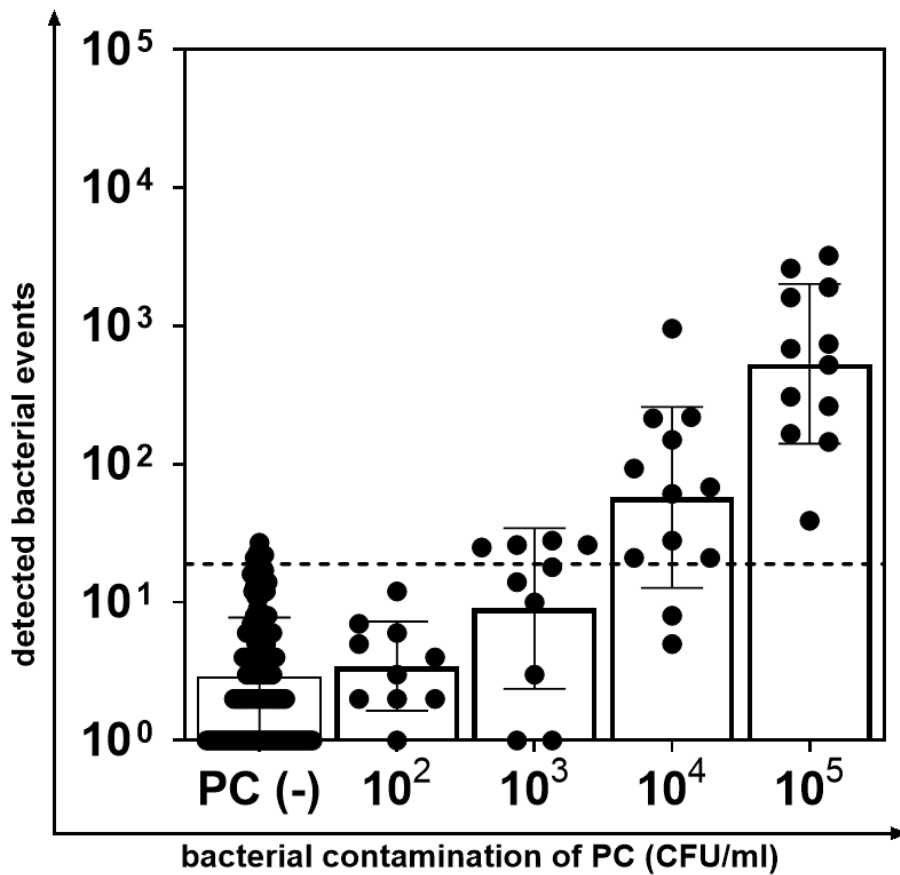


Figure 58: PC spiked with *B. cereus* analysed with the new flow cytometry method with Tirofiban

PC samples were spiked with defined contamination levels of *B. cereus* ranging from 10^2 - 10^5 CFU/ml and analysed using the new flow cytometry method. Non-contaminated PC samples PC (-) were analysed as negative reference to determine the background events. Classification into non-contaminated PC and contaminated PC was performed using the calculated discrimination threshold of 19 (chapter 4.2.4, Fig. 29) (dashed line). Data points with exceptionally high event number and visibly incomplete lysis were excluded from the data set (2 data points at 10^2 , 2 data points at 10^3). Error bars indicate mean of detected events \pm 1 SD.

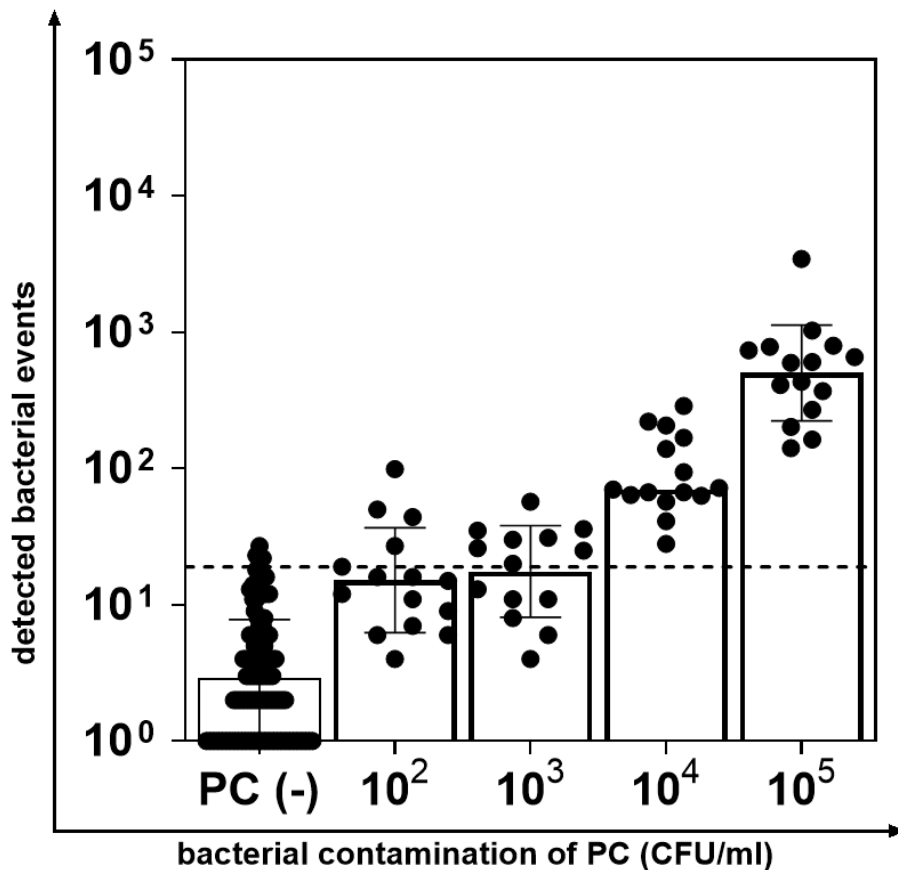


Figure 59: PC spiked with *S. epidermidis* analysed with the new flow cytometry method with Tirofiban

PC samples were spiked with defined contamination levels of *S. epidermidis* ranging from 10²-10⁵ CFU/ml and analysed using the new flow cytometry method. Non-contaminated PC samples PC (-) were analysed as negative reference to determine the background events. Classification into non-contaminated PC and contaminated PC was performed using the calculated discrimination threshold of 19 (chapter 4.2.4, Fig. 29) (dashed line). Data points with exceptionally high event number and visibly incomplete lysis were excluded from the data set (1 data point at 10³). Error bars indicate mean of detected events ± 1 SD.

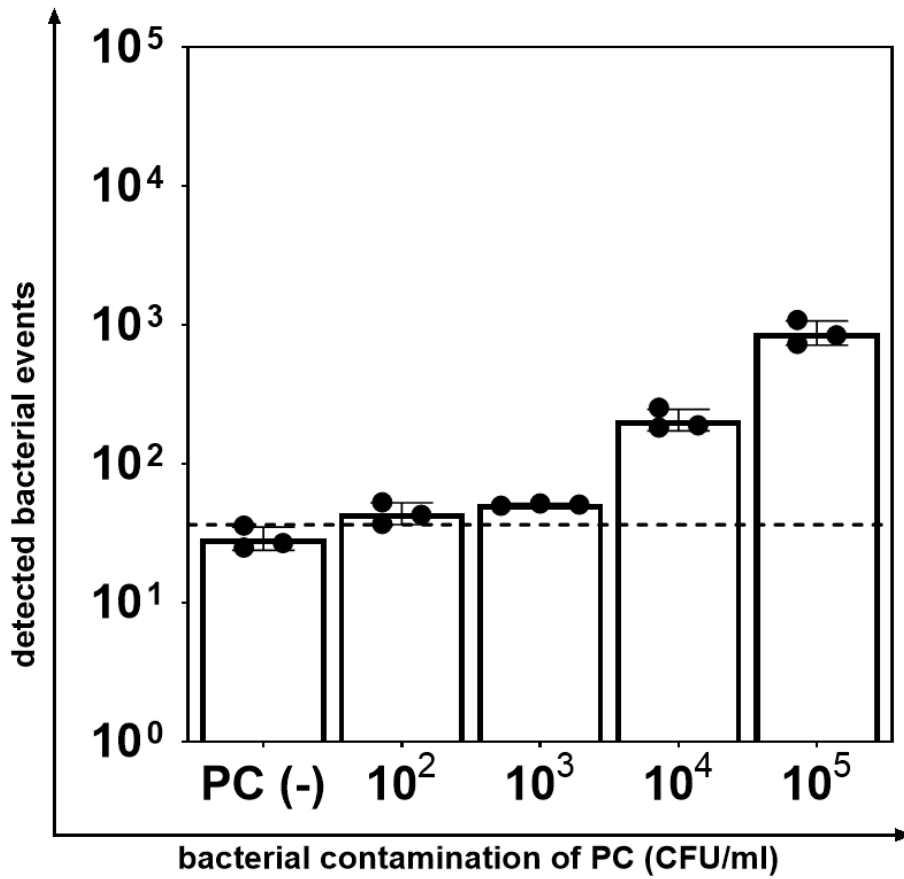


Figure 60: PC spiked with *S. aureus* analysed with the new flow cytometry method with Tirofiban

PC samples were spiked with defined contamination levels of *S. aureus* ranging from 10^2 - 10^5 CFU/ml and analysed using the new flow cytometry method. Non-contaminated PC samples PC (-) were analysed as negative reference to determine the background events. Classification into non-contaminated PC and contaminated PC was performed using the calculated discrimination threshold of 1.562 (chapter 4.2.4, Fig. 30) (dashed line). Error bars indicate mean of detected events ± 1 SD.

7.7 Result graphs of BactiFlow® system

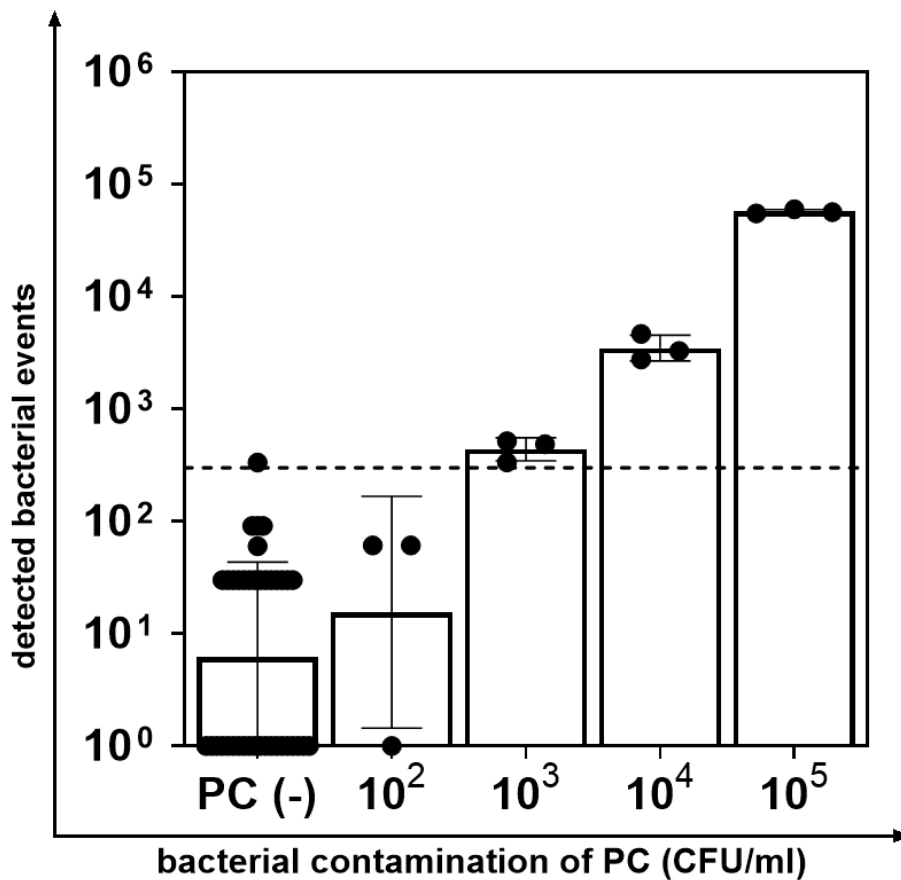


Figure 61: PC spiked with *S. aureus* analysed with the BactiFlow® system

PC samples were spiked with defined contamination levels of *S. aureus* ranging from 10^2 - 10^5 CFU/ml and analysed using the new flow cytometry method. Non-contaminated PC samples PC (-) were analysed as negative reference to determine the background events. Classification into non-contaminated PC and contaminated PC was performed by the BactiFlow® system via its defined LOD of 300 counts/ml (dashed line). Error bars indicate mean of detected events \pm 1 SD.

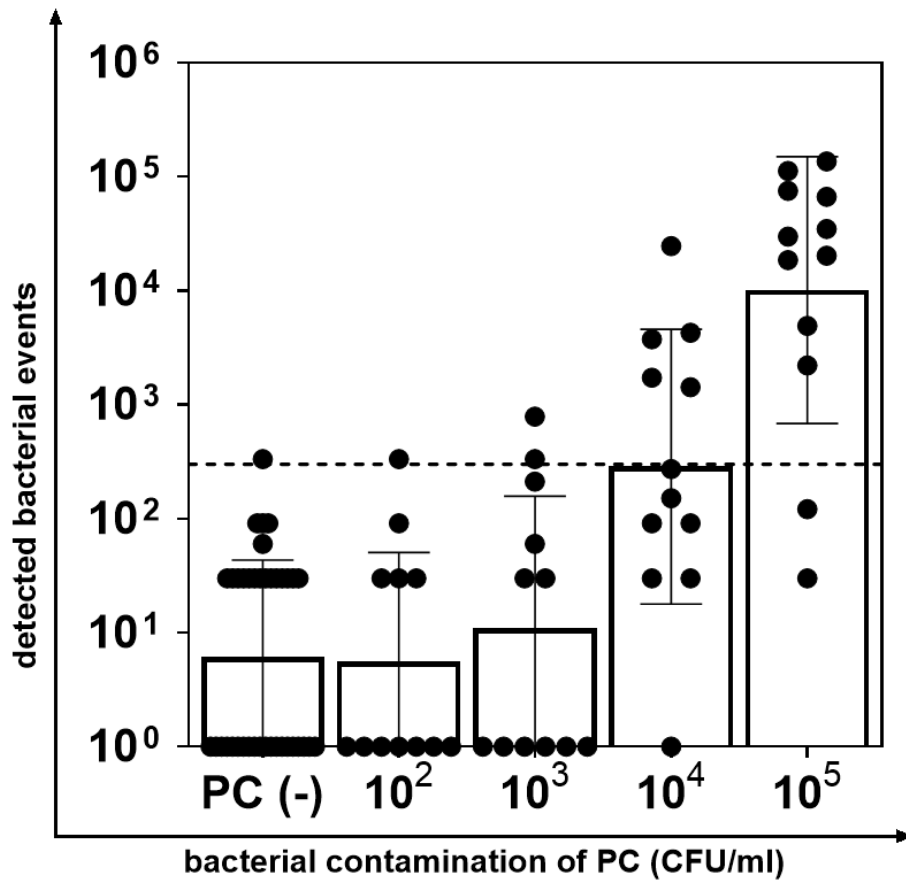


Figure 62: PC spiked with *K. pneumoniae* analysed with the BactiFlow® system

PC samples were spiked with defined contamination levels of *K. pneumoniae* ranging from 10^2 - 10^5 CFU/ml and analysed using the new flow cytometry method. Non-contaminated PC samples PC (-) were analysed as negative reference to determine the background events. Classification into non-contaminated PC and contaminated PC was performed by the BactiFlow® system via its defined LOD of 300 counts/ml (dashed line). Error bars indicate mean of detected events ± 1 SD.

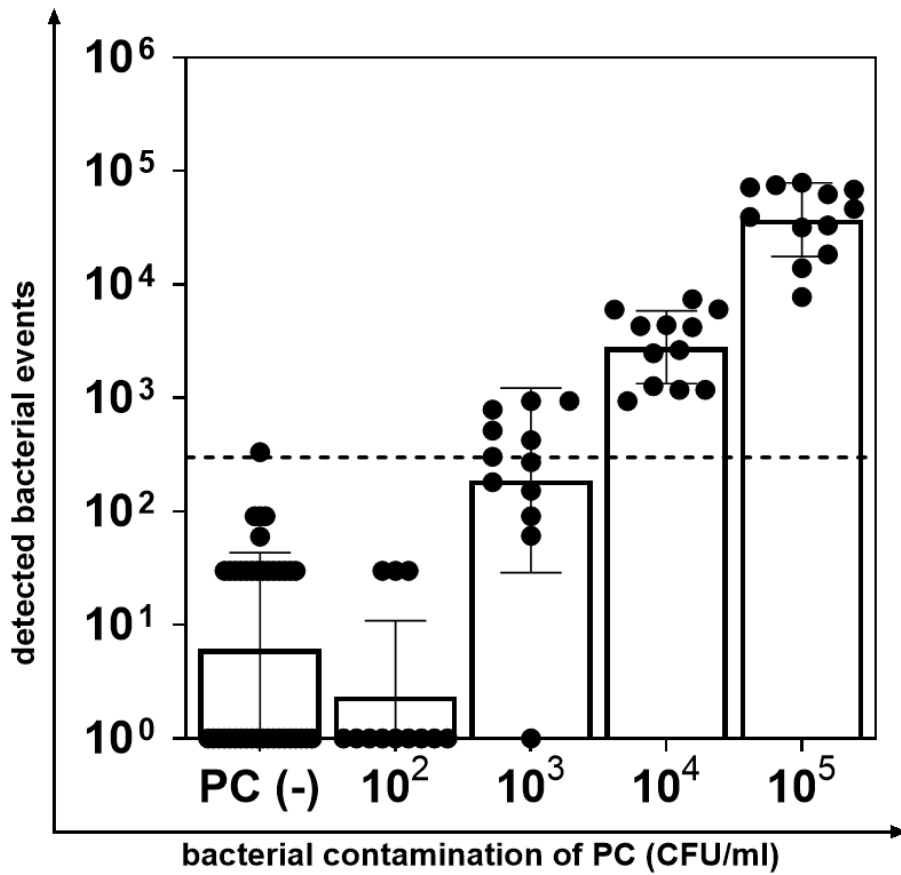


Figure 63: PC spiked with *B. cereus* analysed with the BactiFlow® system

PC samples were spiked with defined contamination levels of *B. cereus* ranging from 10^2 - 10^5 CFU/ml and analysed using the new flow cytometry method. Non-contaminated PC samples PC (-) were analysed as negative reference to determine the background events. Classification into non-contaminated PC and contaminated PC was performed by the BactiFlow® system via its defined LOD of 300 counts/ml (dashed line). Error bars indicate mean of detected events ± 1 SD.

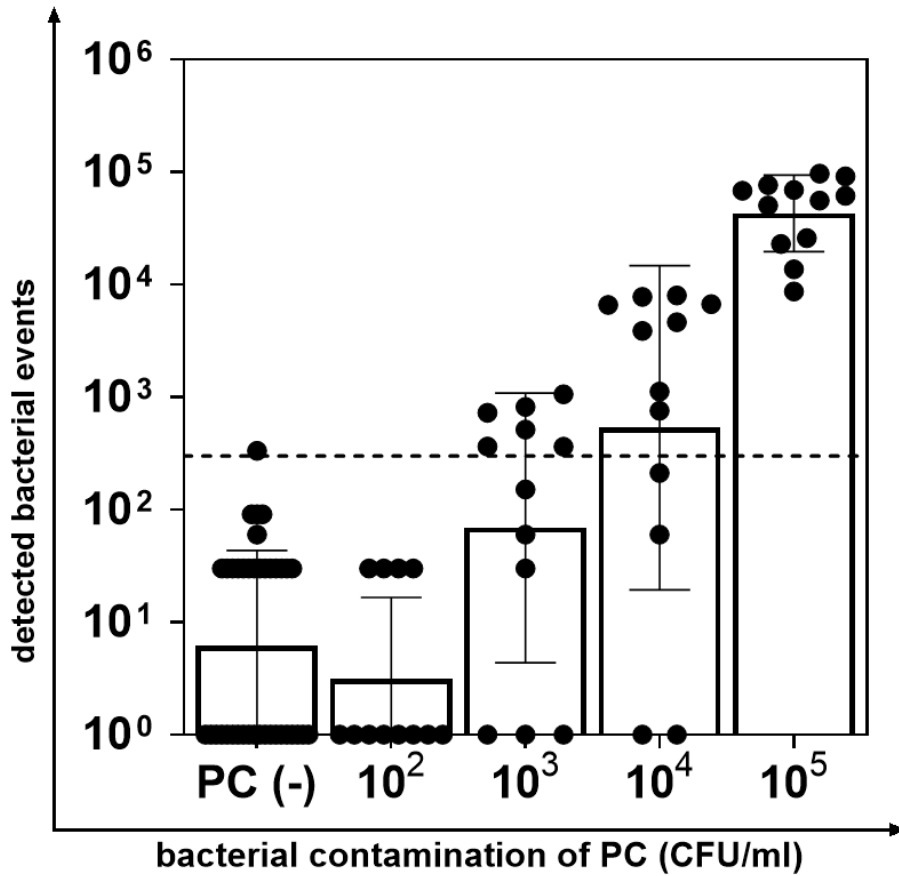


Figure 64: PC spiked with *S. epidermidis* analysed with the BactiFlow® system

PC samples were spiked with defined contamination levels of *S. epidermidis* ranging from 10^2 - 10^5 CFU/ml and analysed using the new flow cytometry method. Non-contaminated PC samples PC (-) were analysed as negative reference to determine the background events. Classification into non-contaminated PC and contaminated PC was performed by the BactiFlow® system via its defined LOD of 300 counts/ml (dashed line). Error bars indicate mean of detected events ± 1 SD.

7.8 Raman parameter folder for the Raman Analyst Software

| | |
|--|--|
| <pre>"despike_type": "default", "despike_threshold": 10, "calib_aggr_by": false, "calib_type": "gauss", "calib_xaxis_x1": 200, "calib_xaxis_x2": 3100, "calib_xaxis_dx": 6, "calib_degree": 3, "calib_peaks": [213.3, 329.2, 390.9, 465.1, 504.0, 651.6, 710.8, 797.2, 834.5, 857.9, 968.7, 1105.5, 1168.5, 1236.8, 1278.5, 1323.9, 1371.5, 1515.1, 1561.5, 1648.4, 2931.1, 3064.6, 3102.4, 3326.6], "calib_peaks_sd": [1.77, 0.52, 0.76, 0.3, 0.6, 0.5, 0.68, 0.48, 0.46, 0.5, 0.6, 0.27, 0.65, 0.46, 0.45, 0.46, 0.11, 0.7, 0.52, 0.5, 0.63, 0.31, 0.95, 2.18], "calib_peaks_which": [213.3, 329.2, 390.9, 465.1, 504, 651.6, 710.8, 797.2, 857.9, 968.7, 1105.5, 1168.5, 1236.8, 1278.5, 1323.9, 1371.5, 1515.1, 1561.5, 1648.4, 2931.1, 3064.6, 3102.4], "baseline_type": "snip", "baseline_iterations": 40, "baseline_smoothing": true, "baseline_emsc_degree": 2, "baseline_emsc_reference": false, "baseline_aggr_by": false, "norm_type": "vector", "norm_area_x1": 400, "norm_area_x2": 3098, "norm_area_exclude_x1": 1800, "norm_area_exclude_x2": 2800, "norm_peak_x1": 2800,</pre> | <pre>"norm_peak_x2": 3050, "qual_snr": false, "qual_spectrum_area_min": false, "qual_spectrum_area_max": false, "qual_bg_area_max": false, "qual_peak_x1": 2800, "qual_peak_x2": 3050, "qual_peak_min": false, "qual_peak_max": false, "qual_corr_calib": false, "qual_corr_prpr": false, "model_type": "pcalda", "model_clusters": 3, "model_ncomp": 10, "model_svm_cost": 1, "model_svm_kernel": "rbf", "model_validation": "10fold", "model_cnn_features": false, "model_cnn_epochs": 0, "model_test": false, "model_meta_included": {"Batches": []}, "Dates": [], "Classes": []}, "model_classes_name": "type", "model_classes_paths": [], "model_responses": "response"</pre> |
|--|--|

Figure 65: Parameters for pre-processing of Raman spectra using the Raman Analyst Software version 0.2.0.0 (Leibniz-IPHT; Jena, Germany)

Parameters for the pre-processing pipeline were defined with the Raman Analyst Software before the data were read into the program. In order to pre-process all examined data with the same parameters, they were exported as a .txt file and stored in the parameter folder of the data structure (chapter 3.5.1, Fig. 4) of the respective data sets for all further experiments, in order to automatically read in the parameters for each subsequent experiment.

7.9 Titration of the optimal Triton X-100 concentration for the lysis of platelets

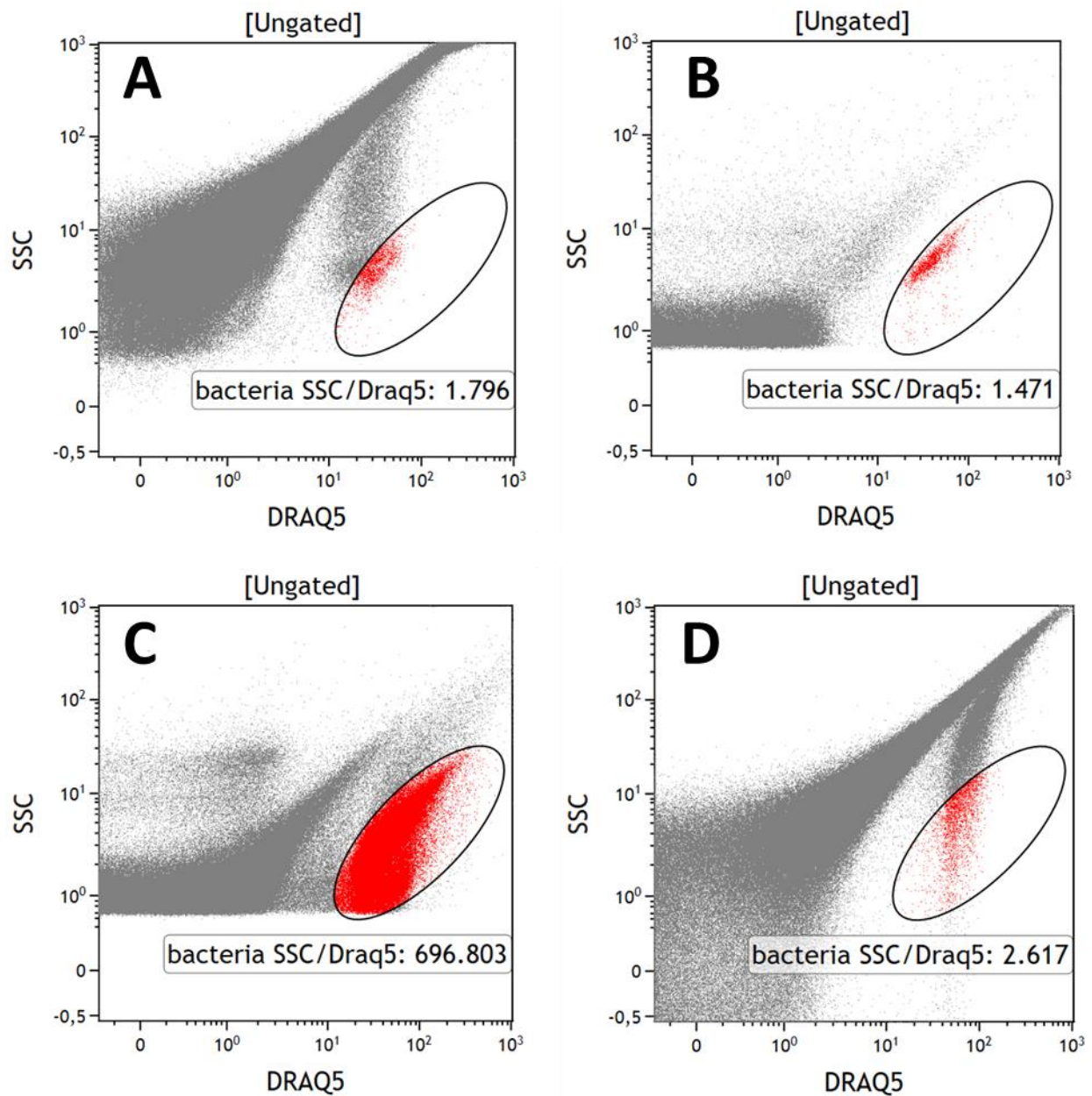


Figure 66: Influence of lysis on bacteria and platelets by different concentrations of Triton X-100

PC samples contaminated with 10^6 CFU/ml of *K. pneumoniae* were centrifuged at 13000 rpm for 1 min. Pellets were resuspended in 1 ml PBS + 1 mM EDTA pH= 7.1 without addition of Triton (A), + 0.5 % Triton X-100 (B), + 0.2 % Triton (C) and + 0.01 % of Triton X-100 (D). All samples were incubated for 30 min at RT prior further sample preparation (chapter 3.6.1) and flow cytometry analysis.

Acknowledgement

First of all, I would like to thank Prof. Dr. Isabelle Bekeredjian-Ding, who gave me the possibility to write my thesis at the Paul-Ehrlich-Institute. I would also like to thank Prof. Dr. Tanja Schneider for taking over the second correction of my thesis and her help for my doctoral studies at the University of Bonn.

A very special thank you goes to Dr. Birgit Blissenbach and Dr. Oleg Krut, who have supervised me for the last 3 years and who have always been there for me with advice and support. I would also like to thank Dr. Birgit Blissenbach for the proof reading of my thesis and the many hours she spent helping me to bring this thesis to a success.

I would also like to thank all the members of division 1/0 and 1/3 of PEI. I would especially like to thank our TAs, who always helped me and had numerous and valuable pieces of advice ready for me. I hope you keep me in good memory, even if I sometimes asked you thousand questions in a day. I want to thank you all for the collegial and friendly working atmosphere.

I would especially like to thank my fellow doctoral students, with whom I not only worked together in a lab, but with whom I also developed valuable friendships and with whom even the long h in the lab became something, that I remember fondly. I wish all those who started after me another successful time and a good completion of their projects.

Finally, I would like to thank my parents and my entire family, without whom I would not have been able to start my studies in biology at the University of Marburg. I will be eternally grateful for their support and hope that with this doctorate I have completed my studies in a worthy manner.